The mechanism of *Nov (Ccn3)* function in haematopoiesis

Thesis submitted for the degree of Doctor of Philosophy (D.Phil)

Yanping Guo

Wolfson College, University of Oxford

Michaelmas term 2012

Weatherall Institute of Molecular Medicine
Nuffield Department of Clinical Laboratory Sciences

THE MECHANISM OF *NOV (CCN3)* FUNCTION IN HAEMATOPOIESIS

Yanping Guo, Wolfson College, Michaelmas term 2012

Thesis submitted for the degree of Doctor of Philosophy (D.Phil.)

Abstract

Haematopoietic stem cells (HSC) are strictly regulated by intrinsic regulators and extrinsic signals from the microenvironment. Nov (CCN3), a matricellular protein of the CCN family, has been reported as a suppressor gene in solid tumours and chronic myeloid leukaemia (CML). Recent study identified *Nov* as a positive regulator in human cord blood CD34+ stem cells. However, the functions of *Nov* in haematopoiesis and adult HSC remain largely unknown.

Gene expression analysis of *Nov* showed that *Nov* was expressed in mouse bone marrow HSCs and was rapidly down regulated during differentiation. Overexpression of *Nov* in HSCs could induce apoptosis and reduce their long term reconstitution efficiency in bone marrow transplantation. Overexpression of *Nov* in HSCs also resulted in a bias of lineage reconstitution with impaired CD3+ T cell differentiation. On the other hand, knockdown of *Nov* expression in HSC did not affect cell growth, differentiation and long term reconstitution activity in bone marrow transplantation. Analysis of Nov^{3del} mutant mice showed normal haematopoiesis and HSC function *in vitro* and *in vivo.* However, there was an increased frequency of HSCs in Nov^{3del} mutant bone marrow which indicated a role of *Nov* in HSC microenvironment.

Analysis of *Nov* function in HSC interaction with microenvironment showed that knockdown of *Nov* in FDCPmix haematopoietic cells resulted in a reduction of cell adherence and migration capacity. At the same time, overexpression of *Nov* in stromal cells enhanced haematopoietic cell migration *in vitro* and could increase their HSC maintaining capacity in co-culture system.

Taken together, these results suggested that *Nov* negatively regulates mouse bone marrow HSC growth and long term reconstitution activity, and plays an important role in HSCs interaction with their bone marrow microenvironment.

Index

Abstract 2
Acknowledgements 8
Abbreviations 9

CHAPTER1 12
INTRODUCTION 12
1.1 Haematopoietic stem cells and haematopoiesis 13
1.1.1 Haematopoietic stem cells 14
1.1.2 Haematopoiesis 15
1.1.3 Intrinsic regulators of HSC 18
1.1.4 Extrinsic regulators of HSC 21
1.1.5 Coordination of intrinsic and extrinsic regulators 32
1.2 Nov 33
1.2.1 Nov and CCN family 33
1.2.2 Regulation and function of *Nov* 34
1.2.3 Nov mutant transgenic mice 36
1.2.4 Nov in HSC and leukaemia 37
1.2.5 Mechanism of Nov function in HSC regulation and HSC niche 39
1.3 Aims of the thesis and project outline 43
Figure.1.1: Road map of HSC differentiation to mature lineage cells: the classical model 44
Figure.1.2: Schematic representation of the key compartments of the HSC niche in bone marrow 46
Figure.1. 3: Structure of the CCN protein family 48
Figure.1.4: The 3D modular arrangement of Nov protein 49
Figure.1.5: Strategy of making Nov^{3del} mutant mice and the expression level of Nov^{3del} mutant protein 50
Table 1.1: The functions of *Nov* in key cellular components of bone marrow HSC niche 52
Figure.1.6: A hypothetical role of *Nov* in HSC and the bone marrow niche. 53

CHAPTER2 55
MATERIALS AND METHODS 55
Mice 56
Cell preparation and flow cytometry analysis 57
Red blood cell lysis 57
Cell enrichment 57
Cell staining for FACS analysis or cell sorts 58
Complete blood count (CBC) test 59
Bone marrow reconstitution assay 59
Cell culture 61
Establishment of bone marrow stroma 61
Culture of cell lines 62
In vitro analysis of HSPC function 63
Cell proliferation assay 63
CAFC assay 63
CFC assay 64
BrdU cell cycle analysis 65

Ki67 cycle analysis....65
Annexin V apoptosis detection....66
Cell migration assay....66
Preparation of lentivirus and lentiviral transduction....67
Production of high titre lentivirus....67
Titration of lentivirus....68
Lentiviral transduction....68
General molecular biology techniques....69
Bacteria transformation and clone selection....69
Plasmids extraction and DNA purification....69
Cloning and ligation for overexpression constructs....70
Constructs for gene expression knockdown....71
DNA sequencing....74
Genomic DNA extraction and genotyping PCR for *Nov*^{3del} transgenic mice 75
Gene expression analysis....77
Total RNA extraction....77
Quantitative RT-PCR analysis....78
Western blots....78
Statistical analysis....79
Table 2.1. FACS instruments configurations....80
Table 2.2. Antibodies used in FACS analysis and their applications....81
Table 2.3. Fluorochromes used in FACS analysis....86
Table 2.4 Primers used for gene expression assay with SYBR GREEN Q-PCR....87
Figure.2.1: Representative FACS plots for bone marrow analysis....88
Figure.2.2: Representative colonies in CFC assay....90

CHAPTER3....91
EFFECTS OF *NOV* OVEREXPRESSION IN HAEMATOPOIETIC STEM AND PROGENITOR CELLS 91
3.1 Introduction....92
3.2 Results....92
3.2.1 Characterisation of *Nov* expression during the early stages of haematopoiesis in bone marrow....92
3.2.2 Cloning of mouse *Nov* cDNA and lentiviral overexpression constructs....93
3.2.3 Functional analysis of *Nov* overexpression in FDCPmix cells....95
3.2.4 Functional analysis of *Nov* overexpression in KLS *in vitro*....97
3.2.5 Effects of *Nov* overexpression in CMP....101
3.2.6 Functional analysis of *Nov* overexpression in KLS *in vivo*....102
3.3 Summary and discussion....111
Figure.3.1: Endogenous expression of *Nov* in mouse haematopoietic stem and progenitor cells....116
Figure.3.2: Constructs for overexpression of *Nov*....117
Figure.3.3: Overexpression of *Nov* in FDCPmix induces apoptosis....119
Figure.3.4: KLS cells transduced with mNov virus grew differently under different culture conditions....121
Figure.3.5: Overexpression of *Nov* in KLS induces apoptosis in expansion condition....122
Figure.3.6: *In vitro* functional assay of *Nov* overexpression in KLS....124
Figure.3.7: *In vitro* functional assay of *Nov* overexpression in CMP....125

Figure.3.8: Overexpression of *Nov* in KLS showed reduced engraftment efficiency in bone marrow reconstitution assay. 126
Figure.3.9: Overexpression of *Nov* in KLS impaired the CD3+ T cell reconstitution in bone marrow reconstitution assay. 127
Figure.3.10: Lineage reconstitution of mNov KLS in bone marrow and spleen. 129
Figure 3.11: The frequency of HSC and progenitors in mNov KLS transplantation. 130
Figure.3.12: T cell developments of mNov donors in recipient thymus in bone marrow transplantation. 132
Figure.3.13: The secondary transplantation of mNov cells shows a reduced engraftment capacity. 134

CHAPTER4. 136
EFFECTS OF KNOCKING DOWN *NOV* EXPRESSION IN HSPC 136
4.1 Introduction 137
4.2 Results 137
4.2.1 LVTHM Novi construct and the limitation 137
4.2.2 LLX Novi knockdown construct 139
4.2.3 Cell growth of FDCPmix was not affected by knocking down of *Nov* expression 139
4.2.4 *In vitro* analysis of knocking down *Nov* in KLS 140
4.2.5 Bone marrow transplantation of KLS transduced with Novi virus 142
4.3 Summary and discussion 147
Figure. 4.1: LVTHM shRNA virus constructs and effects in LVTHM-Novi transduced FDCPmix cells. 149
Figure. 4.2: Bone marrow transplantation of KLS transduced with LVTHM-Novi virus. 151
Figure. 4.3: LLX3.7 shRNA virus construct and consistent expression in FDCPmix cells. 153
Figure. 4.4: Knock down of *Nov* in FDCPmix cells did not affect cell growth. 155
Figure. 4.5: KLS Novi cells showed no obvious change in cell growth. 156
Figure. 4.6: KLS Novi cells showed normal CAFC and CFC frequency. 157
Figure. 4.7: Bone marrow transplantation, KLS Novi cells showed a similar reconstitution capacity to LLX controls. 159
Figure. 4.8: In long term bone marrow transplantation, Novi cells showed a normal lineage distribution in bone marrow and spleen. 161
Figure. 4.9: In long term bone marrow transplantation, KLS Novi cells showed a similar HSC and progenitor frequency in bone marrow. 162
Figure. 4.10: In secondary transplantation, KLS Novi cells showed a similar reconstitution capacity as LLX control KLS. 163

Chapter5. 165
Analysis of Nov^{3del} mutant mice 165
5.1 Introduction 166
5.2 Results 167
5.2.1 Breeding of Nov^{3del} mutant mice 167
5.2.2 Nov^{3del} mutant mice showed normal blood counts and lineage distribution 167

5.2.3 FACS analysis showed an increased frequency of HSC in *Nov*^{3del} bone marrow....169
5.2.4 *In vitro* assays showed an increased CAFC frequency but normal CFC output from *Nov*^{3del} bone marrow....170
5.2.5 *Nov*^{3del} mutant mice bone marrow could long-term reconstitute lethally irradiated recipients....171
5.2.6 Nov^{3del} mutant bone marrow showed increased reconstitution efficiency in serial transplantation....172
5.2.7 The analysis of haematopoiesis in aged *Nov*^{3del} mutant mice....174
5.2.8 The function of HSC from aged *Nov*^{3del} mutant mice was normal in bone marrow transplantation....175
5.3 Summary and discussion....176
Table.5.1: Complete blood test for the wild type, *Nov*$^{3del+/-}$ and *Nov*$^{3del-/-}$ mice. 180
Figure.5.1: Lineage distributions were normal in *Nov*^{3del} mice peripheral blood....181
Figure.5.2: Cellularity and Lineage distributions were normal in *Nov*^{3del} mutant mice bone marrow....182
Figure.5.3: FACS analysis of HSC in *Nov*^{3del} bone marrow....184
Figure.5.4: FACS analysis progenitors in *Nov*^{3del} bone marrow....185
Figure5.5: *In vitro* analysis of *Nov*^{3del} HSC/HPC....186
Figure.5.6: Short term engraftment efficiency of *Nov*^{3del} cells in competitive reconstitution assay. 188
Figure.5.7: Long term engraftment of *Nov*^{3del} cells in competitive reconstitution assay. 189
Figure.5.8: Serial transplantation of *Nov*^{3del} bone marrow cells 191
Figure.5.9: Serial transplantation of *Nov*^{3del} cells....193
Figure.5.10: Analysis of haematopoiesis in aged *Nov*^{3del} mice 194
Figure.5.11: Bone marrow reconstitution of *Nov*^{3del} aged cells....196

CHAPTER6....198
ANALYSIS OF *NOV* FUNCTION IN HSC MICROENVIRONMENT....198
6.1 Introduction....199
6.2 Results 200
6.2.1 Novi FDCPmix cells showed impaired adherent capacity....200
6.2.2 *Nov* knockdown in FDCPmix reduced the migration capacity....201
6.2.3 Gene expression analysis of Novi FDCPmix cells by RT-qPCR 204
6.2.4 Characterization of *Nov* expression pattern in bone marrow cells ...204
6.2.5 Overexpression of *Nov* in stromal cells enhanced FDCPmix migration but *Nov* did not function as chemoattractant *per se*....206
6.2.6 Overexpression of *Nov* in stromal cells can enhance the HSC expansion and CFC frequency *in vitro* 208
6.3 Summary and discussion....210
Figure.6.1: Adherence was impaired in FDCPmix Novi cells and could be rescued by adding Nov protein....214
Figure.6.2: The migration capacity was impaired in FDCPmix Novi cells..215
Figure.6.3: FDCPmix Novi cells show no obvious change in gene expression of CAM and MMP genes by RT-qPCR. 217
Figure.6.4: The expression of *Nov* in stromal cells and primary bone marrow cells. 218
Figure.6.5: The effects of *Nov* in cell migration as extrinsic signal....219

Figure.6.6: The growth rate and CFC frequency of KLS after being cocultured with stromal cells for 7-10 days. 221
Figure.6.7: RT-qPCR results of stromal cells transduced with CSI/mNov or LLX/Novi virus. 223

CHAPTER 7 225
FINAL DISCUSSION AND FUTURE EXPERIMENTS 225
Nov function in HSC: species specific or tissue specific 227
General picture of *Nov* in HSC and bone marrow niche 230
Possible future directions 232
Figure 7.1: Alignment of orthologous human and mouse Nov proteins 233
Figure 7.2: *Nov* function in bone marrow HSC niche 234

REFERENCES: 235
APPENDIX: PUBLICATIONS 253

Acknowledgements

I would like to start by saying thank you to everyone who worked with me and helped me in the past years which has been the most special and memorable experience.

My deepest gratitude goes first to my supervisor Tariq Enver for giving me the opportunity to work in his lab, for providing me plenty flexibility and time to pursue my scientific aims and for being supportive through my study.

I would also like to express my heartfelt gratitude to my co-supervisor Paresh Vyas for helping me whenever I needed and for giving me advice for the thesis.

I feel grateful to all the members in Enver lab: Cristina Fugazza, for those days and nights working side by side at the Cyan machines; Gill May, for teaching me things I need to know in the lab; Alex Tipping, for reading most of this thesis and keeping me hopeful at the final days; Cristina Pina, for your valuable advice*;* John Brown, for help with molecular biology queries; Jason Wray, Rachael Nimmo and Goran Karlsson for reading my thesis and giving me advice; Rajeev Gupta, for providing the HNOV construct. Many thanks to Shamit Soneji, Christina Jensen, and the rest of Enver group for keeping the lab a warm and happy place.

Finally, I would like to thank my family and friends for giving me something to love and to look forward every day. Especially to my parents, thank you for your love and being proud of me. Last but not least, to my dearest kids, thank you for trusting me, loving me and being there for me. **This thesis is dedicated to them.**

Abbreviations

APC	allophycocyanin
B220	CD45R with heavier glycosylation
BFU-E	burst-forming unit erythrocyte
BM	bone marrow
BMP	bone morphogenic proteins
CAFC	cobble stoning forming cell
CD	cluster of differentiation
cDNA	complementary DNA
CFU	colony-forming unit
CFU-E	colony-forming unit erythrocyte
CFU-G	colony-forming unit granulocyte
CFU-GM	colony-forming unit granulocyte-macrophage
CFU-M	colony-forming unit macrophage
CFU-MIX	colony-forming unit of mixed lineages with granulocyte, erythrocyte, megakaryocyte and macrophage
cKit	tyrosine-protein kinase Kit or CD117
CLP	common lymphoid progenitor
CML	chronic myelogenous (or myeloid) leukaemia
CMP	common myeloid progenitor
cPPT	central poly purine tract allows nuclear import of lentivirus in host cells
DMEM	Dulbecco's Modified Eagle Medium
DN	the earliest thymocyte differentiation stage as negative for both CD4 and CD8
DNA	deoxyribonucleic acid
DP	CD4+CD8+ double positive thymic cells
EPO	erythropoietin
FACS	fluorescent activated cell sorter
FBC	fetal bovine serum
FCS	fetal calf serum
FITC	fluorescein isothiocyanate
FLT3	FMS-like tyrosine kinase 3
G0	“gap 0” phase of the cell cycle
G1	“first gap” phase of the cell cycle
G2	“second gap” phase of the cell cycle
G-CSF	granulocyte- colony stimulating factor
GFP	green fluorescent protein
GM-CSF	granulocyte/macrophage colony stimulating factor

GMP	granulocyte-monoctye progenitor
Gr1	granulocyte differentiation antigen 1
H1	histone H1 promoter used to drive shRNA expression
HCT	hematocrit
HGB	Haemoglobin
HSC	haematopoietic stem cell
HSPC	haematopoietic stem and progenitor cell
IL	interleukin
IMDM	Iscove's Modified Dulbecco's Medium
KLS	lineage-cKit+ Sca-1+ cells
LMPP	lymphoid primed multipotent progenitor
LT-HSC	long term haematopoietic stem cells
LTR	long terminal repeat
Mac1	macrophage-1 antigen
MCH	mean corpuscular haemoglobin
MCHC	mean corpuscular haemoglobin concentration
M-CSF	macrophage colony stimulating factor
MCV	mean corpuscular volume
MEP	megakaryocytic and erythroid progenitor
MNC	mononuclear cells
MPP	multipotent progenitor
MPV	mean platelet volume
Nov	nephroblastoma overexpressed gene (CCN3)
P/S	penicillin/ streptomycin
PB	pacific blue
PB	peripheral blood
PBS	phosphate buffered saline
PCR	polymerase chain reaction
PCT	plateletcrit
PE	Phycoerythrin
PLT	platelet count
preCFU-E	early lineage-restricted precursors for erythroid
preGM	early lineage-restricted precursors for the granulocyte/macrophage
preMegE	early lineage-restricted precursors for erythroid, and megakaryocytic lineages
RBC	red blood cells
RDW	Red cell distribution width
RNA	ribonucleic acid
RRE	rev response element
RT	room temperature
Sca-1	stem cell antigen-1
SCF	stem cell factor

SD	the standard deviation
SDS	sodium dodecyl sulphate
SEM	standard error of the mean
SFEM	StemSpan® Serum-Free Expansion Medium
SP	thymocyte positive for either CD4 or CD8
ST-HSC	short term haematopoietic stem cells
TE	Tris-EDTA
Ter119	a glycophorin A-associated protein, also known as Ly-76
TetO	binding site for the tet repressor protein
TF	transcription factor
TPO	thrombopoietin
WBC	white blood cells
WPRE	the woodchuck hepatitis virus posttranscriptional response element

CHAPTER1.

INTRODUCTION

1.1 Haematopoietic stem cells and haematopoiesis

The blood system is a complex, multifunctional tissue which is composed of at least 8 distinct cell lineages, including erythrocytes, megakaryocytes, granulocytes, macrophages and lymphocytes. These mature blood cells are produced via a process known as haematopoiesis, which occurs mainly in the bone marrow of an adult animal. Each cell lineage has a distinct and important function such as supplying oxygen to tissues around the body by red blood cells, blood clotting and wound healing by platelets, and protecting the body against foreign bodies and pathogens by lymphocytes.

Mature blood cells have a high turnover rate and are continuously produced throughout the lifetime of an animal. This demand is fulfilled by rare pluripotent bone marrow stem cells, called haematopoietic stem cells (HSCs). HSCs can give rise to additional HSCs and maintain the HSC pool size through self-renewal. Upon differentiation, HSC can produce all of the different mature blood cell types. Understanding the regulation of HSC function and fate decisions is of great importance not only for understanding basic stem cell biology but also for providing clinical therapy cues for many diseases.

1.1.1 Haematopoietic stem cells

HSCs are rare cells within the bone marrow. HSCs are defined by their capability of long-term self-renewal to propagate themselves and their potency to differentiate into all blood cell lineages. In addition to self-renewal and differentiation, HSCs can also undergo apoptosis which is important in haematopoietic homeostasis and in regulating HSC numbers (Domen J, 2000a).

Most HSCs are in G_0 phase of the cell cycle, and only a small number of HSCs are in cycling and responsible for self-renewal or for producing mature cells at any specific time (Fleming W.H, 1993; Cheshier S.H, 1999). Quiescence of HSCs is critical for protecting the stem cell population and sustaining stem cell pools over long periods (Cheng T, 2000). It is suggested that quiescence of HSC protects stem cells by minimizing their accumulation of replication-associated mutations (Mohrin M.E, 2010; Li. J, 2011).

In homeostasis, the majority of HSCs reside in the bone marrow; however, a small number of HSCs are constantly released into the circulation and migrate among various haematopoietic tissues (Wright D.E, 2001; Wright D.E, 2002). Circulating HSCs can home to the bone marrow and lodge into specific niche which is the principal site for the self-renewal and proliferation of HSCs (Abkowitz J, 2003; Sugiyama T, 2006; Kiel M, 2006).

The gold standard assay to evaluate HSCs is the long term repopulation assay (Metcalf D, 2007). After being transplanted into lethally irradiated recipient mice, HSCs should be able to reconstitute the entire blood system of the recipient for at least 4-6 months. The donor derived cells are then transplanted into secondary lethally irradiated recipients to evaluate their ability of long term self-renewal.

1.1.2 Haematopoiesis

Haematopoiesis describes the ordered and continuous process of blood cell formation. Through a series of developmental steps, HSCs give rise to their downstream multipotent progenitors which are committed to limited blood lineages and have reduced self-renewal capacity. The hierarchy of blood cell development has been proposed on the basis of cellular development and functional readout assays. Roadmaps are often used to describe the sequence of development events and to show the different paths for a haematopoietic cell. The understanding of the determinants and mechanisms in the lineage fate decisions during normal haematopoiesis is of great importance for understanding the aberrations that may occur in haematological diseases.

Figure 1.1 shows the roadmap of the updated classical model and surface markers used for purifying each cell population. The primitive HSC

population in bone marrow is enriched in lineage-cKit+Sca1+ (KLS) compartment (Spangrude G.J, 1988; Ikuta K, 1992). As a heterogeneous population, KLS is made up of the truly long term self-renewing HSC (LT-HSC), followed by ST-HSC with limited self-renewing ability and lastly multipotent progenitors (MPP) which exhibit low or no self-renewal ability (Christensen J.L, 2001; Kiel M.J, 2005; Kim I, 2006).

In the classical model of the haematopoietic development, the first lineage fate decision is taken at the MPP stage and gives strictly separated lymphoid and myeloid progenitors. This model was supported on the basis of the prospective isolation and characterization of common lymphoid progenitors (CLPs) and common myeloid progenitors (CMPs) in bone marrow (Kondo M, 1997; Stinicka E, 2002; Akashi K, 2005; Karsunky H, 2008). CLPs can only differentiate into all types of lymphoid lineages, including B, T and NK cells but not myeloid lineages. CMPs on the other hand can give rise all types of myeloid cells, including granulocyte, monocyte, megakaryocyte and erythroid cells, but not B or T cells. Intermediated progenitors of granulocyte/monocyte progenitor (GMP) and megakaryocyte/erythroid progenitor (MEP) generated by CMP will finally give rise to myeloid cells. The only exceptional cell type is dendritic cells which can be derived from both CLPs and CMPs (Inaba K, 1993; Gatly A, 1995; Martin P, 2000; Manz M.D, 2001; Lu M, 2005).

As more progenitors are identified and characterized, the classical model of haematopoiesis has been challenged and modified. The identification and prospective isolation of a MPP progenitor population in KLS compartment has been demonstrated to have robust lymphoid and G/M potential with little MK/E potential. This lymphoid-primed multipotent progenitor (LMPP) expressing high level of FLT3 is largely committed to the myelo-lymphoid lineage (Adolfsson J, 2001; Adolfsson J, 2005; Yang L, 2005; Mansson R, 2007). Based on the differential cell surface expression of signalling lymphocytic activation molecule family member 1 (Slamf1/CD150), Endoglin (Eng/CD105), and Integrin α 2b (Itgα2b/CD41), a range of myeloid progenitor subsets with developmentally restricted lineage potentials were identified, including early lineage-restricted precursors for the granulocyte/macrophage, erythroid, and megakaryocytic lineages (Cornelis J.H. Pronk,2007).

An alternative model is proposed as myeloid-based model (Kawamoto H, 1997; Lu M, 2002; Kawamoto H, 2009). The model is based on the observations of lineage outcomes from mainly fetal liver cells, in which myeloid potential is retained in an early stage of branches toward erythroid, T-cell, and B-cell lineages. In the myeloid-based model, HSC first diverges into the common myelo-erythroid progenitor (CMEP) and a common myelo–lymphoid progenitor (CMLP); the CMLP then generates T and B cell

progenitors through a bipotential myeloid–T progenitor and a myeloid–B progenitor stage, respectively. The myeloid-base model assumes that blood cells are capable of differentiating into myeloid cells through more than one pathway until their final differentiation into erythrocytes, B lymphocytes, and T lymphocytes. Moreover, there is no CLP like cells in this model. Latest evidence supporting the myeloid-base model came from the study of adult thymus where T-cell thymus progenitors have lost B-cell potential but retain macrophage potential (Wada H, 2008; Kawamoto H, 2010).

1.1.3 Intrinsic regulators of HSC

Both intrinsic and extrinsic mechanisms are involved in the regulation of HSC fate decision and processes of self-renewal, differentiation, apoptosis and quiescence (Zhu J, 2002; Krause D, 2002; Zon L.I, 2008). Intrinsic regulation of HSC refers to the transcription factors, modification of chromatin components and cell cycle status (Orkin S.H, 1995; Park I.K, 2003; Ito K, 2004; Attema J.L, 2007; Pietras E.M, 2011). Recent papers suggested that mitochondrial function and energy homeostasis also contribute to the regulation of HSC function (Nakada D, 2010; Gan B, 2010; Gurumurthy S, 2010; Suda T, 2010).

Transcription factors regulate HSC self-renewal and maintenance through either an activating or repressive manner. Deficiency of transcriptional

repressor Gfi1 causes increased proliferation and exhaustion of stem cells (Zeng H, 2004; Hock H, 2004). HoxB4 potently expands HSC *in vivo* and *in vitro* and conversely, deficiency of HoxB4 leads to reduced proliferative capacity of HSC (Helgason C.D, 1996; Thorsteinsdottir U, 1999; Antonchuk J, 2002; Björnsson J.M, 2003). Oncogene Bmi-1 is required for maintenance of adult self-renewing haematopoietic stem cells (Park I.K, 2003).

Transcription factors play key roles in lineage choice during differentiation, such as GATA-1 for megakaryocyte and erythrocyte development, PU.1 for the myeloid lineage commitment and Ikaros for lymphoid development. Potentially, committed haematopoietic progenitors can also be reprogrammed by the instructive action of transcription factors. For example, forced expression of GATA-1 can reprogram common lymphoid progenitors as well as granulocyte/monocyte (GM) progenitors to differentiate into MegE lineages and inhibit normal lymphoid or GM differentiation (Kulessa H, 1995; Iwasaki H, 2003).

Accumulating evidence shows that transcription factors work in networks called genetic regulatory networks (GRNs) which consist of the interactions between transcription factors and extracellular signals and govern haematopoietic stem cell development and identity (Matt Loose, 2007; Graf T, 2009). Simple module includes as few as two transcription factors. Transcription factors could work in antagonism manner such as the balance

between Bmi1 and Mel-18 regulating self-renewal of HSCs （Kajiume T，2009); or as the reciprocal activation of GATA-1 and PU.1 marking initial myeloerythroid and myelolymphoid lineage choice（Arinobu Y，2007）. They can also work like GATA-1 and FOG-1 which induce terminal erythroid differentiation with FOG-1 acting either as an activator or repressor in conjunction with GATA-1 (Letting D.L, 2004). GATA-1 itself plays a direct role in activating FOG-1 expression through binding to GATA sites throughout the FOG-1 locus (Welch J.J, 2004). More complicated example of regulatory circuit is made up of Gata2, Fli1, and Scl/Tal1 and their enhancers, Gata2-3, Fli1+12, and Scl+19 operates during specification of haematopoiesis in the mouse embryo. (Pimanda, J, 2007, Pimanda J.E, 2010). Gene expression profiles of 38 distinct purified populations of human haematopoietic cells and the probabilistic models of gene expression and analysis of cis-elements in gene promoters were combined to decipher the general organization of their regulatory circuitry. The results revealed many densely interconnected cis-regulatory circuits and a large number of transcription factors that are differentially expressed across haematopoietic states, indicating a complex regulatory system for haematopoiesis (Novershtern N, 2011).

A recent study, armed with advanced techniques of CHIP-seq and mathematical modelling, proved genomic evidence for the existence of a

core network for erythoid of >300 genes that are co-occupied and regulated by GATA-1, SCL, and Klf1. Furthermore, the mathematical modelling revealed that the dual mechanism used by both GATA-1 and PU.1 to repress an alternative lineage-specific transcriptional program for lineage specification (Wontakal S.N, 2012).

1.1.4 Extrinsic regulators of HSC

HSCs are also regulated by combinatorial extrinsic signals produced from the bone marrow microenvironment, including cytokines, signalling pathways and cell-ECM, cell-cell interactions with bone marrow niche (Lymperi S, 2010).

1.1.4.1 Cytokines and signalling pathways

Cytokines are secreted proteins and were identified and purified on the basis of their abilities to support in vitro formation of haematopoietic colonies from progenitors (Kaushansky K, 2006; Zhang C, 2008). For many haematopoietic lineages, one principal cytokine has been identified, such as thrombopoietin (TPO) for platelets (Kaushansky K.,1994; Kobayashi M, 1995, Kaushansky K.,1999); erythropoietin (EPO) for erythroid cells (Koury M.J, 1990; Wu H, 1995), IL-15 for NK cells(Carson, W. E,1994), IL-7 for B and T cells(Grabstein, K.H,1993), and GM-CSF for granulocytes (Metcalf D, 1986). Many cytokines were shown to regulate many HSC functions such as

SCF, Flt3, and TPO to enhance haematopoietic stem and progenitor cells proliferation, prevent apoptosis and support HSC quiescence (Henschler R, 1994; Zandstra P.W, 1997; Buza-Vidas N, 2006; Yoshihara H, 2007).

G-CSF has been clinically used to mobilize HSC in order to increase the number of progenitors in the circulation (Weaver A, 1996). Many soluble cytokines can bind directly to receptors on HSC cell, such as thrombopoietin (TPO) and its receptor Mpl (Yoshihara H, 2007; de Graaf C.A, 2011), SCF and cKit receptor (Ikuta K, 1992).

Chemotactic cytokines, also known as chemokine, are capable of inducing directed chemotaxis in nearby responsive cells including both HSC and lymphocytes. Stromal cell-derived factor-1 (SDF-1/CXCL12), one of well-known chemokine, is responsible for HSC homing towards bone marrow and for retaining HSCs within the bone marrow (Christensen J. L, 2004; Suarez-Alvarez B, 2012).

Many signalling pathways have also been identified that regulate HSC self-renewal and expansion by ligand stimulation or by activation of their internal signals, including Notch, Wnts, TGF-β and BMPs (Calvi L.M, 2003; Duncan A.W, 2005; Reya T, 2003; Trowbridge J.J, 2006; Sugimura R, 2012; Trowbridge, J.J, 2006; Yamazaki S, 2009; Zhang J, 2003) and arguably Shh (Bahardwaj G.B, 2001; Gao J. 2009; Hofmann I, 2009).

1.1.4.2 Extracellular matrix (ECM)

The extracellular matrix (ECM), a three-dimensional fibrillar protein scaffold is an essential no cellular component of the adult stem cell niche (Lu P, 2012; Brizzi M.F, 2012). Both subendosteal reticulocytes and osteoblasts contribute to the production of extracellular matrix molecules, including collagen I, laminin, fibronectin, and decorin (Balduino A, 2005). The function of bone marrow ECM was suggested as allowing some HSCs to lodge at the subendosteal niche and regulating the migration of HSPCs (Reilly G.C, 2009; de Barros A.P, 2010). Analysis of the migratory behaviour of murine haematopoietic progenitor cells factor-dependent-cell-paterson (FDCP)-mix cells on ECM showed that migration on fibronectin (Fn) or laminin (Lam) were β1-integrins dependent (Strobe E.S, 1997). Recent studies, using 3D culture models of human bone marrow mesenchymal stem cells that mimic the subendosteal region or with Fn coated microcavities, showed that human haematopoietic progenitor cells migrated dynamically in and out of these complex structures and lodged within discrete regions (Kurth I, 2009; de Barros A.P, 2010).

ECM proteins could also regulate growth factor bioavailability by establishing stable gradients of growth factors. SDF-1/CXCL12 induction of transendothelial migration in haematopoietic cells was suggested to depend on the immobilized chemokine fraction in the extracellular matrix (ECM) and

bone marrow stromal cells, which could be envisioned as a molecular road map for the migrating HSC (NetelenbosT, 2003; Kopp H.G,2005).

1.1.4.3 Cell-cell interactions

In the bone marrow microenvironment, HSCs are in cell-cell contact with some of the niche forming cells. *In vitro* expansion of HSC was achieved to certain level in co-culture system with stromal cells (Breems D.A, 1998; Jing D, 2010).

It was suggested that HSCs receive messages from adjacent cells via gap junctions of which the expression of Connexin43 (Cx43) was critical in nonhaematopoietic cells of bone marrow (Cancelas J.A, 2000; Montecino-Rodriguez E, 2001; Gonzale-Nieto D, 2012). Cx43 can also play a protective role and regulates the ROS content in HSC through ROS transfer to the microenvironment (Taniguchi Ishikawa E, 2012).Moreover, the secretion of functional SDF-1/CXCL12 from human bone marrow stromal cells (BMSCs) was a cell contact-dependent event mediated by Cx43 and Cx45 gap junctions (Schajnovitz A, 2011).

Cell adhesion molecules (CAM) are also shown to be involved in the crosstalk between HSCs and their niche. Cadherins promote cell-cell adhesion by binding to cadherins expressed by adjacent cells. N-cadherin molecules expressed on osteoblasts and HSCs anchor HSCs within their niche by homotypic adhesion and promote HSC quiescence (Zhang J, 2003;

Xie Y, 2009). However, the role of N-cadherin in HSC regulation within the niche and HSC homeostasis remains controversial (Li P, 2010; Levesque J.P, 2012).

Other than the interaction with ECM proteins, integrin is also the main binding partner of vascular cell adhesion molecule 1(VCAM1), which is expressed on the surface of endothelial cells and osteoblastic lineage (Ulyanova T, 2007; Nakamura Y, 2010). Ingegrins are heterodimetric molecules and can also function as mechanosensors and bi-directional signalling receptors (outside-in and inside-out signalling) (Altrock, E. 2012). Among them, CD41 (Integrinα2b) is a marker of megakaryocytic lineage and key to platelet aggregation. CD41 expression has also been reported to mark the onset of murine primitive and definitive hematopoiesis (Robin C. 2011; Dumon, S, 2012). Latest report shows that CD41+HSCs are mainly quiescent and exhibit myeloerythroid and megakaryocyte gene priming. (Gekas, C, 2013)

1.1.4.4 Cellular compartments of bone marrow niches

Two types of niches in bone marrow have been identified according to its location in the bone as well as their key component cells and they are believed to play different roles in HSC regulation. The osteoblastic-niche is located close to bone endosteal surface, and is later referred as endosteal bone-marrow HSC niche after new cells types along endosteum were

identified to contribute niche forming. Endosteal niche is important for HSC self-renewal and quiescence. The vascular-niche, on the other hand, exists in the centre of bone marrow, close to sinusoids, and is believed to contribute to the regulation of HSC expansion and differentiation (Figure 1.2.) (Kopp, H.G, 2005; Wilson A, 2006; Mendez-Ferrer S, 2010).

Osteoblast (OB)

Osteoblasts are bone-forming cells and interact with HSCs at the interface between the bone and the marrow space. An increase in the number of osteoblasts by administration of parathyroid hormone (PTH) or conditional inactivation of BMP receptor type IA (BMPRIA) resulted in increased HSC numbers (Calvi L.M, 2003; Zhang J, 2003), while osteoblast ablation ultimately results in the loss of HSCs (Visnjic D,2004). HSCs are found in contact with a population of osteoblasts cells on the bone surface, termed spindle-shaped N-cadherin+CD45-osteoblastic (SNO) cells, which express a high amount of N-cadherin (Zhang J, 2003). Osteoblasts secrete cytokines, such as granulocyte colony-stimulating factor (G-CSF), granulocyte-macrophage CSF (GM-CSF) and interleukin-6 (IL-6), which support HSC survival and differentiation. Osteoblasts also express factors that regulate HSC numbers, including angiopoietin, thrombopoietin, WNT, Notch, N-cadherin and osteopontin.

Mesenchymal stem cells (MSCs)

A recent study identified a unique niche component, Nestin+ mesenchymal stem cells (MSCs) that exhibit features of both osteoblastic and endothelial niches (Méndez-Ferrer S, 2010). This nestin-expressing MSC population is closely associated with putative HSCs, and is tightly associated with adrenergic nerve fibers of the sympathetic nervous system (SNS) that regulate HSC mobilization and are responsible for the circadian oscillations in circulating HSC numbers (Katayama Y, 2006; Méndez-Ferrer S, 2008). These MSCs express high levels of HSC maintenance factors, including SDF-1/CXCL12, stem cell factor (SCF), angiopoietin-1 (Ang-1), IL-7, vascular cell adhesion molecule 1 (VCAM1), and osteopontin (OPN), compared with any other stromal cell type including osteoblast cells. Osteoblast cells and mesenchymal stem cells are key cellular components of bone marrow endosteal niche and can be separated with ALCAM (activated Leukocyte Cell Adhesion Molecule) and Sca-1 expression within endosteal populations. Immature mesenchymal cell-enriched ALCAM-Sca-1+ cells express high level of cytokines related genes. Osteoblast-enriched ALCAM+Sca-1-cells significantly enhance the long term reconstitution activity of HSCs by the up-regulation of homing- and cell adhesion–related genes in HSCs (Nakamura Y, 2010).

Bone marrow macrophages

G-CSF mobilization results in a rapid depletion of endosteal osteoblast cells as well as a population of trophic endosteal macrophages (osteomacs or osteoclasts) that support osteoblast function. Depletion of bone marrow macrophages, in particular, a novel CD11b-F4/80-Ly6-G- phagocytic macrophage population, was sufficient to suppress endosteal osteoblasts and inhibit the expression of HSC-supportive cytokines at the endosteum and resulted in the reduction of HSC number (Kollet, 2006; Winkler I.G, 2010; Lymperi S, 2010; Mansour A, 2012). Bone marrow CD169+ mononuclear phagocytes have been lately proved to play a role in HSC/progenitor retention by regulating maintenance of retention gene expression specifically in Nestin+ niche cells (Chow A, 2011).

Sinusoid endothelial Cell (EC)

Endothelial cells (EC) line the interior of all blood vessels, composing the endothelium. Bone marrow ECs were found to support the proliferation and differentiation of haematopoietic progenitors *in vitro* via production of various cytokines and via physical contact (Rafii S, 1994; Rafii S, 1995). *In vivo,* HSCs expressing SLAM markers were detected adjacent to sinusoidal blood vessels throughout the bone marrow revealing a role of sinusoid endothelial cells in bone marrow niches (Kiel M.J, 2005). It has been recently reported

that HSCs require SCF from endothelial cells (Ding L, 2012)

CXCL12-abundant reticular (CAR) cells

CXCL12-abundant reticular (CAR) cells are predominantly found in the more central areas of the marrow, with some tightly associated with sinusoidal endothelium and have a similar morphology to vascular pericytes (Sugiyama T, 2006; Crisan M, 2008). CAR cells express HSC maintenance proteins such as CXCL12 and SCF (Sugiyama T, 2006; Ding L, 2012). HSCs from CAR cell-depleted mice were reduced in number and cell size, were more quiescent, and had increased expression of early myeloid selector genes, similar to the phenotype of wild-type HSCs cultured without a niche(Yoshiki Omatsu,2010).

Bone marrow adipocytes

In human, all bone marrow space is occupied with haematopoietic red marrow at birth, but with age, non-haematopoietic fatty marrow gradually dominates the space in bone marrow. It is generally believed that adipocytes act as passive space fillers in the marrow (Gimble J.M, 1996). A recent study showed that HSCs and progenitors are reduced in number, frequency and cycling capacity in adipocyte-rich bone marrow during homeostasis and that BM-derived adipocytes reduce the expansion of haematopoietic cells in

stromal transwell co-cultures in vitro (Naveiras O, 2009). These results indicate that adipocytes may act as a negative regulator in HSC niche.

Sympathetic nervous system (SNS)

Study showed that signals from the sympathetic nervous system (SNS) trigger G-CSF induced mobilization (Katayaman Y, 2006). In steady state animals, photic cues which are processed in the central nervous system could influence the trafficking of HSCs. The secretion of SDF-1/Cxcl12 in bone marrow stromal cells was regulated through signals from the sympathetic nervous system. (Méndez-Ferrer S.D, 2008). Recent study showed that nonmyelinating Schwann cell was responsible for TGFβ activation for HSC maintenance. These glial cells ensheathed autonomic nerves and were in contact with a substantial proportion of HSCs. Autonomic nerve denervation reduced the number of these active TGFβ-producing cells and led to rapid loss of HSCs from bone marrow (Yamazaki S, 2011). Furthermore, signalling from the sympathetic nervous system was proved to regulate HSC emergence during embryogenesis (Fitch S.R, 2012).

Regulatory T cells

The niche is also suggested to protect stem cells from environmental insults, including cytotoxic chemotherapy and perhaps pathogenic immunity. Latest study with high-resolution *in vivo* imaging proved that regulatory T cells were co-located with HSPS on the endosteal surface in the bone marrow after allogeneic bone marrow transplantation and provided immune privilege to the haematopoietic stem cell niche (Fujisaki J, 2011; Mercier F.E, 2012).

Notably, each cell type described was in close adjacent with one or more of the other cell types in bone marrow and worked in cohort to support HSC function *in vivo*. These results suggest that a single HSC can receive signalling instructions from multiple, distinct types of niche cells and HSCs may move among niches quite readily. One model of marrow haematopoietic cell regulation proposes that the entire bone marrow compartment should be visualized as a niche, with discrete areas and cellular elements serving distinct functions at different stages of haematopoietic development and differentiation (Ehninger A, 2011; Wang L.D, 2011; Ema H, 2012)

1.1.5 Coordination of intrinsic and extrinsic regulators

Accumulating evidence has shown that HSC fate decision is regulated co-ordinately by intrinsic and extrinsic cues. Through their receptors expressed in HSC, many extrinsic signals, such as cytokines and signalling pathway ligands, trigger a cascade of biochemical events and eventually result in the activation or suppression of target genes (Duncan A.W, 2005). On the other hand, the intrinsic regulators play critical roles in controlling the HSC interaction with the environment. Oncogene c-Myc is essential for proliferation of lineage-committed haematopoietic cells *in vivo* and can negatively regulate HSC quiescence by controlling N-cadherin and other adhesion molecules expression. Impaired differentiation of c-Myc-deficient HSCs is linked to their localization in the differentiation-preventative BM niche environment. (Wilson A, 2004). Rho GTPase Cdc42 maintains HSC quiescence and retains HSCs in the correct location in the BM niche by regulating the expression of key cell cycle regulators (including c-Myc and $p21^{Cip1}$) and cell adhesion molecules (such as β_1-integrin and N-cadherin) and the actin structure (Yang L, 2007**;** Cancelas J. A, 2009).

1.2 Nov

1.2.1 Nov and CCN family

NOV (Nephroblastoma overexpressed gene, *CCN3*) was first identified as a proto-oncogene in myeloblastosis-associated virus (MAV)-1-induced avian nephroblastoma, a model of Wilms tumor (Soret J, 1989; V Joliot, 1992). It is one of the three founding members of the CCN family of growth regulators which include *CCN1 (Cyr61)* and *CCN2 (CTGF)*. The CCN family of proteins are secreted extracellular matrix (ECM) associated proteins and are involved in a wide range of important functional pathways, including adhesion, mitogenesis, migration and chemotaxis, cell survival, differentiation, angiogenesis, chondrogenesis, tumourigenesis and wound healing (Holbourn K.P, 2008). This family of proteins share several common structural modules: a signal peptide for secretion, an insulin-like growth factor binding protein domain (IGFBP), Von Willebrand type C repeat (VWC), thrombospondin type I domain (TSP-1) and cysteine knot carboxyl terminal (CT) (Figure 1.3.) (Perbal B, 2001; Perbal B, 2004; McCallum L, 2009).

Latest study using small angle X-ray scattering technique revealed the 3D structure of Nov protein as a long elongated flexible molecule that is

extended and may act as a scaffold for binding and coordinating ligand partners (Figure 1.4.) (Holbourn K.P, 2011).

NOV protein has several isoforms lacking one or two of the basic modules which are found in many types of tissues and tumours (Lazar N, 2007). The full length NOV and its truncated isoforms are believed to have different biological functions (Bleau, A. M, 2007; Katsuki Y, 2008; McCallum L, 2009). For example, the amino-truncated variants of NOV but not the full length protein could be driven to the nucleus by the CT domain (Planque N, 2006). CT domain was also shown to associate with the epidermal growth factor-like repeats of Notch1 and activate the promoters of HES1 and HES5 which are the downstream transducers of Notch signaling (Sakamoto K, 2002).

1.2.2 Regulation and function of *Nov*

NOV is expressed in many tissues, including brain, lung, heart, kidney, liver, spleen, thymus and skeletal muscle (Liu C, 1999). Many reports suggested that Nov regulates cell proliferation, adhesion, migration, differentiation, apoptosis, and extracellular matrix production in a cell-dependent manner (Perbal B, 2001; Manara M.C, 2002; Vallacchi V, 2005).

In fibroblasts, 3T3 cells, treated with recombinant NOV protein, showed a dose-dependent increase in proliferation and an induction of tyrosine

phosphorylation of an unknown 221 kDa protein (Liu C, 1999). Knockdown Nov using small interfering RNA in primary liver cells or cell lines could enhance expression of profibrogenic genes and inhibit cell migration (Borkhan-Kamphorst E, 2012).

Melanoma cells, overexpressing *NOV* showed increased adhesion to ECM proteins, whereas inhibition of *NOV* expression decreased adhesion to laminin and vitronectin. Moreover, NOV secreted by melanoma cells acted as an adhesion matrix protein for melanoma cells themselves (Vallacchi, V, 2008).

In human sarcoma, NOV increases cell motility and MMP-13 and cyclooxygenase (COX) expression through integrin dependent pathway (Tzeng, H. E.2011; Huang C.Y, 2010). Nov promoter could be induced by p53 through a response element +47-+336 in the first intron, and as a result, Nov could be up-regulated by p53 expression (Bohlig L, 2008).

In breast cancer cells, NOV could bind to the cytoplasmic tail of the gap junction protein connexin43 (Cx43). Overexpression of *NOV* reduces growth and increases the activity of the small GTPase Rac1 and intercellular adhesion. (Sin, W. C., 2009)

In glioma cells, overexpression of Cx43 up regulated the expression of *NOV* which resulted in reduced growth rate (Gupta, N, 2001; Sin, W. C, 2008). At the stationary growth phase of glioma C6-Cx43H cells, NOV protein could

be observed in Cx43 gap junction plaques by immunofluorescence imaging (Sin, W. C., 2008).

1.2.3 Nov mutant transgenic mice

Several Nov transgenic mouse lines have been reported recently. The first Nov mutant mice (*Nov*^{3del}) were generated by replacing *Nov* exon 3(VWC domain) with a TK neomycin cassette which results in production of a barely detectable level of mutant NOV protein instead of full length NOV protein (Figure 1.5.) (Heath E, 2008). *Nov*^{3del} mutant mice exhibit several abnormalities including enlarged vertebrae, elongated long bones, enlarged and abnormal modelled endocardial cushions in heart and muscle atrophy. Primary embryo fibroblast (PEF) from *Nov*^{3del} mutant embryos showed enhanced chondrogenesis and osteogenesis (Heath E, 2008). Although the *Nov* knockout mice reported later showed no apparent skeletal abnormalities, there was a similar increase in osteoblast surface, bone formation and bone remodelling in older mice (Canalis E, 2010). The *Nov*^{12del} mutant mice were generated by replacing exon 1, 2 and part of exon 3 with a PGK-neo cassette. Analysis of *Nov*^{12del} mutant mice indicated the function of *Nov* in vascular homeostasis, especially on injury (Shimoyama T, 2010).

On the other hand, transgenic mice overexpressing Nov under the control of the human osteocalcin promoter had normal weight and exhibited a 35% decrease in femoral trabecular bone volume and trabecular cell number. In contrast to Nov^{3del} mice, there was a decrease in osteoblast number per area, but not per surface, indicating no actual change in osteoblast number (Canalis E, 2007).

1.2.4 Nov in HSC and leukaemia

NOV can be detected in human serum (Thibout H, 2003; Gellhaus A, 2007) and is expressed in haematopoietic cells at various stages during haematopoiesis. A micro array study comparing haematopoietic stem and progenitor cells with committed progenitors from human cord blood and bone marrow showed that *NOV* expression level decreases along with differentiation (Eckfeldt C.E, 2005). The function of *NOV* in HSC was reported recently in human cord blood where *NOV* was identified as a positive regulator of haematopoietic stem and progenitor cells and knockdown of *NOV* in HSC abrogates their function (Gupta R, 2007).
In mouse primary haematopoietic cells, *Nov* was found highly expressed in N-cadherin^{lo} HSCs which were proposed to be primed to respond to migratory cues and other regulatory signals (Haug J.S, 2008). *Nov* expression could be induced by GM-CSF treatment in GMP (Kimura A, 2009)

or by IL3 treatment in KLS through STAT5A/B which binds *Nov* promoter (Kimura A, 2010). In FDCPmix cells, a haematopoietic multipotent mouse progenitor cell line, *Nov* expression was down regulated during differentiation (Bruno, L.2004). Furthermore, ChIP-chip analysis of mouse ES cell–derived HSCs/HPCs for Hoxb4, a critical transcription factor of HSCs self-renewal, identified Nov as a target gene as well as Gfi1, Gata2, Runx1 (Ohshima M, 2011).

NOV has been related to leukaemia (McCallum L, 2006; McCallum L, 2009). Transfecting *NOV* into K562, a Chronic Myeloid Leukaemia (CML) cell line, inhibited proliferation, decreased clonogenic potential and enhanced apoptosis (McCallum L, 2009). Cells from CML patients responding to the tyrosine kinase inhibitor, imatinib, showed a decrease in BCR-ABL and increase in *NOV* expression. This correlation between BCR-ABL and *Nov* expression can also be observed in FDCPmix where *Nov* was down regulated as a direct consequence of BCR-ABL kinase activity (McCallum L, 2006). MicroRNA 130α/β has been identified as a target of BCR-ABL to down regulate expression of CCN3 in CML (Suresh S, 2011). A recent study showed a reduced mitogenic signaling in *NOV* overexpressing K562 at the phosphorylation levels of ERK and AKT. *NOV* overexpressing K562 cells also displayed increased adhesion to matrigel™ compared to K562 control where a similar increased expression of the alpha 6 and beta 4 integrins

were observed (McCallum L, 2012).

1.2.5 Mechanism of Nov function in HSC regulation and HSC niche

The study of *Nov* in haematopoiesis is just beginning. The function and its mechanisms of *Nov* in haematopoiesis remain largely unknown.

At the molecular level, knockdown of *NOV* expression (Novi) in human cord blood CD34+ cells resulted in down regulation of *Bmi1* and *Gfi1* which may explain the impaired HSC function. There was also an indication that *NOV* may be involved in the Notch signalling pathway as Nov*i* cells showed an impaired *Hes1* transcriptional response after addition of the Notch ligand Jagged1(Gupta R, 2007).

Lessons learned from other cell types, especially osteoblast, mesenchymal stem cells and endothelial cells present in the HSC niche, may shed light on the function of *Nov* in HSC and niche regulation (Table 1.1). *Nov* is expressed by osteoblasts in bone marrow and *Nov* expression inhibits osteoblast differentiation by binding to bone morphogenic protein-2 (BMP-2), preventing phosphorylation of SMAD proteins and simultaneously activating the Notch signalling pathway (Tokutaro Minamizato, 2007; Kawaki H, 2011; Ouellet V, 2012). In cultured osteoblast, treatment with Nov protein was shown to increase BMP4 expression and bone nodule formation.

Furthermore, monoclonal antibodies for α5β1 and αvβ5 integrins, and inhibitors of integrin-linked kinase (ILK), p38, and JNK, all inhibited Nov-induced bone nodule formation and BMP-4 up regulation of osteoblasts.(Tan T.W,2012) .

In osteogenic mesenchymal stem cells, Kusa-A1, Nov is shown inhibit osteogenic differentiation and cell proliferation; accompanied by up regulation of Hes/Hey, Notch downstream targets, and p21, a CDK inhibitor. Deletion of CT domain abrogated the regulation of Hes/Hey and p21 (Katsuki Y, 2008).

In a recent study, the endosteal niche populations in bone marrow were isolated and characterized for their HSC support activity. The endosteal CD45-TER119-CD31- population could be dissected into 3 populations using ALCAM and Sca1 antibodies: immature mesenchymal cell-enriched ALCAM-Sca-1+cells, osteoblast-enriched ALCAM+Sca-1-, and ALCAM-Sca-1- cells. All three populations were able to maintain the long term repopulation (LTR) activity of HSC *in vitro*. But, the osteoblast enriched ALCAM-Sca-1+ cells showed significantly greater potential for maintenance of LTR activity of HSCs. Interestingly, the immature mesenchymal cell-enriched ALCAM-Sca-1+cells showed reduced capacity to maintain HSC LTR activity after co-culture, in the meantime, these cells could increase the CFU frequency of HSC in the co-culture system. Gene

expression analysis by microarray showed that this immature mesenchymal cell-enriched population expressed higher level of growth factors, cytokines, chemokines and adhesion molecules known to be involved in the regulation of quiescence and proliferation of HSCs. Interestingly, Nov is highly expressed in this population compared to the other two. (Nakamura Y, 2010).

In endothelial cells, *Nov* has been shown to be a positive growth regulator and supports cell-adhesion, migration and survival, possibly through multiple cell surface receptors, including integrins $\alpha5\beta3$, $\alpha5\beta1$, $\alpha6\beta1$, and heparan sulfate proteoglycans (Lin C.G, 2003).

Taken together, these results indicate that Nov may also be involved in the regulation of HSC through niche. Accordingly, it has been hypothesized that NOV secreted by mesenchymal stromal cells may regulate the growth and differentiation of neighbouring osteoblasts and HSCs through Notch and BMP signalling pathways (Katsube K, 2009) (Figure 1.6.).

This model describes a possible functional mechanism of *Nov* in haematopoietic stem cells and indicates a role of *Nov* in the stem cell niche. Indeed, *Nov* expression level is higher in HSC-supportive stromal cells lines than those non-supportive stromal cells (Charbord P, 2005). *Nov* expression can also be up regulated in OP9 stromal cells as a result of direct contact with B-cell progenitors in culture (Zetterblad J, 2010).

However, the proposed model is incomplete as there are some fundamental elements missing:

1) In this model, the function of Nov in HSC is based on the observation of human cord blood. It has not been investigated for Nov function in adult HSCs yet. It is not clear whether the function of *Nov* in adult HSCs is the same as in cord blood HSCs. Other than their fetal developmental stage, HSCs derived from cord blood show distinctive cell division kinetics (da Silva CL, 2009) and reside in a very different microenvironment (Dao M.A, 2007). Umbilical cord is more highly oxygenated than the BM microenvironment, and there is lack of osteoblast cells which is a key cell component in bone marrow niche (Dao M.A, 2007). Therefore, to validate the model, it is necessary to examine the function of Nov in adult HSC.
2) In this proposed model, *Nov* is described as an extrinsic regulator only for HSC function. However accumulating evidence showed that *Nov* is also endogenously expressed in HSCs. In human cord blood CD34+ HSCs, knockdown of Nov resulted in the reduction of long term reconstitution activities of HSC. Therefore, in order to understand the role of *Nov* in HSC and niche, it is important to compare the function of endogenous *Nov* and how HSC response to *Nov* cue from outside.

3) As a protein expressed and possibly secreted by HSC and three key cell components in the niche, does *Nov* represent a bi-directional interaction between HSCs and their niche?

1.3 Aims of the thesis and project outline

The function of *Nov* in haematopoiesis is poorly understood and the mechanisms of *Nov* function in the haematopoietic system remains largely unknown. In this thesis, I aim to delineate the mechanism of *Nov* functions in mouse haematopoiesis using the following approaches:

1). Lentiviral based approach were deployed to modulate *Nov* expression in mouse haematopoietic stem and progenitors to understand the function of *Nov* and to identify its cellular targets during haematopoiesis.

2). The haematopoietic system of Nov^{3del} mutant mice was characterized in order to understand the function of *Nov* during haematopoiesis in homeostatic stage.

3). *Nov* function was examined in haematopoietic stem and progenitor cells' interaction with HSC microenvironment. Nov function was examined for cell adherence and migration with FDCPmix cells. HSC supportive stromal cells were manipulated for Nov expression and tested for their HSC supportive activity in co-culture.

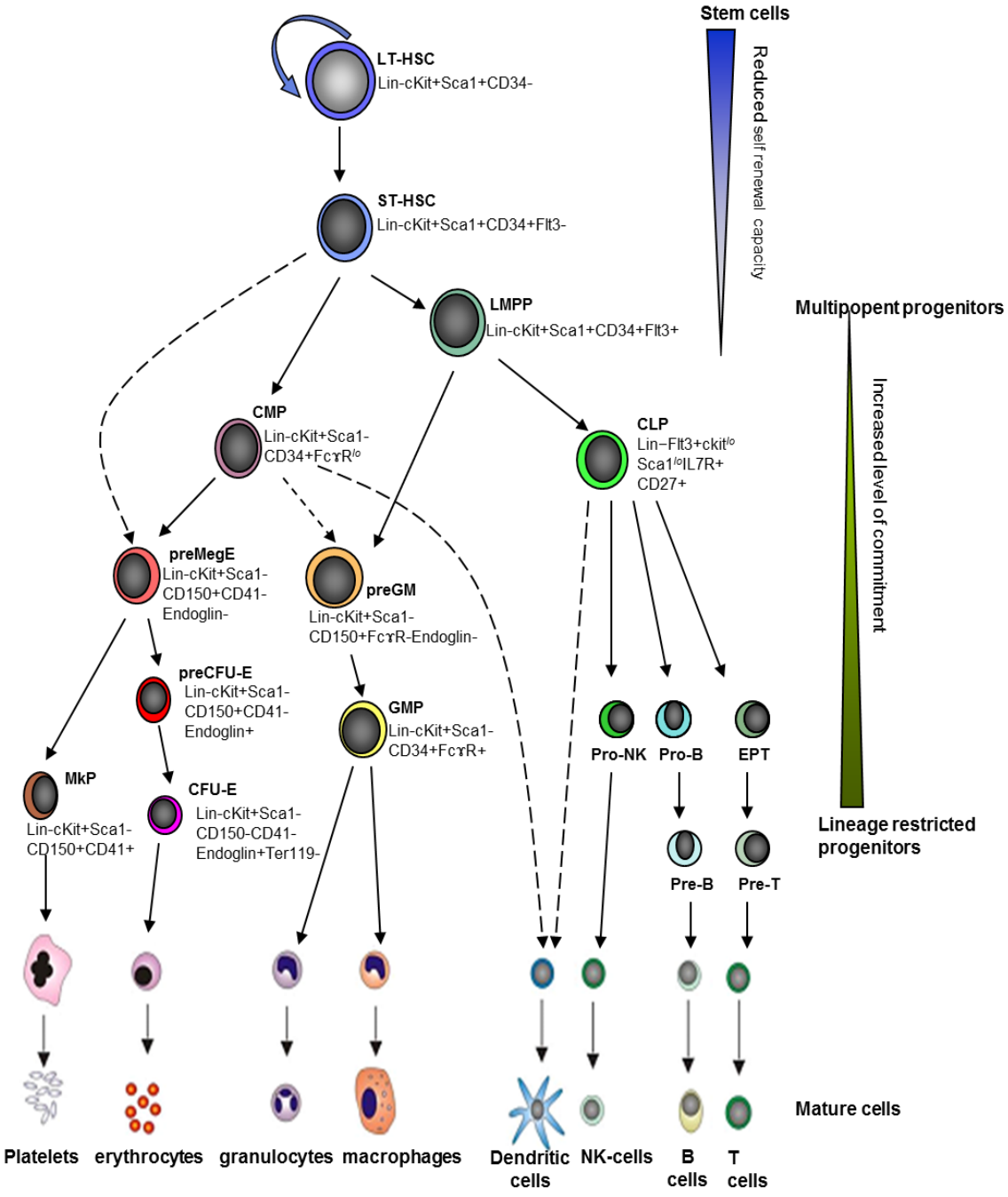


Figure.1.1: Road map of HSC differentiation to mature lineage cells: the classical model

In the classic model of the haematopoiesis, the HSC resides at the top of the hierarchy and is defined as the cell that has both the self-renewal capacity and the potential to give rise to all haematopoietic cell types. Throughout differentiation, HSCs gradually lose their self-renewal capacity and lineage potential as they commit to become functional cells of a certain lineage.

The green oval represents the primitive KLS (Lin−Sca-1+cKit+) “HSC” compartment, which can be divided into LT-HSC, ST-HSC and LMPP according to the timing of repopulation and lineage output in bone marrow reconstitution assays. In the classic model of haematopoiesis, the earliest fate decision downstream of HSC is the separation of common myeloid and common lymphoid commitment pathways, giving rise to CMP and CLP respectively. It is currently believed that restriction of erythroid lineage is the first step of HSC start to commit for differentiation. Recent evidence suggests that CMP may not constitute a single compartment and can be separated into pre-MegE and pre-GM progenitors. Dashed arrows represent differentiation pathway of which the intermediate precursors are yet to be identified. Surface markers for mouse HSC and myeloid progenitors are indicated.

KLS, lineage-, cKit+, Sca1+ cells; LT-HSC, long-term HSC; ST-HSC, short-term HSC; LMPP, lymphoid-primed multipotent progenitor; CLP, common lymphoid progenitor; CMP, common myeloid progenitor; preMegE, early lineage-restricted precursors for erythroid and megakaryocytic lineages; MkP, megakaryocyte progenitor population ; preCFU-E, early lineage-restricted precursors for erythroid; CFU-E colony-forming unit erythrocyte; preGM, early lineage-restricted precursors for the granulocyte/macrophage; GMP, granulocyte/macrophage progenitor; EPT, early T cell progenitor.

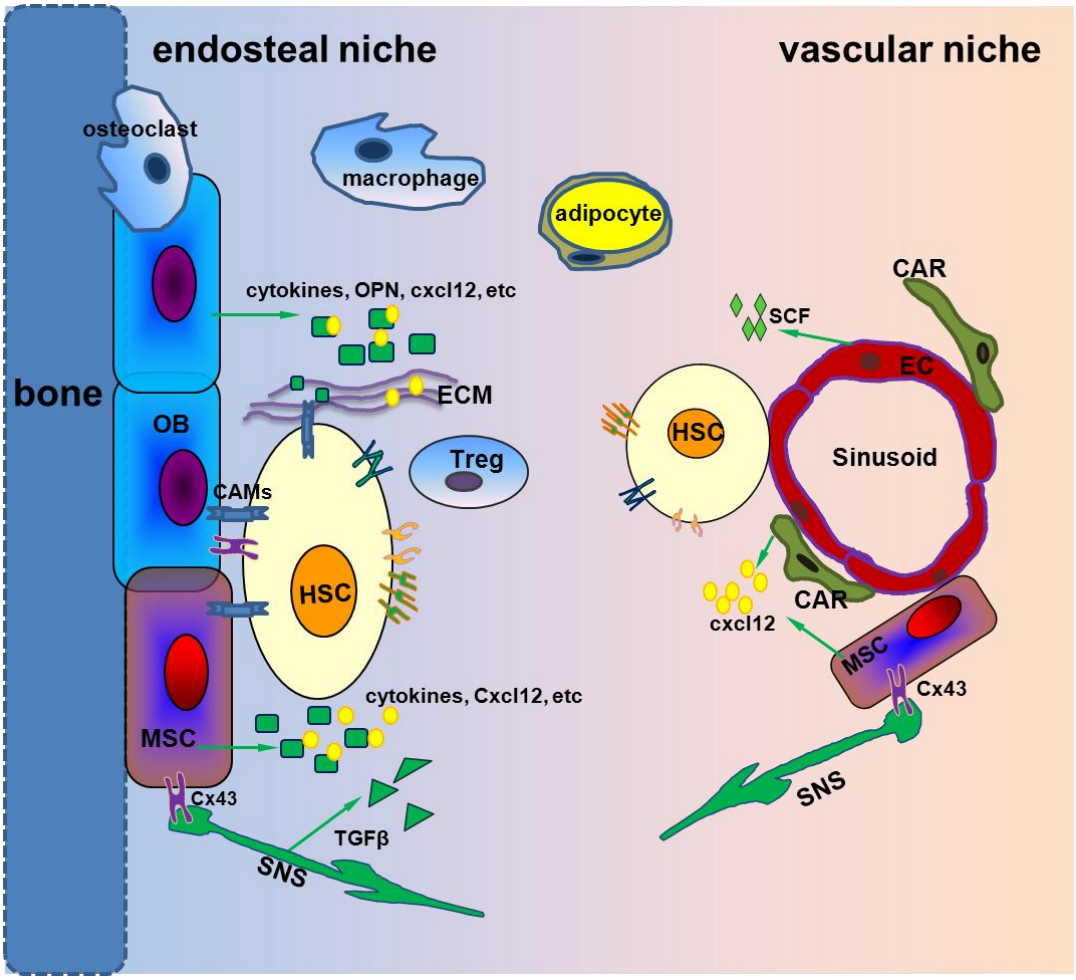


Figure.1.2: Schematic representation of the key compartments of the HSC niche in bone marrow

The HSC microenvironment or niche in bone marrow is made up of a complex of molecular and cellular structures. Two types of niches in bone marrow have been identified according to location in the bone as well as their key component cells and are believed to play different roles in HSC regulation. The endosteal niche, close to bone endosteal surface is important for HSC self-renewal and quiescence. The vascular niche, on the other hand, exists in the centre of bone marrow close to sinusoids, and is believed to regulate HSC expansion and differentiation (Kopp, H.G, 2005; Wilson A, 2006; Mendez-Ferrer S, 2010).

HSC, haematopoietic stem cell; OB, osteoblast; MSC, mesenchymal stem cells; EC, endothelial cells; CAR, CXCL12-abundant reticular cells; SNS, the

sympathetic nervous system; Treg, regulatory T cells; ECM , extracellular matrix ; OPN, osteopontin ; SCF , stem cell factor; CAM, Cell Adhesion Molecules

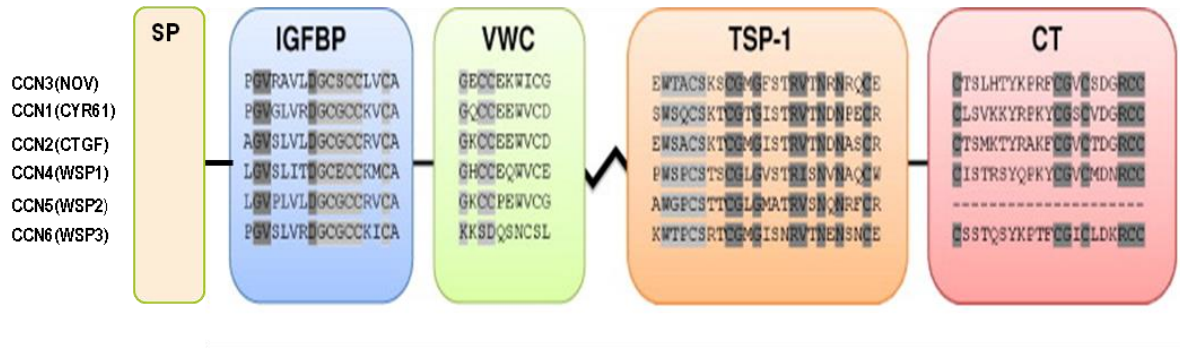


Figure.1. 3: Structure of the CCN protein family

CCN proteins are comprised of a signal peptide (SP) followed by four structurally distinct domains: insulin-like growth factor binding protein domain (IGFBP), von Willebrand type C repeat (VWC), thrombospondin type I domain (TSP-1) and cysteine-rich carboxyl terminal (CT). CCN proteins share 60% amino acid homology and contain highly conserved residues (dark grey) and sequences associated with domain function (light grey).

Adapted from L. McCallum, 2009.

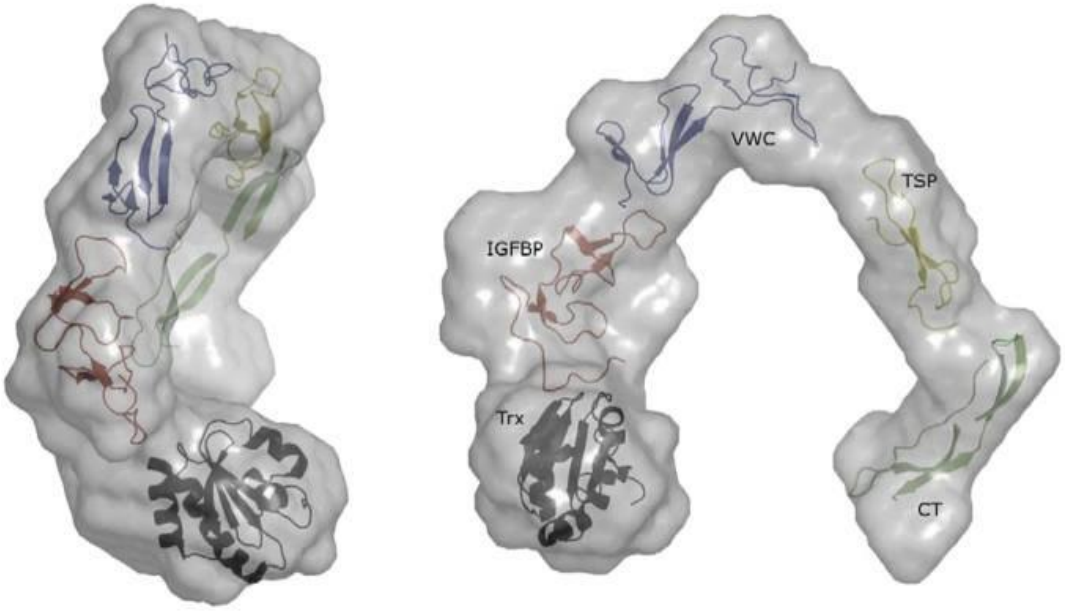


Figure.1.4: The 3D modular arrangement of Nov protein

The small angle x-ray scattering model revealed the molecular shape and possible general three-dimensional modular arrangement of Nov proteins in solution**:** long elongated flexible molecules that are extended and may act as a scaffold for binding and coordinating ligand partners. The protein was made with an N-terminal thioredoxin (Trx) to help with the formation of disulfide bonds. The domains are colored with the Trx tag in black, the IGFBP domain in red, the VWC domain in blue, the TSP domain in yellow, and the CT domain in green.

From Holbourn K P et al. J. Biol. Chem. 2011

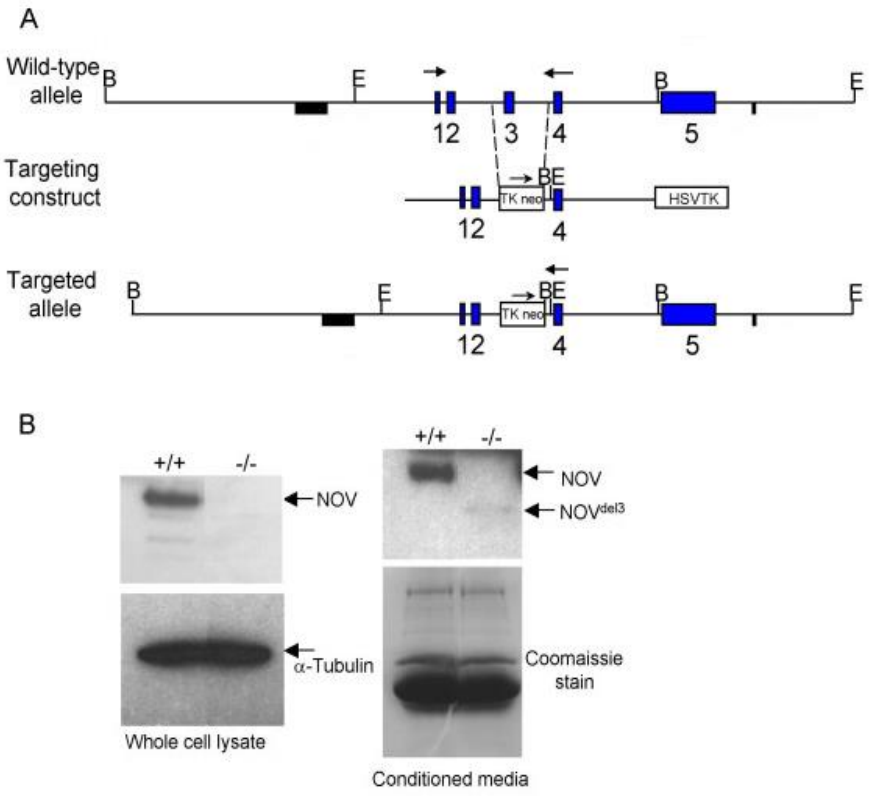


Figure.1.5: Strategy of making *Nov*^{3del} mutant mice and the expression level of *Nov*^{3del} mutant protein

A. Schematic diagram showing wild type and targeted *Nov* alleles, the targeting construct, and the positions of the primers used for genotyping. The TkneopolyA cassette replaces exon 3 in the targeted allele while the HSV TK cassette allows negative selection with Gancyclovir.

B. Western blotting of whole cell lysates and conditioned media from *Nov*^{3del} homozygous and wild type E13.5 primary embryonic fibroblast cells (PEF), using an anti-NOV antibody. Although NOV protein is readily detectable in wild type PEF whole cell lysates, no NOV protein can be detected in *Nov*^{3del} homozygous PEF. Conditioned medium from wild type PEF contains high levels

of secreted NOV, whereas that from *Nov*$^{3del-/-}$ PEF contains trace amounts of mutant NOV protein lacking the VWC domain.

Adapted from E. Heath et al. 2008

Table 1.1: The functions of *Nov* in key cellular components of bone marrow HSC niche

Cell type	Roles in HSC regulation and niche	Endogenous expression level of *Nov*	Functions of *Nov*	References
Osteoblast	express high levels of HSC maintenance factors; direct contact with HSC; important for HSC self-renewal	+	inhibit osteoblast differentiation and cell proliferation	Tokutaro Minamizato, 2007; Katsuki Y, 2008; Kawaki H, 2011; Ouellet V, 2012;
Mesenchymal stem cells	express high levels of HSC maintenance factors; direct contact with HSC; regulate HSC mobilization;	++	inhibit osteogenic differentiation and cell proliferation	Katsuki Y, 2008; Katayama Y, 2006; Méndez-Ferrer S, 2008; Nakamura Y, 2010
Osteoclast	HSPC mobilization and retention in niche; regulation of osteoblast for bone formation	?	suppresses osteoclast differentiation ; enhance osteoclastogenesis and bone resorption	Kollet, 2006; Winkler I.G, 2010; Lymperi S, 2010; Mansour A, 2012; Chow A, 2011Canalis E, 2010; Ouellet V, 2012
Endothelial	support the proliferation and differentiation of HSPC *in vitro* via production of various cytokines and via physical contact; SLAM+ HSCs were detected adjacent to sinusoid endothelial cells	+	positive growth regulator and support cell adhesion, migration	Rafii S, 1994; Rafii S, 1995; Lin C.G, 2003; Kiel M.J, 2005; Ding L, 2012

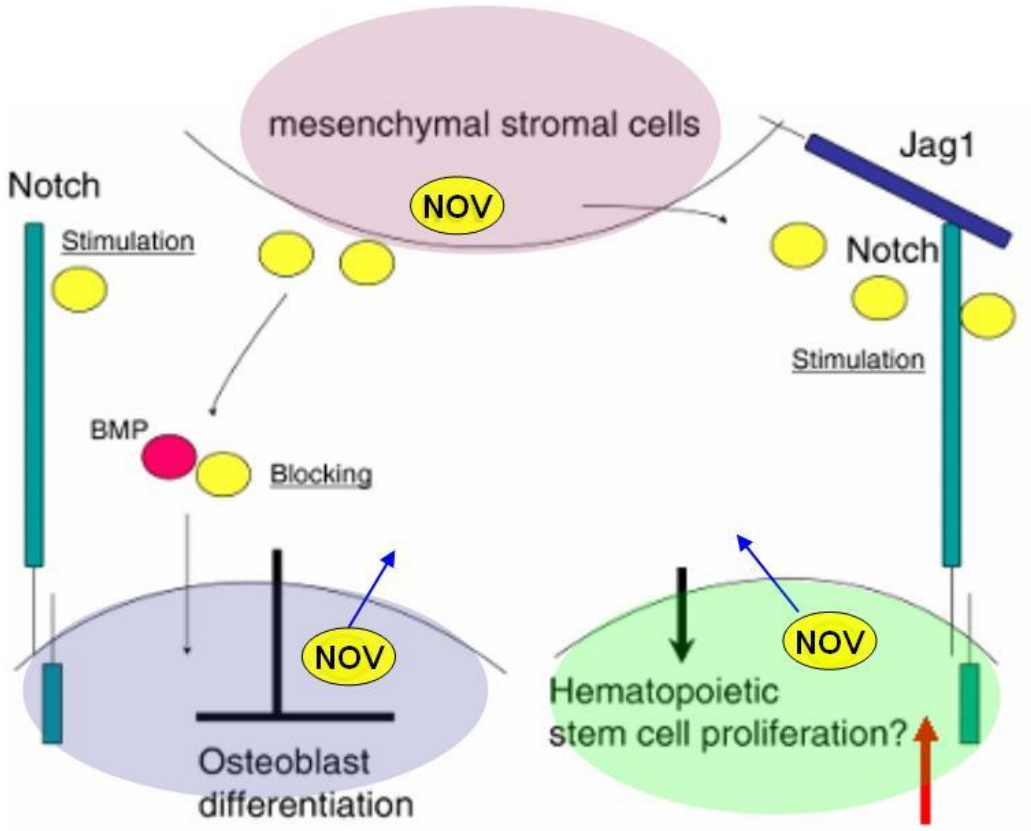


Figure.1.6: A hypothetical role of *Nov* in HSC and the bone marrow niche

In the original model, *Nov* (yellow) secreted by mesenchymal stromal cells regulates the growth and differentiation of neighbouring osteoblasts and HSCs through Notch and BMP signalling pathways. However there are some important elements missing from this model. Firstly, although it is clear that *Nov* negatively regulates osteoblast differentiation; its function in HSCs that reside in the bone marrow niche remains unexplored (red arrow). Secondly, *Nov* is also expressed and may be secreted by osteoblast and HSCs, as indicated by blue arrows. Does *Nov* affect HSC function as an intrinsic regulator or an extrinsic signal, or both?

Finally, as a secreted protein produced by three key components in bone marrow niche, could *Nov* represent bi-direction interaction between HSC and their niche?

Modified from Katsube K., 2009.

CHAPTER2.

MATERIALS AND METHODS

Mice

C57BL/6 (CD45.2) and B6SJLCD45 (CD45.1) were purchased from and kept at the BioMedical Service in John Radcliffe Hospital (BMS), or at Cancer Research UK London Research Institute (Lincoln Inn field).

Nov^{3del} mutant mice (129 backgrounds, CD45.2+) were kindly provided by Dr. Boulter. A (Cambridge University). The re-derivation was performed by Harlan to achieve the Specific Pathogen Free (SPF) health status before the mice were transferred to the BMS.

Animal care and experiment procedures were strictly in accordance with the Guidelines of University of Oxford and London Research Institute (Lincoln Inn field).

Lethal irradiation for bone marrow transplantation was performed according to the regulation of our Project License. Whole body irradiation with maximum dose of 10 Gy was split into two equal fractions with at least 4 hours interval between them. The mice were given antibiotic water one week before the irradiation in order to minimize the possible adverse effects and infection caused by the irradiation. The mice would be humanely killed using a schedule 1 method if severe side effects were observed, such as acute considerable body weight loss.

Cell preparation and flow cytometry analysis

Red blood cell lysis

Peripheral blood, or spleen or bone marrow cells were treated with ACK buffer (0.15M NH_4Cl, 1.0mM $KHCO_3$, and 0.1mM EDTA) for red blood cells lysis before antibody staining or microbeads incubation.

Cell enrichment

Before cell sorts for KLS or progenitor populations, bone marrow cells were enriched by lineage depletion or cKit enrichment using MACS® Cell Separation (Miltenyi Biotec): either MACS magnetic column or autoMACS following the manufacturer's recommendations. The staining buffer for antibodies were PBS/10%FBS (Fetal bovine serum). The MACS buffer used for microbeads incubation was PBS/0.5% FBS.

Lineage depletion

For lineage depletion, cells were incubated with lineage antibody cocktails at 1 in 100 dilution, including: B220, CD3, CD4, CD8, Mac1, Gr1 and Ter119.

If purified antibodies were used, 100µl 10^8 cells were incubated with 10µl Goat-anti-rat IgG microbeads for 15min at 4°C. After washing with PBS, a

maximum of 10^9 cells were applied onto a MACS LD column. The lineage depleted cells were later identified with Goat anti-rat F(ab')2 IgG(H+L) Tricolor/PECY5 antibody by FACS.

If biotin labelled antibodies were used, 100µl 10^8 cells were incubated with 10µl anti-biotin microbeads for 15min at 4°C. After washing with PBS, all cells were applied onto auto MACS machine. The lineage depleted cells were later identified with anti-biotin antibody by FACS.

cKit enrichment

cKit enrichment was performed without red blood cell lysis. Total bone marrow cells were harvested and counted. Up to 10^8 cells were incubated in 100µl with 2.5µl cKit microbeads at 4°C for 20min. After washing with PBS, maximum of 10^9 cells were applied to a MACS LS column. cKit enriched cells were later identified with cKit antibody.

Cell staining for FACS analysis or cell sorts

The instruments used for FACS analysis or cell sorts are listed in Table 2.1. All antibodies used for FACS were titrated before use to optimise the dilution and incubation time. The staining procedures were performed in PBS/10%FBS on ice avoiding direct light. The appropriate unstained, single color controls and isotype controls were used for compensation and

gate definition. Table 2.2 lists all the antibodies used in this thesis and their applications. Information on fluorochromes conjugated to antibodies is listed in Table 2.3.

Representative histograms for KLS, Akashi progenitor dissection and Pronk progenitor dissection are shown in Figure 2.1.A with the gating strategy (Akashi K, 2000; Adolfsson J, 2005; Pronk C.J, 2007). The lineage distribution in bone marrow is showed in Figure 2.1.B. for the staining combination and gate definition. In transplantation experiments, the donor+ and GFP+ cells were gated before lineage analysis (Figure 2.1.C).

Complete blood count (CBC) test

Fresh peripheral blood was evaluated for *Nov*^{3del} mutant mice. The parameters were assessed using an automated instrument (Hemavet FS950; Drew Scientific) according to the manufacturer's recommendations.

Bone marrow reconstitution assay

2×10^4 virally transduced KLS from C57BL6 (CD45.2) mice were harvested, mixed with 2×10^5 fresh competitor bone marrow cells obtained from congenic B6SJL (CD45.1) mice, and were injected via the tail vein into lethally-irradiated (10 Gy) CD45.1 recipient mice.

2×10^6 freshly prepared *Nov*^{3del} (CD45.2$^+$) bone marrow cells were mixed 1:1 with B6SJL (CD45.1) competitor bone marrow and transplanted into lethally-irradiated CD45.1 recipients.

Peripheral blood was collected at 1 month, 2 month and 4 months to determine engraftment efficiency and lineage reconstitution. Engrafted cells detected in peripheral blood at 1 month and 2 month represent the progenitor and short-term stem cells from donors. By 4 months, engrafted multi-lineages cells are mainly derived from long-term stem cells of donor (Yang L. 2005). At the end of the 4th month, recipient animals were sacrificed and analysed for reconstitution in bone marrow and spleen. In some experiments, thymus were collected and analysed for T cell development.

For secondary transplant experiments, whole bone marrow from primary recipient mice were harvested and counted for nucleated cells. Around $5\text{-}6\times10^6$ total nucleated cells were injected via the tail vein of lethally-irradiated recipient (B6SJLCD45.1). Peripheral blood was collected at 1 month, 2 month and 4 months to analyse engraftment efficiency and lineage reconstitution.

Cell culture

Establishment of bone marrow stroma

Flushed or crushed mouse bone marrow was resuspended into single cells without red cell lysis and cultured in MyeloCult™ M5300 with 10^{-6} M hydrocortisone. The culture was incubated at 33°C with half-medium changes weekly for up to three weeks or until an adherent layer has established.

For the CAFC assay, stromal cells were trypsinized and irradiated at 15Gy before being plated into 96-well plates at 10^6 cells per plate in M5300 medium.

To test the stroma function after manipulating *Nov* expression, confluent stromal cells were split the one day before the transduction of lentivirus. The cells were left to grow in M5300 for another 6-7 days until confluent. GFP+ cells were sorted and plated either in 24 wells plate at 10^5 cells per well for migration assay or in 96 wells plate at 10^4 cells per well for KLS co-culture. The cultures were kept in M5300 with hydrocortisone and were ready to be used within 7 days.

Culture of cell lines

K562 cells (Human Chronic Myelogenous Leukaemia) were cultured in RPMI 1640 medium (Gibco) supplemented with 10% FBS. The cells were fed twice a week.

293T cells (Human Embryonic Kidney 293 cells that contain the SV40 Large T-antigen) were cultured with DMEM (Dulbecco's Modified Eagle Medium, Gibco) supplied with 10%FBS. Cells were routinely split every 2-3 days.

FDCPmix (Factor-Dependent Cell Paterson-mix) is a multipotent cell line of haematopoietic stem cells obtained by long-term mouse bone marrow culture. FDCPmix were cultured with Fischer's medium (Gibco) supplied with 20% horse serum (HS) and 2% mIL3 conditioned medium. Both horse serum and IL3 conditioned medium were batch tested before use. SFEM (StemSpan™ Serum-Free Expansion Medium, STEMCELL Technologies) was used for FDCPmix serum free culture supplied with 10ng/ml recombinant mIL3. Cells were split every 3 or 4 days at 3-5×10^4/ml into fresh medium.

In vitro analysis of HSPC function

Cell proliferation assay

To analyse the effects of manipulating Nov expression on HSC/HPC cell growth, cells transduced with either CSGW-mNov virus or LLX-Novi virus were examined for GFP expression 2 days after transduction. In some experiments, GFP+ cells were purified by FACS sorting. Cells were further cultured in expansion or differentiation conditions for another 6-14 days. Cell growth was determined by viable cell counts and GFP+ percentage as checked by FACS.

CAFC assay

The Cobblestone-Area-Forming Cell (CAFC) assay permits determination of frequencies of haematopoietic cells with proliferation potential at limiting dilution *in vitro* (Ploemache R.E, 1989; de Haan G, 2000; Olesen G, 2001). Testing bone marrow cells were plated in five serial dilutions from 10^5 to 6,250 cells each well on pre-irradiated stroma in 96-well plates. For transduced KLS cells, cell density and dilutions were adjusted according to total GFP+ cell number collected. Each dilution was plated in 10 replicate wells. Cells were kept in MyeloCult™ M5300 with half medium changed weekly. After 5 weeks, individual wells were evaluated for the presence of

a cobblestone area. Only wells containing clusters of at least ⩾3 cells growing underneath the stroma were scored as positive. CAFC frequency was then calculated based on the frequencies of negative wells per test cell dilution using Poisson statistics (L-Calc software, Stem Cell Technologies).

CFC assay

Haematopoietic progenitors that are committed to differentiating into a limited number of cell lineages can be detected by the colony forming cell (CFC) assay. Test cells were plated in methylcellulose-based medium to allow individual haematopoietic progenitors to form a discrete colony which contains mature progeny cells. Colonies were scored after 9-14 days. M3234 supplemented with cytokine cocktails of 10ng/ml rmIL3, 10ng/ml rmIL11, 100ng/ml rmSCF, 10ng/ml rmGM-CSF, 10ng/ml rmTPO and 10U/ml hEPO was used for primary cell populations. M3234 supplemented with 10ng/ml rmIL3, 100ng/ml rmSCF and 10U/ml hEPO was used for FDCPmix. M3434 adding 10ng/ml rmTPO was used for whole bone marrow cells. Colony types were scored as described below: CFU-MIX, colony forming unit granulocyte, erythrocyte, monocyte/macrophage, megakaryocyte; CFU-GM, colony forming unit granulocyte, monocyte; CFU-M, colony forming unit monocyte; CFU-G, colony forming unit granulocyte; and BFU/CFU-MegE, burst-forming unit erythrocyte and

colony forming unit megakaryocyte and erythrocyte. Representative colony morphology is shown in Figure 2.2.

For replating experiments, the cells were harvested from the whole dish after colony scoring, and were washed with PBS twice. Cells were counted and plated again into new methylcellulose-based medium.

BrdU cell cycle analysis

The immunofluorescent staining of incorporated bromodeoxyuridine (BrdU) and 7-amino-actinomycin D (7-AAD) that binds to total DNA were used to define cell cycle position (i.e., G0/G1, S, and G2/M phases). APC BrdU Flow Kit (BD Pharmingen™) was used following the manufacturer's protocol.

Ki67 cycle analysis

The Ki-67 protein (also known as MKI67) is a cellular marker for proliferation which is present during all active phases of the cell cycle (G_1, S, G_2, and mitosis), but is absent from resting cells (G_0). Ki67 PE kit (BD Pharmingen™) was used to determine the cell cycle position to replace BrdU assay for primary cells culture. The cells were prepared according to the manufacturer's protocol.

Annexin V apoptosis detection

Annexin V (BD Pharmingen™) that binds membrane phospholipid phosphatidylserine (PS) was used to detect the early apoptosis signal following the manufacturer's protocol. DNA stains Hoechst33258 (pentahydrate (bis-benzimide)) was added to the cells at a final concentration of 5μg/ml at the end of staining to detect dead cells within the culture.

Cell migration assay

Transwell inserts (Costar, 5.0um polycarbonate membrane, 6.5mm inserts) were used for cell migration assay according to the manufacturers' instruction. Briefly, fresh medium were first added to the multiple well plate with/without confluent growing stromal cells. Then the Transwell inserts were placed into the wells, and medium added to the inside compartment of the transwell insert. The plates with transwell insert and medium were either incubated for overnight or used straight for testing cell migration. 2×10^5 FDCPmix cells were applied onto the top of the transwell inserts and incubated for 3-4 hours in 37°C with 5% CO_2 for the cells to migrate through pores to the bottom wells. Cells from both top and bottom of the well were harvested and scored by Trypan Blue viable counts. The

migration rate was calculated as the percentage of the migrated cells at bottom versus the total cell number tested.

Preparation of lentivirus and lentiviral transduction

Production of high titre lentivirus

Lentiviruses pseudotyped with the vesicular stomatitis virus G (VSVG) protein were packaged by transient transfection of 293T cells with FuGene6 (Roche) following the manufacturer's instructions, with modifications. Briefly, 80-90% confluent 293T cells in T75 flask fed with 8ml fresh medium were co-transfected with the plasmids encoding vector components (3rd Generation Packaging Systems) in the presence of 25µl Fugene6. Plasmid mixture was resuspened in 19.3µl TE before adding to Fugene6, containing:

1µg pMDLg/pRRE	encodes Gag and Pol (not Tat)
1µg pRSVrev	encodes only Rev
1µg pMD2-G(VSV-G)	encodes VSVG
2µg vector of interest	

The medium was changed the following morning and the cells were cultured for an additional 48 hours prior to virus collection. Viral stocks were concentrated by ultracentrifugation at 22,000g for 2-4 hours at 4°C.

Titration of lentivirus

Virus titration was performed on 293T cells followed by FACS analysis. Briefly, 10^5 293T cells were plated per well of a 24-well plate, and left for 2-4 hours to adhere. Then 0.01, 0.1, and 1 µl of freshly prepared or thawed lentiviral stock were added to each well. 48 hours later, cells were trypsinised from the wells, and washed with PBS 3 times to remove live viral particles. Cells were then FACS analysed to determine the percentage of GFP+ cells. The viral titre was calculated from the viral dose which provided around 5-15%GFP+ cells, using the formula:

Viral particles/ml = (%GFP+ cells x 10^5) ÷ volume of virus added (µl) x 1000

Lentiviral transduction

Viral transduction was performed at a viral multiplicity of infection (MOI) of 10-200. Freshly sorted primary cells or cell lines were incubated overnight in their normal conditions with virus and were washed with PBS for 3 times before the next step

General molecular biology techniques

Bacteria transformation and clone selection

Bacterial strains used for cloning were *E. coli*: Subcloning Efficiency™ DH5α™ Chemically Competent Cells and MAX Efficiency® Stbl2™ Chemically Competent Cells (Invitrogen). Bacterial transformation was performed according to manufacturer's instructions. All plasmid vectors used contained an Ampicillin resistance cassette for positive selection. Bacterial clone selection was performed by growing transformed bacteria overnight at 37 °C on LB (Luria-Bertani medium) agar plates containing 100µg/ml Ampicillin.

For expansion of bacterial clones, freshly picked clones were added to 5ml, 100ml or 250ml (mini, midi or maxi DNA preparation sizes) of LB broth containing 100µg/ml of Ampicillin and incubated for 16-20 hours at 37°C with shaking .

Plasmids extraction and DNA purification

For the extraction of plasmid DNA, FastPlasmid Mini Kit (Eppendorf), HiSpeed Plasmid Midi Kit (Qiagen) and HiSpeed or EndoFree Plasmid Maxi Kits (Qiagen) were used according to the culture volumes. DNA

concentration and purity was determined by NanoDrop 1000 Spectrophotometer (Thermo Scientific).

For the purification of DNA from PCR and gel bands between enzymatic steps, the GFX PCR DNA and Gel Band Purification Kit (GE Healthcare) were used following the manufacturer's instructions.

Cloning and ligation for overexpression constructs

For overexpression of Nov, full length mouse *Nov* (*mNov*) was amplified from cDNA of FDCPmix cells. Primers were designed according to the sequence of *mNov* mRNA (NCBI: NM_010930) with added FLAG tag at C-terminus (mNov) or N- terminus (mNovB).

The cloning primers are listed below:

mNov: BamHI-Kozak-*mNov*-FLAG

Forward: 5' ACGT GGA TCC GCC ACC ATG AGC CTC TTC CTG CGA AAG 3'

Reverse: 5' ACGT GGA TCC TCA TCA GGG GGG ATC TTT GTC ATC GTC GTC CTT GTA GTC CAT AAT TTC TCC TCT GCT TGT 3'

mNovB: BamHI-Kozak-FLAG –*mNov*

Forward: 5' ACGT GGA TCC GCC ACC ATG GAC TAC AAG GAC GAC GAT GAC AAA GAT CCT CCT ATG AGC CTC TTC CTG CGA AAG

Reverse: 5' ACGT GGA TCC TCA TTA AAT TTC TCC TCT GCT TGT

PCR product was first cloned into pGEM T-easy vector (Promega) according to manufacturer's instructions. The insert was recovered from T-easy vector by restriction digestion with BamHI, and was then sub-cloned into a lentiviral expression construct *pHR-SIN-CSGW-IRES-emGFP*(CSI). The CSI vector was obtained from Enver lab general plasmids stock. CSI vector was digested with BamHI at 37°C for overnight. Purified vector backbone was dephosphorylated (calf intestine alkaline phosphatase – CIAP, NEB or Fermentas) before ligation in order to minimize self-ligation in the reaction. The ligation of insert DNA with backbone vector was performed with T4 DNA ligase (NEB or Fermentas), following manufacturer's protocols.

Constructs for gene expression knockdown

Short-hairpin RNAs (shRNA) directed at *mNov* (NCBI: NM_010930) were designed according to the algorithms available at http://www.rockefeller.edu/labheads/tuschl/sirna.html by identifying targets with the sequence AAG(N)18TT. The target sequence was subjected to BLAST analysis with no near full-length or in-common homologies to other known transcripts.

LVTHM oligos:

Upper:

5’-cgcggtGCGAGAATTGCACTAGCTTGTTCAAGAGAACAAGCTAGTGC

AATTCTCGTTTTTTgaattc-3’

Lower:

5’-cggaattcAAAAAACGAGAATTGCACTAGCTTGTTCTCTTGAACAAGCT

AGTGCAATTCTCGCac-3’

LLX

Upper:

5’-tCGAGAATTGCACTAGCTTGTTCAAGAGACAAGCTAGTGCAATTCTC

GTTTTTTc-3’

Lower:

5’-tcgagAAAAAACGAGAATTGCACTAGCTTGTCTCTTGAACAAGCTAGT

GCAATTCTCGa-3’

The synthesized sense and antisense strands were annealed in OAN annealing buffer at 100μM concentration under the following condition:

95°C, 4min,

70°C, 10min,

69°C, 1min,

68°C, 1min,

then gradual temperature reduction at 1°C per minute until 4°C,

final hold step at 4°C for 10min.

OAN annealing buffer:

10mM Tris-HCl (pH7.5)

100mNNaCl

1mM EDTA

In DEPC treated H2O

The annealed product includes either MluI/ClaI or XhoI compatible sequence overhang for cloning purposes with LVTHM or LLX vector. The ligation to enzyme digested and non-dephosphorylated LVTHM or LLX lentiviral backbone was performed overnight at room temperature and used a ≥500-fold molar excess of insert.

Recombinant clones were identified on the basis of product size by restriction digestion.

DNA sequencing

The inserted elements of vector constructs were sequenced before packaging for viral transduction. The sequencing services were provided by the sequencing team at WIMM or by Source Bioscience Cambridge UK. Primers used for sequencing were as followed:

CSI-mNov overexpressing construct:

SFFV-F: 5’-TGCTTCTCGCTTCTGTTCG-3’

IRES-R: 5’-ATAGACAAACGCACACCG-3’

LVTHM-Novi knockdown construct:

LVTHM-F: 5'-GTGCGCCCTGGCAGGAAGATG-3'

LVTHM-R: 5'-TCTGAGCCTGGGAGCTCTCTGGCTAACTAGG-3'

LLX-Novi knockdown construct:

Lenti-lox3.7-F: 5'-CAGTGCAGGGGAAAGAATAGTAGAC-3'

Genomic DNA extraction and genotyping PCR for *Nov*^{3del} transgenic mice

Mouse ear notch samples were incubated with 550µl digestion buffer and 30µl proteinase K (10 mg/ml stock) at 55°C for overnight followed by 5 minutes treatment at 70°C to inactivate proteinase K. The digested samples were centrifuged at 13000rpm for 5-10 minutes to get rid of insolvable fur and dust. The clear supernatant was transferred into a new tube and an equal volume of phenol/chloroform/isoamyl alcohol (25:24:1) was added. The mixture was shook by hand but not vortex. The samples were spun at the top speed for 10minutes and the aqueous phase transferred to a new tube. DNA was precipitated with 1 ml ethanol at room temperature for 10 minutes and spun at 13000rpm for 5 minutes. DNA pellet was washed with 70% ethanol and air dried for 5-10 minutes at room temperature. DNA was resuspended in 100µl TE and incubated at 55°C for 10 minutes to facilitate dissolution. Genomic DNA samples were stored at 4°C before use.

Digestion Buffer (100 ml)

1 ml, 1M TRIS, pH 7.8 (final 10 mM)

1 ml, 500 mM EDTA (final 5 mM)

10 ml, 10% SDS (final 1%)

20 ml, 1.5 M NaOAc (final 0.3 M)

67 ml ddH20

The PCR primers and programs were specifically designed by our collaborator who made the *Nov*^{3del} mutant mice.

Primer pairs of Neo86 and Ex4R using PCR program DT1 will identify a 700bp band for the mutant deletion. Primer pairs of Ex3.1 and Ex4R using PCR program CB5 will give a 1.2kb band for the normal allele

Neo86 5' GGACGAAGAGCATCAGGGGCTCGC 3'

Nov Ex4R 5' CACACTGGCGATTCCTGTTG 3'

Nov Ex3.1 5' GAGTGCTGCGAAAAGTGGAC 3'

Program DT1

Step Number	Temp (°C)	Time (min)
1	96	1
2	94	1
3	62	1
4	72	1
Repeat steps 2-4 for 35 times		
5	4	hold

Programme CB5

Step Number	Temp (°C)	Time
1	95	5 min
2	93	30 sec
3	65	50 sec
4	70	6 min
Repeat steps 2-4 for 3 times		
5	93	30 sec
6	64	50 sec
7	70	6 min
8	93	30 sec
9	63	50 sec
10	70	6 min
11	93	30 sec
12	62	50 sec
13	70	6 min
14	93	30 sec
15	61	50 sec
16	70	6 min
17	93	30 sec
18	60	50 sec
19	70	6 min
Repeat steps 17-19 for 29 times		
20	4	hold

Gene expression analysis

Total RNA extraction

Cell pellets were resuspended and homogenised in Trizol reagent (Invitrogen) and total RNA was isolated following the manufacturer's protocol. RNA pellets were dissolved in DEPC-treated water and concentrations determined by NanoDrop 1000 Spectrophotometer (Thermo Scientific).

Quantitative RT-PCR analysis

Equivalent amounts of total RNA from test and control samples were DNase treated (RNase-free DNase, Promega) and reverse transcribed using Superscript II and random primers (250ng/reaction), according to manufacturer's protocols. The cDNA samples were then analysed using either inventoried Taqman gene expression assays (Applied Biosystems) or SYBR Green master mix (Qiagen) in ABI Prism Sequence Detector Systems 7000 (Applied Biosystems). Primers used for SYBR Green assays were designed using Roche ProbeFinder online service. The sequences of those primers were listed in the table2.4.

Western blots

Cell pellets were lysed in RIPA buffer (150 mM NaCl, 1.0% Triton X-100, 0.5% Na Deoxycholate, 0.1% SDS, 50 mM Tris HCl, pH 8.0) on ice for 30 minutes, followed by centrifugation at 12000g for 20 minutes at 4°C. Clear supernatants were removed to a fresh tube and stored at -80°C. Supernatants from K562 cells were taken directly from culture and stored in -80°C. All samples were then mixed 1:4 with 4× NuPAGE loading buffer (Invitrogen) and denatured by heating at 95°C for 2-4 minutes before loading. Lanes were loaded with approximate cell equivalents onto Bis-Tris

4-12% NuPAGE gel and run in MES running buffer. Proteins were transferred to pre-equilibrated Novex membrane using a wet transfer system (transfer buffer: 192 mM glycine, 25mM Tris HCl pH 8.0, 0.0375% SDS, 20% methanol). Membranes were blocked in TBS/0.05% Tween/5% fat-free milk and incubated with anti-Nov (CCN3) antibody (R&D) or anti β-tublin antibody (Santa Cruz) followed by HPR(horse radish peroxides)-conjugated secondary antibody. Protein binding was detected by ECL (Enhanced chemiluminescence) detection system (GE Healthcare).

Statistical analysis

Significance of differences between groups was determined using a two-tailed *t*-test. Significance was achieved at value $p<0.05$.

Table 2.1. FACS instruments configurations

Instrument	**laser wavelength**	**laser power**
CyAn ADP Flow Cytometer	Violet 413nm	25mW
	Blue 488nm	25mW
	Red 638nm	60mW
MOFLO sorter	Violet 413nm	100mW
	Blue 488nm	100mW
	Red 638nm	40mW
Gallios Flow Cytometer	Violet 405nm	40mW
	Blue 488nm	22mW
	Red 638nm	25mW

Table 2.2. Antibodies used in FACS analysis and their applications

Antibody	Clone	Supplier	Catalogue No.	Application	Dilution
B220 APC	RA3-6B2	eBioscience	17-0452-83	peripheral blood analysis	1 in 100
B220 biotin	RA3-6B2	eBioscience	13-0452-85	lineage cocktail for BM HSPC staining	1 in 100
B220 PE/Cy5	RA3-6B2	Biolegend	103210	lineage cocktail for BM HSPC staining	1 in 100 or 1 in 300 for lineage cocktail
B220 purified	RA3-6B2	Biolegend	16-0452-85	lineage cocktail for BM HSPC staining	1 in 100
CD105 PE	MJ7/18	eBioscience	12-1051-82	BM progenitor staining	1 in 100
CD11b(MAC1) APC	M1/70	eBioscience	17-0112-83	peripheral blood analysis	1 in 100
CD11b(MAC1) biotin	M1/70	eBioscience	13-0112-85	lineage cocktail for BM HSPC staining	1 in 100
CD11b(MAC1) PE/Cy5	M1/70	Biolegend	101210	lineage cocktail for BM HSPC staining	1 in 100 or 1 in 300 for lineage cocktail
CD11b(MAC1) purified	M1/70	eBioscience	16-0112-85	lineage cocktail for BM HSPC staining	1 in 100
CD150 APC	TC15-12F12.2	Biolegend	115910	BM HSPC staining	1 in 30
CD16/CD32 (FC Receptor block) biotin	93	eBioscience	13-0161-82	lineage cocktail for BM HSPC staining	1 in 100
CD16/CD32 (FC Receptor block) PE	2.4G2	BD Pharmingen	553145	BM progenitor staining	1 in 100
CD16/CD32 (FC Receptor block) PE/Cy7	93	eBioscience	25-0161-81	BM progenitor staining	1 in 100
CD16/CD32 (FC Receptor block) purified	2.4G2	BD Pharmingen	553142	lineage cocktail for BM HSPC staining	1 in 100
CD25 APC	3C7	Biolegend	101910	thymus lineage	1 in 100
CD31 APC	390	eBioscience	17-031-80	BM endothelial staining	1 in 100
CD31 PE	MEC13.3	Biolegend	102508	BM endothelial staining	1 in 100
CD34 -biotin	MFC14.7	Biolegend	119304	BM HSPC staining	1 in 100
CD34 eFluor660(APC)	RAM34	eBioscience	50-0341-82	BM HSPC staining	1 in 100

Table2.2. Antibodies used in FACS analysis and their applications: continued

Antibody	Clone	Supplier	Catalogue No.	Application	Dilution
CD34 FITC	RAM34	eBioscience	11-0341-85	BM HSPC staining	1 in 20
CD3e biotin	145-2C11	eBioscience	36-0031-85	lineage cocktail for BM HSPC staining	1 in 100
CD3e PE	eBio500A2	eBioscience	12-0033-83	peripheral blood analysis	1 in 100
CD3e PE/Cy5	145-2C11	Biolegend	100310	lineage cocktail for BM HSPC staining	1 in 100 or 1 in 300 for lineage cocktail
CD3e purified	17A3	eBioscience	16-0032-85	lineage cocktail for BM HSPC staining	1 in 100
CD4 biotin	GK1.5	eBioscience	36-0041-85	lineage cocktail for BM HSPC staining	1 in 100
CD4 PE/Cy5	GK1.5	Biolegend	100410	lineage cocktail for BM HSPC staining	1 in 100 or 1 in 300 for lineage cocktail
CD4 purified	GK1.5	eBioscience	16-0041-85	lineage cocktail for BM HSPC staining	1 in 100
CD41 PE	MWReg30	BD Pharmingen	558040	peripheral blood analysis	1 in 100
CD41 purified	MWReg30	BD Pharmingen	553847	lineage cocktail for BM HPC staining	1 in 100
CD45 APC	LCA.Ly.5(30-F11)	BD Pharmingen	559864	BM reconstitution readout	1 in 100
CD45.1 APC	A20	eBioscience	17-0453-82	BM reconstitution readout	1 in 100
CD45.1 APC/Cy7	A20	Biolegend	110716	BM reconstitution readout	1 in 100
CD45.1 FITC	A20	eBioscience	11-0453-85	BM reconstitution readout	1 in 100
CD45.1 Pacific Blue	A20	Biolegend	110722	BM reconstitution readout	1 in 100
CD45.1 PE/Cy5	A20	eBioscience	15-0453-82	BM reconstitution readout	1 in 100
CD45.1 PE/Cy7	A20	eBioscience	25-0453-82	BM reconstitution readout	1 in 100
CD45.2 APC	104	eBioscience	17-0454-82	BM reconstitution readout	1 in 100
CD45.2 APC/Cy7	104	Biolegend	109824	BM reconstitution readout	1 in 100

Table2.2. Antibodies used in FACS analysis and their applications: continued

Antibody	Clone	Supplier	Catalogue No.	Application	Dilution
CD45.2 Pacific Blue	104	Biolegend	109820	BM reconstitution readout	1 in 100
CD45.2 PE	104	eBioscience	12-0454-83	BM reconstitution readout	1 in 100
CD45.2 PE/Cy7	104	Biolegend	109830	BM reconstitution readout	1 in 100
CD71 PE	R17217	eBioscience	12-0711-82	peripheral blood analysis	1 in 100
CD8 biotin	53-6.7	eBioscience	13-0081-85	lineage cocktail for BM HSPC staining	1 in 100
CD8 PE/Cy5	53-6.7	Biolegend	100710	lineage cocktail for BM HSPC staining	1 in 100 or 1 in 300 for lineage cocktail
CD8 purified	53-6.7	eBioscience	16-0081-85	lineage cocktail for BM HSPC staining	1 in 100
ckit eFluor780(APC/Cy7)	2B8	eBioscience	47-1171-82	BM HSPC staining	1 in 100
ckit-APC	2B8	eBioscience	11-1171-82	BM HSPC staining	1 in 100
ckit-PE/Cy7	2B8	Biolegend	105814	BM HSPC staining	1 in 100
CXCR4 APC	2B11	eBioscience	17-9991-82	FDCPmix mobility assay	1 in 50
CXCR4 PE	2B11	eBioscience	12-9991-82	FDCPmix mobility assay	1 in 50
FLT3 biotin	A2F10	eBioscience	13-1351-85	BM HSPC staining	1 in 100
FLT3 PE	A2F10	eBioscience	12-1351-83	BM HSPC staining	1 in 50
GR1-biotin	RB6-8C5	eBioscience	36-5931-85	lineage cocktail for BM HSPC staining	1 in 100
GR1-Pacific Blue	RB6-8C5	Biolegend	108430	peripheral blood analysis	1 in 100
GR1-PE/Cy5	RB6-8C5	Biolegend	108410	lineage cocktail for BM HSPC staining	1 in 100 or 1 in 300 for lineage cocktail
GR1-PE/Cy7	RB6-8C5	eBioscience	25-5931-82	peripheral blood analysis	1 in 100
GR1-purified	RB6-8C5	eBioscience	16-5931-85	lineage cocktail for BM HSPC staining	1 in 100

Table2.2. Antibodies used in FACS analysis and their applications: continued

Antibody	Clone	Supplier	Catalogue No.	Application	Dilution
IL7-R eFluro450 (violet1)	A7R34	eBioscience	48-1271-80	BM progenitors staining	1 in 100
IL7-R PE/Cy5	A7R34	Biolegend	135016	BM progenitors staining	1 in 100
IL7-R purified	A7R34	eBioscience	16-1271-85	BM progenitors staining	1 in 100
SCA1 Pacific Blue	E13-161.7	Biolegend	122520	BM HSPC staining	1 in 30
SCA1 PE	E13-161.7	BD Pharmingen	553336	BM HSPC staining	1 in 50
SCA1 PE/Cy5	E13-161.7	Biolegend	122510	lineage cocktail for BM HPC staining	1 in 100
SCA1 PE/Cy7	E13-161.7	BD Pharmingen	558162	BM HSPC staining	1 in 100
SCA1 purified	D7	eBioscience	14-5981-82	lineage cocktail for BM HPC staining	1 in 100
ter119 APC	TER119	eBioscience	17-5921-82	peripheral blood analysis	1 in 100
ter119 biotin	TER119	eBioscience	13-5921-82	lineage cocktail for BM HSPC staining	1 in 100
ter119 PE/Cy5	TER119	eBioscience	15-5921-82	lineage cocktail for BM HSPC staining	1 in 100 or 1 in 300 for lineage cocktail
ter119 purified	TER119	Biolegend	116202	lineage cocktail for BM HSPC staining	1 in 100
Goat anti-rat F(ab')2 IgG(H+L) Tricolor/PECY5		Invitrogen	A10691	lineage cocktail for BM HSPC staining	1 in 100
Strepavidin APC		eBioscience	17-4317-82	lineage cocktail for BM HSPC staining	1 in 100
Strepavidin PE/Cy7		eBioscience	25-4317-82	lineage cocktail for BM HSPC staining	1 in 100

Table2.2. Antibodies used in FACS analysis and their applications: continued

Antibody	Clone	Supplier	Catalogue No.	Application	Dilution
Hoechst 33258, pentahydrate(bis-benzimide)		Invitrogen	H3569	viability, cell cycle staining	5mg/ml stock, 1 in 1000
Propidium Iodide (PI)		Invitrogen	P3566	viability	1mg/ml stock, 1 in 1000
7-aminoactinomycin D (7-AAD)		BD Pharmingen	559925	viability, cell cycle staining	1 in 100
AQUA		Invitrogen	L34957	viability	1in 300
Annexin-PE Apoptosis Detection kit		BD Pharmingen	559763	viability, apoptosis staining	
APC BrdU Flow Kit		BD Pharmingen	557892	cell cycle staining	
PE Mouse Anti-human Ki67 set		BD Pharmingen	556027	cell cycle staining	

Table 2.3. Fluorochromes used in FACS analysis

Fluorochrome	Excitation(nm)	Peak Emission (nm)	channel used in Cyan/Moflo	channel used in Gallios	bandpass filter
FITC/GFP	488	525	FL1	FL1	530/30
PE	488	575	FL2	FL2	575/26
PI	488	617	FL3	FL3	610/20
7-AAD	488	647	FL4	FL4	660/20
PE/Cy5	488	667	FL4	FL4	670/14
PE/Cy7	488	785	FL5	FL5	780/60
Hoechst 33258	351	460	FL6	FL9	450/50
Pacific Blue	360,405,407	455	FL6	FL9	450/50
eFluor450	405,407	450	FL6	FL9	450/50
aqua	405	512	FL7	FL10	550/40
APC	595,633,635,647	660	FL8	FL6	660/20
eFluor660	355,405,407,633	650	FL8	FL6	660/20
APC/Cy7	595,633,635,647	774	FL9	FL8	780/60
APC eFluor780	633, 635, 640	780	FL9	FL8	780/60

Table 2.4 Primers used for gene expression assay with SYBR GREEN Q-PCR

primers name	Position	Tm	%GC	Sequence
ALCAM-F	1334 - 1353	60.0	50.0%	CTTCAGTGTTTGGGGAATGG
ALCAM-R	1390 - 1409	59.0	50.0%	TTATGCCTTCAGGCTGTCCT
CXCR4-F	516-536	60.0	66.7%	CGCCACCAACAGTCGAGGCC
CXCR4-R	736-755	59.2	65.0%	ATGACGATGCCGGGCAGGAC
HPRT1-F	104 - 122	59.0	53.0%	TCCTCCTCAGACCGCTTTT
HPRT1-R	173 - 193	59.0	48.0%	CCTGGTTCATCATCGCTAATC
ICAM1-F	97 - 114	59.0	67.0%	CCCACGCTACCTCTGCTC
ICAM1-R	148 - 168	59.0	52.0%	GATGGATACCTGAGCATCACC
MMP2-F	1458 - 1475	59.0	61.0%	GGGCTTCTGTCCTGACCA
MMP2-R	1565 - 1589	60.0	44.0%	AAGTTCTTGGTGTAGGTGTAGATCG
MMP3-F	912 - 935	60.0	50.0%	CCAAGTCTAACTCTCTGGAACCTG
MMP3-R	1019 - 1038	60.0	45.0%	AGAGATTTGCGCCAAAAGTG
MMP9-F	1307 - 1325	60.0	53.0%	ACGACATAGACGGCATCCA
MMP9-R	1374 - 1393	60.0	55.0%	GCTGTGGTTCAGTTGTGGTG
NCAD-F	334-3363	60.2	70.0%	CTGGCGGACATGTACGGCGG
NCAD-R	3479-3498	59.6	65.0%	AGCCTCCAGCAAGCACGGTG
Nov F1	779-798	53.1	52.6%	AGTGTCTCCGCACCAAGAA
Nov R1	861-881	55.1	60.0%	CACTGCAGACCCCACAGAAC
OSN-F	205-225	60.2	70.0%	GCCTCAGTCCCCAGCCCAGA
OSN-R	363-382	59.6	65.0%	GCCAAAGCCGAGCTGCCAGA
OPN-F	45-64	60.0	65.0%	GCAGTCTTCTGCGGCAGGCA
OPN-R	172-192	57.3	57.1%	AGCTTCTCCTCTGAGCTGCCA
SDF1-F	427-450	60.6	62.5%	GAGAAGGCTGACATCCGTGGGAG
SDF1-R	587-608	60.4	63.6%	CGGGCGAGGGCAGGGATGAATA
VCAM-F	1788 - 1808	59.0	43.0%	TGGTGAAATGGAATCTGAACC
VCAM-R	1855 - 1873	59.0	53.0%	CCCAGATGGTGGTTTCCTT

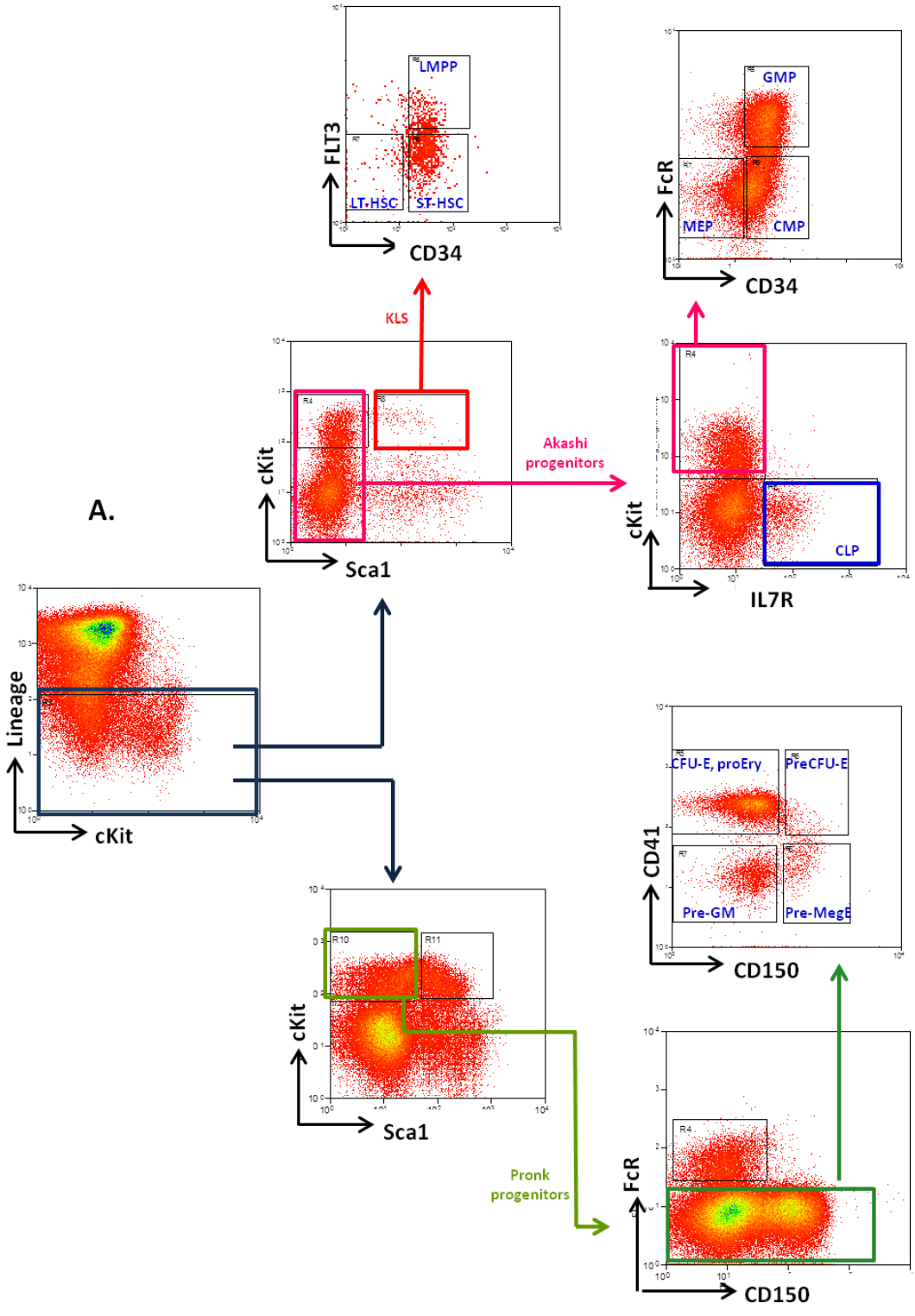


Figure.2.1: Representative FACS plots for bone marrow analysis

Continued opposite

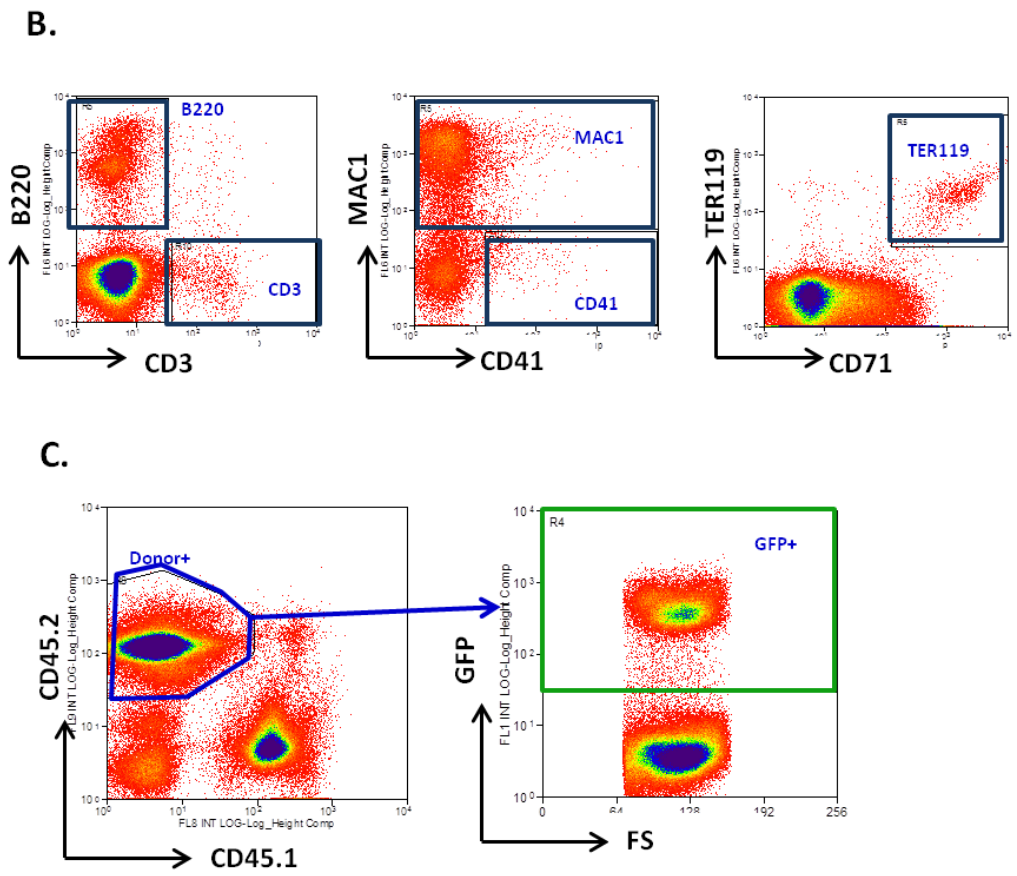
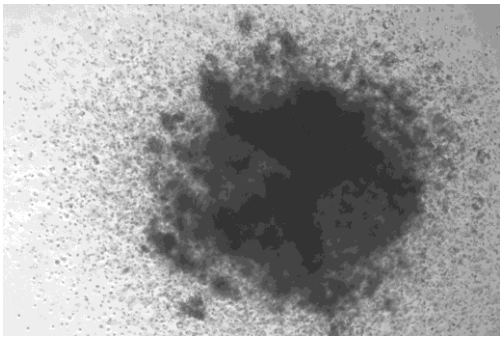


Figure2.1: Representative FACS plots for bone marrow analysis

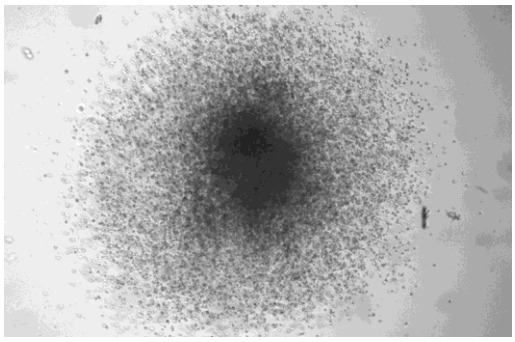
A. The gating strategies for KLS, Akashi progenitor dissection and Pronk progenitor dissection.

B. Staining combination and lineage gates for bone marrow analysis, showing the B220+, CD3+, Mac1+ gates. CD41 and Ter119 were analyzed in some experiments.

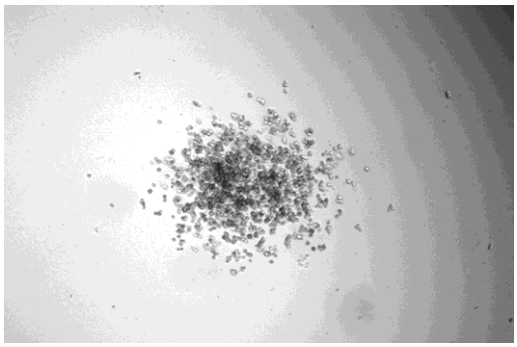
C. The representative reconstitution profiles of donor+ and GFP+ cells in transplantation experiments.



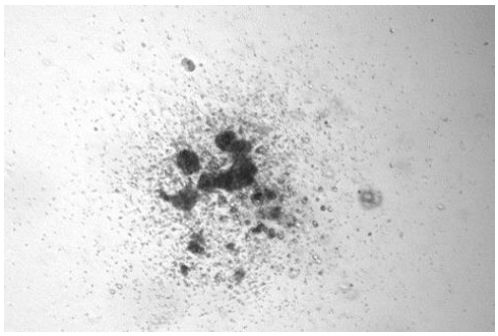
CFU-GEMM, 40×



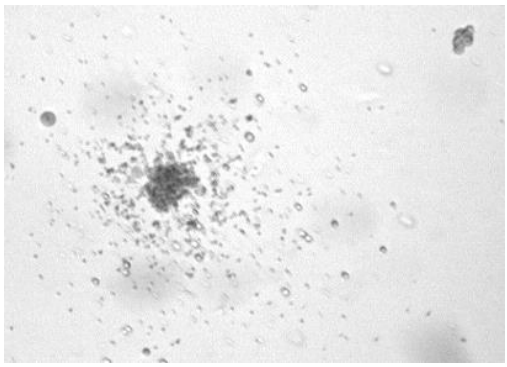
CFU-GM, 40×



CFU-M, 40×



CFU-G, 40×



BFU-E, 60×

Figure.2.2: Representative colonies in CFC assay

It should be noted that, in CFC assays from cultured HSPCs which had been stimulated by TPO, there could be megakaryocytic blast cells presented in BFU-E colonies. I therefore scored both types as CFU-MegE.

CHAPTER3.

EFFECTS OF *NOV* OVEREXPRESSION IN HAEMATOPOIETIC STEM AND PROGENITOR CELLS

3.1 Introduction

In this chapter, I characterized the expression of *Nov* along the haematopoiesis hierarchy in bone marrow and investigated the functional effects of *Nov* overexpression in haematopoietic stem and progenitor cells. Cell growth and function of haematopoietic stem and progenitor cells with forced expression of *Nov* were examined *in vitro* with liquid culture, CAFC assay and CFC assay. Effects of *Nov* overexpression on stem cell function were also tested *in vivo* by bone marrow transplantation.

3.2 Results

3.2.1 Characterisation of *Nov* expression during the early stages of haematopoiesis in bone marrow

In order to determine the profile of *Nov* expression during the early stages of haematopoiesis in mouse bone marrow, cells were purified from adult C57BL/6 mouse bone marrow for LT-HSC, ST-HSC, LMPP, CMP, GMP and MEP populations within the haematopoietic hierarchy (chapter 2, Figure 2.1 for the sorting strategy). Quantitative real-time PCR (RT-qPCR) with TaqMan oligos showed that *Nov* expression could only be detected in populations within the KLS compartment including LT-HSC, ST-HSC and LMPP. The expression of *Nov* could not be detected in any other progenitor compartments tested, including CMP, GMP and MEP (data not shown).

Within the KLS compartment, *Nov* expression level was highest in LT-HSC which is the most primitive stem cell population (Figure 3.1.). Expression levels in each population were normalised to the housekeeping gene β-actin. These results were consistent with the microarray data of Nov expression in human HSPC where *NOV* expression level decreases along with differentiation (Eckfeldt C.E, 2005). These results suggested that *Nov* is likely to be involved in HSC function in self-renewal and early stages during differentiation.

3.2.2 Cloning of mouse *Nov* cDNA and lentiviral overexpression constructs

Full length mouse *Nov* was amplified from cDNA derived from FDCPmix cells. Primers were designed according to the sequence of *Nov* mRNA (NCBI: NM_010930) with added FLAG tag at either the C- terminus (mNov) or N- terminus (mNovB). The FLAG tagged mNov PCR product was subcloned into Teasy-vector and then subcloned into lentiviral vector CSI (Figure 3.2.A). The internal ribosome entry site (IRS) in CSI vector enables translation of both Nov and eGFP from the same transcript; therefore cells that express GFP also express Nov. Both constructs were sequence verified. The purpose of making two constructs with FLAG tag added at

either C- or N- terminus was to monitor the possible defect of steric hindrance where FLAG tag may affect the protein expression and function. K562 cells is a human CML cell line with no *NOV* expression, which make the cell line an ideal material to test the expression of Nov protein from mNov and mNovB constructs. K562 cells were transduced with either mNov or mNovB virus and cultured for 2-3 days. GFP+ cells were purified by FACS, and cell pellets were checked for protein expression by western blot (Figure 3.2.B). hNOV (CSI-human NOV) (kindly provided by Dr R. Gupta: Gupta.R,2007) was tested in parallel as a positive control. Protein expression was detected by anti-Nov specific antibody or anti-FLAG antibody. Western blots showed that Nov was expressed in both mNov and mNovB transduced cells, but the expression from mNovB constructs was lower compared to mNov and hNOV constructs. Anti-FLAG antibody could detect the C-terminal FLAG signal from mNov transduced cells, but did not detect the N-terminal FLAG signal from mNovB transduced cells. This result indicated that the N-terminal FLAG peptide of mNovB may be cleaved inside the cells before the secretion.

To verify the secretion of Nov protein from transduced cells, the supernatant was collected from purified GFP+ cell culture and tested with anti-Nov antibody. The results of western blots showed that the secretion of Nov protein was normal from mNov transduced cells (Figure 3.2.C). Nov

protein could also be detected in the supernatant of mNovB transduced cells which was designed with FLAG at the N-terminus in front of the secretion signal. These results indicated that, although the FLAG peptide is cleaved inside the cell, the secretion signal is not affected.

The bands at 32kDa from mNov, mNovB and hNOV K562 cells supernatants might be the putative N-terminal truncated isoform (Lazar N, 2007; Su B.Y, 2001). It was noticed that there were also bands at 50kDa detected by anti-Nov antibody from K562 negative and CSI control cells supernatants. These bands may represent the homologue Nov proteins from the serum used in the medium (Thibout.H, 2003).

Because of the low protein level detected from mNovB by western blots, only the mNov construct was tested in this thesis.

3.2.3 Functional analysis of *Nov* overexpression in FDCPmix cells

In order to understand the function of *Nov* in mouse haematopoietic cells, FDCPmix, a multipotent haematopoietic stem and progenitor cell line, was tested first for cell growth and colony forming activity after the transduction with CSI and mNov virus.

3.2.3.1 FDCPmix cell growth was impaired by *Nov* overexpression

FDCPmix cells were transduced with either CSI or mNov virus and cultured for 2 days in normal expansion condition with 20% horse serum and 2% IL3 conditioned medium. GFP+ cells were purified by FACS for RNA extract. RT-qPCR was performed to confirm the overexpression of *Nov* (Figure 3.3.A). Virally transduced cells were cultured for 7-8 days in expansion medium and were monitored for cell growth. The results showed that mNov transduced FDCPmix cells expanded at a significantly lower rate in expansion medium compared to CSI control (Figure 3.3.B).

3.2.3.2 Overexpression *Nov* in FDCPmix cell did not affect cell cycle status

To understand the impacts of *Nov* overexpression on cell growth, cell cycle status was analysed using the APC BrdU Flow Kit (BD Pharmingen™). FDCPmix cells transduced with CSI or mNov were incubated with BrdU and monitored for cell cycle status with FACS following the manufacturer's protocol. On average, there were around 60% cells at G0/G1 phase and 35% cells at S phase from both CSI and mNov FDCPmix cells (Figure 3.3.C). The percentage of cells in G2/M phase as detected by BrdU and 7AAD staining in FDCPmix cells were low (data not shown) which could be due to the fast proliferation rate and short G2/M phase. The results showed that there was no obvious change in cell cycle status in mNov FDCPmix cells.

3.2.3.3 Apoptosis levels were increased in mNov FDCPmix cells

FDCPmix cells overexpressing *Nov* showed impaired cell growth but this growth defect was not due to changes in the cell cycle. I therefore tested the effect of *Nov* on apoptosis in FDCPmix cells. AnnexinV staining showed an increase of apoptosis in mNov FDCPmix cells. Figure 3.3.D shows one representative experiment of 3 experiments.

In summary, overexpression of *Nov* in FDCPmix impaired the cell growth in their expansion condition via apoptosis.

3.2.4 Functional analysis of *Nov* overexpression in KLS *in vitro*

3.2.4.1 Growth of mNov KLS was impaired in expansion culture

In order to determine the function of *Nov* in primary haematopoietic stem cells, KLS cells were purified and transduced with CSI or mNov virus. KLS cells were first tested for their growth in liquid culture under different cytokine combinations. The growth of GFP+ KLS cells was monitored after 7-10 days culture.

The first test condition was serum free medium SFEM with the addition of expansion cytokines including SCF, FLT3 and TPO which were shown to be able to maintain and expand mice HSC *in vitro* (Ramsfjell V, 1999; Chou S, 2010). In agreement with the FDCPmix growth result, KLS cells

transduced with mNov grew significantly slower than CSI control cells (Figure 3.4.A).

I then tested the cell proliferation and differentiation in IMDM with 10% FCS and complete cytokines including IL3, IL11, GM-CSF, SCF, TPO and EPO (Akashi K, 2000). This condition contains cytokines that can promote differentiation to both myeloid and erythroid pathways. mNov KLS cells showed a trend of reduction in growth compared to CSI control, but it was not statistically significant (Figure 3.4.B). This result indicated that under differentiation condition, *Nov* may have little or no effects on KLS cell growth.

The results of liquid culture experiments showed that the *Nov* impaired KLS cells growth in expansion condition but not in differentiation conditions. It implies that *Nov* plays a negative role in HSC expansion.

3.2.4.2 *Nov* overexpression induced apoptosis in KLS growing in expansion condition without changing the cell cycle

In order to understand the mechanism of impaired growth of mNov KLS in expansion condition, I did FACS analysis of expanded cells to determine the cell types within the culture. The expressions of cKit varied from experiment to experiment but were always comparable between CSI control and mNov transduced cells (data not shown). The profile of CD41 and Mac1 showed that, after 7-9 days cultured in SCF, FLT3 and TPO,

cells showed signs of differentiation by expressing CD41 (megakaryocytic differentiation marker) and Mac1 (myeloid differentiation marker). Figure 3.5.A. shows representative FACS plots of CSI and mNov transduced cells where an increased expression of CD41 and a reduction of Mac1 expression were observed in mNov transduced cells compared to CIS control. These results indicated Nov overexpression in KLS may favour a spontaneous differentiation towards megakaryocytes *in vitro*.

The overexpression of *Nov* induced apoptosis in FDCPmix. Therefore, I checked the apoptosis of KLS proliferated cells in expansion conditions. Consistent with the observation of mNov FDCPmix cells, the level of apoptosis was increased in mNov KLS cells (Figure 3.5.B).

Because the protocol for BrdU staining for cell cycle required a large amount of cells which proved to be difficult for primary KLS cells, I chose Ki67 and DNA stain Hoechst33258 to determine the cell cycle status of mNov KLS cells as it requires fewer cells. The results showed no difference in cell cycle between CSI and mNov cells (Figure 3.5.C).

The results indicated that the negative regulation of *Nov* overexpression in primary KLS cell growth in expansion *in vitro* may due to the induction of apoptosis but not altered cell cycle.

3.2.4.3 *Nov* overexpression in KLS did not affect the CAFC and CFC activity

To investigate the effect of *Nov* overexpression on the function of primary HSC *in vitro,* Cobblestone-Area-Forming Cell (CAFC) assay and colony-forming cell (CFC) assays were performed. CAFC assay permits to determine the frequencies of haematopoietic stem cells with proliferation potential at limiting dilution *in vitro*. CFC assay is used to study the proliferation and differentiation pattern of haematopoietic progenitors by their ability to form colonies in a semisolid medium.

For the CAFC assay, KLS cells were transduced with CSI or mNov virus under expansion conditions and cultured for 2 days. GFP+ cells were purified by FACS sort and plated on to 96 wells pre-prepared with stromal cells growing at the bottom. For limiting dilution, cell density and dilutions were adjusted in each experiment according to total GFP+ cell number collected. Each dilution was plated in 10 replicate wells. Cells were kept in MyeloCult™ M5300 with half medium changed weekly. After 5 weeks, individual wells were evaluated for the presence of a cobblestone area and the frequency of CAFC was calculated with L-Calc software. The results of showed that, on average, the frequency of CAFC in mNov KLS cells was similar to CSI control (Figure 3.6.A).

In the CFC assay, GFP+ purified KLS were plated into Methocult M3234 plus cytokine cocktails of IL3, IL11, SCF, GM-CSF, TPO and EPO to support the growth of all types of myeloid lineage colonies. 10-14 days later, colonies were scored according to their morphology. The results showed that colony forming activity was similar between mNov and CSI KLS cells. The output of different colony types was also similar between mNov and CSI KLS cells (Figure 3.6.B).

Overall, the results of the *in vitro* functional assays suggested that overexpression of *Nov* did not affect the stem and progenitor cell frequency and colony forming efficiency *in vitro*.

3.2.5 Effects of *Nov* overexpression in CMP

CMP is a progenitor cell population in bone marrow which can give rise to myeloid lineages including both megakaryocyte/erythrocyte and granulocyte/macrophage. In order to test if *Nov* could affect the function of haematopoietic progenitors downstream of KLS, primary CMP were transduced with CSI and mNov virus and were examined for cell growth and CFC activity.

CMP cells were purified as Lineage-cKit+Sca1-CD34+FcR- by FACS. Cells were cultured in SFEM supplemented with IL3, IL6 and SCF (Luskey B.D, 1992; Bryder D, 2000). CSI or mNov transduced CMP cells were cultured

for 7-9 days and were monitored for GFP+ cells growth. The results showed that mNov CMP cells proliferated at a similar rate as the CSI control (Figure 3.7.A). In CFC assay, GFP+ purified CMP were plated into Methocult M3234 supplemented cytokine cocktails of IL3, IL11, GM-CSF, SCF, TPO and EPO. Colonies were scored according to their colony morphology 10-14 days later. The results of 2 experiments showed a trend of increased colony forming activity in mNov transduced cells (Figure 3.7.B).

In summary, CMP progenitor functional analysis indicated that *Nov* did not affect cell growth in liquid culture, and it may enhance progenitors' colony forming activity *in vitro*.

3.2.6 Functional analysis of *Nov* overexpression in KLS *in vivo*

To investigate the capacity of mNov HSC to proliferate and repopulate lethally irradiated animals, I performed the bone marrow reconstitution assay with KLS cells overexpressing CSI or mNov. Purified C57BL/6(CD45.2) KLS cells were transduced with CSI or mNov virus under expansion condition (SFEM with SCF, FLT3 and TPO) overnight. The cells were washed three times with PBS to remove the virus. Around 2×10^4 KLS cells were mixed with 2×10^5 B6SJCD45.1 helper bone marrow cells for

each recipient animal. Cell mixtures were injected into B6SJCD45.1 recipient mice through the tail vein. In each experiment, 1-2×10^3 KLS transduced cells were kept in the same condition for another 2 days to examine transduction efficiency by GFP. Peripheral blood of recipient was examined at 1 month, 2 month and 4 month for GFP and lineage reconstitution (Figure 3.8.A). The engraftment efficiency of transduced KLS cells was calculated using the formula:

$$\text{Engraftment efficiency} = \frac{\%\text{GFP+ within donor cells}}{\%\text{GFP+ of input}}$$

Animals were then sacrificed and were analysed for lineage reconstitution in bone marrow and spleen, and HSC and progenitor frequency in bone marrow.

3.2.6.1 *Nov* overexpression in KLS showed a reduced engraftment efficiency

The results showed that the percentage of GFP+ within donor cells was the same as the input GFP+ percentage in CSI control recipients. In contrast, in the mNov recipients, the GFP+ percentage within donor cells was only around 25% of input GFP. These data indicated that there were no effects in KLS reconstitution activity caused by the treatment of viral transduction and overnight culture, as there was no change in transplant efficiency in

control CSI recipients. But there was a significant reduction of engraftment from mNov KLS cells. The significant reduction of GFP+ cells after 1 month of transplantation was maintained throughout the rest of the experiment (Figure 3.8.B). These results indicated that there may be a transient effect of *Nov* overexpression which reduced the engraftment efficiency within 1 month of transplantation. The engrafted cells were persisted in the recipient and contributed to the production of circulating peripheral blood cells at a steady frequency.

3.2.6.2 *Nov* overexpression in KLS reduced CD3+ T cells reconstitution and enhanced Mac1+and CD41+ myeloid reconstitution in peripheral blood

The lineage reconstitutions in peripheral blood were analysed by FACS for B220 (B-cell), CD3 (T-cell), Mac1 (myeloid cell) and CD41 (megakaryocytic cell) expression after 1 month, 2 month and 4 month of transplantation. After one month of transplantation, around 70% of engrafted GFP+ cells were B220+ from both CSI and mNov KLS derived cells indicating no difference in B cell reconstitution capacity between CSI and mNov KLS cells (Figure 3.9.A, panel 1). However, there was a 4 fold reduction of CD3+ T cell reconstitution from mNov cells, with 16% CD3+ in CSI cells and only 3.8% in mNov cells. This reduction of CD3+ cells at 1 month was statistically significant at p=0.0161 (Figure 3.9.A, panel 2). Interestingly,

there was a statistically significant increase of Mac1+ myeloid cell reconstitution in mNov derived cells, at around19.8% comparing to only 7.3% in CSI cells (Figure 3.9.A, panel 3). And consistent with the results of *in vitro* experiments (Figure 3.5.A) where overexpression of Nov favoured the differentiation towards CD41+ cells, there was also a statistically significant increase of CD41+ cells derived from mNov KLS cells (Figure 3.9.A, panel 4).These lineage biases were maintained in mNov derived cells when checked at 2 months (Figure 3.9.B) and 4 months (Figure 3.9.C), except the B220+ cell percentage at 2 month where there was a mild increase in mNov derived cells.

These results showed that there was an impact in lineage choice during differentiation after forced expression of mNov in KLS in transplantation in peripheral blood.

3.2.6.3 Lineage reconstitution in bone marrow and spleen

The lineage distributions were also analysed in bone marrow and spleen after 4 months of transplantation with FACS for B cell, T cell, myeloid cell and megakaryocytic cell lineage reconstitution.

In bone marrow, the reconstitutions of B220+, Mac1+ and CD41+ cells were similar in mNov donor cells compared to CSI control (Figure 3.10.A). The percentage of CD3+ T cells were low in the bone marrow from both CSI and mNov donors but were similar between the two groups.

In spleen, the lineage distribution bias was similar to the bias seen in peripheral blood from mNov recipients. The CD3+ T cells percentage was significantly reduced in mNov donors and Mac1+ and CD41+ cells were increased, compared to CSI control (Figure 3.10.B).

3.2.6.4 *Nov* overexpression in KLS showed no changes in primitive HSC frequency but a reduction in progenitor frequencies in bone marrow

In order to understand the cellular mechanism of *Nov* induced reduction of engraftment efficiency and lineage bias, recipients' bone marrow were FACS analysed for HSC and progenitor frequency.

Because the percentage of total GFP+ in some of mNov recipients were very low (<1% within donor cells, data not shown), the GFP+ subpopulations within KLS compartment which was of low frequency in total bone marrow failed to form a proper population for gating. Therefore, the data were analyzed as the ratio of the GFP percentage in each population compared to the total GFP percentage within donors and the HSC population was analyzed as FLT3- HSC only which included both LT-HSC and ST-HSC populations.

FACS analysis showed that the frequency of HSC and LMPP were similar between mNov and CSI donors (Figure 3.11.A). At progenitor level, the frequency of GMP was also similar between mNov and CSI donors.

However, the frequencies of CMP, MEP and CLP were significantly reduced in mNov donors (Figure 3.11.B).

The MEP progenitor frequency was reduced in bone marrow which seemed to be inconsistent with the observation of increased CD41+ cell in peripheral blood and spleen. Several studies reported that Nov could regulate integrin expression (Benini S, 2005; Vallacchi V, 2008; Huang C.Y, 2011). However, it was not clear the functional meaning of the correlation between Nov overexpression and CD41 expression in haematopoietic cells *in vivo*.

The unaltered GMP frequency in mNov donor cells was consistent with the myeloid functional assay *in vitro* where *Nov* overexpression did not affect the myeloid colony forming activity (Figure 3.6.B). And the unaltered frequency in GMP but reduced frequency in MEP and CLP may contribute to the phenotypes observed in peripheral blood with increased Mac1+ myeloid cells.

However, the reduced CLP frequency alone could not explain the reduced CD3+ T cell reconstitution because B220+ B cells reconstitution was normal in peripheral blood and spleen (Figure 3.9; Figure 3.10.B). Although T cells are originated from HSC and progenitors in bone marrow, mature T cells are produced in the thymus. I therefore decided to test the differentiation of T cells in thymus.

3.2.6.5 *Nov* overexpression blocked the T cell development in thymus at the stage of CD4/CD8 Double Negative

The thymus is a specialized organ of the immune system for T cell differentiation and selection. Circulating T-lymphoid progenitor cells originated from bone marrow need to migrate into the thymus for T cells development and maturation. The most primitive progenitor in thymus is called the ETP (early T cell progenitor) which can be found in the DN1 (double negative 1) compartment. DN1 has been defined as Lineage-cKit+CD25- and can differentiate into DN2 cells (Lineage-Kit+CD25+) cells that migrate from the entry site in the perimedullary cortex to the inner cortex (Lind E.F., 2001; Porritt H.E., 2003). DN2 cells then further differentiate to become DN3 cells (Lineage- Kit-CD25 +) at the outer cortex of thymus. DN3 cells are committed to the T cell lineage and start rearrangement of TCRβ, γ, and δ gene loci. CD4-CD8- (DN) cells then proliferate and generate CD4+CD8+ double positive (DP) thymocytes, which are the most abundant cells within the thymus(Ciofani M., 2006). These DP thymocytes develop into CD4 and CD8 single positive (SP) immunocompetent T cells through serial changes in TCRα locus rearrangement and selection (Bhandoola A., 2007).

In Figure 3.12.A, typical FACS profiles of T cell development compartments in thymus are presented for staining and gating strategy.

To address at which stage *Nov* overexpression affects T cell development, the frequency of subpopulations during T cell development were analyzed by FACS. The percentage of double negative (CD4-CD8-) was almost 23% within mNov derived cells, compared to only 11% within CSI donors (Figure 3.12.B). The two fold increase of total CD4-CD8- DN population in mNov donor cells was statistically significant at p=0.0007.When the subpopulations within the heterogeneous DN cells were examined, the results showed a clear trend of increased frequency of early T cell precursors (DN1, DN2 and DN3) in mNov donor cells (Figure 3.12.C).

In contrast, as the most abundant population in thymus, the percentage of double positive cells was significantly reduced in mNov donors to 50% compared to 70% in CSI donors. However, the frequencies of more mature single positive populations, both CD4+CD8- and CD4-CD8+, were comparable between CSI and mNov donors. Despite the significant reduction of CD3+ cells in peripheral blood and spleen in mNov donors, CD3+ cell frequency in thymus was similar between CSI and mNov donors (Figure 3.12.C).

The increased frequency of DN population and reduced frequency of DP population in mNov donor cells suggested a negative role of *Nov* during DN to DP transition. The difference of CD3+ frequency between thymus and

peripheral blood and spleen implied another role of *Nov* in T cell migration from thymus into circulating blood.

3.2.6.6 Secondary transplantation of KLS overexpressing *Nov*

To test the mNov HSC function in serial transplantation, bone marrow collected from first recipients were tail-vein injected into secondary recipients. The engraftment efficiency was calculated as the ratio of %GFP+ donors in secondary recipient to %GFP+ donors in primary recipient.

On the basis of the observations in primary recipients that the CMP and CLP frequencies were reduced while GMP frequency were intact, it was predicted that the short-term secondary engraftment efficiency would be reduced in mNov donors together with a reduction in lymphoid cell reconstitution. Indeed, after one month of secondary transplantation, there was a significant reduction in engraftment efficiency from mNov donors (Figure 3.13.A). The engraftment efficiency after 2 months of transplantation, the reduction of GFP+ percentage in mNov recipient was maintained, except one mNov recipient.

The lineage reconstitution in peripheral blood after 1 month of transplantation was altered in mNov donors compared to CSI controls. There was a significant reduction of both B220+ and CD3+ lymphoid cells and an increase of Mac1+ myeloid cells in mNov donors compared to CSI

control. 2 months after transplantation, B220+ cells repopulation in mNov donors recovered to normal level as CSI control while the bias of CD3+ between Mac1+ cells was maintained.

Although preliminary, the data from the secondary transplantation experiments was consistent with the results that *Nov* overexpression impaired the expansion of HSC and inhibited T cell development.

3.3 Summary and discussion

RT-qPCR of HSC and downstream populations showed that *Nov* was expressed in HSC and was down regulated rapidly during differentiation *in vivo*. To elucidate the functional effects of *Nov* down regulation accompanying the differentiation of HSC, I attempted to counter *Nov* down-regulation by forcing expression of *Nov* and examined its effects on HSC growth and differentiation.

The growth of *Nov* overexpressed FDCPmix and KLS was significantly reduced in expansion condition *in vitro* (Figure 3.3.B; Figure 3.4.A), while the growth of KLS was not affected in differentiation condition (Figure 3.4.B. C). This data indicated a role of *Nov* specifically in HSC growth. To understand the inhibitory effect of *Nov* in HSC *in vitro* expansion, I analyzed the cell cycle status and apoptosis of *Nov* overexpressing KLS and FDCPmix. The results showed that *Nov* overexpression impaired the

growth of KLS by induction of apoptosis, but did not affect cell cycle. Consistent with the observation *in vitro*, the engraftment efficiency was significantly reduced in mNov KLS cells in bone marrow transplantation and serial transplants.

The inhibitory effect of *Nov* on cell growth has been reported in many transformed cell types including melanoma, glioblastoma, adrenocortical tumors and in CML (Fukunaga-Kalabis M, 2006; Fukunaga-Kalabis M, 2008; Fu C.T, 2004; Sin W.C, 2008; Gupta N, 2001; Benini S, 2005; Martinerie C, 2001; McCallum L, 2006; McCallum L, 2009). These reports, together with my data on *Nov* overexpression in mouse HSPC were not in agreement with the results reported for human where overexpression of hNOV in human cord blood CD34+ cells increased the CAFC frequency and enhanced the HSC engraftment efficiency in secondary transplantation into mice. Discrepancies between these two experimental systems will be discussed further in the final discussion after more functions of *Nov* have been examined in mouse haematopoietic cells and HSC niche.

It is noted that overexpression of *Nov* in primary KLS cells also increase the expression of integrin CD41 both *in vitro* and *in vivo*. CD41 has been known as a specific marker for megakaryocyte differentiation, and is expressed in HSCs which are primed for myeloerythroid and megakaryocyte differentiation (Gekas C, 2013). *Nov* has been reported to

regulate the expression of integrin α7, β1, αv, and β5 in melanoma cells (Vallacchi V,2008) and activate a signal transduction pathway that included αvβ3 integrin, integrin-linked kinase (ILK), Akt and nuclear factor-kappaB (NF-κB) in prostate cancer cells (Chen P. C, 2012). Possible explanation between the expression of CD41 and *Nov* in hematopoietic cells could be similar to the mechanism in other cell types. However, the effect of *Nov* overexpression in megakaryocyte development has not been reported before, and further experiments should be carried out to look into the function of *Nov* in megakaryocyte differentiation.

Also emerging from these data is the negative effects of *Nov* on T cell development during bone marrow transplantation. There was significant reduction of CD3+ T cell reconstitution from *Nov* overexpressed donor in peripheral blood and spleen. In thymus, there were a significant increase of DN population and a reduction of DP population in mNov donor cells. There are two possible mechanisms to explain this phenotype. The first is through the block of DP development. During T cell development in thymus, Notch signalling is active and critical in DN, CD4+, and CD8+ single positive (SP) thymocytes, but is down regulated in CD4+8+ double positive (DP) thymocytes (Hasserjian R. P,1996; Deftos M. L, 1998). *NOV* has been reported to associate with the epidermal growth factor-like repeats of Notch1 by the CT domain and activate the promoters of HES1

and HES5, which are the downstream transducers of Notch signalling (Sakamoto K., 2002). It is possible that overexpression of *Nov* in thymocytes activated the activity of Notch signalling pathway. During the transition from DN to DP, the mNov cells would therefore fail to switch off the downstream targets of Notch signalling pathway, resulting in a block in DP development.

The other possible explanation is related to the apoptosis effect induced by *Nov*. During the development of T cell in thymus, DP thymocytes are highly sensitive to apoptosis in order to eliminate inappropriate or auto-reactive T lymphocytes. Caspase-3 and caspase-8-like proteases activities have been reported to be involved in the T-cell receptor (TCR)-mediated apoptosis (Jiang D, 1999). In the CML line K562, NOV has been reported to reduce cell growth and increase apoptosis through reducing the level of phosphorylation of Erk and enhancing caspase 3 cleavages (McCallum, L.2012). Therefore, it is reasonable to argue that overexpression of *Nov* at the DP stage enhanced the level of apoptosis and results in the reduction of DP population in thymus.

Another interesting phenomenon was that there was no obvious reduction of CD3+ and single positive CD4+ or CD8+ population in thymus although there was significant reduction of CD3+ T cell in peripheral blood and spleen. This data indicated that there may be another inhibitory effect

induced by *Nov* overexpression for CD3+ cells to leave the thymus and enter the peripheral blood.

Taken together, the results of overexpressing *Nov* in mouse haematopoietic cells indicated that i). *Nov* overexpression impaired the growth of HSC in expansion condition *in vitro* and increased the apoptosis level; ii). Overexpression of *Nov* in KLS cells reduced the engraftment efficiency and T cell reconstitution in bone marrow transplantation.

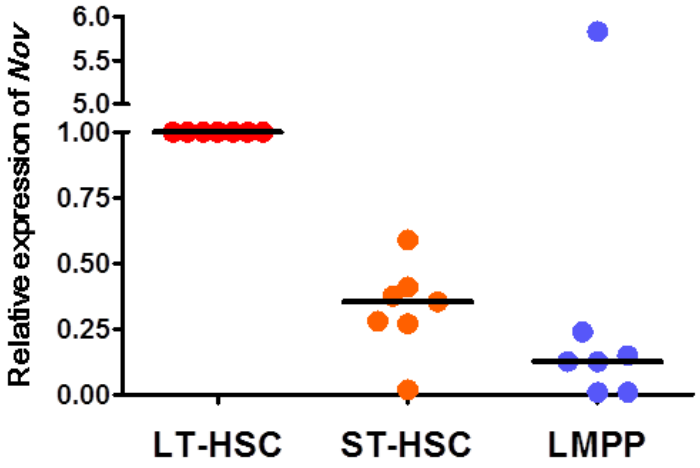


Figure.3.1: Endogenous expression of *Nov* in mouse haematopoietic stem and progenitor cells

Within the KLS compartment, *Nov* expression levels in ST-HSC and LMPP were compared to LT-HSC after normalization with β-actin. The expression of *Nov* was highest in LT-HSC and decreased rapidly during differentiation. The expression of *Nov* could not be detected in progenitors CMP, GMP and MEP (data not shown). There was one experiment where LMPP showed an unusual high expression of *Nov*. Each dot represents one sample analysed; the line indicates the medians of 5 independent samples.

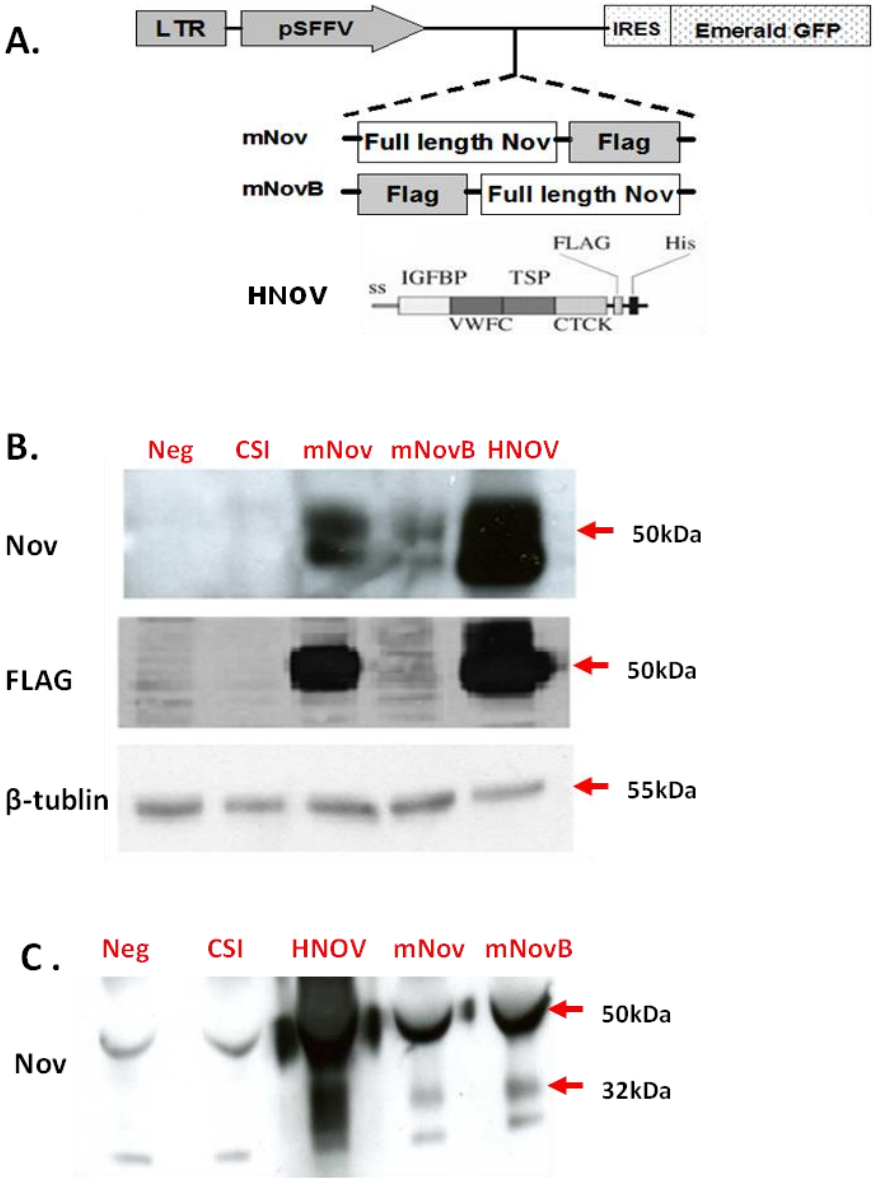


Figure.3.2: Constructs for overexpression of *Nov*

A. Schematic representation of the lentiviral constructs for overexpression of *mNov* and *hNOV* (kindly provided by Dr. R. Gupta). mNov has FLAG tag at the C-terminus of full length mouse *Nov* cDNA; mNovB has FLAG tag full at the N-terminus of full length mouse *Nov* cDNA in the front of the signal peptide; hNOV has FLAG tag and HIS tag at the N-terminus of full length human NOV. The expressions of *mNov* and *hNOV* are driven by the SFFV promoter. Emerald-GFP is the reporter for expression and purification.

B. Western blot of transduced K562 cell pellets showed the expression of Nov protein was detected from all 3 constructs using anti-Nov antibody. The expression level of mNovB was much lower than the mNov and hNOV constructs in K562. The anti-FLAG antibody failed to detect mNovB expression in cell pellets.

C. Western blot of supernatant from GFP+ cell culture showed that cells transduced with all three overexpression constructs could secrete Nov protein into medium, even though mNovB was designed with a FLAG tag in front of the signal peptide. Two bands can be seen: 50kDa for the full length Nov and 32kDa for a putative N-terminal truncated isoform. Bands detected at 50kDa in Negative and CSI control supernatant might represent the homologue Nov proteins from serum.

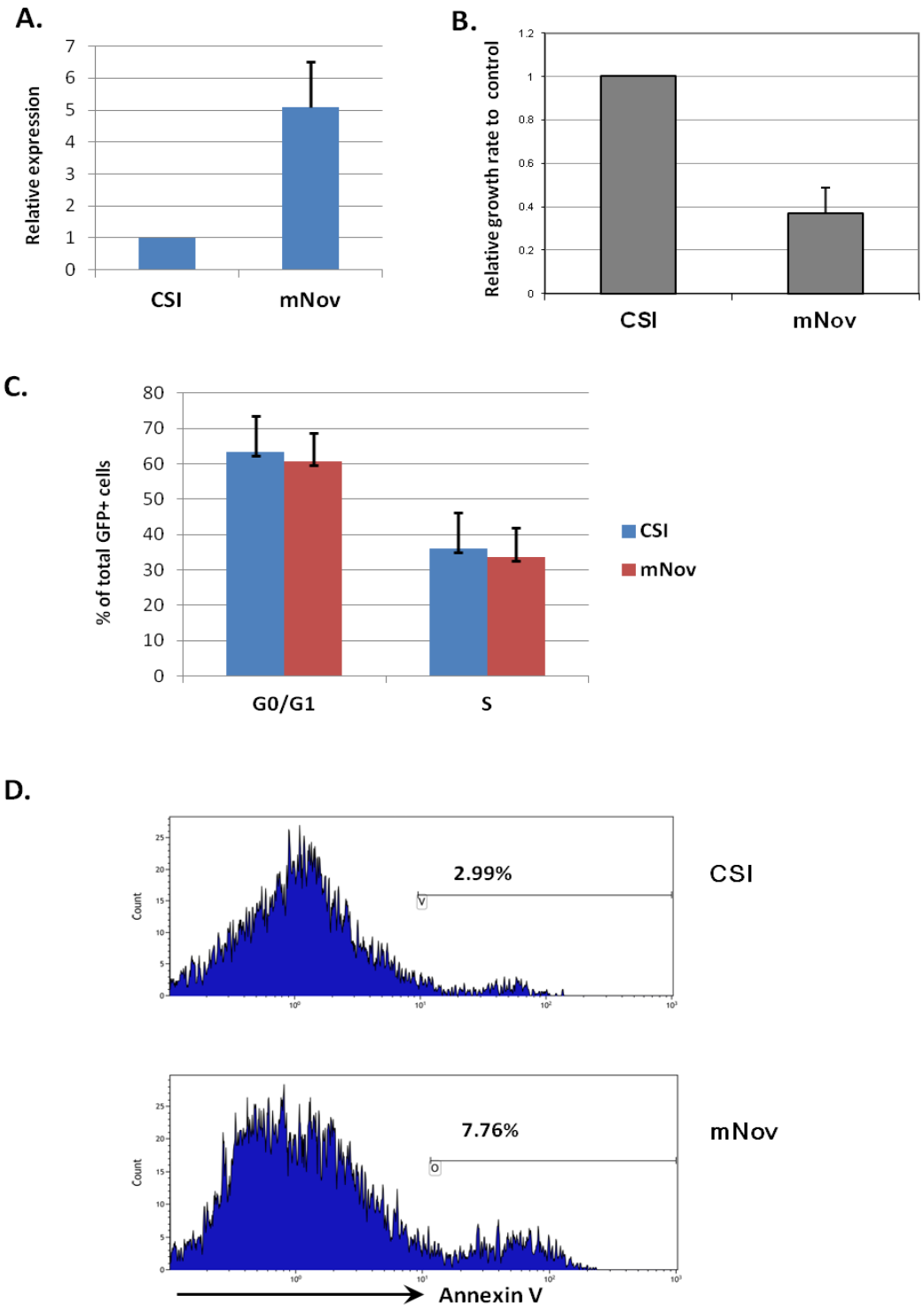


Figure.3.3: Overexpression of *Nov* in FDCPmix induces apoptosis

A. RT-qPCR of FDCPmix cells transduced with CSI or mNov virus confirmed the

increased expression levels of *Nov*. n=3

B. Relative growth rate of FDCPmix cells transduced with mNov virus compared to CSI control cells in expansion conditions (Fishers' medium with 20% Horse serum and 2% IL3 conditioned medium). n=3±SD, p=0.0007

C. BrdU cell cycle analysis of FDCPmix cells transduced with CSI or mNov virus showed that there was no obvious difference between mNov transduced cells and control cells indicating cell cycle was not affected by Nov overexpression. n=3±SD

D. Representative FACS plots of Annexin V staining showing an increase in apoptosis in mNov transduced cells. Cells were gated on Hoechst333258- for live cells.

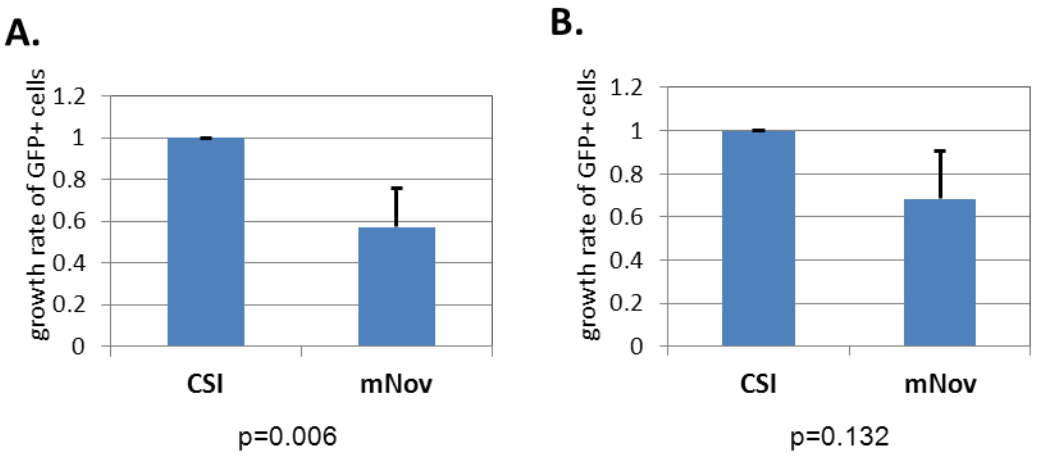


Figure.3.4: KLS cells transduced with mNov virus grew differently under different culture conditions

A. Relative growth rate of KLS cells transduced with CSI or mNov virus in serum free expansion medium SFEM with cytokines SCF, FLT3 and TPO. n=3±SD

B. Relative growth rate of KLS cells transduced with CSI or mNov virus in IMDM/10% FCS medium with cytokine cocktails IL3, IL11, SCF, GM-CSF, TPO and EPO to support proliferation and differentiation. n=3±SD

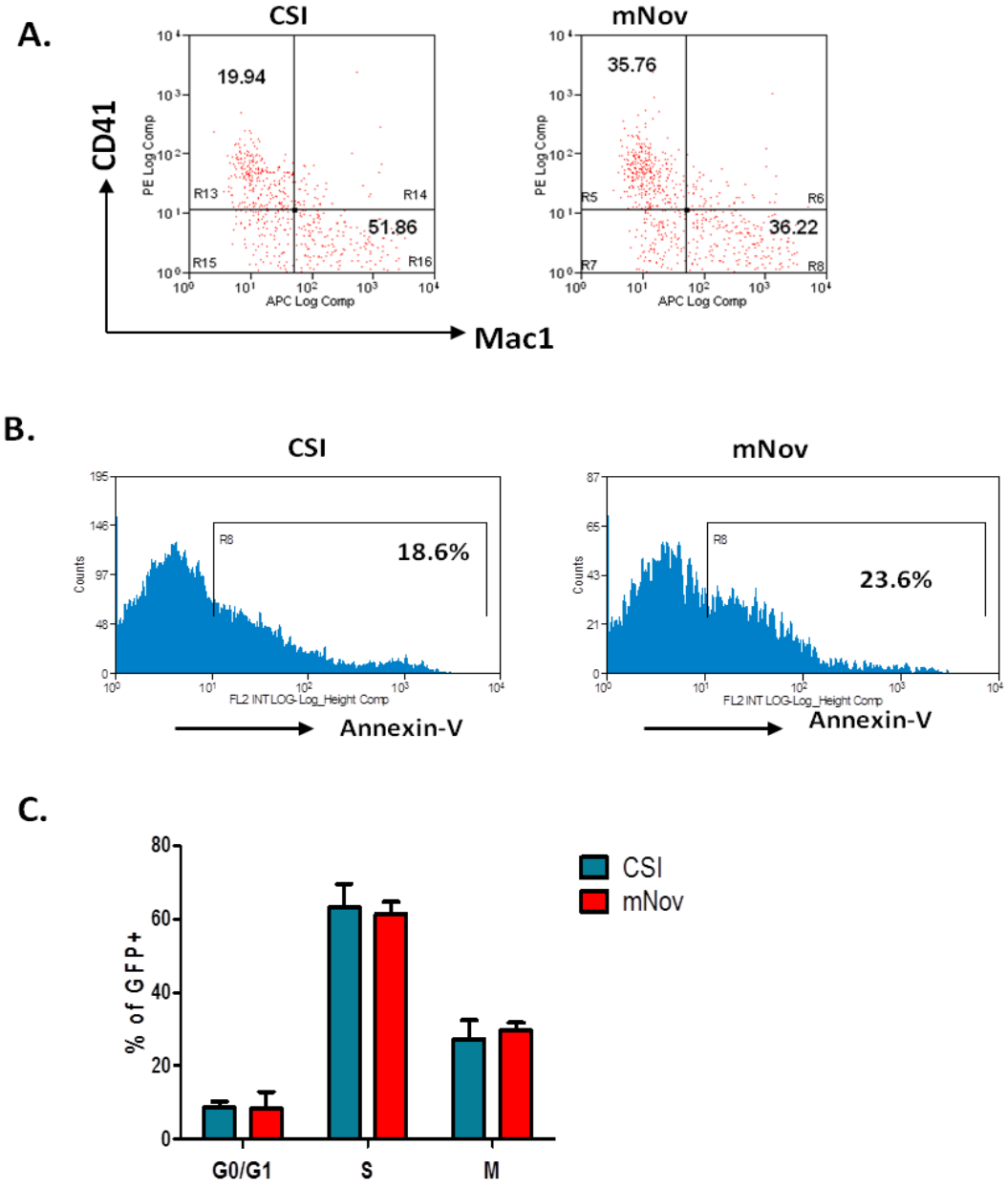


Figure.3.5: Overexpression of *Nov* in KLS induces apoptosis in expansion condition

A. Overexpressing *Nov* in KLS induced CD41 expression and reduced expression of Mac1 in SFEM supplemented with SCF, FLT3 and TPO. Plots showed one representative experiment from 3 experiments.

B. Representative FACS plots of AnnexinV staining showed a mild increase of apoptosis in mNov transduced cells.

C. Ki67 staining of KLS cells growing in expansion condition showed no difference in cell cycle status between CSI and mNov cells. n=3±SEM

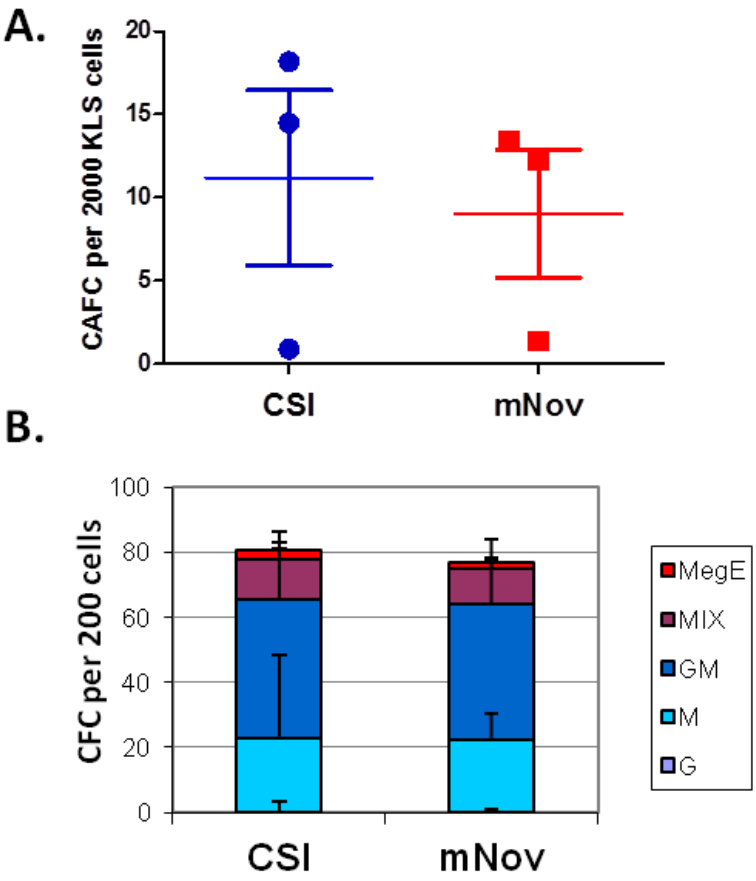


Figure.3.6: *In vitro* functional assay of *Nov* overexpression in KLS

A. Overexpression of *Nov* in KLS did not change their cobble-stone- area forming frequency in CAFC assay. Each dot represents one experiment performed. The lines represent the mean value with SEM.

B. CFC assay of KLS transduced with CSI or mNov showed no difference in colony forming activity and colony output. n=3±SD

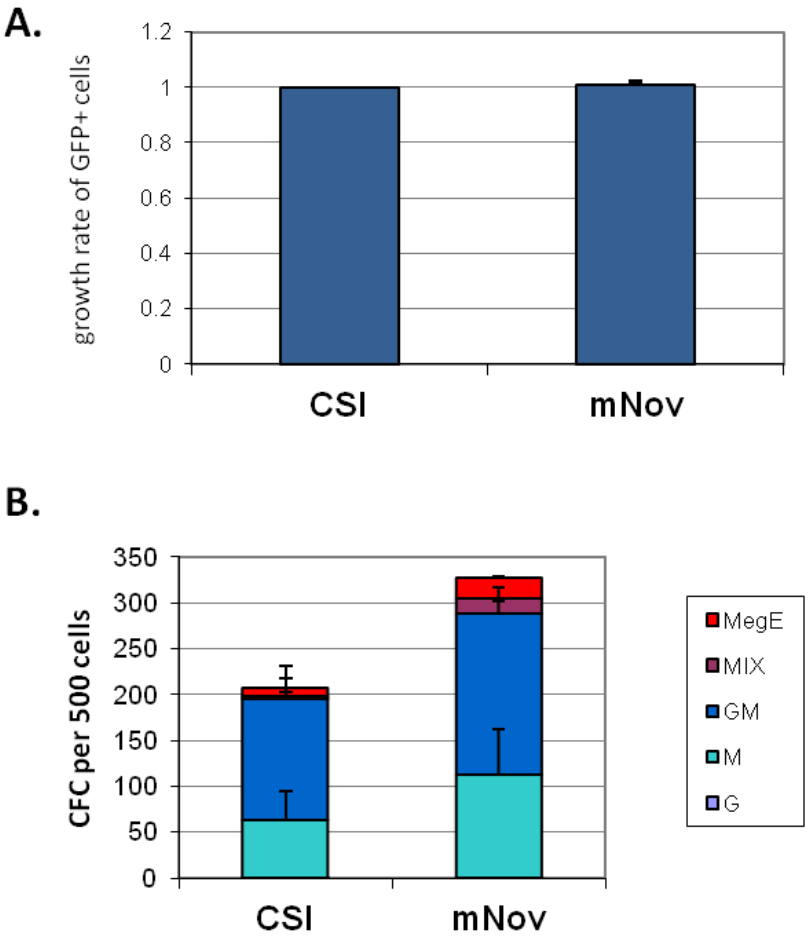


Figure.3.7: *In vitro* functional assay of *Nov* overexpression in CMP

A. Growth rate of CMP cells transduced with CSI or mNov virus in serum free medium SFEM with SCF, IL3 and IL6. n=2±SD

B. CFC assay of CMP transduced with CSI or mNov showed a trend of enhanced colony forming cell potential. Cells were cultured in M3234 supplemented with IL3, IL11, GM-CSF, SCF, TPO and EPO. n=2±SD

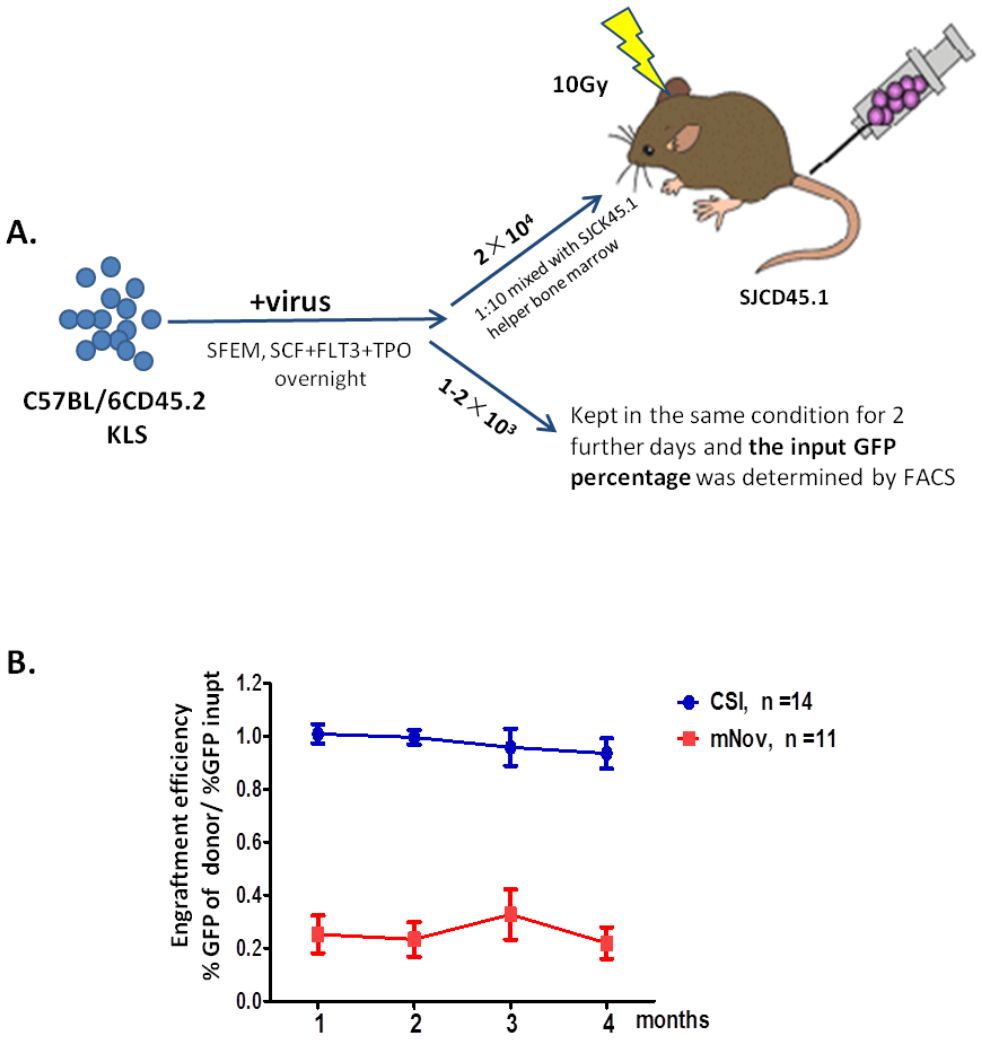


Figure.3.8: Overexpression of *Nov* in KLS showed reduced engraftment efficiency in bone marrow reconstitution assay.

A. Schematic representation of the experimental protocol for bone marrow transplantation.

B. The engraftment efficiency of KLS transduced with CSI or mNov is presented as the ratio between the percentages of GFP+ cells within donor cells to the input GFP percentages. The results indicated a significant reduction of GFP+ cells after 1 month of transplantation of mNov donor cells and the GFP expression was maintained at low percentage. The line shows the mean of engraftment efficiency with SEM.

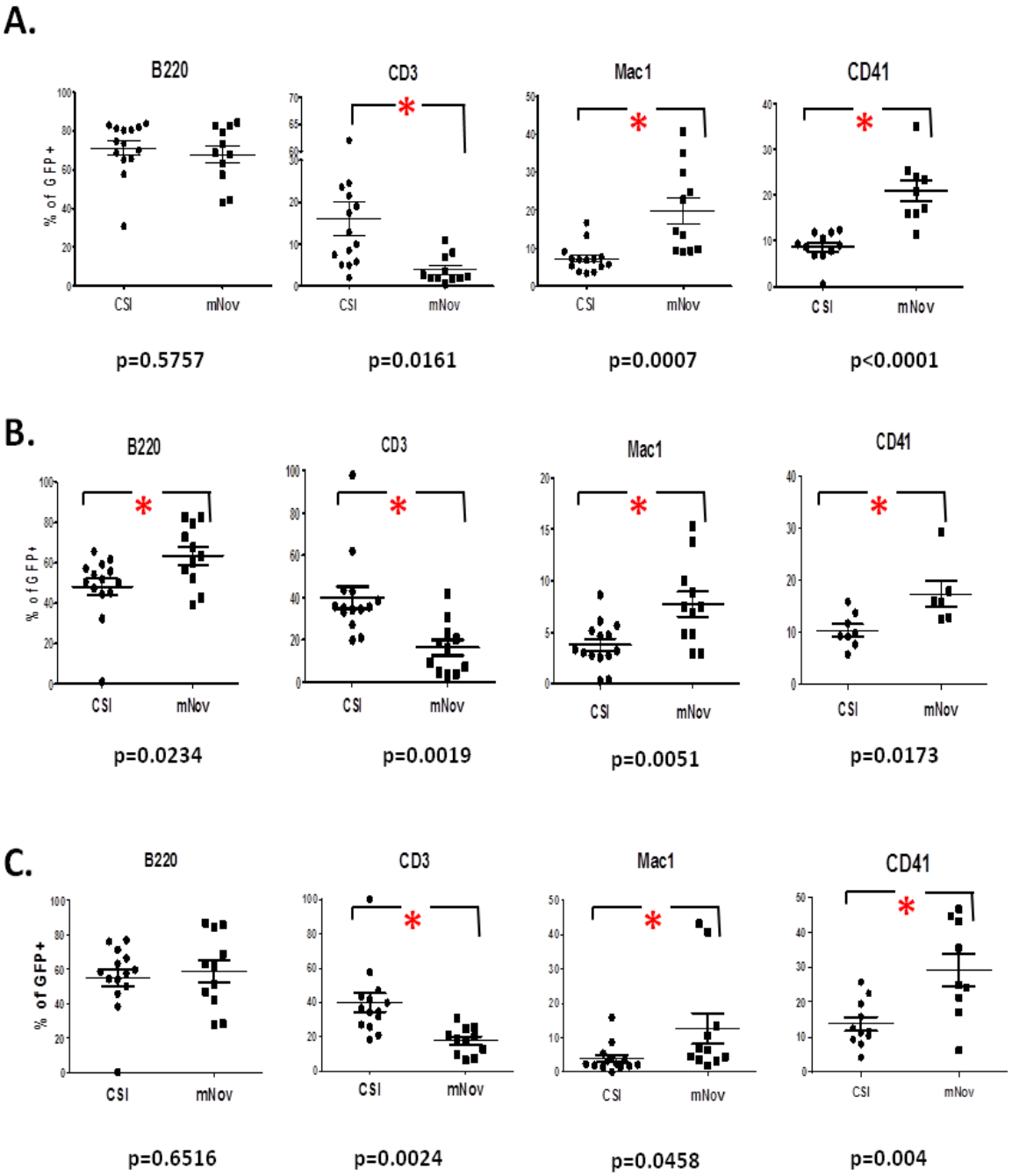


Figure.3.9: Overexpression of *Nov* in KLS impaired the CD3+ T cell reconstitution in bone marrow reconstitution assay.

The lineage distribution of GFP+ donor cells in peripheral blood at each month A. 1month, B. 2month and C. 4month. There was a consistent reduction of CD3+ T cell reconstitution which was statistically significant at each time point. In parallel, the

reconstitutions of Mac1+ and CD41+ cells were increased in mNov donor cells. Each dot represents one recipient analysed. The line shows the mean of the percentage of each lineage within GFP+ donor cells. p-value is indicated under each group of comparison.

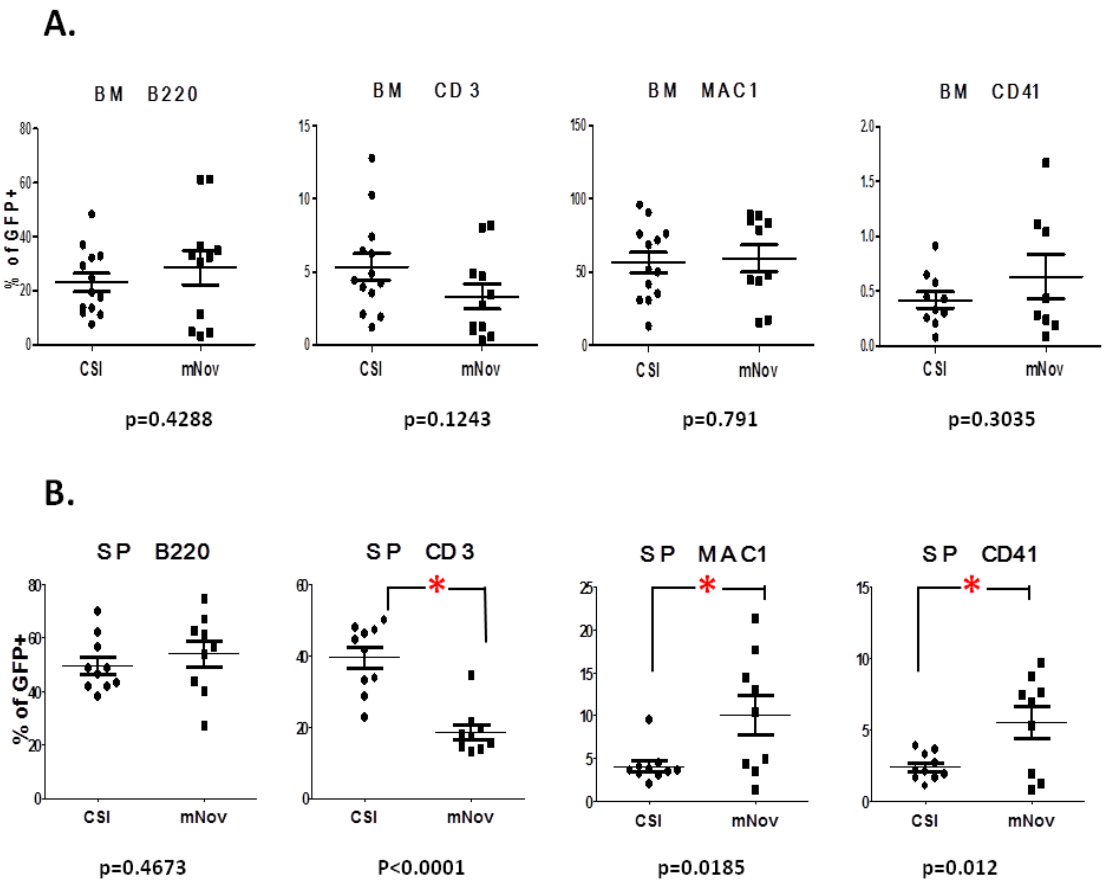


Figure.3.10: Lineage reconstitution of mNov KLS in bone marrow and spleen.

The lineage distribution of GFP+ donor cells in A. bone marrow and B. spleen after 4month of transplantation. In bone marrow, the lineage distribution was similar between CSI and mNov donors. In spleen, there was a significant reduction of CD3+ T cells reconstitution and increases of Mac1 and CD41 reconstitution. Each dot represents one recipient analysed. The line shows the mean of the percentage of each lineage within GFP+ donor cells with SEM. p-value is indicated under each group of comparison.

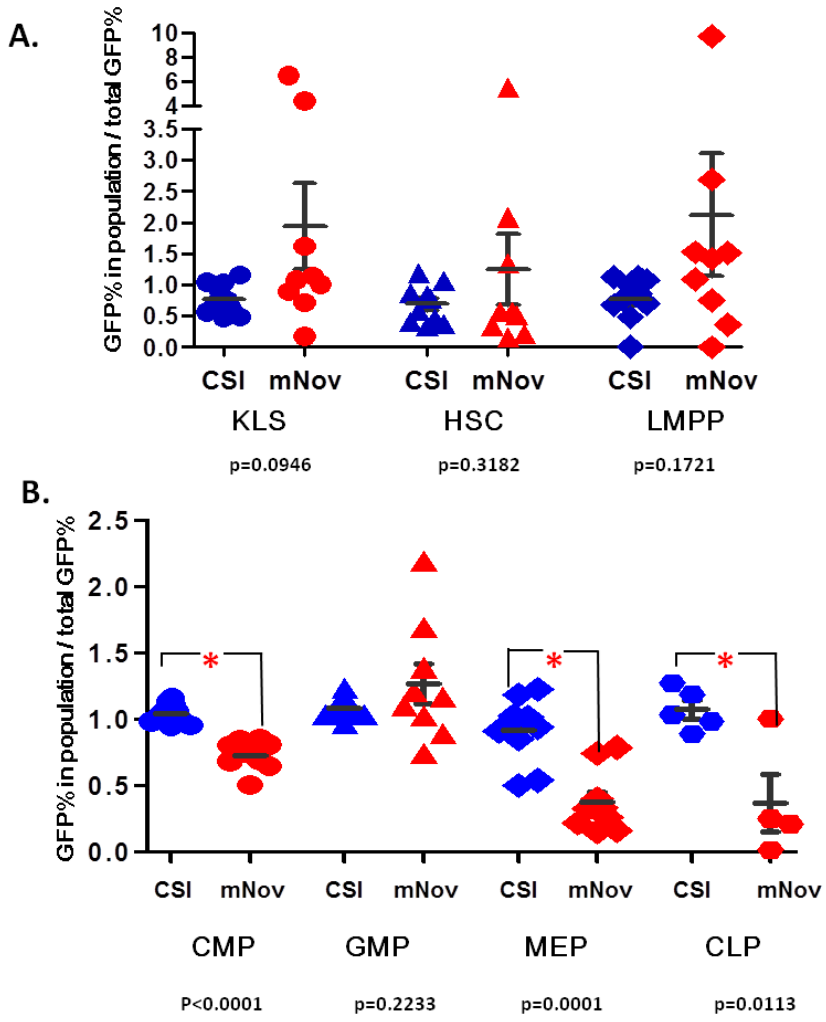


Figure 3.11: The frequency of HSC and progenitors in mNov KLS transplantation.

The data showed the ratio of the GFP percentage in each population compared to the total GFP percentage within the donor derived cells. The HSC population was analysed as FLT3- HSC (LT-HSC and ST-HSC).

A. The GFP+ percentages within KLS compartments were comparable to total GFP+ percentage within donors in both CSI and mNov cells. This result indicated normal KLS compartment frequencies within both CSI and mNov donor cells.

B. The GFP+ percentages in progenitors' compartments were reduced compared

to total GFP+ percentage within donors in mNov cells, except GMP progenitors. This result indicated an impaired differentiation of mNov cells toward CMP, MEP and CLP.

Each dot represents one recipient analysed. The lines show the mean of the percentage of each lineage within GFP+ donor cells±SEM. p-value is indicated under each group of comparison.

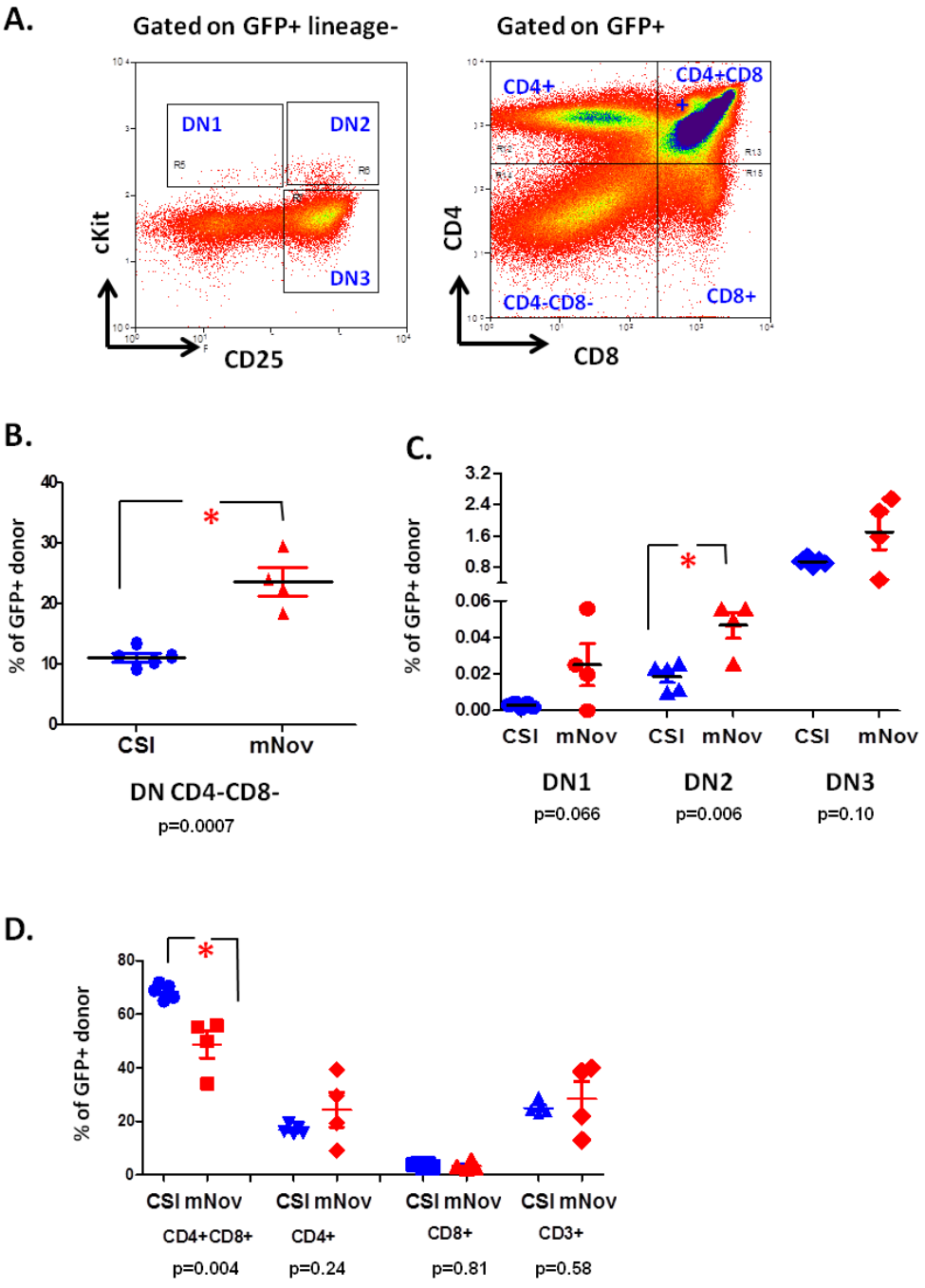


Figure.3.12: T cell developments of mNov donors in recipient thymus in bone marrow transplantation.

A. Representative FACS plots of T cell development in thymus. Lineage negative cells defined as B220-, Mac1-, Gr1-, CD4-, CD8-, CD3- and Ter119- were gated before defining DN subpopulations.

B. The frequencies of DN in GFP+ donors were increased in mNov cells. Each dot represents one recipient analysed. The line shows the mean of the percentage of each lineage within GFP+ donor cells ± SEM.

C. There was a clear trend of increase of DN subpopulation in GFP+ donors in mNov cells. Each dot represents one recipient analysed. The line shows the mean of the percentage of each lineage within GFP+ donor cells ± SEM.

D. The frequency of double positive cells in GFP+ donors was decreased in mNov derived cells. However, the frequencies of more mature single positive CD4+ or CD8+ cells were not altered. The frequency of CD3+ was similar between CSI and mNov donors. Each dot represents one recipient analysed. The line shows the mean of the percentage of each lineage within GFP+ donor cells ± SEM.

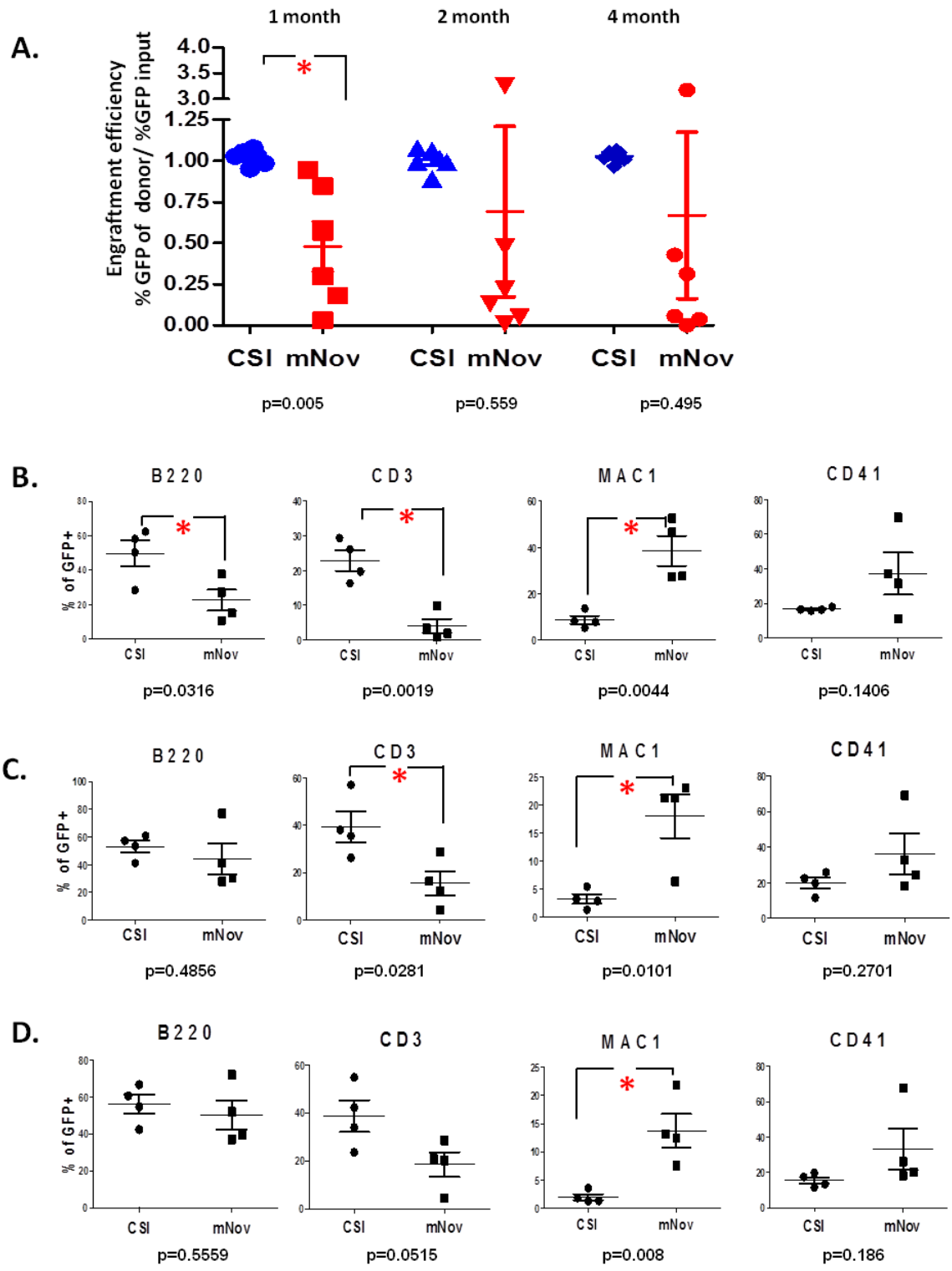


Figure.3.13: The secondary transplantation of mNov cells shows a reduced engraftment capacity.

A. The engraftment efficiency was calculated as the ratio of %GFP+ donor cells

in secondary recipients to %GFP+ donor cells in primary recipient. The results indicated a significant reduction of GFP+ cells after 1 month of secondary transplantation. 2 months and 4 months after secondary transplantation, the reduction of engraftment efficiency remained in all but one mNov recipients. n=6±SEM

B. The lineage distribution of GFP+ donor cells in peripheral blood after 1 month of secondary transplantation. The B220+ and CD3+ lymphoid cells were significantly reduced in mNov donor cells compared to CSI control donor cells. The frequency of Mac1+ was increased in mNov cells. Each dot represents one recipient analysed. The line shows the mean of the percentage of each lineage within GFP+ donor cells with SEM.

C. The lineage distribution of GFP+ donor cells in peripheral blood after 2 months of secondary transplantation. B220+ B cell reconstitution recovered to normal level in mNov donors compared to CSI control donors. CD3+ T cells were still significantly reduced in mNov donor derived cells. The frequency of Mac1+ was increased in mNov cells. Each dot represents one recipient analysed. The line shows the mean of the percentage of each lineage within GFP+ donor cells with SEM.

D. The lineage distribution of GFP+ donor cells in peripheral blood after 4 months of secondary transplantation. B220+ B cell reconstitution maintained at normal level in mNov donor cells compared to CSI control donor cells. CD3+ T cells were reduced in mNov donor cells, but not statistically significant. The frequency of Mac1+ was increased in mNov cells. Each dot represents one recipient analysed. The line shows the mean of the percentage of each lineage within GFP+ donor cells with SEM.

CHAPTER4.

EFFECTS OF KNOCKING DOWN *NOV* EXPRESSION IN HSPC

4.1 Introduction

Forced expression of *Nov* appeared to negatively regulate cell growth *in vitro* and overall engraftment efficiency *in vivo*; however, these results did not answer whether *Nov* is genetically required for HSC maintenance.

To determine the impact of Nov loss on cell intrinsic HSC function, I analysed the effects of Nov knockdown in HSC growth and differentiation *in vitro* and long term bone marrow reconstitution activity *in vivo*.

4.2 Results

4.2.1 LVTHM Novi construct and the limitation

The lentiviral LVTHM knockdown construct was chosen to test Nov knockdown effects. Schematic representation of the LVTHM vector for knocking down *Nov* is shown in Figure 4.1.A. Reporter GFP is driven by EF1α (elongation factor 1α) promoter and short hairpin interfering RNA (shRNA) is driven by H1 promoter. shRNA was designed by targeting at the C-terminal of Nov coding sequence with the sequence AAG(N)18TT.

In order to determine the effects of knocking down Nov expression on progenitor output, FDCPmix cells were transduced with control LVTHM and Novi lentivirus overnight. GFP+ cells were sorted 2 days after transduction. RT-qPCR results of FDCPmix cells confirmed that *Nov* expression was efficiently knocked down by 50% on average in the cells transduced by Novi

virus comparing to LVTHM control (Figure 4.1.B). In CFC assay, *Nov* knockdown did not affect total colony forming efficiency but resulted in a reduction of mixed (CFU-GEMM) colony output from 30% in LVTHM to 20% in Novi transduced cells (Figure 4.1.C.D).

To investigate the capacity of Novi HSC to proliferate and repopulate lethally irradiated animals, I performed a bone marrow reconstitution assay with KLS cells transduced with LVTHM or Novi virus. KLS cells were transfected with virus under SFEM medium supplemented with SCF, FLT3 and TPO for overnight. Transduced KLS cells were tail-vein injected into lethally irradiated recipient mice. The engraftment efficiency was checked after 1 month of transplantation by FACS analysis of peripheral blood. The results indicated a reduction of GFP expression in both LVTHM and Novi donor cells. In one of the experiments, the transduction efficiency was around 50% in both LVTHM and Novi KLS cells as checked 2 days after transduction (Figure 4.2.A). 1 month after transplantation, the average GFP+ percentage within the donor cells was only around 2% in LVTHM and 0.5% in Novi recipients in peripheral blood. Representative FACS plots are presented in Figure 4.2.B. At the end of 4 months, the GFP+ cells remained lower than 2% of donor cells in all recipients but one LVTHM recipient (Figure 4.2.C).

The overall low detection of GFP expression in recipient peripheral blood from both LVTHM and Novi cells prevented a detailed analysis of reconstitution and

a proper interpretation of lineage reconstitution. Therefore, LVTHM Novi transplantation experiments failed to provide any useful information to understand the effects of *Nov* knockdown in primary KLS cells.

4.2.2 LLX Novi knockdown construct

The LVTHM knockdown lentivirus showed an unexpected problem in the detection of GFP reporter in bone marrow transplantation. I therefore switched to the *LLX3.7* vector in which U6 promoter drives the shRNA and a separate CMV promoter for GFP expression. Schematic representation of LLX construct for knocking down *Nov* is shown in Figure 4.3.A.

The same shRNA sequence directed at the C-terminal of *Nov* coding sequence was designed and cloned into LLX vector. The GFP expression was monitored in FDCPmix for at least 3 weeks as shown in Figure 4.3.B.

RT-qPCR results of FDCPmix cells confirmed that *Nov* expression was knocked down and maintained at low level during the culture of FDCPmix Novi cells (Figure 4.3.C).

4.2.3 Cell growth of FDCPmix was not affected by knocking down of *Nov* expression

The FDCPmix cells transduced with LLX and Novi virus were purified for GFP+ cells and cultured in their normal self-renewal condition which was Fischer medium containing 20% horse serum and 2% IL3 conditioned medium. The

cell growth rate was monitored for 3 passages, and the results showed that there were no obvious defects in Novi FDCPmix cells in cell growth (Figure 4.4.A).

It has been reported that Nov protein is present in serum (Thibout.H, 2003) and, indeed, the western blots of supernatant from K562 culture detected a band at similar size as Nov protein while no Nov was detected in cell pellets (Chapter 3, Figure 3.2.B and C). Therefore, the lack of phenotype in cell growth from Novi cells could be due to the presence of homologue Nov protein in serum in the culture condition. In order to test this hypothesis, I tested the cell growth of FDCPmix in a serum free medium SFEM supplemented with 10ng/ml IL3. During the culture of FDCPmix in serum free condition, no obvious change was observed in Novi cells compared to LLX control (Figure 4.4.B). This result indicated that, although highly expressed in FDCPmix cells, *Nov* was dispensable for FDCPmix cell growth with or without serum.

4.2.4 *In vitro* analysis of knocking down *Nov* in KLS

In order to determine the consequences of *Nov* expression knockdown on primary HSC cells, I tested its effects in KLS cells. KLS are a heterogeneous population which contains LT-HSC, ST-HSC and LMPP. Previous work showed that these three primitive populations are the only populations expressing *Nov* along the haematopoietic hierarchy (Chapter 3, Figure 3.1).

4.2.4.1 Proliferation assay and FACS analysis

I firstly tested the proliferation rate of KLS in expansion condition of SFEM with 100ng/ml SCF and 10ng/ml FLT3. The cell growth rate was monitored after 7-9 days of virus transduction. Knocking down Nov in KLS cells showed no obvious effects in cell growth compared to LLX control (Figure 4.5.A). This result was in agreement with the observation of Nov knockdown in FDCPmix cells (Figure 4.4.A.B), which indicated that Nov was dispensable for cell growth *in vitro*.

In the previous chapter, overexpression of mNov in KLS could increase spontaneous differentiation toward CD41+ megakaryocyte *in vitro*. However, when cultured in the same condition, proliferated Novi cells showed that *Nov* knockdown cells contained a similar percentage of Gr1+ cells (myeloid) and CD41+ cells (megakaryocyte) (Figure 4.5.B).

4.2.4.2 CAFC and CFC assay with KLS Novi cell

The function of Novi KLS cells was tested *in vitro* with CAFC assay and CFC assay for their self-renewal and differentiation outcome.

In CAFC assay, GFP+ KLS transduced with LLX or Novi virus were sorted directly onto stroma in 96 well plates at 1:2 serial dilutions. The cobble-stone forming areas were scored 5 weeks later. Of the two experiments performed, there seemed to be no difference between LLX and Novi cells in CAFC forming

capacity. These results indicated that CAFC frequency of KLS was not affected by *Nov* knockdown (Figure 4.6.A).

In CFC assay, the total colony forming frequency was comparable between Novi and control cells (Figure 4.6.B). However, in agreement with the data obtained from CFC assay with LVTHM-Novi FDCPmix cells (Figure 4.1.D), the mixed-lineage colony output was reduced in *Nov* knockdown cells. When the colonies were plated again, there was an indication of a mild increase in secondary colony forming efficiency, but it is not statistically significant (Figure 4.6.C).

In vitro analysis of Nov knockdown in both FDCPmix cells and primary KLS cells showed that Nov was dispensable in cell growth, CAFC frequency and colony forming efficiency.

4.2.5 Bone marrow transplantation of KLS transduced with Novi virus

4.2.5.1 The engraftment efficiency of Novi KLS was comparable to LLX control

To investigate the capacity of HSC transduced with Novi virus to repopulate lethally irradiated animals, I performed a bone marrow reconstitution assay with KLS cells transduced with LLX or Novi virus. KLS cells were transfected with virus under SFEM medium supplemented with SCF, FLT3 and TPO

overnight. Transduced KLS cells were injected into lethally irradiated recipient mice through tail vein. The engraftment efficiency was checked after 1 month by FACS analysis of peripheral blood. Although the expression of GFP was maintained and could be detected *in vitro* for at least 2 weeks in transduced KLS and for more than 2months in transduced FDCPmix cells (data not shown), the GFP level in recipient mice was reduced by almost 40% in both LLX and Novi donors. There was a further reduction of GFP percentage from both donor cells, where there was only 20% of input GFP percentage detected two months after transplantation. The GFP percentage remained at a similar low level throughout the rest period of the experiment in both LLX and Novi recipients (Figure.4.7.A).

Two possibilities could be considered to explain this phenotype of reduced GFP level. The first is that the reduction of GFP level was due to the limitation of lentiviral construct where the promoter was prone to be inactivated *in vivo* by methylation (Almarza E, 2007; Gilhan D.E, 2010; Gonzalez-Murillo A.2010). The second possibility is that the transduced cells were heavily contaminated by progenitors which failed to long term reconstitute in recipient bone marrow and resulted in a gradual reduction of engraftment. In a similar project in our group, we purified GFP+ and KLS double sorted cells before transplantation in order to avoid the contamination with transduced progenitors. In that experiment, the percentage of GFP + cells within LLX donor was still reduced

as well (data not shown). This result argued against the possibility that contamination was the possible reason for reduced GFP+ engraftment. Despite the reduction of GFP percentage, because the reduction of GFP percentage were similar and stable in both LLX and Novi donors, I considered the engraftment efficiency as reliable and valid by comparing GFP+ cells in recipients of both groups. The data observed so far indicated that Novi KLS did not affect the engraftment efficiency in bone marrow transplantation.

4.2.5.2 The lineage reconstitution capacity were normal in Novi KLS comparing to LLX control

The lineage distributions in peripheral blood were analysed by FACS for B220 (B cell), CD3 (T cell), Mac1 (myeloid cell) and CD41 (megakaryocytic cell) expression at 1month, 2 month and 4 month after transplant (Figure 4.7.B). The results showed that, at each time point, the percentages of each lineage within the GFP+ cells were similar between LLX and Novi recipients. In contrast to the lineage bias in mNov KLS in transplantation, where there was a reduced CD3+ T cells reconstitution and an increased Mac1+ myeloid reconstitution, there was no effects in lineage reconstitution by knocking down of Nov in KLS (Figure 4.7.B).

After 4 months of transplantation, bone marrow and spleen cells were collected and FACS analysed for lineage reconstitution. The results were consistent with the peripheral blood results where the percentages of each

lineage were comparable between LLX and Novi KLS derived cells in both bone marrow and spleen (Figure 4.8.).

These results indicated that knocking down of Nov in KLS cells did not affect their lineage differentiation in transplantation *in vivo*.

4.2.5.3 The HSC and progenitor frequencies were similar in LLX and Novi donor cells

In order to understand the effects of Nov knockdown during the most primitive levels of the haematopoietic hierarchy, I analysed the frequency of HSCs and progenitors within the LLX and Novi transduced cells in bone marrow. The results showed that the frequency of HSC and progenitors were comparable between the LLX and Novi cells. These results were consistent with the engraftment efficiency and lineage reconstitution in peripheral blood, bone marrow and spleen and suggested that Nov knockdown in KLS didn't affect the lineage choice and differentiation of HSC *in vivo* (Figure 4.9.).

4.2.5.4 Novi cells showed a similar reconstitution efficiency in secondary transplant assay

In order to test the Novi HSC self-renewal capacity, I performed the secondary transplantation of Novi KLS cells. Bone marrow collected from first recipient was injected into secondary recipient through tail vein. The engraftment

efficiency was calculated as the ratio of GFP% in secondary recipient to GFP% in first recipient.

The GFP expression level decreased mildly in secondary recipients comparing to their first recipients (Figure 4.10.A). Between LLX and Novi groups, the engraftment efficiencies were similar. Although there was an increase of Mac1+ and CD41+ cells derived from Novi donors after 1 month of transplantation, this phenotype disappeared after 2 months of transplantation which indicated that the lineage bias observed at 1 month was a transient phenotype induced by Nov knockdown. 6 months after the secondary transplantation, the GFP+ percentage were very low in some recipients (<0.5% of total donor CD45.2 cells) which prevented a proper analysis for lineage distribution (Figure 4.10.B). Although only 3 recipients in LLX group and 2 in Novi group were valid for analysis of lineage distribution, the results showed no difference between LLX and Novi cells.

Taken together, these results showed that Novi cells had a normal function in long term reconstituting secondary recipients and a normal lineage differentiation capacity. These data suggested that Nov knockdown in HSC didn't affect their self-renew and differentiation capacity which was in line with the observations of unaltered HSC and progenitor frequencies in first transplanted recipients.

4.3 Summary and discussion

In this chapter, I tested the effects of *Nov* knockdown in HSC and progenitors. The results of knocking down *Nov* in FDCPmix did not affect the cell growth and total colony forming efficiency in CFC assay, but reduced the mix colony output. Knocking down of *Nov* expression in primary KLS cells did not affect cells growth and CAFC forming efficiency. The total CFC activity was not affected, but the mix colony output was reduced which was also shown in FDCPmix as well. Bone marrow transplant experiment showed a similar reconstitution efficiency and lineage distribution in both LLX and Novi donor KLS cells. The secondary transplantation of Novi cells showed normal reconstitution efficiency. These data indicated Novi HSC function was normal compared to LLX control, indicating that *Nov* may be dispensable for HSC function.

However, there is a possibility that may mislead the results of *Nov* knockdown in HSC in bone marrow transplantation and also those assays with serum. In the bone marrow transplantation, the recipient animals were wild type and could produce Nov protein. Novi HSC engrafted into recipients may take up Nov from their microenvironment and function normally as a result.

Another limitation of the transient knockdown of Nov by lentiviral approach is introduced by lack of suitable antibodies that are specific to Nov protein and can detect weak expression of Nov protein (data not shown). For this chapter, I

have tried several commercially available antibodies, but failed to detect the knockdown level of Nov protein, even though the RT-qPCR results clearly indicated that, at mRNA level, Nov expression has been effectively reduced. Half-life of Nov protein within alived cells is not clear. Therefore, the possibility that Novi cells may still contain enough active Nov proteins to maintian their key functions can not be excluded.

In order to understand the function of *Nov* in haematopoiesis at steady state and without extrinsic or residue *Nov* activity, in the next chapter, I decided to look at the haematopoiesis and HSC function using Nov^{3del} mutant mice.

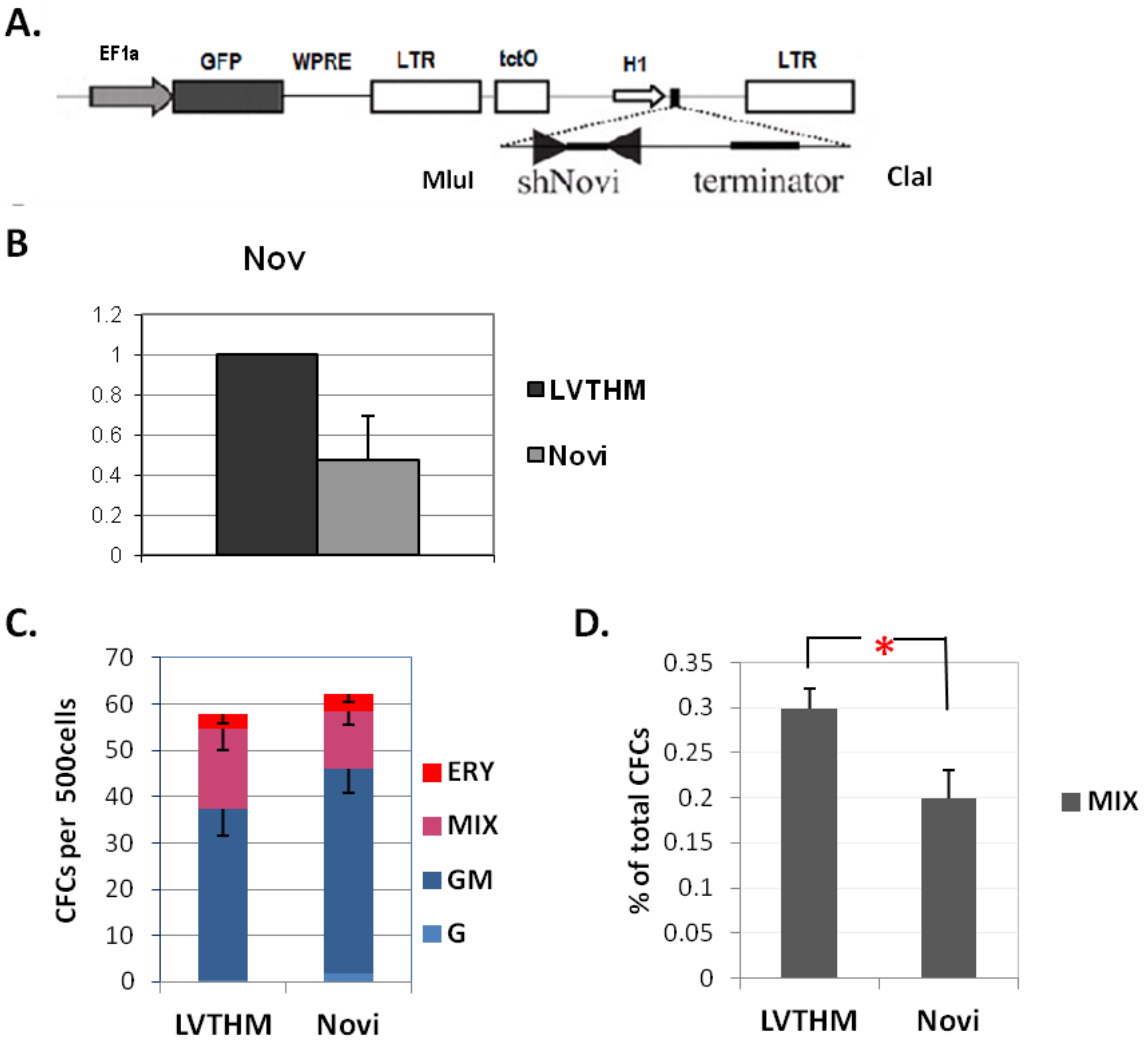


Figure. 4.1: LVTHM shRNA virus constructs and effects in LVTHM-Novi transduced FDCPmix cells.

A. Schematic representation of the pLVTHM vector. (EF1α: Promoter for elongation factor 1α; GFP: Green fluorescent protein; WPRE: woodchuck hepatitis virus post-transcriptional regulatory element; LTR: long-terminal repeat; tetO*: tet* operator; H1: Histone H1 promoter ;)

B. RT-qPCR of FDCPmix cells transduced with LVTHM-Novi virus. The results confirm the effect of the shRNA and showed 50% of remaining endogenous expression on average. n=3

C. *Nov* knockdown does not affect the colony forming efficiency in CFC assay. GFP+ cells were plated in M3234 with 10ng/ml rmIL3, 100ng/ml rmSCF and 10U/ml hEPO. n=3±SD

D. *Nov* knockdown impairs mixed colony output in FDCPmix CFC assay. n=3±SD

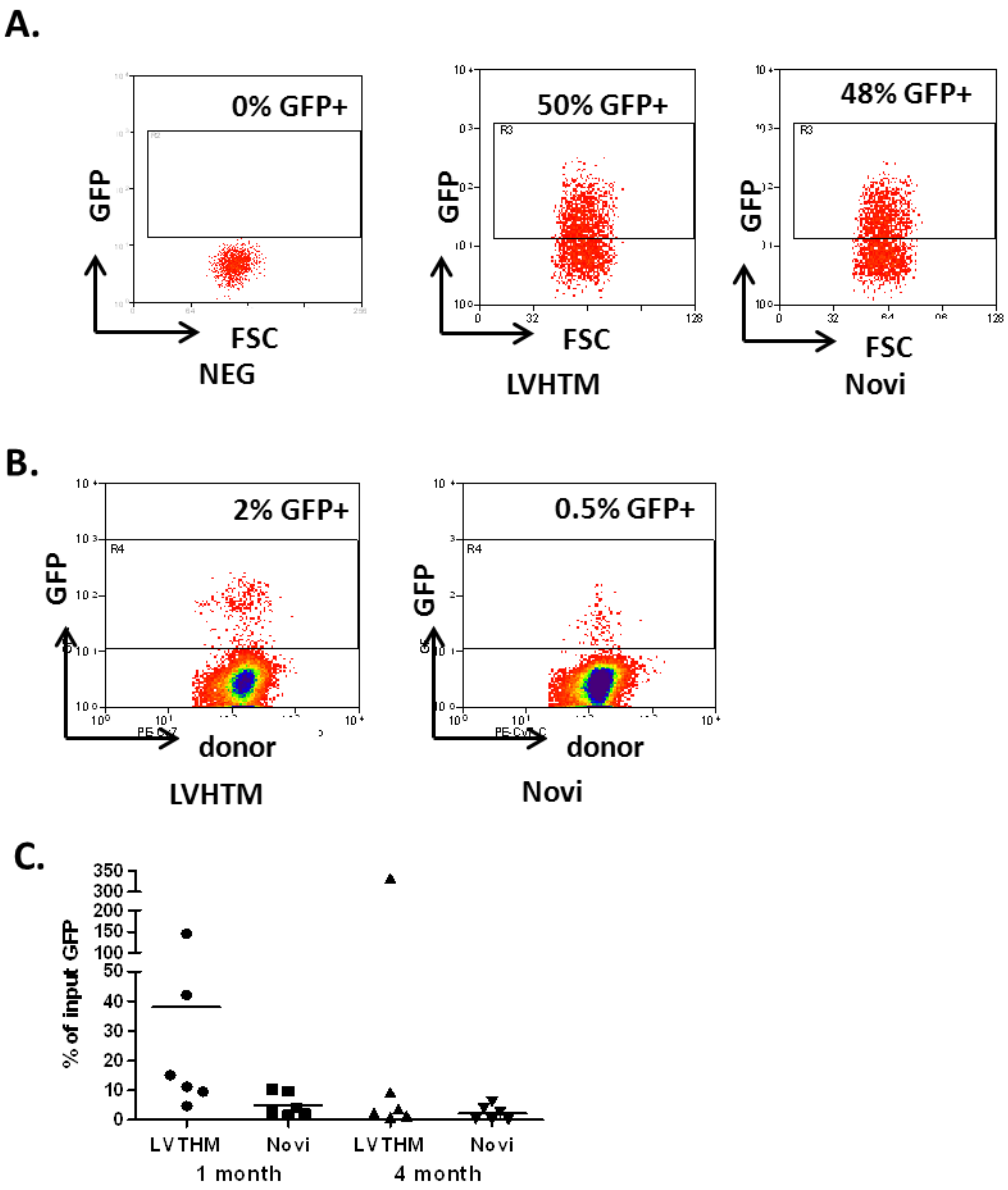


Figure. 4.2: Bone marrow transplantation of KLS transduced with LVTHM-Novi virus.

A. Representative flow cytometry plots of KLS with LVTHM Novi virus shows transduction efficiency.

B. Representative flow cytometry plots show the GFP percentage in donor derived cells after 1 month of bone marrow transplantation. This result indicates a significant reduction of GFP+ cells in donor derived cells.

C. Summary of GFP+ percentage remaining in donor cells at 1 month and 4 month. There were less than 1% of GFP+ cells in donor derived cells at 4 month from both LVTHM and Novi KLS transplantation except 1 LVTHM KLS recipient mouse. The low frequency of GFP+ cells in both Novi and control recipients make it difficult to analyse the lineage distribution and draw a conclusion on the effects of Nov knock-down on KLS cells in bone marrow transplantation. Each dot represents one recipient analysed. The line shows the mean of the percentage of input GFP.

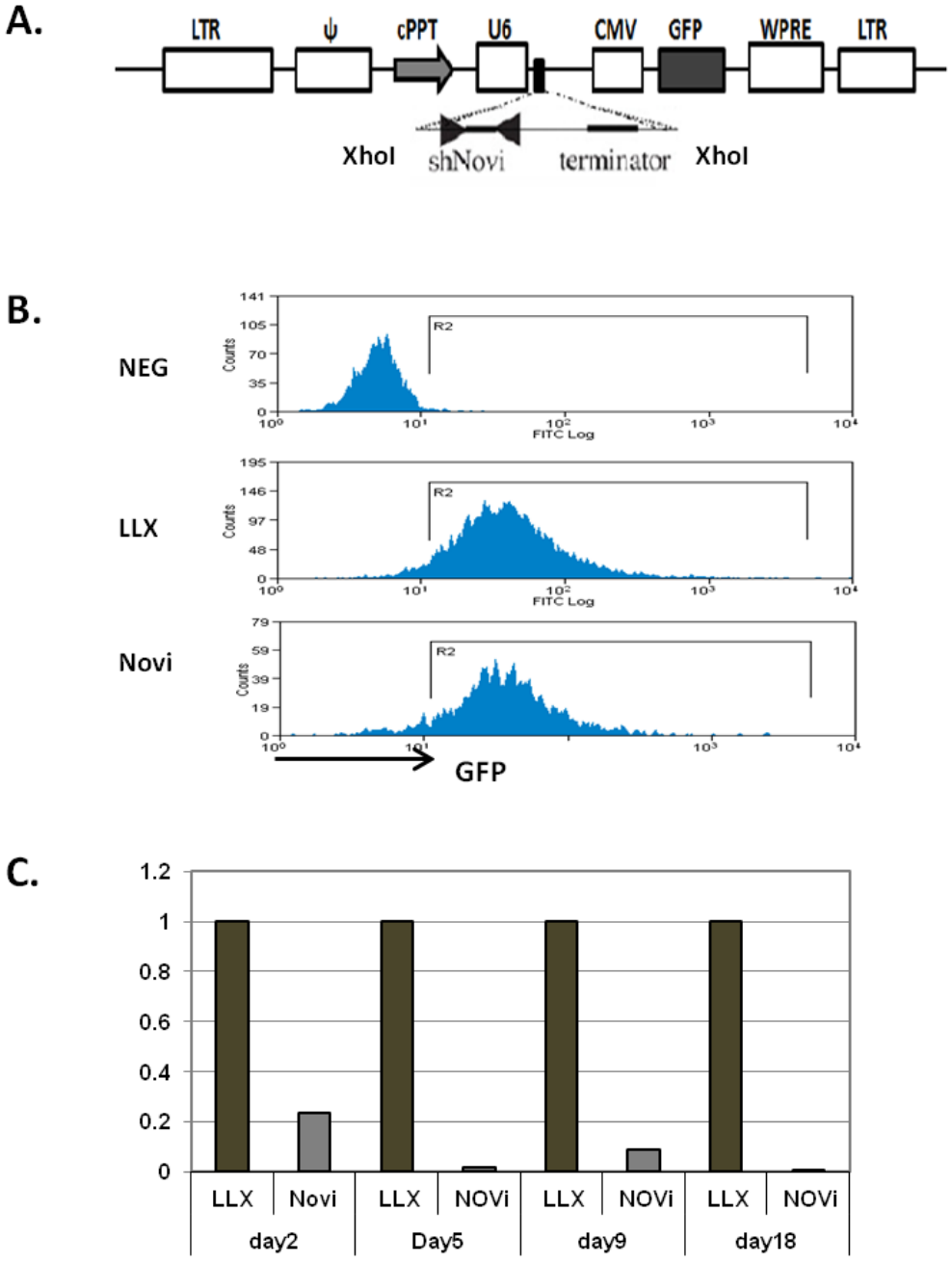


Figure. 4.3: LLX3.7 shRNA virus construct and consistent expression in FDCPmix cells.

A. Schematic representation of the pLLOX3.7 vector (LLX); LTR: long-terminal repeat; Ψ: HIV packaging signal; CPPT: central polypurine track; U6: U6 promoter; CMV: cytomegalovirus promoter; GFP: enhanced GFP; WPRE:

woodchuck hepatitis virus post-transcriptional regulatory element.

B. Expression of GFP in FDCPmix 18 days after GFP+ sort.

C. RT-PCR check of *Nov* expression in Novi FDCPmix cells after GFP+ sort and the result shows effective *Nov* knock-down even after 18 days.

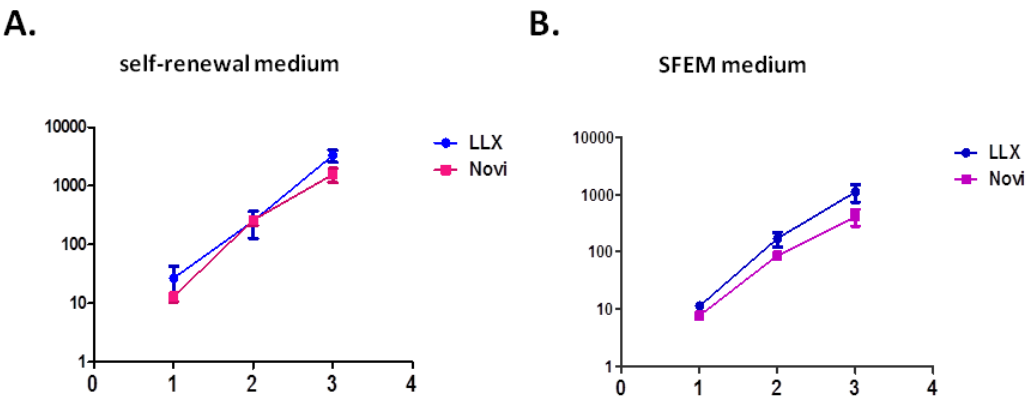


Figure. 4.4: Knock down of *Nov* in FDCPmix cells did not affect cell growth.

A. The cell growth rate of Novi FDCPmix in complete medium containing horse serum and 2% IL3 conditional medium. The cell growth rate was monitored for 3 passages, and the results showed that there were no obvious defects in Novi FDCPmix cell growth. n=2±SEM

B. The cell growth rate of Novi FDCPmix cells in SFEM medium with 10ng/ml rmIL3. The cell growth rate was monitored for 3 passages, and the results showed that there were no obvious defects in Novi FDCPmix cell growth in serum free condition. n=2±SEM

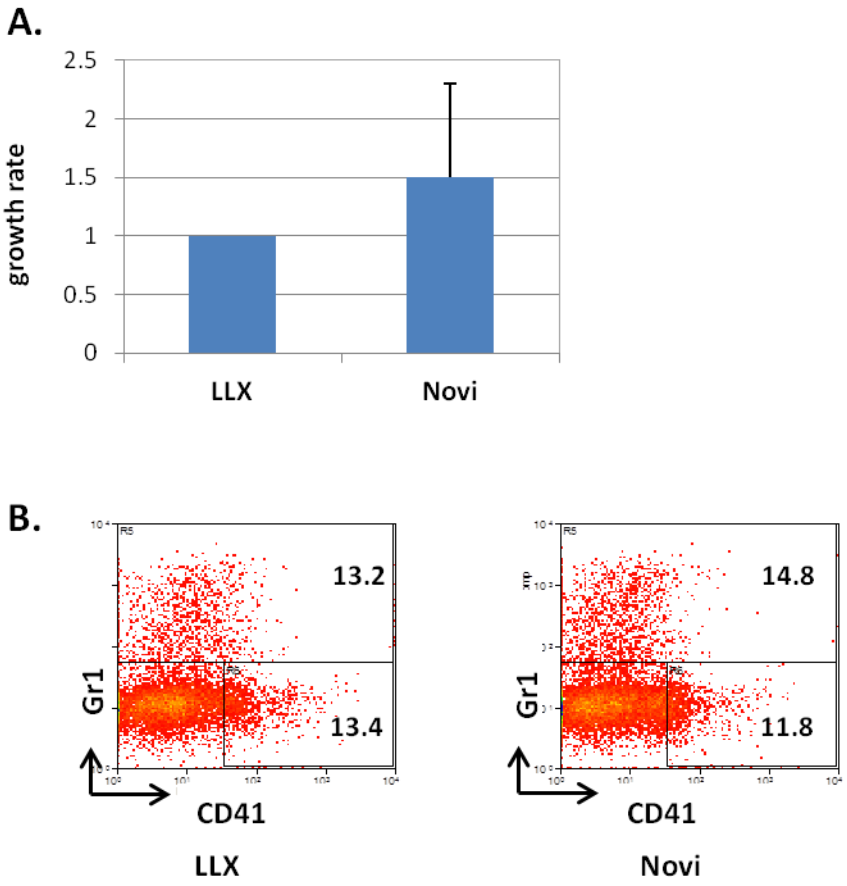


Figure. 4.5: KLS Novi cells showed no obvious change in cell growth.

A. Cells growth rate of viral transduced KLS cells cultured in SFEM with 100ng/ml SCF and 50ng/ml FLT3. Proliferated cells were counted 9 days after transduction with LLX-Novi virus. There was no obvious difference in cell growth between LLX and Novi transduced cells. n=2±SD

B. Representative FACS plots of KLS proliferated cells showed no difference in Gr1 and CD41 expression in LLX and Novi cell in expansion condition.

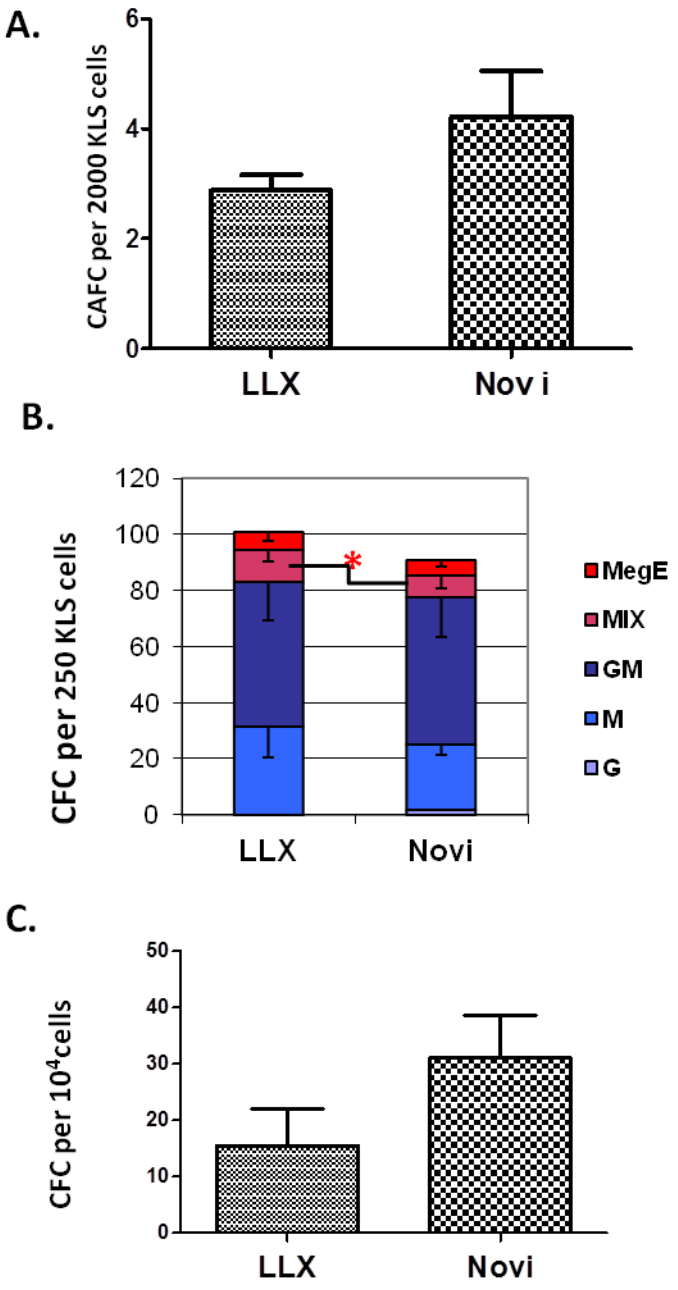


Figure. 4.6: KLS Novi cells showed normal CAFC and CFC frequency.

A. GFP+ sorted KLS cells were cultured on stroma to test their CAFC forming capacity at 5 weeks. The result shows no obvious difference between control and Novi cells. n=2±SEM

B. GFP+ Novi KLS cells were plated in M3234 with Weissman cytokine cocktails (10ng/ml rmIL3, 10ng/ml rmIL11, 100ng/ml rmSCF, 10ng/ml rmG-CSF,

10ng/ml rmTPO and 10U/ml hEPO). The total colony number in Novi KLS cells is similar to LLX cells, but the mix colony output is reduced to a statistically significant degree in Novi cells. n=3±SEM, *p=0.043

C. Secondary plating of CFC assay, Novi cells, despite the reduction in mixed colony output, showed no statistically significant difference in colony forming efficiency. n=3±SEM, p=0.20

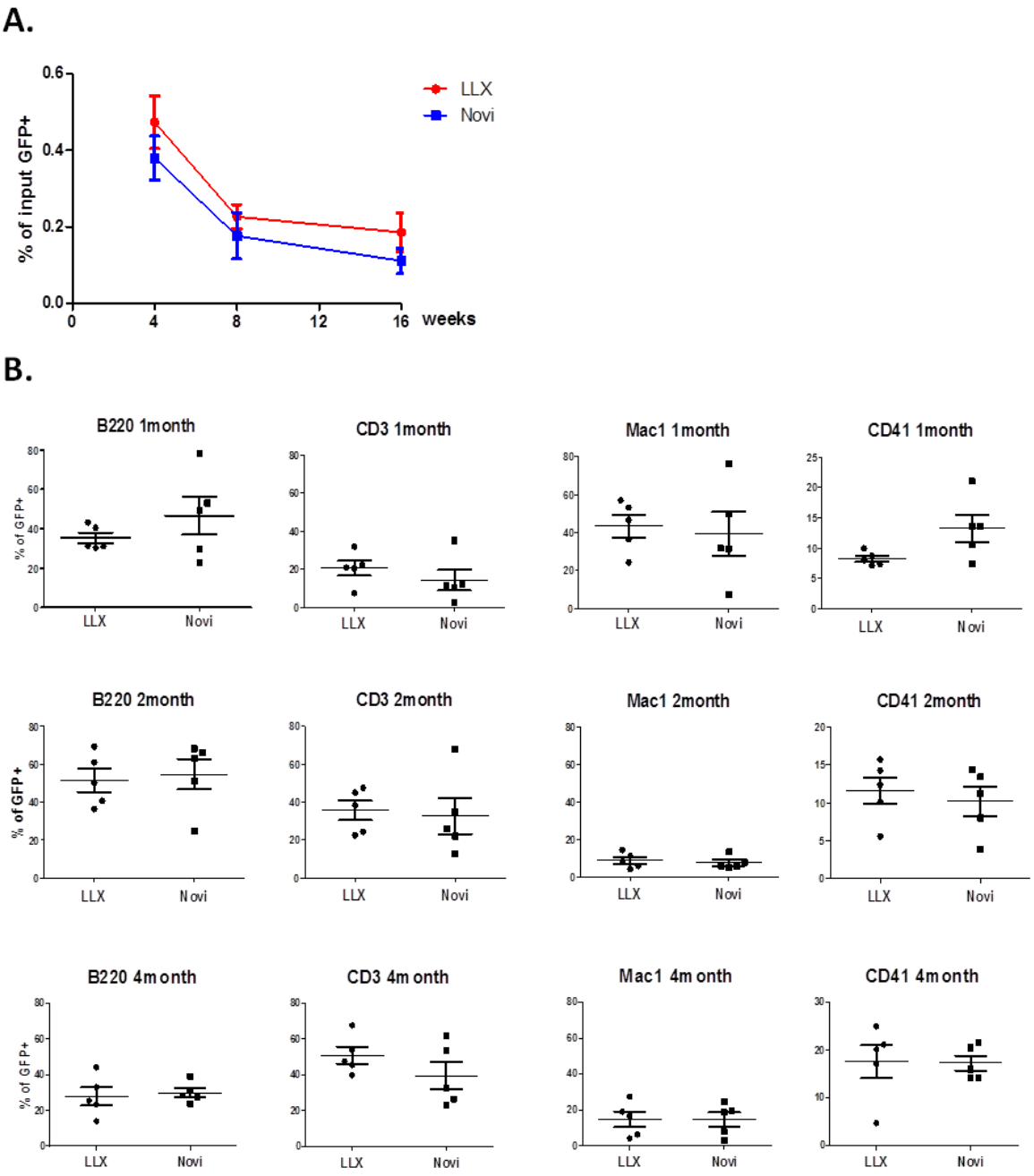


Figure. 4.7: Bone marrow transplantation, KLS Novi cells showed a similar reconstitution capacity to LLX controls.

A. The engraftment efficiency of KLS transduced with LLX or Novi. The percentage of GFP+ cells within donor cells were compared with the input GFP percentage. The results indicated a reduction of GFP+ cells during the

period of transplantation in both LLX and Novi cells. n=5. The line shows the mean of the percentage of input GFP with SEM.

B. The lineage distribution of GFP+ donor derived cells in peripheral blood at each time point indicated. The FACS results showed that there were no differences in B cell (B220+), T cell (CD3+), myeloid cell (Mac1+) and megakaryocytic cell (CD41+) differentiation between Nov knockdown cells and the controls. Each dot represents one recipient analysed. The line shows the mean of the percentage of each lineage within GFP+ donor cells.

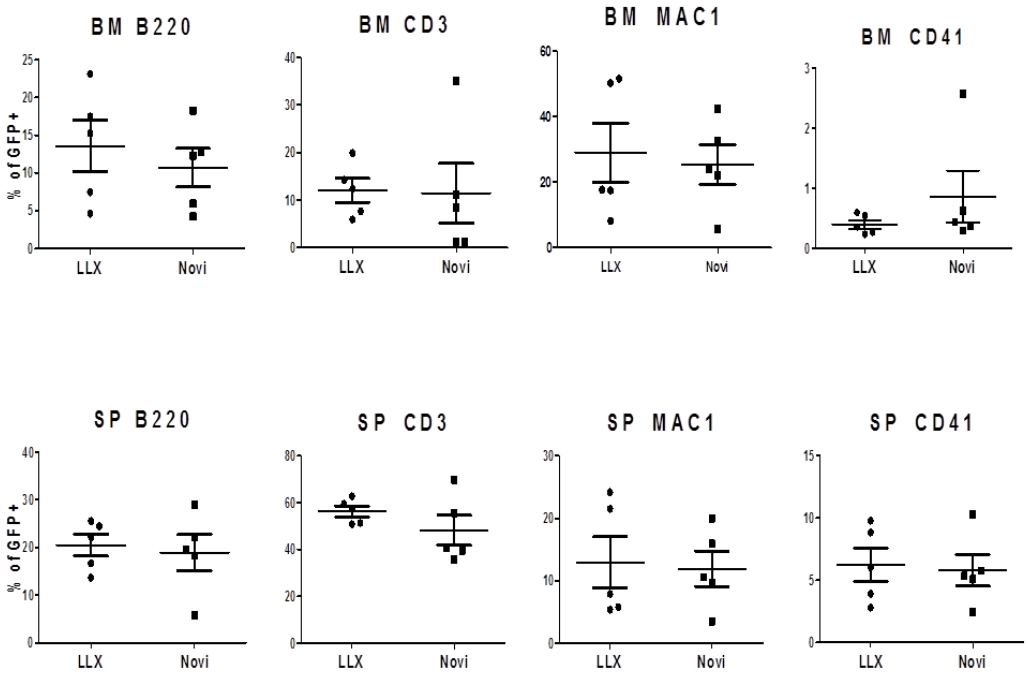


Figure. 4.8: In long term bone marrow transplantation, Novi cells showed a normal lineage distribution in bone marrow and spleen.

The lineage distribution of GFP+ donor cells in bone marrow and spleen 4 months after transplant. Each dot represents one recipient analysed. The line shows the mean of the percentage of each lineage within GFP+ donor cells with SEM.

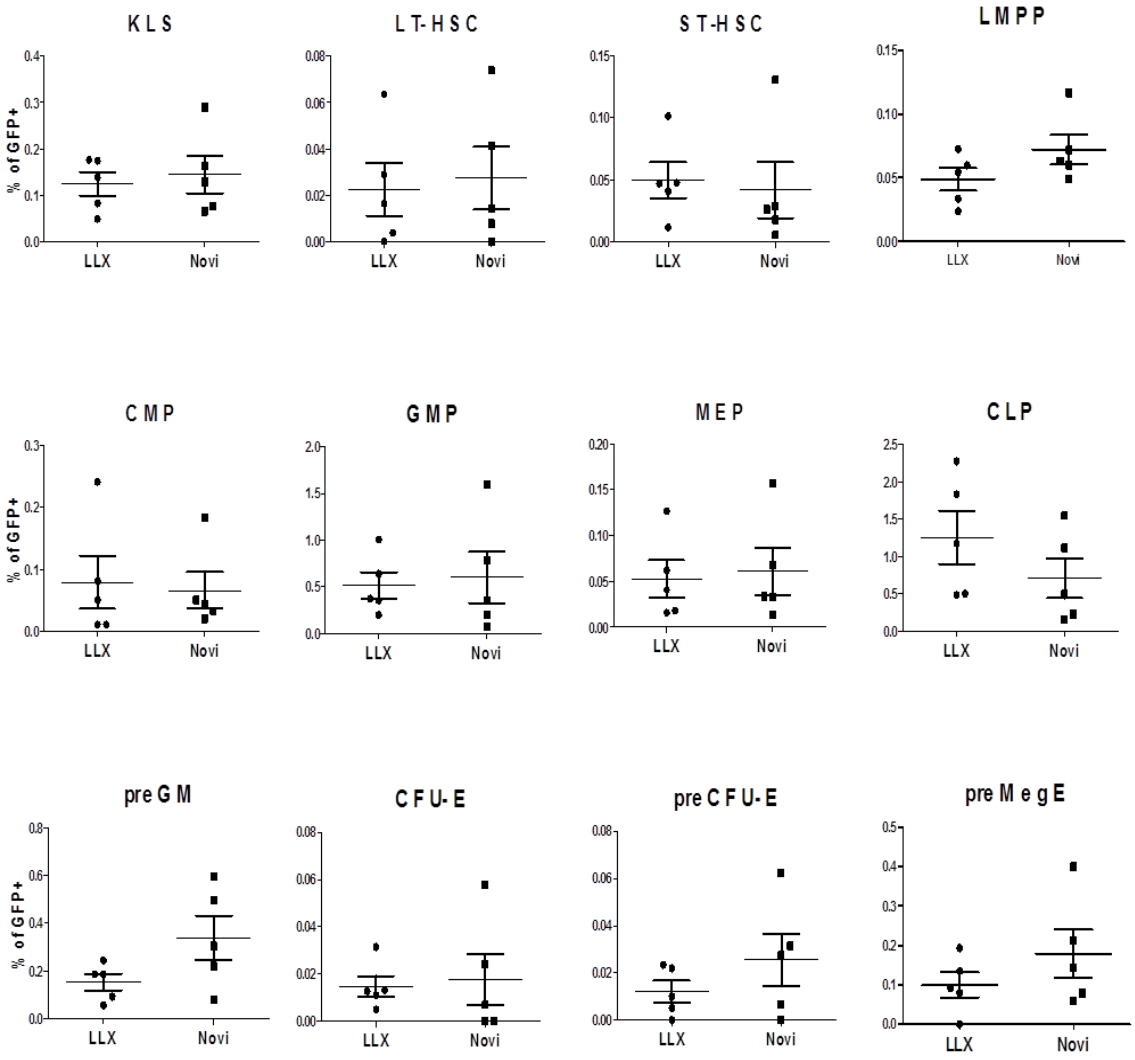


Figure. 4.9: In long term bone marrow transplantation, KLS Novi cells showed a similar HSC and progenitor frequency in bone marrow.

The frequencies of HSC and progenitors within GFP+ donor cells in bone marrow 4 months after transplant were similar between LLX and Novi cells. Each dot represents one recipient analysed. The line shows the mean of the percentage of each lineage within GFP+ donor cells with SEM.

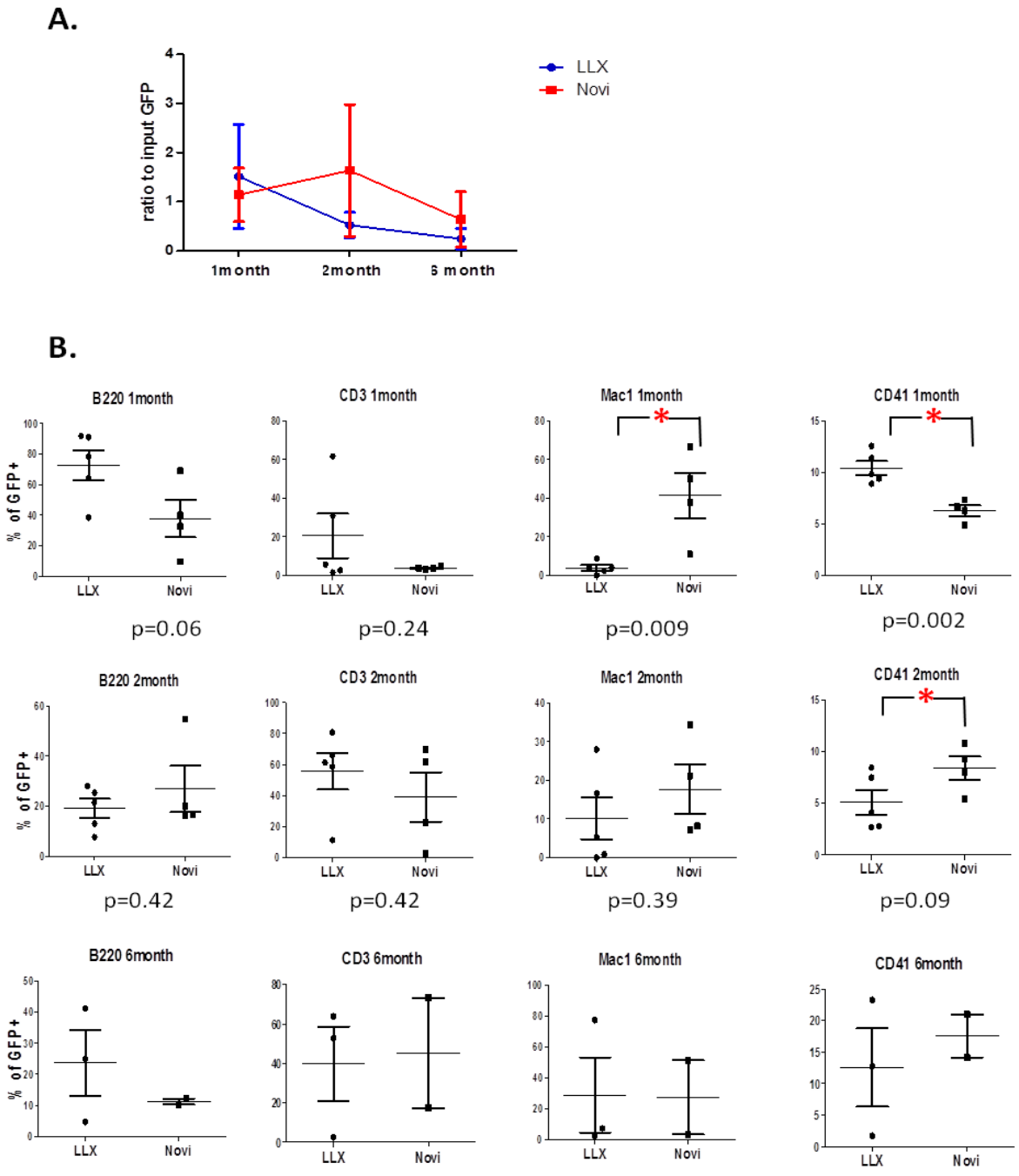


Figure. 4.10: In secondary transplantation, KLS Novi cells showed a similar reconstitution capacity as LLX control KLS.

A. The engraftment efficiency of LLX and Novi donor in secondary recipients are similar. There was a mild and continuous decrease of GFP+ percentage within the CD45.2 donors derived cells which was also observed during the first

transplantation. The percentages of GFP+ cells within donor derived cells were comparable between the LLX and Novi cells. These results indicated that Novi HSCs have a similar secondary reconstitution capacity to the controls. n=4; the line shows the mean of the percentage of input GFP with SEM.

B. The lineage distribution of GFP+ donor derived cells in peripheral blood at each time point indicated. There was a statistically significant increase of Mac1 output and a significant reduction of CD41 output after 1 month of secondary transplantation. However, this lineage bias disappeared at 2 months, and there were similar lineage distributions from Novi and LLX control. 6 months after the secondary transplantation, the GFP+ percentage were very low in some recipients (<0.5% of donor CD45.2 cells), and only 3 recipients in LLX group and 2 in Novi group were valid for analysis of lineage distribution. The results showed no difference in lineage distribution between LLX and Novi cells. Each dot represents one recipient analysed. The line shows the mean of the percentage of each lineage within GFP+ donor derived cells with SEM. p-value is indicated under each comparison group.

Chapter5.

Analysis of *Nov*^{3del} mutant mice

5.1 Introduction

The Nov mutant mice (*Nov*^{3del}) were generated by replacing *Nov* exon 3(VWC domain) with a TK neomycin cassette which resulted in production of a barely detectable level of mutant NOV protein instead of full length NOV protein (Heath E, 2008). *Nov*^{3del} mutant mice exhibit several abnormalities including enlarged vertebrae, elongated long bones, enlarged and abnormal modelled endocardial cushions in heart and muscle atrophy. Primary embryo fibroblast (PEF) from *Nov*^{3del} mutant embryos showed enhanced chondrogenesis and osteogenesis. Our collaborators also observed some features of early aging in *Nov*^{3del} mice indicating a general role of Nov in maintenance of tissue viability in adults.

In this chapter, I characterized the haematopoiesis of *Nov*^{3del} mutant mice in order to understand Nov function *in vivo* under homeostatic conditions. The complete blood test was performed to examine the erythroid and megakaryocytic differentiation and function. The myeloid and lymphoid differentiations were assessed by FACS for lineage distribution in peripheral blood and bone marrow. The frequencies and function of *Nov*^{3del} HSC and progenitors were determined by FACS analysis and *in vitro* CAFC and CFC assay. The *Nov*^{3del} HSC function was further tested in bone marrow reconstitution assay and serial transplantation. The haematopoiesis in aged *Nov*^{3del} mice were also examined by FACS analysis and bone marrow

reconstitution assay.

5.2 Results

5.2.1 Breeding of *Nov* ^{3del} mutant mice

The original paper describing *Nov*^{3del} mutant mice reported that 35% of heterozygote and 55% of homozygote were lost prior to postnatal day 10, resulting in only 17% homozygote and 46% heterozygote from a total of 30 live born. However, during the period of expanding the *Nov*^{3del} colony in Oxford, the loss of homozygote and heterozygote within the live born pups were not observed. Within the 241 offspring from mating of F1 and F2 *Nov*^{3del} heterozygote, there were 108 mice were heterozygote, 67 homozygote and 66 wild type, representing 45%, 28% and 27% of total respectively.

5.2.2 *Nov*^{3del} mutant mice showed normal blood counts and lineage distribution

The blood tests were performed to measure the peripheral blood counts in *Nov*^{3del} mutant mice and their wild type littermates. Table 5.1 showed the average readings of blood tests for wild type, heterozygous and homozygous mice with standard deviation. In general, the *Nov*^{3del} mutant mice had normal blood counts in all parameters compared to their wild type littermates.

The lineage distributions of white blood cells in peripheral blood were then checked by FACS analysis. The results (Figure 5.1.) showed that the distributions of both lymphoid B-cells (B220+), T-cells (CD3+) and myeloid cells (Mac1+) were similar in *Nov*^{3del} homozygous mice and wild type controls. Interestingly, in heterozygous peripheral blood, there is a tendency of decreased frequency of B-cells (B220+) although it is not statistically significant. And there was a statistically significant increase of T-cells (CD3+) frequency in heterozygous peripheral blood which was 60% comparing to around 40% in their wild type and homozygous litter mates.

The original report described a phenotype of enlarged long bone in *Nov*^{3del} mutant mice. However, of all the animals I analysed, there were no obvious differences of the sizes of femur and tibia noticeable between wild type and mutant mice. Other than the size, there were also no differences in total bone marrow cellularity. On average, the total number of mononuclear cells from one femur of each mouse is around 1.5×10^7 cells and 1.7×10^7 cells in wild type and homozygous respectively (Figure 5.2.A).

In the bone marrow, the lineage distributions of myeloid and lymphoid cells were again similar between wild type and homozygous animals as shown in Figure 5.2.B. Consistent with the observation in peripheral blood, there was a mild decrease of B220+ cells in heterozygous bone marrow, though no difference in CD3+ cells (Figure5.2.B).

5.2.3 FACS analysis showed an increased frequency of HSC in *Nov*^{3del} bone marrow

Given that *Nov* is expressed only in the KLS compartments of haematopoietic cells, the next question investigated was whether loss of *Nov* affected the frequency of the various HSC/HPC subpopulations in the bone marrow.

On average, the percentage of KLS cell in total bone marrow in wild type mice was around 0.41%; 0.63% in homozygous bone marrow. The increase of KLS frequency was mild (1.5 fold) but statistically significant. The KLS population is a heterogeneous population and can be dissected into more primitive stem cell population and multipotent lymphoid and myeloid progenitors with the surface marker of FLT3. When dissecting the KLS compartment into LT-HSC, ST-HSC and LMPP, the results indicated that this frequency increase was due to the increase of LT-HSC and ST-HSC compartments, but not LMPPs. In heterozygotes, the increases of all the compartments were less obvious and not statistically significant (Figure 5.3).

Downstream of haematopoietic stem cells differentiation, the percentages of myeloid progenitors (CMP, GMP and MEP) were similar between homozygous and wild type animals. However, there seemed to be a mild increase in all the progenitor populations in heterozygote bone marrow (Figure 5.4).

5.2.4 *In vitro* assays showed an increased CAFC frequency but normal CFC output from *Nov*^{3del} bone marrow

Limiting dilution CAFC assay is widely used to test the frequency of HSCs *in vitro*. Cobble-stone-forming-areas were scored after 5 weeks and the frequency of long-term stem cells were calculated by L-Calc program from Stem Cell Tech. On average, there were 1.5 CAFC per 10^5 wild type bone marrow cells plated; 2.2 and 3.4 CAFC per 10^5 heterozygous and homozygous mutant bone marrow cells plated. The increases were 1.4 fold and 2.2 fold in *Nov*^{3del} heterozygote and homozygote bone marrow respectively, and the increase was statistically significant between wild type and mutant littermates (Figure 5.5.A). This result was consistent with the observation of mild increase in LT-HSC frequency in mutant bone marrow by FACS.

CFC assays were used to test the progenitor frequency and function *in vitro*. Total of 2×10^5 bone marrow mononuclear cells from *Nov*^{3del} homozygous and wild type mice were plated into M3434 with 10ng/ml TPO. The colonies were scored according to their morphologies 10-14 days later. The results showed that *Nov*^{3del} cells had a normal colony forming efficiency. And the outputs of different colony types were also similar between *Nov*^{3del} cells and their wild type counterparts. There was a mild increase of the total colony number from heterozygous cells which was in line with the FACS results (Figure 5.5.B).

There was no obvious reduction of colony forming efficiency in *Nov*^{3del} cells in secondary replating experiments (Figure 5.5.C). These results indicated a normal progenitor function of *Nov*^{3del} cells *in vitro*.

5.2.5 *Nov*^{3del} mutant mice bone marrow could long-term reconstitute lethally irradiated recipients

To test the function of HSC, currently the golden standard is to examine their reconstitution capacity of lethally irradiated recipients in the competitive bone marrow transplant assay.

The same amount of *Nov*^{3del} (CD45.2) mutant bone marrow and CD45.1 competitive bone marrow cells were injected into lethally irradiated recipients. After one month, the peripheral bloods were checked by FACS for the engraftment efficiency and lineage constitution. The results showed that *Nov*^{3del} bone marrow had a similar efficiency to reconstitute lethally irradiated recipient comparing to their wild type littermate (Figure 5.6.A). They could also give all lineages of blood cells analysed with normal distribution (Figure 5.6.B). After 4 months, the engraftment efficiency was maintained in *Nov*^{3del} mutant donor cells in both peripheral blood and bone marrow (Figure 5.7.A). The lineage distribution in peripheral blood (Figure 5.7.B) and bone marrow (Figure 5.8.C) were also comparable between wild type and *Nov*^{3del} donors. Although the KLS frequency was increased in *Nov*^{3del} mutant primary bone marrow as

detected by FACS analysis, this phenotype was not carried over in the transplant recipient bone marrow with enhanced long term engraftment efficiency. There were also no differences of KLS and LT-HSC (CD34-KLS) frequencies within wild type and *Nov*^{3del} mutant donor cells (Figure 5.7.D). The progenitor frequencies of both Akashi's (Figure 5.7.E) and Pronk's (Figure 5.7.F) dissections were also comparable between *Nov*^{3del} derived cells and the wild type donor cells.

5.2.6 Nov^{3del} mutant bone marrow showed increased reconstitution efficiency in serial transplantation

The primary transplants showed normal lineage distribution in primary recipients and no difference in the engraftment efficiency. However, this was not compatible with the observations of increased HSC frequency from both in vivo FACS analysis and in vitro CAFC assay. Therefore I decided to perform a serial transplant with those reconstituted bone marrows in hope to read out the HSC frequency in a more strict setting.

The same amounts of bone marrow cells from first recipients were collected and injected into lethally irradiated recipients. After 4 months, the peripheral blood was FACS analysed to determine the engraftment efficiency. Of the engrafted recipients in the secondary transplant experiments, as judged by more than 0.3% of donor cells within total mononuclear cells, the average

engraftment efficiency was around 15.3% from wild type donors and 43.6% from *Nov*^{3del} donors. Consistent with the peripheral blood results, the percentages of *Nov*^{3del} donors were also higher in spleen and bone marrow which were 46.9% and 46% respectively; instead, the percentages of wild type donors were only 20% and 12% respectively in spleen and bone marrow (Figure 5.8.A).

The lymphoid cell reconstitutions in recipients were similar from both wild type and *Nov*^{3del} donors. However, there was an unexpected augment of myeloid reconstitution from Nov^{3del} donors, and the increase was statistically significant in bone marrow (Figure 5.8.B).

Even though there was significantly increased secondary engraftment capacity from *Nov*^{3del} donor cells and disruption in lineage distribution, the frequencies of KLS and HSC subpopulations were not significantly increased in *Nov*^{3del} donors comparing to the wild type control (Figure 5.9.A); and the frequencies of progenitors were also similar between the *Nov*^{3del} and wild type donors (Figure 5.9.B).

The result of enhanced reconstitution efficiency in a serial transplant experiment reflected the observation of increased HSC frequency in *Nov*^{3del} mutant bone marrow. However, it was not clear what might cause the enhanced differentiation into myeloid cells in secondary recipients.

5.2.7 The analysis of haematopoiesis in aged *Nov*^{3del} mutant mice

The observation in the original *Nov*^{3del} mice paper indicated that Nov had a general role in maintenance of tissue viability in adults. Especially, these mice showed some early aging features. In Nov knock-out mice, the phenotype of increased osteoblast surface, bone formation and bone remodelling was more obvious in older mice. These observations indicated that Nov may have a role in aging and it would be possible that the haematopoietic phenotype shown in *Nov*^{3del} young mice will be more readily observed. To test this hypothesis, I did the FACS analysis and transplant experiments with aged (more than14 months old) *Nov*^{3del} mutant bone marrow.

Just as there was no obvious increase of bone size and cellularity in young *Nov*^{3del} mutant bones, the aged *Nov*^{3del} mutant mice showed no differences in bone cellularity. The average numbers of total bone marrow mononuclear cells in one femur were around 2.1×10^7 and 2.4×10^7 in wild type and homozygote respectively. (Figure 5.10.A)

The lineage distribution of aged *Nov*^{3del} mutant peripheral blood was similar to that of young mice. The B cells, T cells and myeloid cells were around 43.5%, 42.8% and 10.3% respectively in *Nov*^{3del} mutant peripheral blood which were similar in their wild type control. (Figure 5.10.B)

The lineage distributions were also similar in aged mice bone marrow. There were 16%, 9% and 15% of B cell, T cell and myeloid cells in *Nov*^{3del} mutant bone marrow respectively with similar lineages distribution in wild type bone marrow (Figure 5.10.B).

Surprisingly, the frequencies of KLS and HSCs were decreased to a level comparable to their wild type control. Similar frequencies of all progenitors were observed in both aged wild type and *Nov*^{3del} cells (Figure 5.10.C).

5.2.8 The function of HSC from aged *Nov*^{3del} mutant mice was normal in bone marrow transplantation.

To test the function of aged *Nov*^{3del} HSC, I performed a competitive bone marrow reconstitution assay. After 4 months of engraftment, the percentages of donor cells in the recipient's peripheral blood were around 70% from both wild type and *Nov*^{3del} derived cells (Figure 5.11.A). In peripheral blood, the lymphoid (B220+ and CD3+) and myeloid (Mac1+) cells were replenished at similar frequencies as their wild type control (Figure 5.11.B).

The percentages of donor cells in bone marrow were also similar at around 86% and 87% for both wild type and *Nov*^{3del} donors (Figure 5.11.A). There were also no differences in lineage distributions in bone marrow (Figure 5.11.B).

The frequencies of haematopoietic stem and progenitor cells derived from aged donor cells were similar for *Nov*^{3del} mutant and wild type controls, implicating an unaltered function of *Nov*^{3del} HSC (Figure 5.11.C).

5.3 Summary and discussion

In this chapter, I characterized haematopoiesis in *Nov*^{3del} mutant mice and tested *Nov*^{3del} HSC function with both *in vitro* and *in vivo* assays. In general, the *Nov*^{3del} mice showed normal haematopoietic cell differentiation and function in peripheral blood and bone marrow. There was a mild increase of HSC frequency in *Nov*^{3del} mice bone marrow by FACS analysis. This result was later confirmed by the *in vitro* CAFC assay with the increased frequency of cobble-stone-forming cells and by the secondary transplantation with the enhanced engraftment efficiency in secondary recipients. The haematopoiesis and HSPC function appeared to be normal in aged *Nov*^{3del} mutant mice as well.

In the original paper, the author reported a loss of 35% of heterozygote and 55% of homozygote prior to postnatal day10 which resulted in only 17% homozygote and 46% heterozygote from a total of 30 live born (Heath, E.2008). However, of the total 241 offspring I obtained from breeding between heterozygote in the BMS oxford, there were 45% heterozygote, 28% homozygote and 27% wild type. The similar percentage of homozygous

offspring with wild type indicated there was no homozygote lost prior to postnatal. The increased survival rate of homozygote during the successive breeding could be explained partly by a selection for a less severe phenotype through generations which was also suggested in the paper (Heath, E.2008) to explain the reduced levels of neonatal loss comparing to surviving littermates.

Nov^{3del} mutant mice exhibited several abnormalities including enlarged vertebrae, elongated long bones at both embryonic and adult stages in the original paper (Heath, E.2008). It is therefore reasonable to predict that the *Nov*^{3del} mice will contain more bone marrow cells per long bone. Surprisingly, the bone marrow cellularity in each femur counted showed no difference between *Nov*^{3del} and their wild type controls. This observation, together with the increased survival rate of homozygote, indicated that this *Nov*^{3del} transgenic mouse line may have adapted to the mutation in Nov gene during the successive breeding and lose certain severe phenotypes. There are two possible explanations for these changes. Firstly, the phenotypes caused by losing normal Nov expression may be compensated by the upregulation of other genes during breeding, although it is not clear which candidate genes are involved. Secondly, *Nov*^{3del} mutant mice I used have been rederived to clean out the viruses, bacterias and pathogens, such as mouse *Hepatitis virus*, mouse *Norovirus* and *Helicobacter spp*, found in these animals before they were imported in BMS Oxford. Several proteins from CCN family, including

Nov, have been reported to involve in the response of inflammation and viral infection (Perbal B, 2006; Kular L, 2011). The presents of these pathogens may activate the CCN proteins; therefore, contribute the severe phenotypes observed in the original paper.

In general, *Nov*^{3del} mice had normal haematopoiesis throughout their adulthood. *Nov*^{3del} HSC showed an unaltered function as tested by both *in vivo* and *in vitro* assays. Obviously, there is the possibility that the low level expression of *Nov*^{3del} mutant protein in the mutant animal could act as the full length protein and therefore mask the phenotype in haematopoiesis which would have been induced by loss of Nov. However, these results were also consistent with the results described in Chapter 4 where Nov knockdown KLS showed no effects in cell growth and viability or the reconstitution capacity in lethally irradiated recipients. It may therefore be reasonable to conclude, based on these results above, that Nov may be dispensable for mouse HSC function under differentiation or self-renewal condition.

Despite all the normalities observed in haematopoiesis, interestingly, there was an increase of HSC frequency in *Nov*^{3del} mice. Accumulating evidence revealed that Nov regulates bone turnover and is a novel regulator of skeletal metastasis (Minamizato T, 2007; Canalis E, 2007; Heath E. 2008; Katsube K,2009; Canalis et al. 2010; Ouellet, V., 2012) . Nov inhibits osteoblast differentiation and would cause significantly diminished bone mineral density in

transgenic mice when overexpressed specifically in osteoblasts (Canalis E, 2007). In Nov null mice, though no obvious skeletal abnormalities were observed during development, female mice at ten months old showed an increase in osteoblast numbers/bone surface, mineralization and bone formation. As a known key component of the HSC niche, altered osteoblast cell number and function in bone marrow will often affect the HSC number and self-renewal ability (Zhang, J.2003; Calvi, L.M.2006). HSC niche function in *Nov*^{3del} mice has not been examined. It is intriguing then to propose that the increased frequency of HSC in *Nov*^{3del} mice is due to either increased niche forming osteoblast cells or enhanced osteoblast function that contribute to the interaction of HSC and its microenvironment.

In order to understand the Nov function in HSC niche and the interaction between HSC and its microenvironment, I carried out the following *in vitro* assays which are described in Chapter6.

	WBC ($10^{\wedge 3}/mm^3$)	RBC ($10^{\wedge 6}/mm^3$)	HGB (g/dl)	HCT (%)	MCV (um^3)	MCH (pg)	MCHC (g/dl)	RDW (%)	PLT ($10^{\wedge 3}/mm^3$)	MPV (um^3)	PCT (%)
WT	**8.54**	**9.81**	**15.43**	**47.74**	**48.50**	**15.68**	**32.35**	**13.23**	**438.88**	**5.613**	**0.25**
	±2.09	**±2.37**	**±3.54**	**±11.85**	**±1.37**	**±0.55**	**±1.59**	**±0.56**	**±130.75**	**±0.20**	**±0.08**
$Nov^{3del+/-}$	**6.76**	**9.10**	**14.51**	**44.75**	**49.13**	**15.97**	**32.48**	**13.30**	**376.13**	**5.69**	**0.21**
	±3.29	**±1.41**	**±2.00**	**±6.79**	**±0.74**	**±0.35**	**±0.69**	**±0.60**	**±91.29**	**±0.28**	**±0.05**
$Nov^{3del-/-}$	**6.86**	**9.13**	**14.50**	**45.18**	**49.20**	**15.88**	**32.22**	**12.74**	**374.80**	**5.58**	**0.21**
	±1.11	**±1.82**	**±3.00**	**±9.93**	**±1.48**	**±0.34**	**±0.74**	**±0.10**	**±98.08**	**±0.25**	**±0.05**

Table.5.1: Complete blood test for the wild type, *$Nov^{3del+/-}$* and *$Nov^{3del-/-}$* mice.

Blood counts were assessed in 8 wild-type (WT), 8 age-matched *$Nov^{3del+/-}$* and 5 age-matched *$Nov^{3del-/-}$* mice at 8-12 weeks old. All hematologic parameters measured for both genotypes were in the normal range. The mean value ± SD are presented for each parameter.

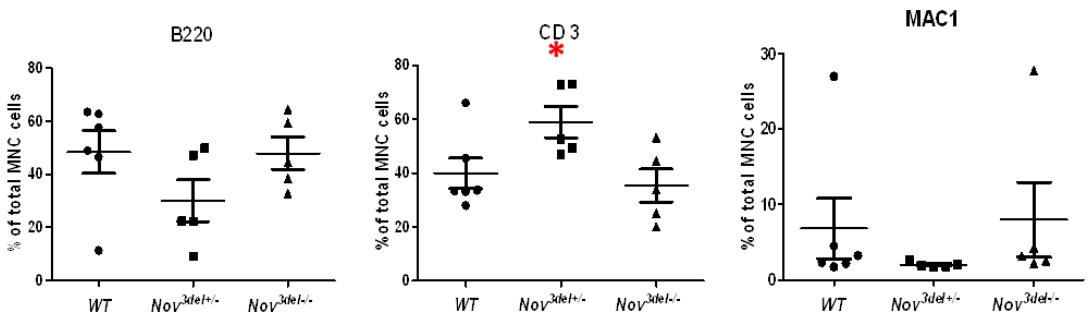


Figure.5.1: Lineage distributions were normal in *Nov*^{3del} mice peripheral blood.

Peripheral blood from wild type and *Nov*^{3del} mutant mice were analysed by FACS. The results showed that there were no difference in B220, CD3 and Mac1 expression except from the CD3 expression in heterozygous mice. There was a tendency of reduced frequency of B220 expression in heterozygotes, but it was not statistically significant. Each dot represents individual mouse analysed; the line indicates the mean with SEM. * indicate that the t-test result between wild type and heterozygous group is statistically significant at $p<0.05$.

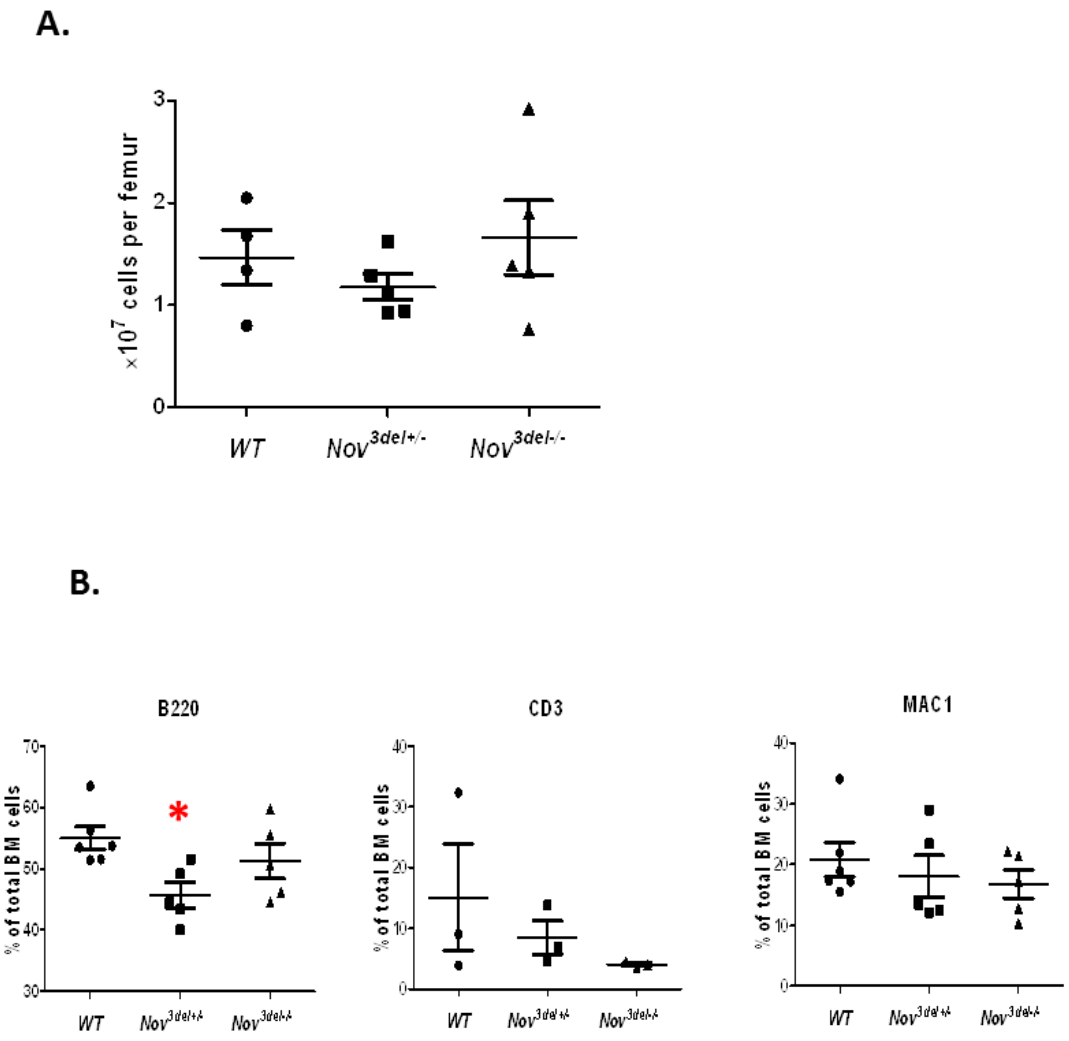


Figure.5.2: Cellularity and Lineage distributions were normal in *Nov*^{3del} mutant mice bone marrow.

A. Total mononuclear cell numbers from one femur of each type of animals were flushed and counted after red blood cell lysis. The results showed no obvious increase of cellularity in both heterozygous and homozygous animals compared to their wild type littermates.

B. Lineage distributions were analysed by FACS and showed no difference between wild type and *Nov*^{3del} homozygous mice. But in heterozygotes, there was a mild reduction in B220+ cell frequency, which was consistent with the observation in peripheral blood.

Each dot represents an individual mouse analysed; the line indicates the mean with SEM. * indicate the t-test result between wild type and heterozygous group is statistically significant at $p<0.05$.

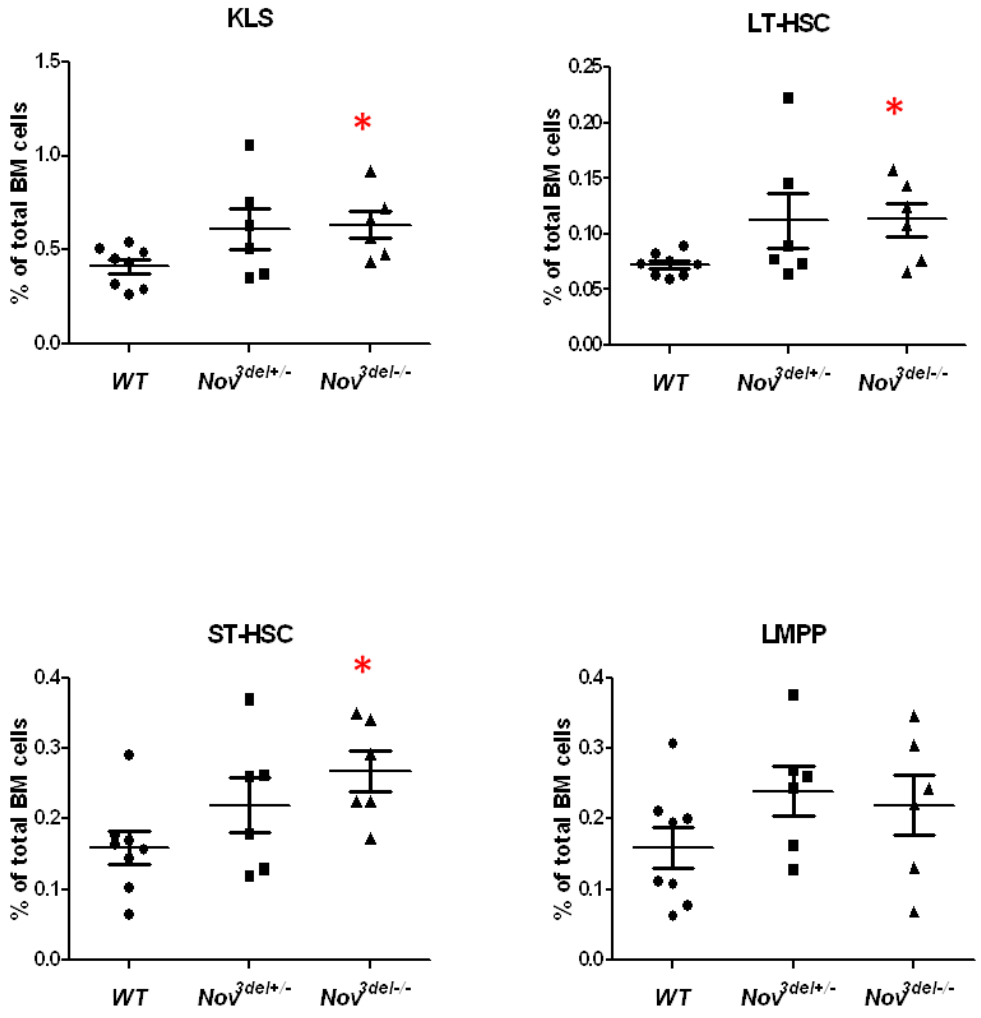


Figure.5.3: FACS analysis of HSC in *Nov*^{3del} bone marrow

The frequency of KLS in total bone marrow was increased by 1.5 fold in homozygote bone marrow. This enrichment could be observed in the LT-HSC and ST-HSC compartments, but not LMPPs. In heterozygotes, the increases of all the compartments were less obvious and not statistically significant.

Each dot represents an individual mouse analysed; the line indicates the mean with SEM. * indicate the t-test result between wild type and homozygous group is statistically significant at $p<0.05$.

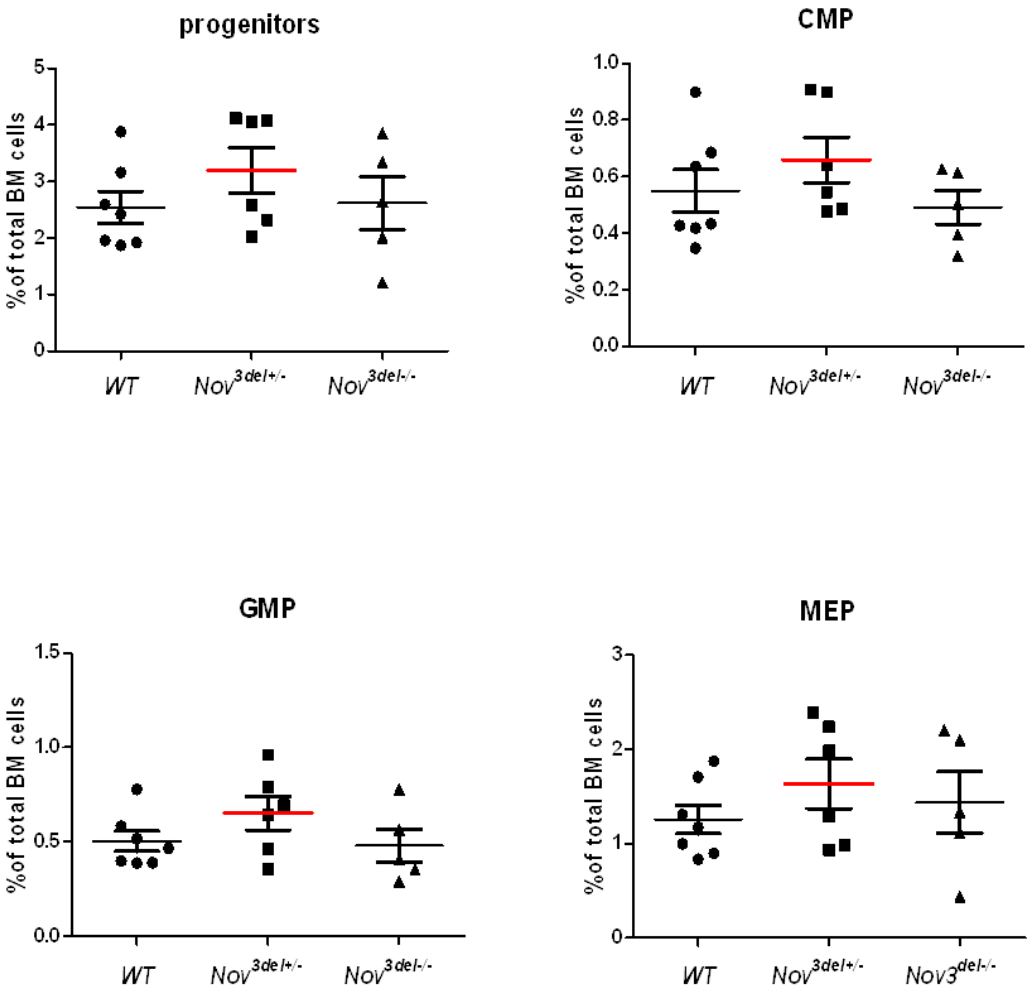


Figure.5.4: FACS analysis progenitors in *Nov*^{3del} bone marrow

The percentages of myeloid progenitors (CMP, GMP, and MEP) were similar between homozygote mutant and wild type animals. There seemed to be a mild increase in all the progenitor populations in heterozygote bone marrow, though this is not statistically significant.

Each dot represents an individual mouse analysed; the line indicates the mean with SEM.

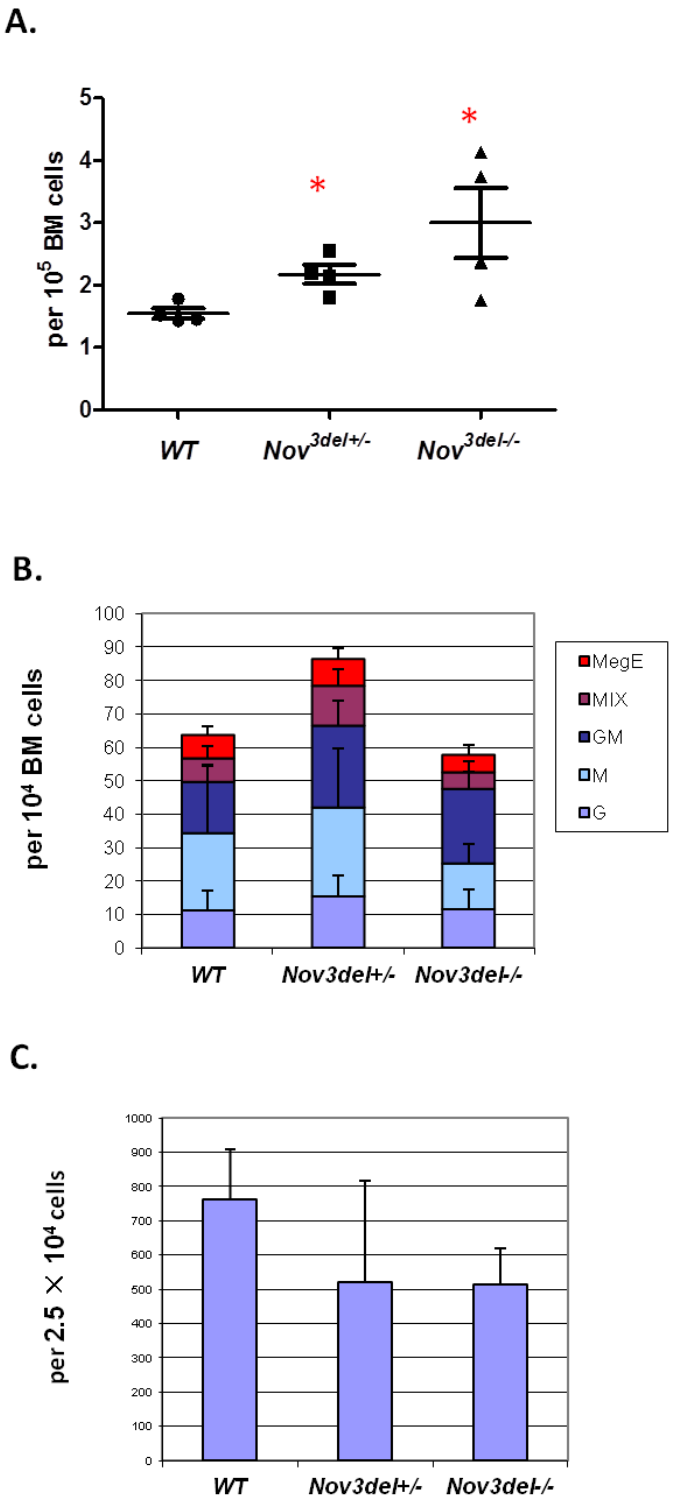


Figure5.5: *In vitro* analysis of *Nov*^{3del} HSC/HPC

A. The frequency of CAFC from 5 weeks limiting dilution CAFC assay. The results showed that there were 1.4 fold and 2.2 fold increase of CAFC

frequency in *Nov*^{3del} heterozygous and homozygous bone marrow respectively. Each dot represents an individual mouse analysed; the line indicates the mean with SEM. * indicate the t-test result between wild type and heterozygous group is statistically significant at $p<0.05$.

B. CFC assay. Bone marrow from *Nov*^{3del} homozygote mice had similar colony forming ability as their wild type control. There was a mild increase of total colony number from heterozygote bone marrow. Cells were cultured in Methocult M3434 with TPO. (n=5, mean ± SD).

C. Secondary replating of CFC assay. There was no obvious difference in the replating efficiency between wild type and *Nov*^{3del} mutant cells. (Average of 3-5 mice analysed for each genotypic group, mean ± SD).

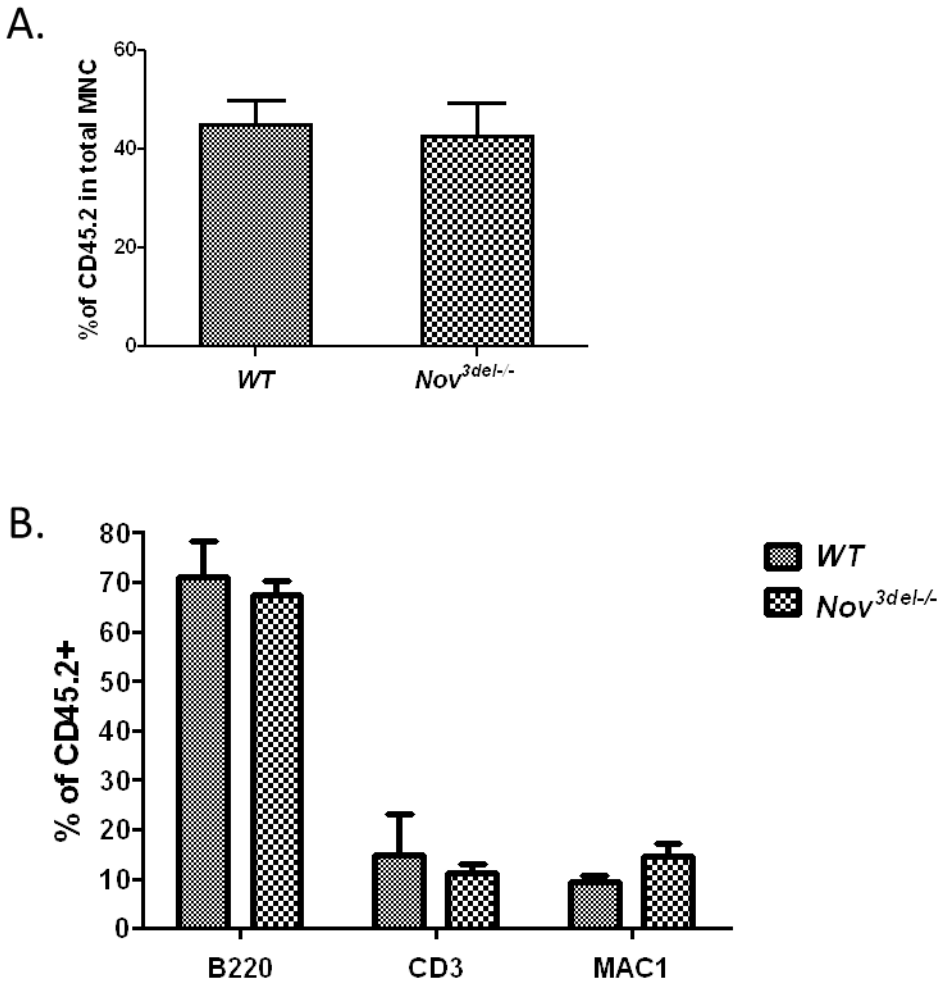


Figure.5.6: Short term engraftment efficiency of *Nov*^{3del} cells in competitive reconstitution assay.

A. The engraftment efficiency at one month from wild type and *Nov*^{3del} cells. The results showed comparable engraftment efficiency at short term from wild type and *Nov*^{3del}cells. n=8±SEM

B. The reconstitutions of different lineages in peripheral blood derived from *Nov*^{3del} cells were similar to wild type donors. n=8±SEM

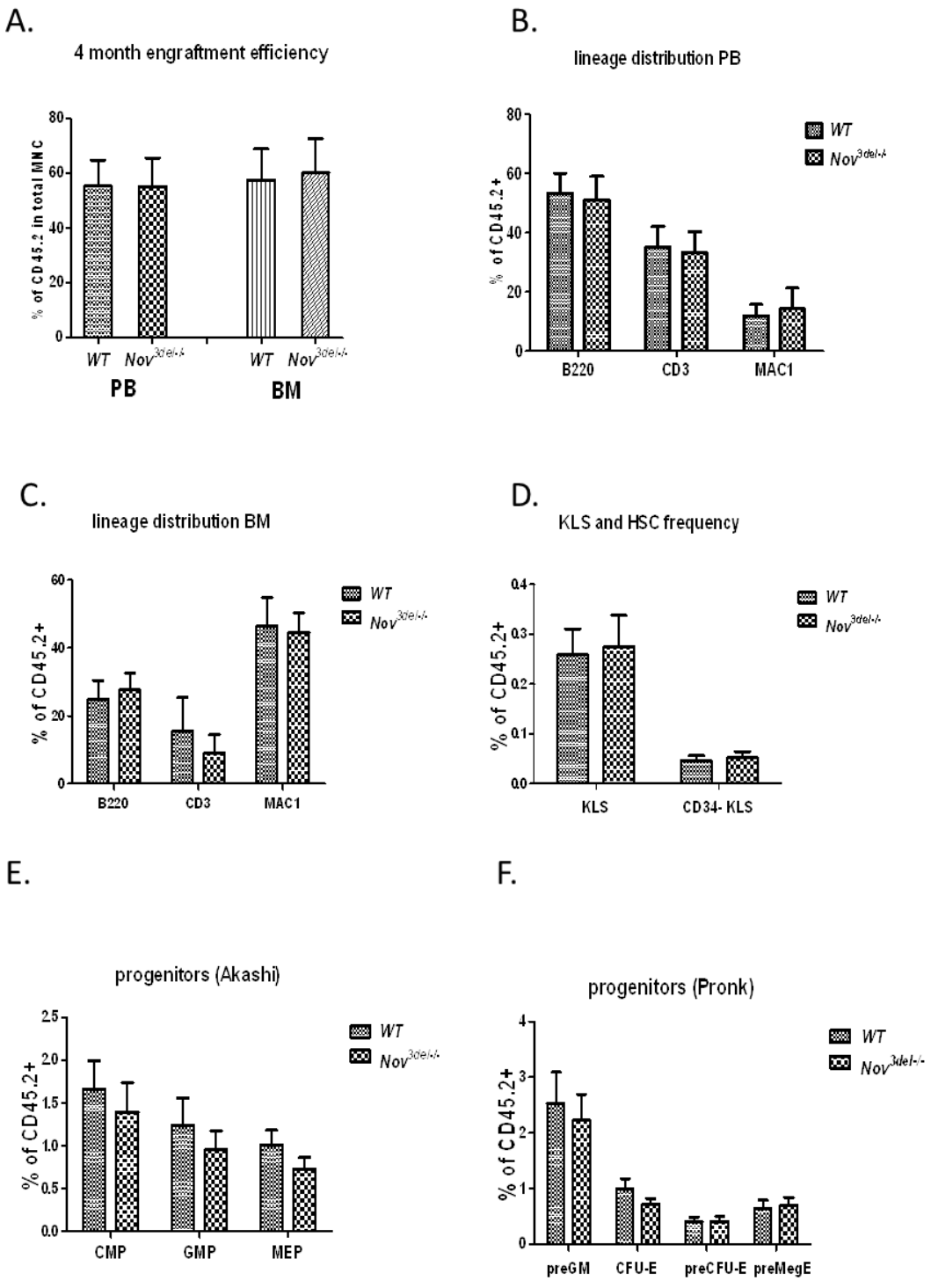


Figure.5.7: Long term engraftment of *Nov*^{3del} cells in competitive reconstitution assay.

A. This graph showed the engraftment efficiency at 4 month in peripheral blood and bone marrow. The *Nov*^{3del} donor cells had a similar long term

reconstitution capacity compared to their wild type control. n=6±SEM

B. The lineage distribution of engrafted donor cells in peripheral blood. n=8±SEM

C. The lineage distribution of engrafted donor cells in bone marrow. n=8±SEM

D. In the donor derived cells, the KLS and CD34-HSC frequency were similar between the wild type and *Nov*^{3del} cells n=8±SEM

E.F. The progenitors frequencies were similar in both wild type and *Nov*^{3del} donor cells. n=8±SEM

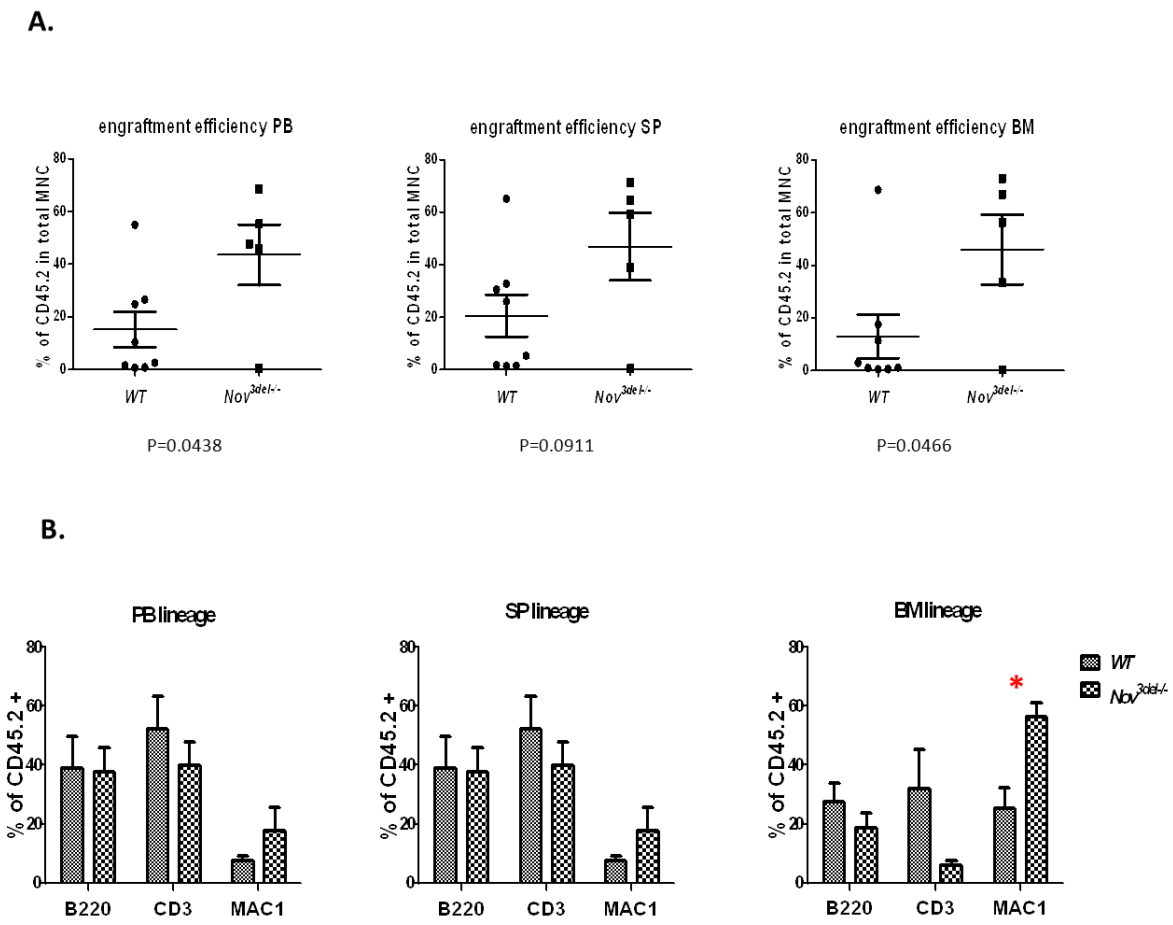


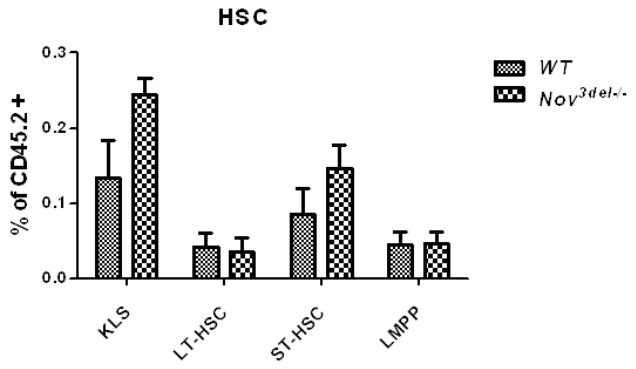
Figure.5.8: Serial transplantation of *Nov*^{3del} bone marrow cells

A. This graph showed the engraftment efficiency of donor cells in peripheral blood, spleen and bone marrow 4 months after being transplanted into secondary recipients. There was a significant increase in reconstitution from *Nov*^{3del} donor cells in all three organs comparing to the wild type control. Each dot represents an individual mouse analysed; the line indicates the mean with SEM.

B. The lineage distributions were examined in peripheral blood, spleen and bone marrow. The *Nov*^{3del} cells that reconstituted secondary recipients showed no difference in lymphoid (B220+, CD3+) reconstitution. The myeloid outputs (Mac1+) were increased in all three organs checked; and

the increase was statistically significant in bone marrow. n=8 wild type and 5 homozygote ±SEM. * indicate the t-test result between wild type and heterozygous group is statistically significant at $p<0.05$.

A.



B.

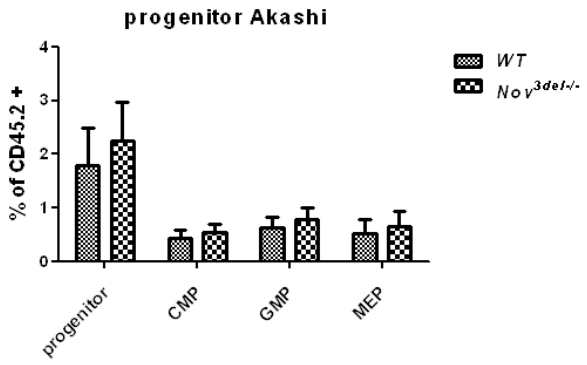


Figure.5.9: Serial transplantation of *Nov*^{3del} cells

A. FACS results of the haematopoietic stem cell frequency of donor cells in bone marrow 4 months after being transplanted into secondary recipients. The frequencies of all HSPC subpopulations were similar between *Nov*^{3del} donor cells and the wild type control.

B. FACS analysis of the progenitor cell frequency in bone marrow 4 months after being transplanted into secondary recipients. The frequencies of progenitors (Akashi dissection) were similar between *Nov*^{3del} donor cells and the wild type control.

n=8 wild type and 5 homozygote ±SEM.

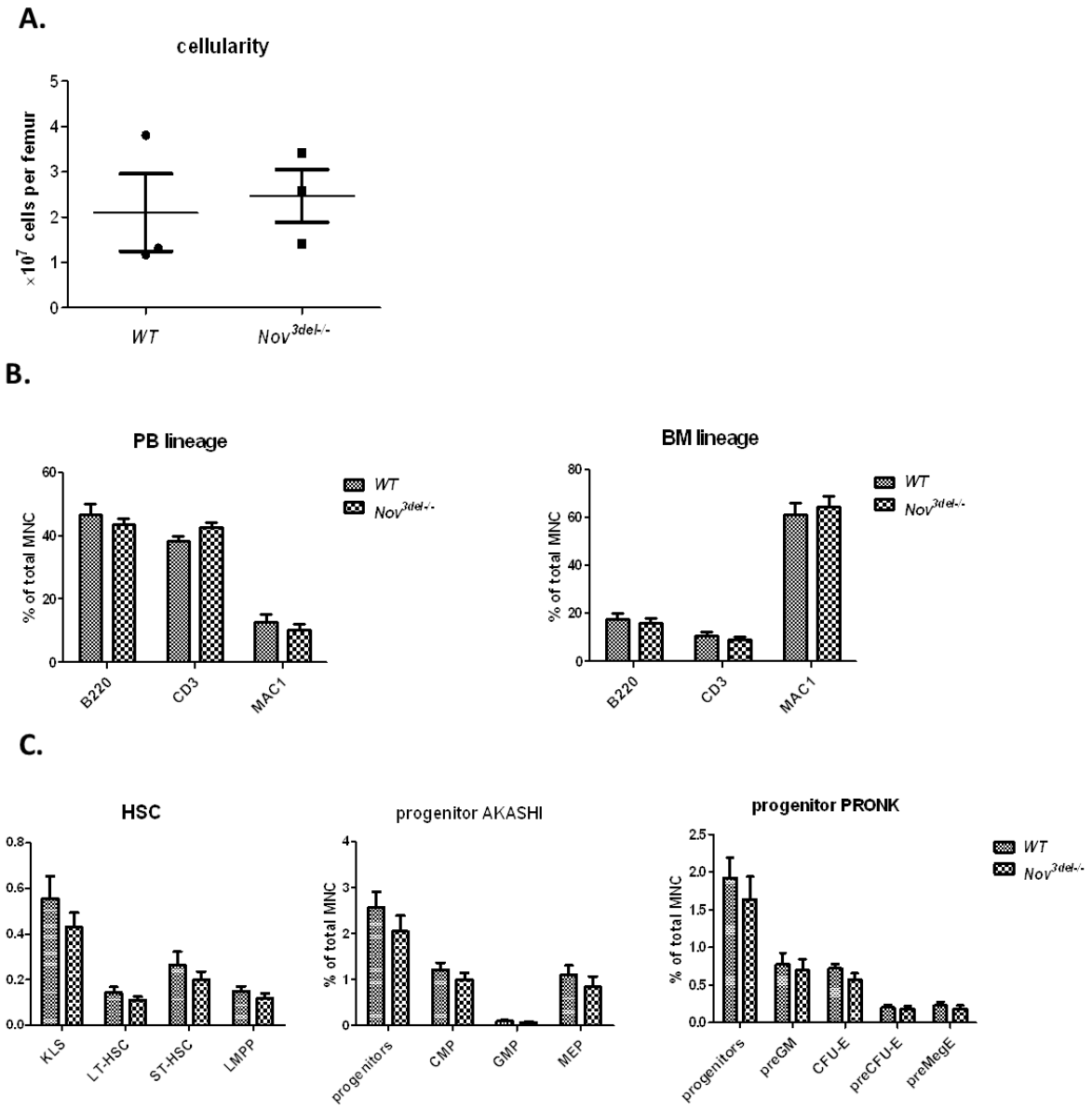


Figure.5.10: Analysis of haematopoiesis in aged *Nov*^{3del} mice

A. The bone marrow cellularities of aged *Nov*^{3del} mice were assessed and showed no difference to their wild type control. Each dot represents individual mouse analysed; the line indicates the mean with SEM.

B. FACS analysis of lineage distribution in peripheral blood and bone marrow showed a normal lineage distribution in *Nov*^{3del} aged mice. n=6 ±SEM

C. The frequencies of KLS, HSC and progenitors in aged mice were comparable between wild type and *Nov*^{3del}. n= 5wild type and 8 homozygote ± SEM

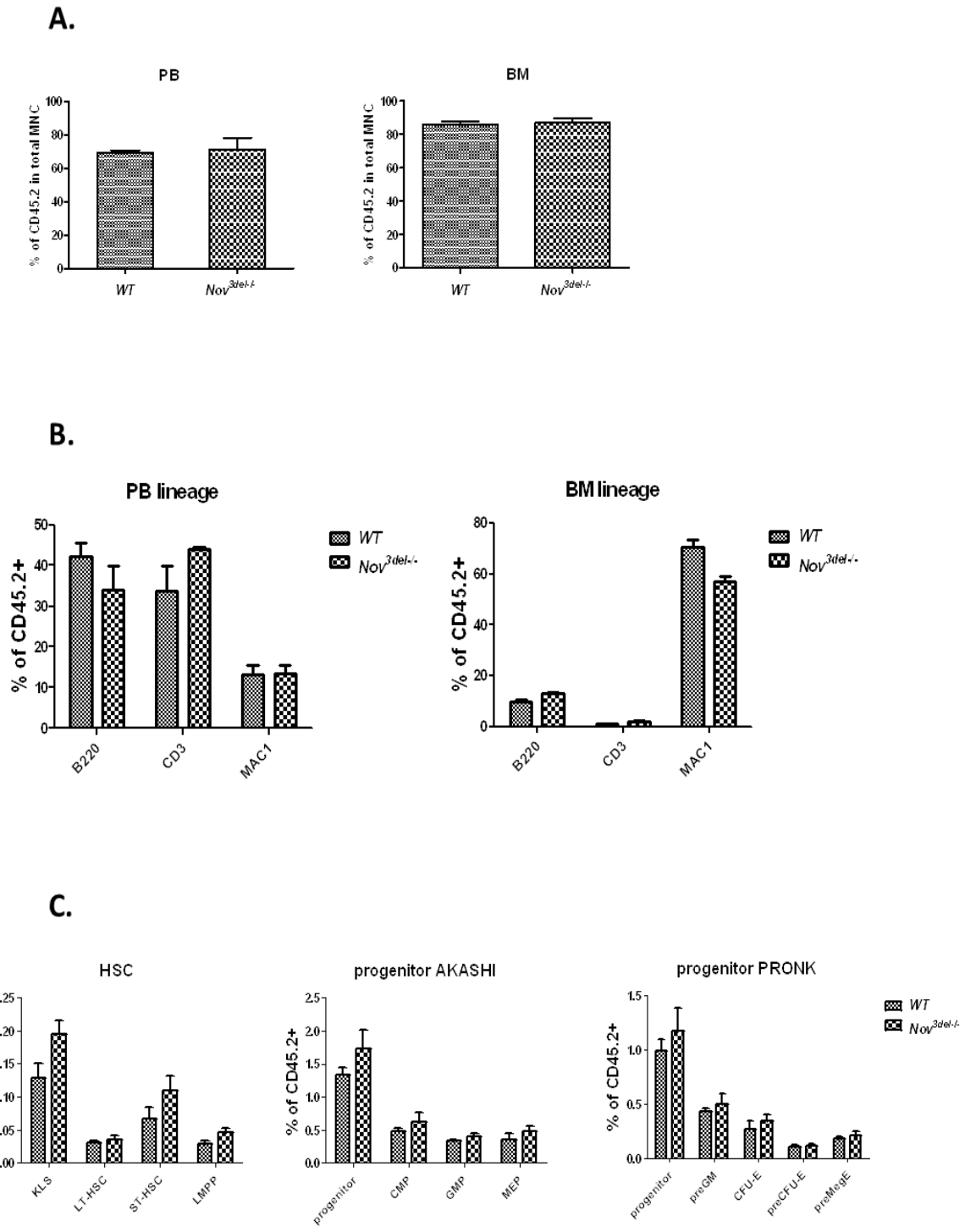


Figure.5.11: Bone marrow reconstitution of *Nov*^{3del} aged cells

A. The engraftment efficiency at 4 months. The results showed a comparable reconstitution capacity of *Nov*^{3del} aged cells to their wild type counterparts.

B. FACS analysis of lineage distribution in peripheral blood and bone marrow showed a normal lineage distribution in *Nov*^{3del} aged donors.

C. The frequencies of HSPC in aged donor cells were comparable between wild type and *Nov*^{3del}. n=4±SEM

CHAPTER6.

ANALYSIS OF *NOV* FUNCTION IN HSC MICROENVIRONMENT

6.1 Introduction

In previous chapters, I tested the function of *Nov* in HSC through gain and loss of function analysis. Forced expression of Nov in KLS cells induced apoptosis and reduced their long term reconstitution activity. *Nov* knockdown in haematopoietic stem and progenitor cells did not affect cell growth, differentiation and long term reconstitution activity. *Nov*^{3del} mutant mice also showed normal HSC function in differentiation and self-renewal. However, *Nov*^{3del} mutant mice showed an increased HSC frequency possibly due to the enlarged bone and enhanced osteoblast cell function. This raised the possibility that *Nov* could play a role in the interaction between HSC and the microenvironment. Therefore, I moved on to investigate the role of *Nov* in HSC interaction with microenvironment.

To model the interactions between HSCs and bone marrow stromal cells and to test the function of Nov in HSC microenvironment, I set up several *in vitro* assays with FDCPmix cells and bone marrow stromal cells. Firstly, Nov functions in haematopoietic cell adherent and migration capacity were tested with FDCPmix cells. Secondly, the expression levels of Nov were compared by RT-qPCR in bone marrow stromal cells, primary bone marrow endothelial cells and osteoblast cells to identify the expression pattern of *Nov* within bone marrow. To model the function of Nov in HSC microenvironment, stromal cells were manipulated for Nov expression and examined for their function as HSC niches.

6.2 Results

6.2.1 Novi FDCPmix cells showed impaired adherent capacity

During the serum free culture of FDCPmix, I consistently observed a layer of adherent cells at the bottom of flask in LLX cell culture but not in Novi cell culture (Figure 6.1.A). The majority of these adherent cells were round and bright under the light field microscope. There were also some cells showing fibroblast-like morphology which could be fully differentiated macrophage cells.

This interesting phenotype of *Nov* knockdown in FDCPmix indicated that, as a matrix protein, *Nov* may be involved in the process of cell adhesion. A role for Nov in cell adhesion had been reported in many different tissues (Benini S, 2005; Vallacchi V, 2008; Bohlig L, 2008), and a recent study showed that Nov-overexpressing K562 CML cells displayed increased adhesion to matrigel (McCallum L, 2012). In order to test whether the observed reduction of adherent cells from Novi culture was due to the loss of Nov, I did a rescue experiment by adding recombinant murine Nov protein (R&D) into the culture (Figure 6.1.B). The addition of exogenous Nov protein did not affect the percentage of adherent cells within the LLX culture. However, when rmNov was added to Novi cells at increasing concentrations, the percentage of adherent cells increased as the

concentration of rmNov was increased from 0 to 0.1 and then 0.5 μg/ml. However, at the highest concentration tested 1μg/ml, adherence was reduced (Figure 6.1.B).

These results indicated that *Nov* may be a positive regulator for cell adherent capacity and could enhance cells adherent capacity in a concentration dependent manner. As a secreted protein, the level of Nov produced by LLX FDCPmix cells may have reached its saturated level and this could explain why there was no effect on cell adherence when rmNov was added to LLX culture.

6.2.2 *Nov* knockdown in FDCPmix reduced the migration capacity

An important aspect of haematopoietic stem and progenitor cells interaction with the microenvironment is the capacity of HSPC to respond and migrate to chemokine and other signals released from bone marrow. It has been reported that primed HSC (N-cadherin^{low} HSCs) are specifically prepared for tasks involving reconstitution, mobilization, or response to stimuli and may have more flexible interactions with their environment. Gene expression assays showed that *Nov* is highly expressed in this population (Haug J.S, 2008). Moreover, accumulating evidence observed from other tissue system such as sarcoma (Tzeng, H. E.2011, Huang, C. Y.2011, Benini, S2005), prostate cancer (Chen, P. C.2012), smooth

muscle cells (Shimoyama, T.2010) and glioblastoma cell line (Lin C.G, 2003) showed that *Nov* functions in cell migration and mobility. Therefore, I decided to investigate whether *Nov* also plays a role in HSC migration.

I performed an *in vitro* transwell assay with FDCPmix cells which are known to express a high level of *Nov* (Bruno., 2004) and can home to bone marrow in recipient mice (data not shown). This assay provides a quick and simple model to test *Nov* function in haematopoietic stem and progenitor cell migration. All experiments using FDCPmix for migration assays employed serum free conditions to reduce the possible effects of serum present in normal culture.

Novi FDCPmix cells were maintained in SFEM medium with 10ng/ml rmIL3 for one passage before the transwell assay. 500µl of SFEM (10ng/ml rmIL3) was applied onto the top chamber and left in the incubator overnight to equilibrate the transwell. 1-2×10^5 FDCP Novi or control cells were added onto the top chamber and incubated for up to 3-4 hours at 37°C with 5% CO_2. Then cells were washed off from both top and bottom chambers and counted. The migration rate was calculated as the number of cells migrated to the bottom chamber as a fraction of the total number of cells in both top and bottom chambers (Figure 6.2.A).

When no chemoattractants such as SDF-1 were added in the bottom chambers the migration rate should represent the intrinsic capacity for cell mobility. After 4 hours of incubation, around 15% of total plated LLX cells

migrated through the membrane and entered the bottom chamber in control wells, while only 10% of Novi FDCPmix cells migrated to the bottom chamber (Figure 6.2.B, left panel). The difference of migration rate between Novi and control FDCPmix cells is statistically significant. This result indicated that reducing the level of *Nov* expression may impair the capacity of FDCPmix cells to migrate and thus *Nov* could play a positive role in the migration capacity of haematopoietic stem and progenitor cells. In order to test how Novi FDCPmix cells respond to homing signals, 100ng/ml SDF-1 was added to the bottom of the well before adding 1-2×10^5 FDCPmix cells into the top chamber. After 3-4 hours of incubation, the average migration rate of Novi FDCPmix cells to SDF-1 was 48% compared to 58% of LLX FDCPmix cells (Figure6.2.B, right panel). The mild decrease of migration rate in Novi cells was not statistically significant, but the level was consistent with the observation of decreased intrinsic migration capacity of Novi cells.

FACS analysis of CXCR4, the receptor of SDF-1, showed that FDCPmix cells have high expression of CXCR4 and *Nov* knockdown did not affect CXCR4 protein level at cell surface (Figure 6.2.C). This result indicated that the mild reduction of Novi FDCPmix response to SDF-1 was not due to reduced receptor expression but rather due to reduced intrinsic capacity of migration.

6.2.3 Gene expression analysis of Novi FDCPmix cells by RT-qPCR

In order to understand the molecular mechanism of *Nov* involvement in FDCPmix adherence and migration, I checked the gene expression of known cell adherence molecules (CAMs) and matrix metalloproteinase (MMPs). Consistent with the protein level, the expression of CXCR4 was not changed at mRNA level in Novi cells. Moreover, there was no obvious change in the expression of the other genes analysed (Figure 6.3). These results implied that *Nov* did not affect cell adherence and mobility via effects on expression of these adherence/migration related genes. The mechanism of *Nov* function in cell adherence and mobility could be either through protein interaction or other pathways.

6.2.4 Characterization of *Nov* expression pattern in bone marrow cells

Katsube.K. (2009) proposed that *Nov* expressed by bone marrow mesenchymal stem cells could be the main source of Nov supply in the bone marrow to suppress the osteoblast function and enhance the HSC function. Stromal cells derived from long term bone marrow culture have been used to support and test HSC function in various *in vitro* assays (Alberico T.A, 1987; Toksoz D, 1992; Jing D, 2010; de Barros A.P, 2010; Zetterblad J, 2010). Stromal cells derived from bone marrow or fetal liver

are immature and heterogeneous populations. A prominent cell type in these cultures is a multipotential population which can differentiate into osteoblasts, chondrocytes and adipocytes under suitable conditions, and is therefore referred to as a mesenchymal stem cell. The other populations in the culture include adipocytes, macrophages, fibroblasts and endothelial cells. Stromal cells derived from bone marrow culture provide a unique *in vitro* system to study HSC microenvironment.

In order to verify if these stromal cells derived from long term bone marrow culture could be used as a model to investigate Nov function in HSC microenvironment, I firstly tested whether *Nov* was expressed in stromal cells and what the level of Nov expression was.

I compared the expression of *Nov* in stromal cells to LT-HSC and primary bone marrow osteoblast and endothelial cells (Figure 6.4). Primary endosteal osteoblast (CD45-Ter119-CD31-) and endothelial (CD45-Ter119-CD31+) cells were isolated by FACS from bone marrow. RT-qPCR results using TaqMan oligos showed that *Nov* was expressed in stromal cells at a similar level to LT-HSC. The expression was lower in endothelial cells and osteoblast cells compared to stromal cells and LT-HSC. These results suggested that stromal cells derived from long term bone marrow culture could be used as an *in vitro* model to test Nov function in HSC microenvironment.

6.2.5 Overexpression of *Nov* in stromal cells enhanced FDCPmix migration but *Nov* did not function as chemoattractant *per se*

The niche cells provide not only ECM and the cell-cell contacts with HSC to provide them an anchor; they are also known to secret critical cytokines and signals for HSC homing and other functions. Therefore, I tested the homing capacity of FDCPmix towards *Nov* overexpressing or *Nov* knockdown stromal cells in transwell assay.

Long term bone marrow culture cells were maintained as normal in M5300 for two weeks and split one day before viral transduction. The cells were cultured for another week and GFP+ cells were purified with FACS sorts. Stromal cells were transduced with either mNov virus to overexpress *Nov* or Novi virus to knockdown *Nov* with empty virus as controls. GFP+ cells were sorted and plated into 24 well plates at 10^5 cells per well in M5300. The plates were incubated at 33°C and were ready to be used within 7 days. Effects on *Nov* expression were confirmed by RT-qPCR (Figure 6.5.A). The day before the experiment, the medium was changed to SFEM to avoid the possible effects of serum in the system. The transwell inserts were placed into the well with stromal cells growing at bottom. 10^5 FDCPmix cells were added onto the top chamber and incubated for 3-4 hours. Then cells from both top and bottom chambers were collected and counted for calculation of migration rate (Figure 6.5.B). The results showed

that FDCPmix cells had higher migration rate towards *Nov*-overexpressing stromal cells while knocking down of *Nov* in stromal cells did not affect FDCPmix migration towards them.

SDF-1/CXCL12 is a known chemoattractant produced by bone marrow as a signal for HSC homing to bone marrow. I next checked if *Nov* overexpression in stromal cells induced SDF-1 expression which in turn enhanced the migration of FDCPmix cell towards mNov stromal cells. RT-qPCR results however indicated that *Nov* did not regulate the expression of *SDF-1/Cxcl12* in stromal cells (Figure 6.5.C).

The lack of changes in *SDF-1/Cxcl12* expression indicated that the enhanced FDCPmix cell migration toward mNov stromal cells was not due to an increased level of homing signal SDF-1. I therefore asked whether *Nov* itself plays a role as a chemoattractant in HSC homing and whether Nov affects cell response to SDF-1. These were tested by adding 100ng/ml recombinant mouse Nov protein into medium in the bottom wells in the absence or presence of SDF-1. The results (Figure 6.5.D) showed that the overall migration rates were similar between the wells with or without rmNov indicating Nov alone did not affect the migration efficiency. In agreement with the enhanced migration towards mNov stromal cells, when adding rmNov into wells with SDF-1, there was a tendency of enhanced migration towards SDF-1, from 56% to 65%, although this result was not statistically significant.

These results indicated that *Nov* did not work as chemoattractant *per se*, but may enhance the effect of SDF-1 to FDCPmix cells migration.

6.2.6 Overexpression of *Nov* in stromal cells can enhance the HSC expansion and CFC frequency *in vitro*

In order to avoid the activity of Nov or similar proteins from serum, a serum free co-culture system was designed to test the function of *Nov* in the HSC microenvironment. GFP+ stromal cells transduced with either CSI/mNov or LLX/Novi virus were sorted and plated into 96 well plates at 10^4 cells per well in M5300. When the cells grew to about 80% confluent in 96 well plates, the whole plate was irradiated to deactivate the growth of haematopoietic cells from the culture. Medium of the culture was changed from M5300 to SFEM one day before adding KLS cells. This step allowed the secretion of cytokines and other essential proteins into the medium from stromal cells before KLS cells were seeded onto the stromal cells. Half-medium change was performed every week for up to 4 weeks.

The KLS cells proliferated rapidly on the stromal cells for the first two weeks even though there was no serum or cytokines present in the culture. KLS cells can retain their progenitor capacity even after two weeks co-culture in serum and cytokine-free condition. However, the cells grown in serum-free condition lost their haematopoietic morphology gradually after 3 weeks culture (data not shown).

The assay therefore did not allow long-term analysis of *Nov* function in stromal cells' supporting haematopoietic stem cell culture. However, it still provided a good indication for stromal functions in short term assay. The proliferation rates of KLS cells on the *Nov* manipulated stromal cells after two weeks were compared. On average, KLS expanded more than 700-fold in two weeks when cultured on the mNov stromal cells (Figure 6.6.A). There was only around 300-fold proliferation of KLS on control stromal cells. Knocking down *Nov* in stromal cells did not affect KLS cell proliferation.

After two weeks co-culture with mNov or Novi stromal cells, KLS derived cells were taken out from 96 wells and put into methylcellulose with cytokines to test their progenitor function. The progenitor frequency was determined by the number of colonies formed per 100 KLS initially plated on stroma. The results showed that *Nov* overexpressing stromal cells can not only enhance the proliferation of KLS cells, but also help maintaining their progenitor function (Figure 6.6.B). In contrast, *Nov* knockdown stromal cells showed an impaired capacity to support progenitors although they can support KLS cell proliferation as effectively as their vector controls. Taken together, these results suggested that *Nov* plays an important role in stromal cells for supporting haematopoietic stem and progenitor cells *in vitro*.

In order to investigate the possible mechanism of *Nov* function in HSC supportive stromal cells, I did a preliminary test for expression of some genes known to be involved in interactions of HSC and niche cells, namely CAMs and MMPs. The results showed that mNov stromal cells had reduced expression at the mRNA level of *Mmp9* and *N-cadherin*.

6.3 Summary and discussion

Migration and adherent capacity are critical for homing of HSC to their bone marrow niche and replenishing the blood cells both during homeostasis and in lethally irradiated recipients. Many studies have tried to develop an *in vitro* experimental system mimicking the functional haematopoietic stem cell niche to recapitulate the specialized properties of the marrow microenvironment and achieve the expansion of functional HSC *in vitro* (Ferreira M.S, 2012; Sharma M.B, 2012). These *in vitro* models also provide powerful tools to investigate the interaction between HSCs with their microenvironments (de Barros A.P, 2010; Shen Y, 2012). In this chapter, I deployed *in vitro* analysis to investigate the function of Nov in the interactions between HSCs and their microenvironment. Serum free culture of FDCPmix cells showed that *Nov* knock down reduced the capacity of FDCPmix cells to adhere to flask. The defect of adhesion in Novi cells could be rescued by adding recombinant Nov protein into the culture medium. These data suggested that *Nov* impacts cell adherent

functions through an extra cellular mechanism, which also explains the normal reconstitution of Novi KLS observed in wild type recipients.

In vitro transwell assay of Novi FDCPmix cells showed a reduction of spontaneous migration capacity and a trend of reduced migration capacity towards chemoattractant SDF-1 *in vitro*. Interestingly, overexpression of *Nov* in stromal cells could enhance the migration of FDCPmix cells. The further migration assays suggested that *Nov* did not function as a chemoattractant, but could enhance the homing effect of SDF-1. These data identified an important role of *Nov* in HSC migration and were consistent with a recent study where *Nov* was found highly expressed in N-cadherin+ HSCs, a subpopulation of primed HSC that was proposed to response to microenvironmental cues (Haug J. S, 2008).

RT-qPCR results of some known *Nov* targets involved in cell migration and adherence (Tzeng H.E, 2011; Liu S, 2012; Shimoyama T, 2010; Lin C.G, 2003) showed no obvious changes in gene expression at mRNA level. These data suggested that the function of Nov in cell adherence and migration involves in other mechanisms without CAM and MMP.

When KLS cells were cultured in serum-free medium in the presence of stromal cells without any cytokines, significant expansion was observed in wells with *Nov* overexpressing stromal cells. CFC assay of the expanded cells showed increased colony forming activity from mNov stromal cells co-cultured KLS. These results indicated that *Nov* overexpression in

stromal cells can enhance the function of stromal cells in HSC microenvironment which efficiently expand and maintain HSC progenitor function in co-culture. These results were in line with several recent reports. Microarray assay and cDNA subtraction studies comparing HSC supportive fetal liver stromal cells cell lines versus non-supportive lines showed that *Nov* was highly expressed in HSC supportive stromal cells (Charbord, P.2005). *Nov* has also been reported to be highly expressed in ALCAM-Sca1+ endotheal population in bone marrow which could enhance the progenitor read out of HSC in CFC assay after coculture (Nakamura, Y.2010).

Overexpression of *Nov* in stromal cells reduced the expression of *Mmp9* and *N-cadherin.* Recent studies showed that MMP-9 activated the HSC mobilizing factor cytokines (e.g. SCF), degrades osteopontin, induces HSC cycling and reduces HSC anchorage to the osteoblastic niche (Heissig, B. 2002). *N-cadherin* is expressed in osteoblasts, mesenchymal stem cells and haematopoietic stem and progenitor cells (ZHANG.J, 2003; Haug.J.S, 2008; Xie.Y, 2009; Wein.F, 2010). *In vitro* culture of HSCs with osteoblasts that expressed high levels of N-cadherin or primary N-cadherin^{hi} ALCAM+ Sca- osteoblast cells enhanced the long term reconstitution activity of HSCs (Nakamura, Y. et al. 2010). However, the studies of N-cadherin function in HSC and niche had been controversial. There are also

evidences showed that N-cadherin is not required for maintenance of HSC (Kiel, M.J, 2007; Greenbaum.A.M, 2012).

Further studies of the interaction among Nov, Mmp9 and N-cadherin may shed light on the mechanism of HSC interaction with microenvironment.

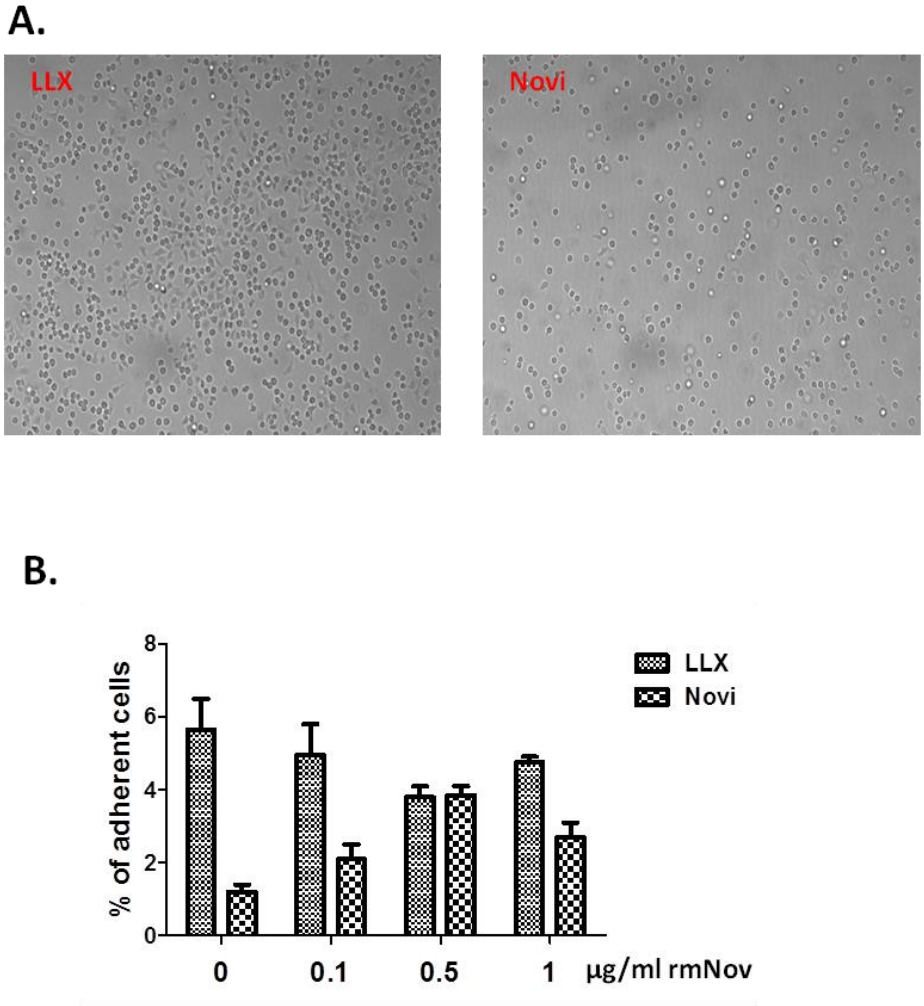


Figure.6.1: Adherence was impaired in FDCPmix Novi cells and could be rescued by adding Nov protein.

A. The photos show the adherent cells at the bottom of flasks after being washed with PBS. There were much less cells attached to the bottom of the flask from culture of Novi cell comparing to the LLX culture. This result indicated that Nov is involved in the process of cell adherence.

B. The rescue of Novi FDCPmix cell adherence by adding rmNov in the SFEM medium. The result indicates that the impairment of Novi cell adherence could be rescued by adding rmNov to culture and this rescue is concentration dependent. n=3±SEM

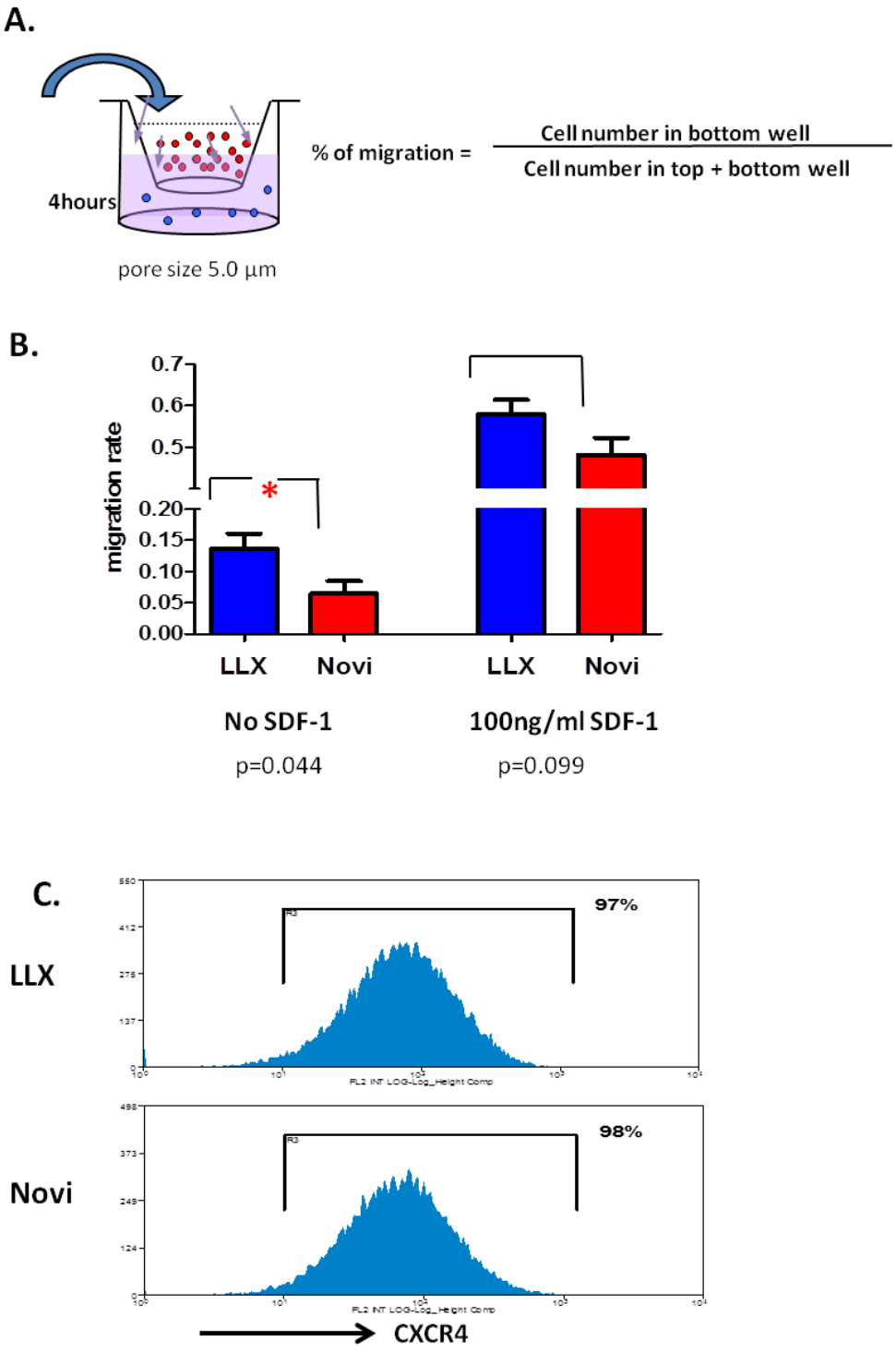


Figure.6.2: The migration capacity was impaired in FDCPmix Novi cells.

A. Schematic representation of the transwell migration assay.

B. The transwell assay shows an impaired spontaneous migration capacity in

FDCPmix Novi cells when there is no chemoattractant SDF-1 in the bottom well. There is a trend of reduced migration capacity towards the SDF-1 in FDCPmix Novi cells, but it is not statistically significant. N=6±SEM

C. The FACS analysis plots of CXCR4 expression show that FDCPmix cells have high expression level of CXCR4 which is not affected by Nov knock-down.

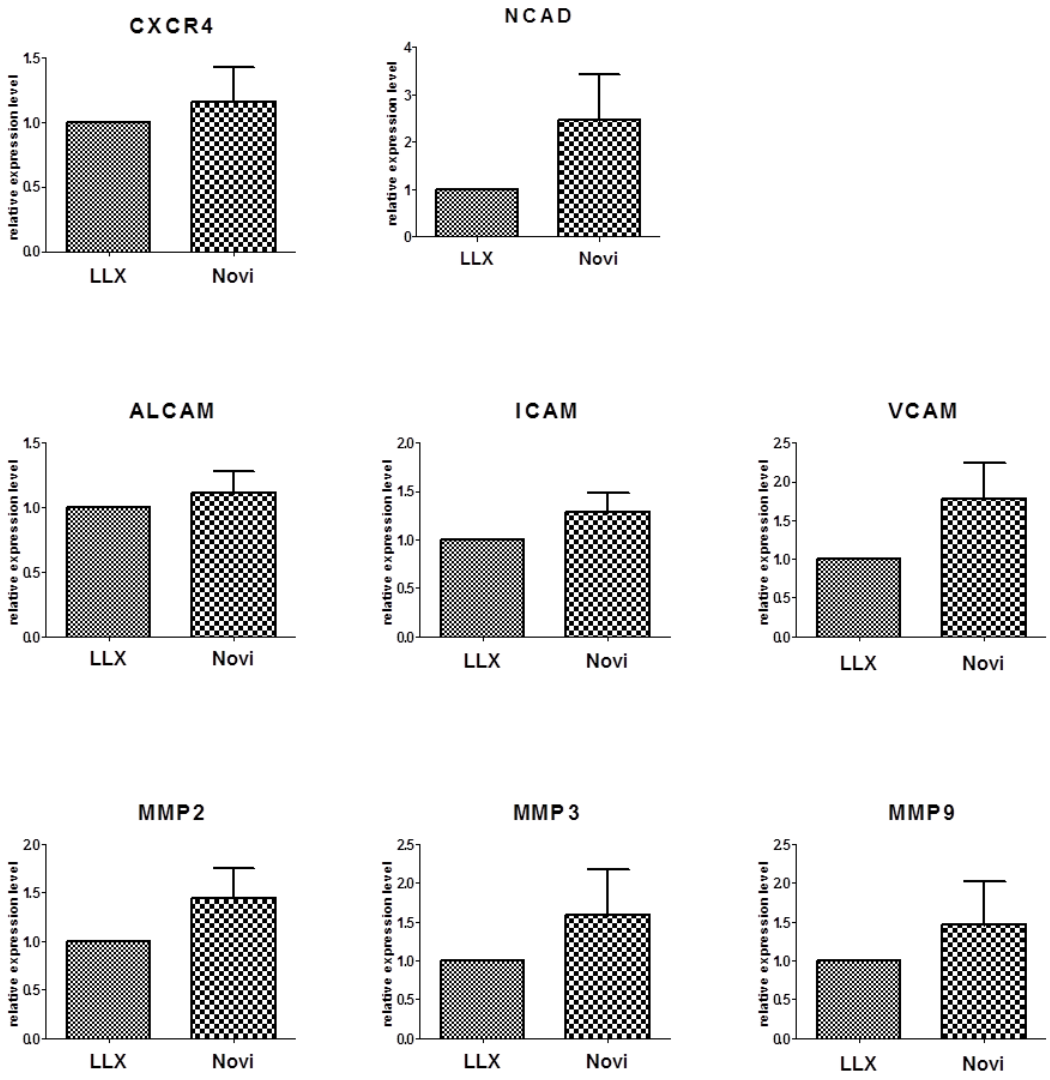


Figure.6.3: FDCPmix Novi cells show no obvious change in gene expression of CAM and MMP genes by RT-qPCR.

The RT-PCR results show that CXCR4 expression is not changed in Novi cells which are consistent with the FACS analysis. The expression level of various adherent molecules (CAMs) and matrix metalloproteases (MMPs) are not changed by Nov knock-down. n=6±SEM

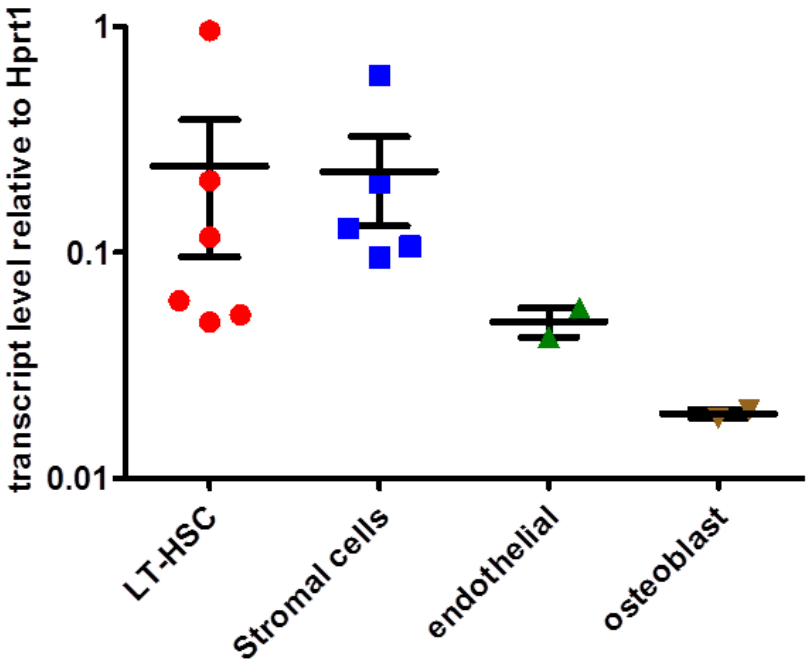


Figure.6.4: The expression of *Nov* in stromal cells and primary bone marrow cells.

The RT-qPCR results showed that *Nov* is expressed in cultured bone marrow stromal cells and primary bone marrow cells. The expression level is comparable between the LT-HSC and stromal cells and the expression levels were lower in primary bone marrow endothelial (CD45-Ter119-CD31+) and osteoblast (CD45-Ter119-CD31-) cells. The expression level of *Nov* is relative to the expression of Hprt1. Each dot represents one sample tested. The line shows the mean ±SEM.

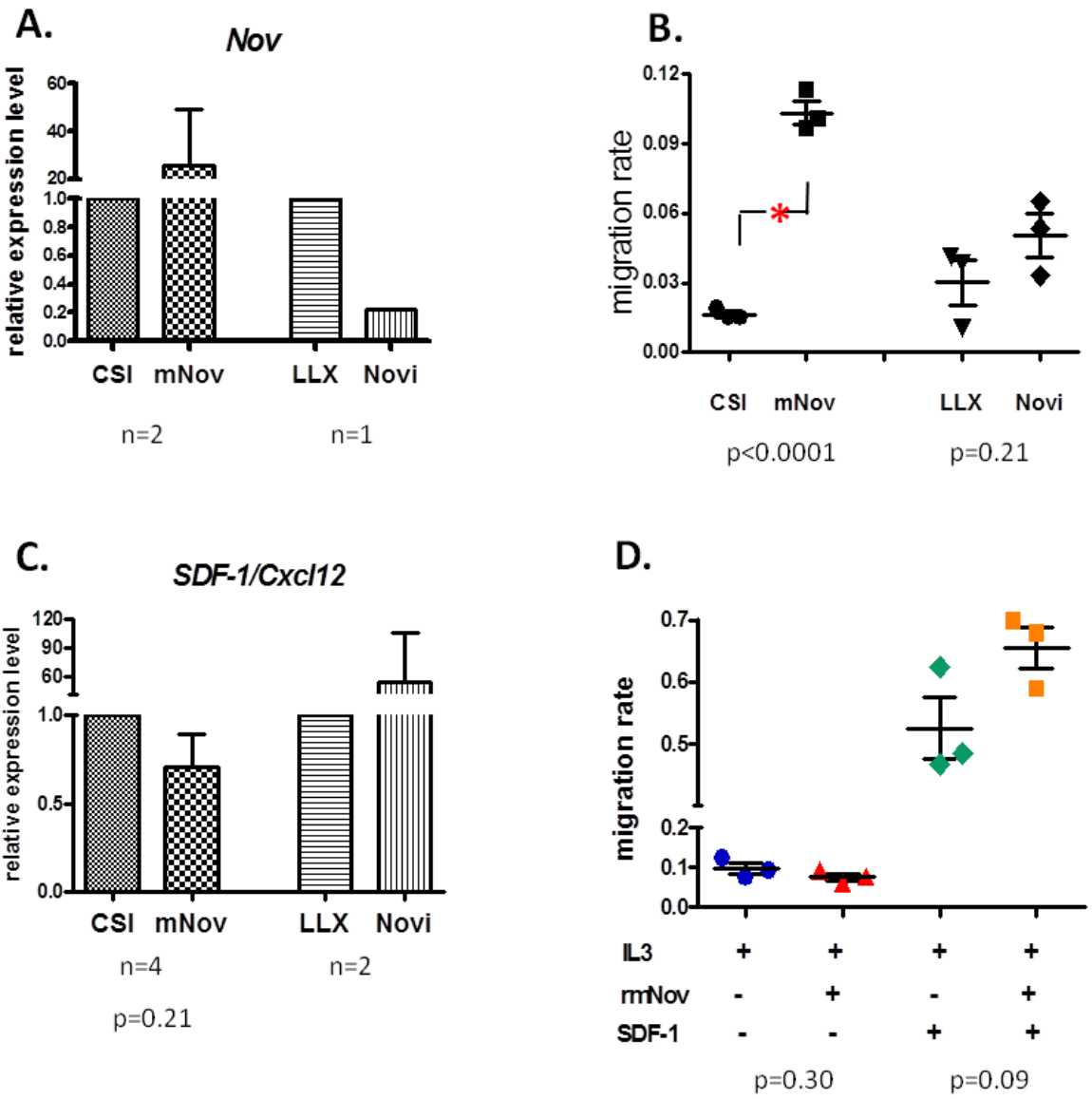


Figure.6.5: The effects of *Nov* in cell migration as extrinsic signal.

A. RT-qPCR results show that *Nov* expression is altered in CSI-mNov and LLX-Novi stromal cells.

B. Migration assay of FDCPmix towards stromal cells in the bottom wells. The results showed that overexpression of *Nov* in stromal cells could enhance FDCPmix cells migration while knocking down of *Nov* did not

affect the FDCPmix cells migration. Each dot represents individual well tested. The line indicates the mean ±SEM.

C. The RT-qPCR of *SDF-1/Cxcl12* mRNA was not changed in *Nov* overexpressing stromal cells. The expression of *SDF-1* in one of the LLX-Novi samples was extremely high which contributed the high mean value.

D. The migration rates of FDCPmix cells are similar between wells with or without rmNov in the bottom chambers. However, when SDF-1 was added to the bottom wells, there was a trend of increased migration toward rmNov and SDF-1, although it was not statistically significant. Each dot represents individual well tested.

The line indicates the mean ±SEM.

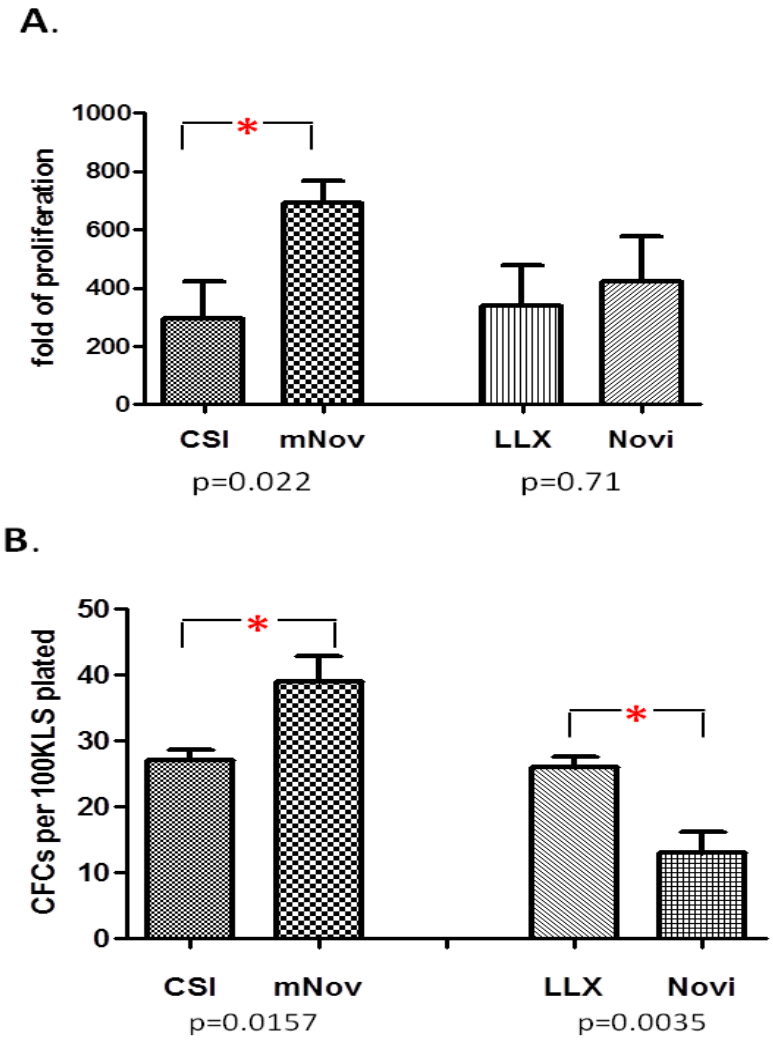


Figure.6.6: The growth rate and CFC frequency of KLS after being cultured with stromal cells for 7-10 days.

A. KLS were sorted directly onto stromal cells in SFEM without any cytokines and the proliferation rate was calculated after 7-10 days of co-culture. The results showed that stromal cells overexpressing *Nov* can increase KLS cells growth in co-culture. However, knock-down of *Nov* did not affect their supportive capacity.

B. Proliferated cells from KLS co-cultured with stromal cells were collected

and plated in M3434 to check their progenitor frequency. The results showed that there was significant increased frequency of colony forming cells expanded from KLS co-cultured with mNov stromal cells. In the meantime, cells expanded from KLS co-cultured on Novi stromal cells showed a decreased frequency of progenitors in CFC assay.

n=6, mean±SEM; p value is indicated under each group of comparison.

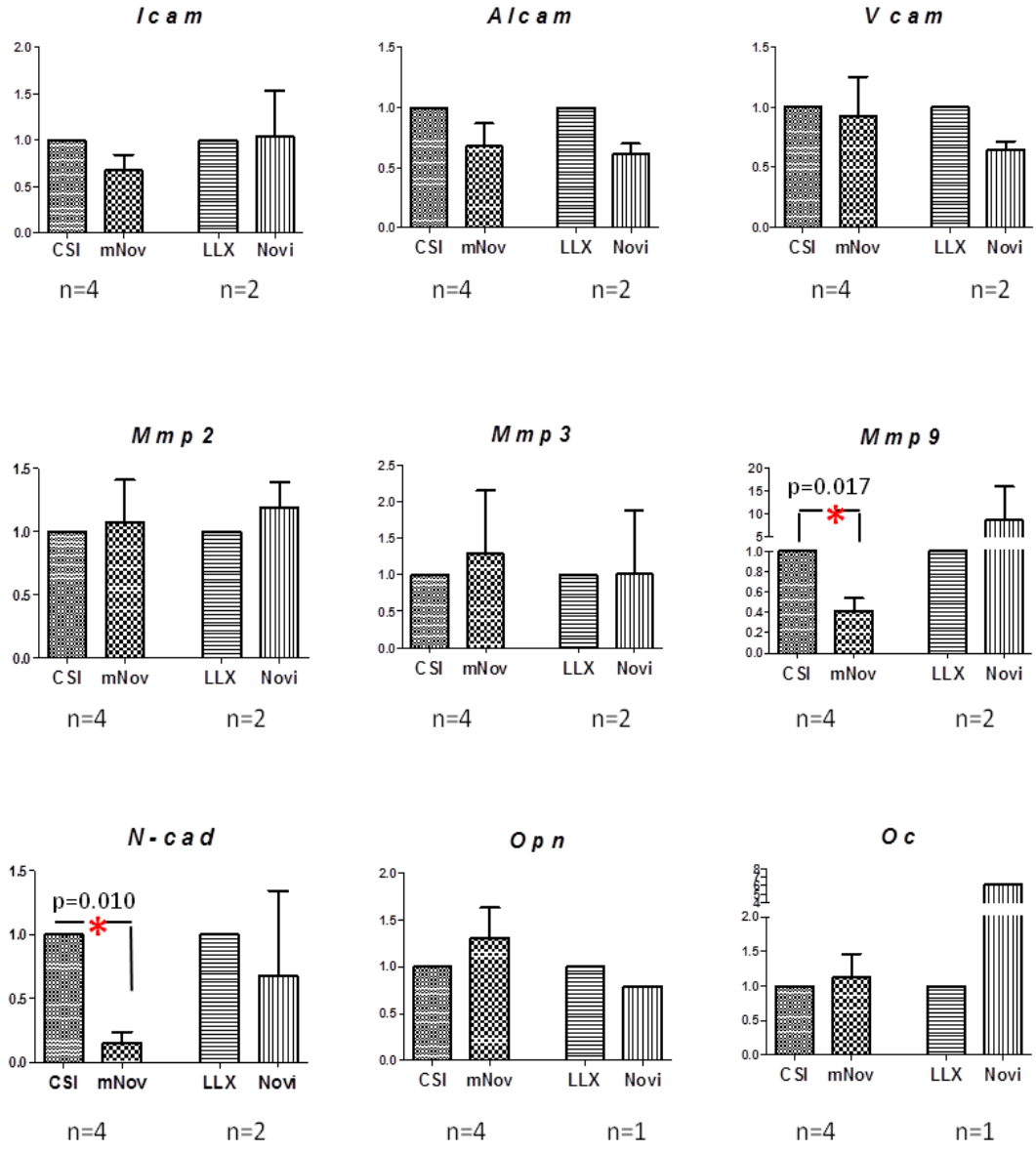


Figure.6.7: RT-qPCR results of stromal cells transduced with CSI/mNov or LLX/Novi virus.

All expression levels were normalized with Hprt1. The expression in cells transduced with control virus were set to 1 and compared with test cells. There were no significant changes of expression in CAM genes and MMPs except

Mmp9. There was also a consistent reduction of *N-cadherin* expression in mNov stromal cells. *Nov* had no effects on *Opn (*Osteopontin) and *Oc (*Osteocalcin) expression which were markers for osteoblast and osteoclast cells which were also presented in the stromal cells culture.

CHAPTER 7

FINAL DISCUSSION AND FUTURE EXPERIMENTS

Haematopoietic stem and progenitor cells (HSPC) are strictly regulated by intrinsic regulators and extrinsic signals from the microenvironment. Nov (CCN3), a matricellular protein of the CCN family, has been reported as a tumor suppressor gene in solid tumors and chronic myeloid leukaemia (CML), and as a positive regulator of HSPC function in human cord blood CD34+ cells. However, the functions of *Nov* in haematopoiesis of adult HSCs remain largely unknown. The studies described in this thesis aim to elucidate the function of *Nov* in mouse haematopoiesis in the hope of understanding the regulation of HSC and its interaction with the microenvironment.

Microarray data of human cord blood HSPC showed that *Nov* expression decreases during differentiation (Eckfeldt C.E, 2005). Similarly, I observed that the expression of *Nov* in mouse bone marrow HSC was down regulated rapidly during differentiation. *Nov* overexpression in mouse KLS cells could reduce their expansion rate and increase apoptosis *in vitro*. Moreover, overexpression of *Nov* in mouse KLS cells significantly reduced their long term reconstitution efficiency in bone marrow transplantation assay. Another interesting phenotype identified in bone marrow transplantation assay was that *Nov* overexpression could impair T cell differentiation in the thymus of irradiated recipients.

Surprisingly, ablation of *Nov* expression in mouse HSC did not affect their growth and differentiation *in vitro* and long term reconstitution *in vivo*. The analysis of *Nov*^{3del} mutant mice also showed normal haematopoietic and HSC function. On the whole, the data suggest that haematopoietic stem cells do not depend on *Nov* to regulate their maintenance and differentiation. However, the increased frequency of HSC observed from *Nov*^{3del} mutant mice indicated that *Nov* may play an important role in the interaction between HSCs and their niche. Indeed, the analysis showed that *Nov* is a positive regulator in HSC adhesion and migration. Further analysis of primary bone marrow stromal cells showed that *Nov* plays a positive role in stromal cells function in HSPC maintenance and may be involved in regulation of HSC niche through N-cadherin and MMP9.

Nov function in HSC: species specific or tissue specific

It was noted that *Nov* function in mouse bone marrow HSCs appeared to be a negative regulator and was dispensable for HSC maintenance and differentiation. Overexpression of *Nov* in mouse bone marrow HSC resulted in apoptosis and reduction of long term bone marrow reconstitution, while ablation of *Nov* expression in mouse HSC did not affect the growth and differentiation *in vitro* and long term reconstitution *in vivo*. In contrast, in human cord blood CD34+ HSCs, forced expression of *Nov* resulted in enhanced HSC function in CAFC assay and xenotransplantation assay of

immunodeficient NSG mice (Gupta R, 2007). Moreover, in human cord blood, knockdown of *Nov* expression significantly reduced their CAFC frequency and secondary bone marrow reconstitution in immunodeficient NSG mice. These data indicated that *Nov* was a positive intrinsic regulator for human HSC function (Gupta R, 2007). The conflicting observations on mouse bone marrow HSC from this thesis could be due to the fundamental difference between the two experimental systems deployed: the species difference- i.e. human vs. mouse; and the tissue and developmental difference- i.e. cord blood vs. bone marrow.

Firstly, the orthologous *Nov proteins* of human and mouse share more than 90% conservation (Figure 7.1). Therefore, it is unlikely that the difference observed in these two systems is due to sequence differences between the two proteins. This hypothesis is supported by preliminary experiments of overexpression of human *Nov* in mouse HSCs where *hNov* HSC showed similar defects in cell growth and reduction in bone marrow reconstitution efficiency (data not shown).

Alternatively, *Nov* may function differently in human and mouse haematopoiesis. It is not unusual for one gene to function differently in different species, for example, the contrasting expression of and response to FLT3 and cKIT in mouse and human HSCs (Sitnicka E, 2003). However, *hNov* function in human haematopoietic cells has been controversial as Nov

was initially reported as growth inhibitor in human haemotopoietic cells. Forced expression of Nov in human CML cells has been reported to confer growth regulation by causing growth inhibition and regaining sensitivity to the induction of apoptosis (McCallum, L 2006; McCallum, L 2009). Nov can also be down-regulated in CML by BCR-ABL through microRNAs 130a/b (Suresh, S, 2011). It is possible that the conflicting observation of Nov function in CML cells is simply due to the deregulation of stem cell function in leukemic cells. Notably, similar growth defects are induced by *Nov* in mouse HSC and human CML cells. In FDCPmix cells, a multipoint hemaetopoietic cell line derived from mouse, down-regulation of Nov has been shown to be a direct consequence of BCR-ABL kinase activity similar to the observation in human CML CD34+ cell (McCallum L, 2006). Therefore, the different effects observed in human cord blood HSCs and mouse bone marrow HSCs may not simply due to the species difference. The other fundamental difference between the two test systems was that the human experiments were performed with cord blood HSCs while the mouse experiments were with adult bone marrow HSCs. It has been known that there are certain biologic differences between HSCs in cord blood and bone marrow, including cloing efficiency in culture and cell division kinetics (Hao QL, 1995; da Silva C.L, 2009).

Other than the biological differences between their developmental stages, cord blood HSCs and bone marrow HSCs are located in different microenvironments. Cord blood HSCs are located in a microenvironment where there is more oxygen and no osteoblast cells compared to bone marrow (Dao M.A, 2007). Different microenvironment will provide different extrinsic regulation signals to HSC. Especially, *Nov* is expressed in several cell types in bone marrow and is an important regulator for bone formation (Katsube K, 2009). The *in vitro* analysis of Nov function in HSC cultured on stroma cells showed a positive effect in cell growth and cloning efficiency (Figure 6.6, page 221). It is therefore reasonable to consider that *Nov* function in haematopoiesis is tissue specific through bone marrow HSC niche.

General picture of *Nov* in HSC and bone marrow niche

It has been hypothesized that Nov secreted by mesenchymal stromal cells may regulate the growth and differentiation of neighbouring osteoblasts and HSCs through Notch and BMP signalling pathways (Katsube K, 2009). This model describes the functional mechanism of *Nov* in bone marrow and indicates a role of *Nov* in the HSC niche. Data from my thesis provides more detailed information of *Nov* function in the HSC and niche. In bone marrow, *Nov* is expressed in both HSC and niche cells. The expression levels are

similar in HSC and stromal cells, but lower in osteoblast and endothelial cells. In agreement with the model (Katsube K, 2009), forced expression of *Nov* in stromal cells enhanced the maintenance of HSC. *Nov* was also shown to positively regulate HSC adhesion and migration. These results indicate that the expression of *Nov* in mesenchymal stromal cells, although not the sole source of *Nov* in bone marrow, is a critical player in HSC niche; and *Nov* is involved in the intrinsic regulation of HSC interaction with niche, namely, adhesion and migration (Figure 7.2). RT-qPCR results suggest that N-cadherin and MMP9 as possible candidates in the regulation of HSC niche through *Nov*. Recent studies show that Connexin-43 (Cx43), a gap junction protein, controls the cellular content of the BM osteogenic microenvironment and prevents haematopoietic stem cell senescence through transfer of reactive oxygen species to bone marrow stromal cells (Gonzalez-Nieto D, 2012; Taniguchi Ishikawa E, 2012). It is worth noting that an interaction of Nov protein with the C terminus of Cx43 has been reported in glioma cells and overexpression of Cx43 in glioma cells could reduce proliferation and leads to production of soluble growth-inhibitory factors, including Nov (Fu C.T, 2004). Therefore, more detailed molecular analysis, especially the interaction of Cx43 and Nov in niche may shed light on the mechanism of *Nov* function in HSC niche.

Possible future directions

Data from this thesis have raised several interesting questions. Firstly, the experiments identified different responses of human HSC and mouse HSC to *Nov* and therefore further studies should address whether these two distinct results are due to the distinct HSC niche in which these cells normally reside *in vivo*. This could be achieved by comparing the function of Nov in human bone marrow HSC and cord blood HSC; and by comparing the function of *Nov* in mouse HSC from different HSC residing tissues, such as fetal liver, cord blood and bone marrow.

Further studies should also be focused on the mechanism of *Nov* function in the HSC niche which will lead to better understanding of where HSCs reside and how they are regulated. The detailed mechanism of *Nov* function in bone marrow stromal cells could be revealed by microarray assay of *Nov*-perturbed stromal cells. Examination of the interaction between *Nov* and *Cx43* within HSC niche will also add detailed information to the mechanism of HSC niche regulation of HSC.

Lastly, an interesting phenotype observed from mNov KLS bone marrow transplantation assay showed that *Nov* may regulate T cell differentiation in thymus. A relationship between *Nov* and T cell development has not been reported before, therefore, further study should be performed to understand the function of *Nov* in thymus and T cell development.

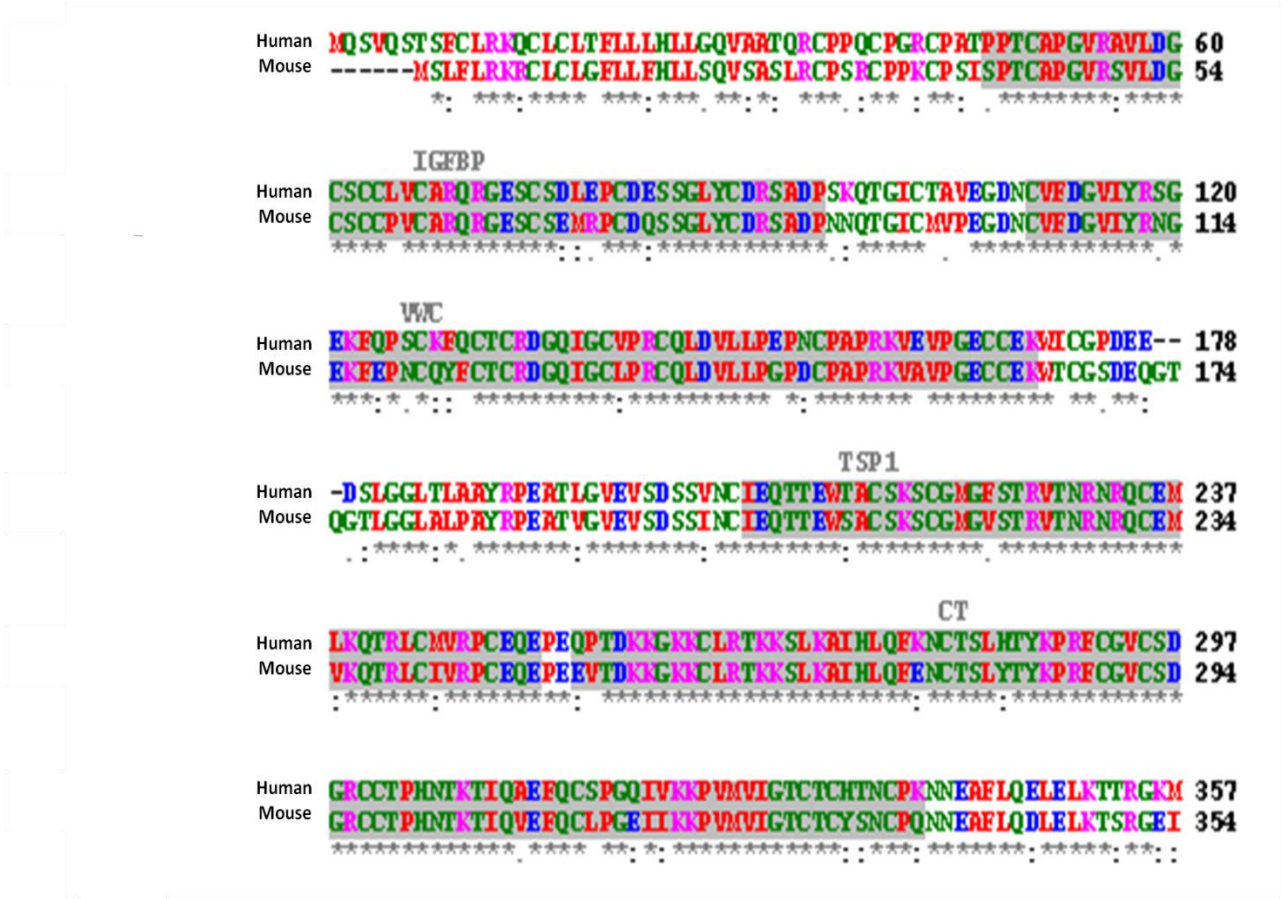


Figure 7.1: Alignment of orthologous human and mouse Nov proteins

The amino acid sequences of human and mouse proteins were aligned using MacVector software. The result shows that Nov proteins are highly *conserved proteins* with more than *90*% identity between *human* and mouse.

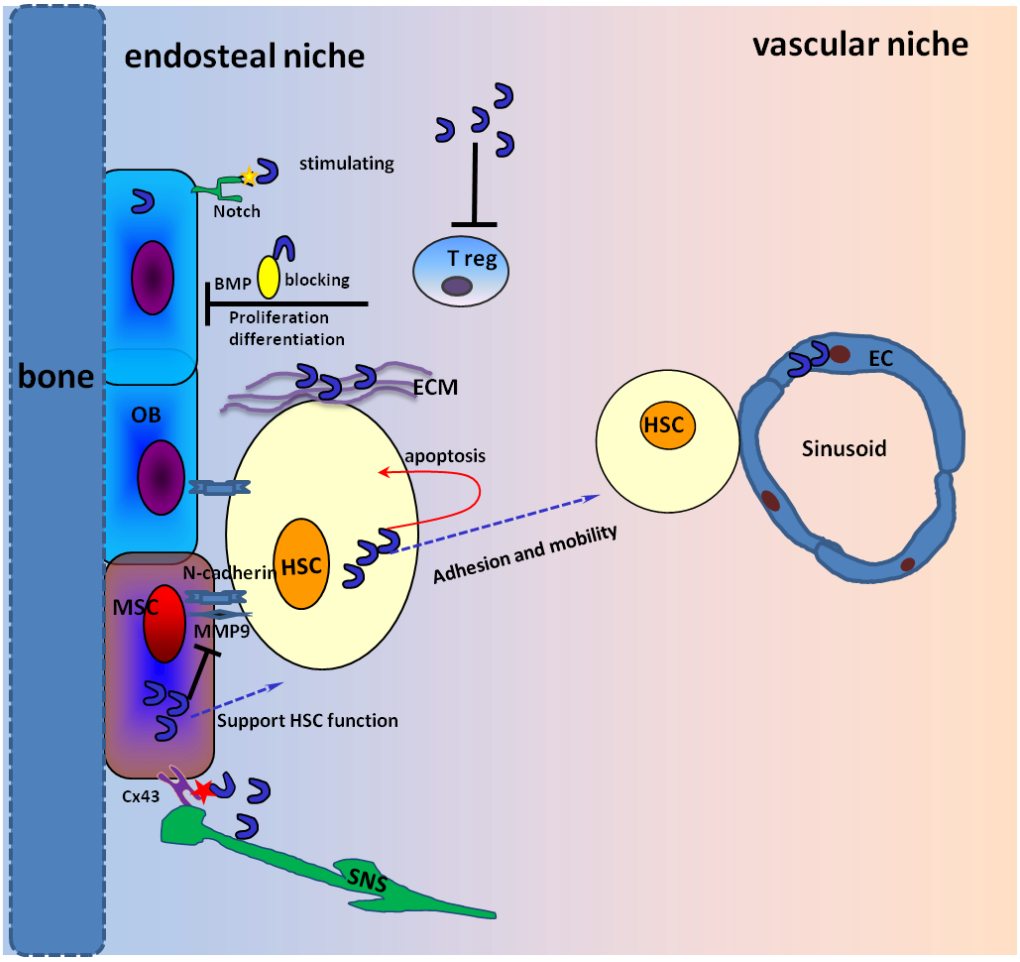


Figure 7.2: *Nov* function in bone marrow HSC niche

In bone marrow, *Nov* is expressed in both HSC and niche cells including MSC, OB and EC cells. The expression levels are similar in HSC and MSC cells, but lower in osteoblast and endothelial cells. Overexpression of *Nov* in HSC would result in apoptosis and reduction of long term bone marrow reconstitution with impaired T cell differentiation. Endogenous *Nov* is dispensable for HSC maintenance and differentiation, but is a positive regulator for HSC adhesion and migration.

The expression of *Nov* in stromal cells could enhance the maintenance of HSC which is possibly regulated through N-cadherin, MMP9 and Cx43.

HSC, haematopoietic stem cell; OB, Osteoblast; MSC, mesenchymal stromal cells; SNS, the sympathetic nervous system; T reg, Regulatory T cells; ECM , Extracellular matrix ; , Nov protein.

References:

Abkowitz, J. L., A. E. Robinson, S. Kale, M. W. Long, and J. Chen. 2003. Mobilization of hematopoietic stem cells during homeostasis and after cytokine exposure. *Blood* 102 (4):1249-1253.

Adolfsson, J., O. J. Borge, D. Bryder, K. Theilgaard-Monch, I. Astrand-Grundstrom, E. Sitnicka, Y. Sasaki, and S. E. Jacobsen. 2001. Upregulation of Flt3 expression within the bone marrow Lin(-)Sca1(+)c-kit(+) stem cell compartment is accompanied by loss of self-renewal capacity. *Immunity* 15 (4):659-669.

Adolfsson, J., R. Mansson, N. Buza-Vidas, A. Hultquist, K. Liuba, C. T. Jensen, D. Bryder, L. Yang, O. J. Borge, L. A. Thoren, K. Anderson, E. Sitnicka, Y. Sasaki, M. Sigvardsson, and S. E. Jacobsen. 2005. Identification of Flt3+ lympho-myeloid stem cells lacking erythro-megakaryocytic potential a revised road map for adult blood lineage commitment. *Cell* 121 (2):295-306.

Akashi, K., D. Traver, T. Miyamoto, and I. L. Weissman. 2000. A clonogenic common myeloid progenitor that gives rise to all myeloid lineages. *Nature* 404 (6774):193-197.

Alberico, T. A., J. N. Ihle, C. M. Liang, H. E. McGrath, and P. J. Quesenberry. 1987. Stromal growth factor production in irradiated lectin exposed long-term murine bone marrow cultures. *Blood* 69 (4):1120-1127.

Almarza, E., P. Rio, N. W. Meza, M. Aldea, X. Agirre, G. Guenechea, J. C. Segovia, and J. A. Bueren. 2007. Characteristics of lentiviral vectors harboring the proximal promoter of the vav proto-oncogene: a weak and efficient promoter for gene therapy. *Mol Ther* 15 (8):1487-1494.

Altrock, E., C. A. Muth, G. Klein, J. P. Spatz, and C. Lee-Thedieck. 2012. The significance of integrin ligand nanopatterning on lipid raft clustering in hematopoietic stem cells. Biomaterials 33 (11):3107-3118.

Antonchuk, J., G. Sauvageau, and R. K. Humphries. 2002. HOXB4-induced expansion of adult hematopoietic stem cells ex vivo. *Cell* 109 (1):39-45.

Arinobu, Y., S. Mizuno, Y. Chong, H. Shigematsu, T. Iino, H. Iwasaki, T. Graf, R. Mayfield, S. Chan, P. Kastner, and K. Akashi. 2007. Reciprocal activation of GATA-1 and PU.1 marks initial specification of hematopoietic stem cells into myeloerythroid and myelolymphoid lineages. *Cell Stem Cell* 1 (4):416-427.

Attema, J. L., P. Papathanasiou, E. C. Forsberg, J. Xu, S. T. Smale, and I. L. Weissman. 2007. Epigenetic characterization of hematopoietic stem cell differentiation using miniChIP and bisulfite sequencing analysis. *Proc Natl Acad Sci U S A* 104 (30):12371-12376.

Balduino, A., S. P. Hurtado, P. Frazao, C. M. Takiya, L. M. Alves, L. E. Nasciutti, M. C. El-Cheikh, and R. Borojevic. 2005. Bone marrow subendosteal microenvironment harbours functionally distinct haemosupportive stromal cell populations. *Cell Tissue Res* 319 (2):255-266.

Benini, S., B. Perbal, D. Zambelli, M. P. Colombo, M. C. Manara, M. Serra, M. Parenza, V. Martinez, P. Picci, and K. Scotlandi. 2005. In Ewing's sarcoma CCN3(NOV) inhibits proliferation while promoting migration and invasion of the same cell type. *Oncogene* 24 (27):4349-4361.

Bhandoola, A., H. von Boehmer, H. T. Petrie, and J. C. Zuniga-Pflucker. 2007. Commitment and developmental potential of extrathymic and intrathymic T cell precursors: plenty to choose from. *Immunity* 26 (6):678-689.

Bhardwaj, G., B. Murdoch, D. Wu, D. P. Baker, K. P. Williams, K. Chadwick, L. E. Ling, F. N. Karanu, and M. Bhatia. 2001. Sonic hedgehog induces the proliferation of primitive human hematopoietic cells via BMP regulation. *Nat Immunol* 2 (2):172-180.

Bjornsson, J. M., N. Larsson, A. C. Brun, M. Magnusson, E. Andersson, P. Lundstrom, J. Larsson, E. Repetowska, M. Ehinger, R. K. Humphries, and S. Karlsson. 2003. Reduced proliferative capacity of hematopoietic stem cells deficient in Hoxb3 and Hoxb4. *Mol Cell Biol* 23 (11):3872-3883.

Bleau, A. M., N. Planque, N. Lazar, D. Zambelli, A. Ori, T. Quan, G. Fisher, K. Scotlandi, and B. Perbal. 2007. Antiproliferative activity of CCN3: involvement of the C-terminal module and post-translational regulation. *J Cell Biochem* 101 (6):1475-1491.

Bohlig, L., R. Metzger, K. Rother, H. Till, and K. Engeland. 2008. The CCN3 gene coding for an extracellular adhesion-related protein is transcriptionally activated by the p53 tumor suppressor. *Cell Cycle* 7 (9):1254-1261.

Borkham-Kamphorst, E., C. R. van Roeyen, E. Van de Leur, J. Floege, and R. Weiskirchen. 2012. CCN3/NOV small interfering RNA enhances fibrogenic gene expression in primary hepatic stellate cells and cirrhotic fat storing cell line CFSC. *J Cell Commun Signal* 6 (1):11-25.

Breems, D. A., E. A. Blokland, K. E. Siebel, A. E. Mayen, L. J. Engels, and R. E. Ploemacher. 1998. Stroma-contact prevents loss of hematopoietic stem cell quality during ex vivo expansion of CD34+ mobilized peripheral blood stem cells. *Blood* 91 (1):111-117.

Brizzi, M. F., G. Tarone, and P. Defilippi. 2012. Extracellular matrix, integrins, and growth factors as tailors of the stem cell niche. *Curr Opin Cell Biol*.

Bryder, D., and S. E. Jacobsen. 2000. Interleukin-3 supports expansion of long-term multilineage repopulating activity after multiple stem cell divisions in vitro. *Blood* 96 (5):1748-1755.

Buza-Vidas, N., J. Antonchuk, H. Qian, R. Mansson, S. Luc, S. Zandi, K. Anderson, S. Takaki, J. M. Nygren, C. T. Jensen, and S. E. Jacobsen. 2006. Cytokines regulate postnatal hematopoietic stem cell expansion: opposing roles of thrombopoietin and LNK. *Genes Dev* 20 (15):2018-2023.

Calvi, L. M., G. B. Adams, K. W. Weibrecht, J. M. Weber, D. P. Olson, M. C. Knight, R. P. Martin, E. Schipani, P. Divieti, F. R. Bringhurst, L. A. Milner, H. M. Kronenberg, and D. T. Scadden. 2003. Osteoblastic cells regulate the haematopoietic stem cell niche. *Nature* 425 (6960):841-846.

Canalis, E. 2007. Nephroblastoma overexpressed (Nov) is a novel bone morphogenetic protein antagonist. *Ann N Y Acad Sci* 1116:50-58.

Canalis, E., A. Smerdel-Ramoya, D. Durant, A. N. Economides, W. G. Beamer, and S. Zanotti. 2010. Nephroblastoma overexpressed (Nov) inactivation sensitizes osteoblasts to bone morphogenetic protein-2, but nov is dispensable for skeletal homeostasis. *Endocrinology* 151 (1):221-233.

Cancelas, J. A., W. L. Koevoet, A. E. de Koning, A. E. Mayen, E. J. Rombouts, and R. E. Ploemacher. 2000. Connexin-43 gap junctions are involved in multiconnexin-expressing stromal support of hemopoietic progenitors and stem cells. *Blood* 96 (2):498-505.

Cancelas, J. A., and D. A. Williams. 2009. Rho GTPases in hematopoietic stem cell functions. *Curr Opin Hematol* 16 (4):249-254.

Carson, W. E., J. G. Giri, M. J. Lindemann, M. L. Linett, M. Ahdieh, R. Paxton, D. Anderson, J. Eisenmann, K. Grabstein, and M. A. Caligiuri. 1994. Interleukin (IL) 15 is a novel cytokine that activates human natural killer cells via components of the IL-2 receptor. *J Exp Med* 180 (4):1395-1403.

Charbord, P., and K. Moore. 2005. Gene expression in stem cell-supporting stromal cell lines. *Ann N Y Acad Sci* 1044:159-167.

Chen, P. C., Lin, T. H., Cheng, H. C., & Tang, C. H. 2012. CCN3 increases cell motility and ICAM-1 expression in prostate cancer cells. *Carcinogenesis*, 33(4):937-945

Cheng, T., N. Rodrigues, H. Shen, Y. Yang, D. Dombkowski, M. Sykes, and D. T. Scadden. 2000. Hematopoietic stem cell quiescence maintained by p21cip1/waf1. *Science* 287 (5459):1804-1808.

Cheshier, S. H., S. J. Morrison, X. Liao, and I. L. Weissman. 1999. In vivo proliferation and cell cycle kinetics of long-term self-renewing hematopoietic stem cells. *Proc Natl Acad Sci U S A* 96 (6):3120-3125.

Chou, S., P. Chu, W. Hwang, and H. Lodish. 2010. Expansion of human cord blood hematopoietic stem cells for transplantation. *Cell Stem Cell* 7 (4):427-428.

Chow, A., D. Lucas, A. Hidalgo, S. Mendez-Ferrer, D. Hashimoto, C. Scheiermann, M. Battista, M. Leboeuf, C. Prophete, N. van Rooijen, M. Tanaka, M. Merad, and P. S. Frenette. 2011. Bone marrow CD169+ macrophages promote the retention of hematopoietic stem and progenitor cells in the mesenchymal stem cell niche. *J Exp Med* 208 (2):261-271.

Christensen, J. L., and I. L. Weissman. 2001. Flk-2 is a marker in hematopoietic stem cell differentiation: a simple method to isolate long-term stem cells. *Proc Natl Acad Sci U S A* 98 (25):14541-14546.

Christensen, J. L., D. E. Wright, A. J. Wagers, and I. L. Weissman. 2004. Circulation and chemotaxis of fetal hematopoietic stem cells. *PLoS Biol* 2 (3):E75.

Ciofani, M., G. C. Knowles, D. L. Wiest, H. von Boehmer, and J. C. Zuniga-Pflucker. 2006. Stage-specific and differential notch dependency at the alphabeta and gammadelta T lineage bifurcation. *Immunity* 25 (1):105-116.

Crisan, M., S. Yap, L. Casteilla, C. W. Chen, M. Corselli, T. S. Park, G. Andriolo, B. Sun, B. Zheng, L. Zhang, C. Norotte, P. N. Teng, J. Traas, R. Schugar, B. M. Deasy, S. Badylak, H. J. Buhring, J. P. Giacobino, L. Lazzari, J. Huard, and B. Peault. 2008. A perivascular origin for mesenchymal stem cells in multiple human organs. *Cell Stem Cell* 3 (3):301-313.

da Silva, C. L., R. Goncalves, C. D. Porada, J. L. Ascensao, E. D. Zanjani, J. M. Cabral, and G. Almeida-Porada. 2009. Differences amid bone marrow and cord blood hematopoietic stem/progenitor cell division kinetics. *J Cell Physiol* 220 (1):102-111.

Dao, M. A., M. H. Creer, J. A. Nolta, and C. M. Verfaillie. 2007. Biology of umbilical cord blood progenitors in bone marrow niches. *Blood* 110 (1):74-81.

de Barros, A. P., C. M. Takiya, L. R. Garzoni, M. L. Leal-Ferreira, H. S. Dutra, L. B. Chiarini, M. N. Meirelles, R. Borojevic, and M. I. Rossi. 2010. Osteoblasts and bone marrow mesenchymal stromal cells control hematopoietic stem cell migration and proliferation in 3D in vitro model. *PLoS One* 5 (2):e9093.

de Graaf, C. A., and D. Metcalf. 2011. Thrombopoietin and hematopoietic stem cells. *Cell Cycle* 10 (10):1582-1589.

de Haan, G., S. J. Szilvassy, T. E. Meyerrose, B. Dontje, B. Grimes, and G. Van Zant. 2000. Distinct functional properties of highly purified hematopoietic stem cells from mouse strains differing in stem cell numbers. *Blood* 96 (4):1374-1379.

Deftos, M. L., Y. W. He, E. W. Ojala, and M. J. Bevan. 1998. Correlating notch signaling with thymocyte maturation. *Immunity* 9 (6):777-786.

Ding, L., T. L. Saunders, G. Enikolopov, and S. J. Morrison. 2012. Endothelial and perivascular cells maintain haematopoietic stem cells. *Nature* 481 (7382):457-462.

Domen, J., S. H. Cheshier, and I. L. Weissman. 2000. The role of apoptosis in the regulation of hematopoietic stem cells: Overexpression of Bcl-2 increases both their number and repopulation potential. *J Exp Med* 191 (2):253-264.

Domen, J., and I. L. Weissman. 2000. Hematopoietic stem cells need two signals to prevent apoptosis; BCL-2 can provide one of these, Kitl/c-Kit signaling the other. *J Exp Med* 192 (12):1707-1718.

Dumon, S., D. S. Walton, G. Volpe, N. Wilson, E. Dasse, W. Del Pozzo, J. R. Landry, B. Turner, L. P. O'Neill, B. Gottgens, and J. Frampton. 2012. Itga2b regulation at the onset of definitive hematopoiesis and commitment to differentiation. PLoS One 7 (8):e43300.

Eckfeldt, C. E., E. M. Mendenhall, C. M. Flynn, T. F. Wang, M. A. Pickart, S. M. Grindle, S. C. Ekker, and C. M. Verfaillie. 2005. Functional analysis of human hematopoietic stem cell gene expression using zebrafish. *PLoS Biol* 3 (8):e254.

Ehninger, A., and A. Trumpp. 2011. The bone marrow stem cell niche grows up: mesenchymal stem cells and macrophages move in. *J Exp Med* 208 (3):421-428.

Ema, H., and T. Suda. 2012. Two anatomically distinct niches regulate stem cell activity. *Blood* 120 (11):2174-2181.

Ferreira, M. S., W. Jahnen-Dechent, N. Labude, M. Bovi, T. Hieronymus, M. Zenke, R. K. Schneider, and S. Neurs. 2012. Cord blood-hematopoietic stem cell expansion in 3D fibrin scaffolds with stromal support. *Biomaterials* 33 (29):6987-6997.

Fitch, S. R., G. M. Kimber, N. K. Wilson, A. Parker, B. Mirshekar-Syahkal, B. Gottgens, A. Medvinsky, E. Dzierzak, and K. Ottersbach. 2012. Signaling from the Sympathetic Nervous System Regulates Hematopoietic Stem Cell Emergence during Embryogenesis. Cell Stem Cell 11 (4):554-566.

Fleming, H. E., V. Janzen, C. Lo Celso, J. Guo, K. M. Leahy, H. M. Kronenberg, and D. T. Scadden. 2008. Wnt signaling in the niche enforces hematopoietic stem cell quiescence and is necessary to preserve self-renewal in vivo. *Cell Stem Cell* 2 (3):274-283.

Fleming, W. H., E. J. Alpern, N. Uchida, K. Ikuta, G. J. Spangrude, and I. L. Weissman. 1993. Functional heterogeneity is associated with the cell cycle status of murine hematopoietic stem cells. *J Cell Biol* 122 (4):897-902.

Frimberger, A. E., A. I. Stering, and P. J. Quesenberry. 2001. An in vitro model of hematopoietic stem cell homing demonstrates rapid homing and maintenance of engraftable stem cells. *Blood* 98 (4):1012-1018.

Fu, C. T., J. F. Bechberger, M. A. Ozog, B. Perbal, and C. C. Naus. 2004. CCN3 (NOV) interacts with connexin43 in C6 glioma cells: possible mechanism of connexin-mediated growth suppression. *J Biol Chem* 279 (35):36943-36950.

Fujisaki, J., J. Wu, A. L. Carlson, L. Silberstein, P. Putheti, R. Larocca, W. Gao, T. I. Saito, C. Lo Celso, H. Tsuyuzaki, T. Sato, D. Cote, M. Sykes, T. B. Strom, D. T. Scadden, and C. P. Lin. 2011. In vivo imaging of Treg cells providing immune privilege to the haematopoietic stem-cell niche. *Nature* 474 (7350):216-219.

Fukunaga-Kalabis, M., G. Martinez, Z. J. Liu, J. Kalabis, P. Mrass, W. Weninger, S. M. Firth, N. Planque, B. Perbal, and M. Herlyn. 2006. CCN3 controls 3D spatial localization of melanocytes in the human skin through DDR1. *J Cell Biol* 175 (4):563-569.

Fukunaga-Kalabis, M., G. Martinez, S. M. Telson, Z. J. Liu, K. Balint, I. Juhasz, D. E. Elder, B. Perbal, and M. Herlyn. 2008. Downregulation of CCN3 expression as a potential mechanism for melanoma progression. *Oncogene* 27 (18):2552-2560.

Galy, A., M. Travis, D. Cen, and B. Chen. 1995. Human T, B, natural killer, and dendritic cells arise from a common bone marrow progenitor cell subset. *Immunity* 3 (4):459-473.

Gan, B., J. Hu, S. Jiang, Y. Liu, E. Sahin, L. Zhuang, E. Fletcher-Sananikone, S. Colla, Y. A. Wang, L. Chin, and R. A. Depinho. 2010. Lkb1 regulates quiescence and metabolic homeostasis of haematopoietic stem cells. *Nature* 468 (7324):701-704.

Gao, J., S. Graves, U. Koch, S. Liu, V. Jankovic, S. Buonamici, A. El Andaloussi, S. D. Nimer, B. L. Kee, R. Taichman, F. Radtke, and I. Aifantis. 2009. Hedgehog signaling is dispensable for adult hematopoietic stem cell function. *Cell Stem Cell* 4 (6):548-558.

Gekas, C., and T. Graf. 2013. CD41 expression marks myeloid-biased adult hematopoietic stem cells and increases with age. Blood 121 (22):4463-4472

Gellhaus, A., M. Schmidt, C. Dunk, S. J. Lye, and E. Winterhager. 2007. The circulating proangiogenic factors CYR61 (CCN1) and NOV (CCN3) are significantly decreased in placentae and sera of preeclamptic patients. *Reprod Sci* 14 (8 Suppl):46-52.

Gilham, D. E., A. L. M. Lie, N. Taylor, and R. E. Hawkins. 2010. Cytokine stimulation and the choice of promoter are critical factors for the efficient transduction of mouse T cells with HIV-1 vectors. *J Gene Med* 12 (2):129-136.

Gimble, J. M., C. E. Robinson, X. Wu, and K. A. Kelly. 1996. The function of adipocytes in the bone marrow stroma: an update. *Bone* 19 (5):421-428.

Gonzalez-Murillo, A., M. L. Lozano, L. Alvarez, A. Jacome, E. Almarza, S. Navarro, J. C. Segovia, H. Hanenberg, G. Guenechea, J. A. Bueren, and P. Rio. 2010. Development of lentiviral vectors with optimized transcriptional activity for the gene therapy of patients with Fanconi anemia. *Hum Gene Ther* 21 (5):623-630.

Gonzalez-Nieto, D., L. Li, A. Kohler, G. Ghiaur, E. Ishikawa, A. Sengupta, M. Madhu, J. L. Arnett, R. A. Santho, S. K. Dunn, G. I. Fishman, D. E. Gutstein, R. Civitelli, L. C. Barrio, M. Gunzer, and J. A. Cancelas. 2012. Connexin-43 in the osteogenic BM niche regulates its cellular composition and the bidirectional traffic of hematopoietic stem cells and progenitors. *Blood* 119 (22):5144-5154.

Grabstein, K. H., T. J. Waldschmidt, F. D. Finkelman, B. W. Hess, A. R. Alpert, N. E. Boiani, A. E. Namen, and P. J. Morrissey. 1993. Inhibition of murine B and T lymphopoiesis in vivo by an anti-interleukin 7 monoclonal antibody. *J Exp Med* 178 (1):257-264.

Graf, T., and T. Enver. 2009. Forcing cells to change lineages. *Nature* 462 (7273):587-594.

Gupta, N., H. Wang, T. L. McLeod, C. C. Naus, S. Kyurkchiev, S. Advani, J. Yu, B. Perbal, and R. R. Weichselbaum. 2001. Inhibition of glioma cell growth and tumorigenic potential by CCN3 (NOV). *Mol Pathol* 54 (5):293-299.

Gupta, R., D. Hong, F. Iborra, S. Sarno, and T. Enver. 2007. NOV (CCN3) functions as a regulator of human hematopoietic stem or progenitor cells. *Science* 316 (5824):590-593.

Gurumurthy, S., S. Z. Xie, B. Alagesan, J. Kim, R. Z. Yusuf, B. Saez, A. Tzatsos, F. Ozsolak, P. Milos, F. Ferrari, P. J. Park, O. S. Shirihai, D. T. Scadden, and N. Bardeesy. 2010. The Lkb1 metabolic sensor maintains haematopoietic stem cell survival. *Nature* 468 (7324):659-663.

Hao QL, Shah AJ, Thiemann FT, Smogorzewska EM, Crooks GM. 1995. A functional comparison of CD34 + CD38- cells in cord blood and bone marrow. Blood 86: 3745-3753

Hasserjian, R. P., J. C. Aster, F. Davi, D. S. Weinberg, and J. Sklar. 1996. Modulated expression of notch1 during thymocyte development. *Blood* 88 (3):970-976.

Haug, J. S., X. C. He, J. C. Grindley, J. P. Wunderlich, K. Gaudenz, J. T. Ross, A. Paulson, K. P. Wagner, Y. Xie, R. Zhu, T. Yin, J. M. Perry, M. J. Hembree, E. P. Redenbaugh, G. L. Radice, C. Seidel, and L. Li. 2008. N-cadherin expression level distinguishes reserved versus primed states of hematopoietic stem cells. *Cell Stem Cell* 2 (4):367-379.

Heath, E., D. Tahri, E. Andermarcher, P. Schofield, S. Fleming, and C. A. Boulter. 2008. Abnormal skeletal and cardiac development, cardiomyopathy, muscle atrophy and cataracts in mice with a targeted disruption of the Nov (Ccn3) gene. *BMC Dev Biol* 8:18.

Helgason, C. D., G. Sauvageau, H. J. Lawrence, C. Largman, and R. K. Humphries. 1996. Overexpression of HOXB4 enhances the hematopoietic potential of embryonic stem cells differentiated in vitro. *Blood* 87 (7):2740-2749.

Henschler, R., W. Brugger, T. Luft, T. Frey, R. Mertelsmann, and L. Kanz. 1994. Maintenance of transplantation potential in ex vivo expanded CD34(+)-selected human peripheral blood progenitor cells. *Blood* 84 (9):2898-2903.

Hock, H., M. J. Hamblen, H. M. Rooke, J. W. Schindler, S. Saleque, Y. Fujiwara, and S. H. Orkin. 2004. Gfi-1 restricts proliferation and preserves functional integrity of haematopoietic stem cells. *Nature* 431 (7011):1002-1007.

Hofmann, I., E. H. Stover, D. E. Cullen, J. Mao, K. J. Morgan, B. H. Lee, M. G. Kharas, P. G. Miller, M. G. Cornejo, R. Okabe, S. A. Armstrong, N. Ghilardi, S. Gould, F. J. de Sauvage, A. P. McMahon, and D. G. Gilliland. 2009. Hedgehog signaling is dispensable for adult murine hematopoietic stem cell function and hematopoiesis. *Cell Stem Cell* 4 (6):559-567.

Holbourn, K. P., K. R. Acharya, and B. Perbal. 2008. The CCN family of proteins: structure-function relationships. *Trends Biochem Sci* 33 (10):461-473.

Holbourn, K. P., M. Malfois, and K. R. Acharya. 2011. First structural glimpse of CCN3 and CCN5 multifunctional signaling regulators elucidated by small angle x-ray scattering. *J Biol Chem* 286 (25):22243-22249.

Huang, C. Y., C. Y. Lee, M. Y. Chen, H. C. Tsai, H. C. Hsu, and C. H. Tang. 2011. Nephroblastoma overexpressed gene (NOV) enhances cell motility and COX-2 upregulation of human osteosarcoma involves alphavbeta5 integrin, ILK and AP-1-dependent pathways. *Biochem Pharmacol* 81 (5):577-585.

Ikuta, K., and I. L. Weissman. 1992. Evidence that hematopoietic stem cells express mouse c-kit but do not depend on steel factor for their generation. *Proc Natl Acad Sci U S A* 89 (4):1502-1506.

Inaba, K., M. Inaba, M. Deguchi, K. Hagi, R. Yasumizu, S. Ikehara, S. Muramatsu, and R. M. Steinman. 1993. Granulocytes, macrophages, and dendritic cells arise from a common major histocompatibility complex class II-negative progenitor in mouse bone marrow. *Proc Natl Acad Sci U S A* 90 (7):3038-3042.

Ito, K., A. Hirao, F. Arai, S. Matsuoka, K. Takubo, I. Hamaguchi, K. Nomiyama, K. Hosokawa, K. Sakurada, N. Nakagata, Y. Ikeda, T. W. Mak, and T. Suda. 2004. Regulation of oxidative stress by ATM is required for self-renewal of haematopoietic stem cells. *Nature* 431 (7011):997-1002.

Iwasaki, H., S. Mizuno, R. A. Wells, A. B. Cantor, S. Watanabe, and K. Akashi. 2003. GATA-1 converts lymphoid and myelomonocytic progenitors into the megakaryocyte/erythrocyte lineages. *Immunity* 19 (3):451-462.

Jiang, D., L. Zheng, and M. J. Lenardo. 1999. Caspases in T-cell receptor-induced thymocyte apoptosis. *Cell Death Differ* 6 (5):402-411.

Jing, D., A. V. Fonseca, N. Alakel, F. A. Fierro, K. Muller, M. Bornhauser, G. Ehninger, D. Corbeil, and R. Ordemann. 2010. Hematopoietic stem cells in co-culture with mesenchymal stromal cells--modeling the niche compartments in vitro. *Haematologica* 95 (4):542-550.

Joliot, V., C. Martinerie, G. Dambrine, G. Plassiart, M. Brisac, J. Crochet, and B. Perbal. 1992. Proviral rearrangements and overexpression of a new cellular gene (nov) in myeloblastosis-associated virus type 1-induced nephroblastomas. *Mol Cell Biol* 12 (1):10-21.

Kajiume, T., N. Ohno, Y. Sera, Y. Kawahara, L. Yuge, and M. Kobayashi. 2009. Reciprocal expression of Bmi1 and Mel-18 is associated with functioning of primitive hematopoietic cells. *Exp Hematol* 37 (7):857-866 e852.

Karsunky, H., M. A. Inlay, T. Serwold, D. Bhattacharya, and I. L. Weissman. 2008. Flk2+ common lymphoid progenitors possess equivalent differentiation potential for the B and T lineages. *Blood* 111 (12):5562-5570.

Katayama, Y., M. Battista, W. M. Kao, A. Hidalgo, A. J. Peired, S. A. Thomas, and P. S. Frenette. 2006. Signals from the sympathetic nervous system regulate hematopoietic stem cell egress from bone marrow. *Cell* 124 (2):407-421.

Katsube, K., S. Ichikawa, Y. Katsuki, T. Kihara, M. Terai, L. F. Lau, Y. Tamamura, S. Takeda, A. Umezawa, K. Sakamoto, and A. Yamaguchi. 2009. CCN3 and bone marrow cells. *J Cell Commun Signal* 3 (2):135-145.

Katsuki, Y., K. Sakamoto, T. Minamizato, H. Makino, A. Umezawa, M. A. Ikeda, B. Perbal, T. Amagasa, A. Yamaguchi, and K. Katsube. 2008. Inhibitory effect of CT domain of CCN3/NOV on proliferation and differentiation of osteogenic mesenchymal stem cells, Kusa-A1. *Biochem Biophys Res Commun* 368 (3):808-814.

Kaushansky, K. 1999. Thrombopoietin and hematopoietic stem cell development. *Ann N Y Acad Sci* 872:314-319.

Kaushansky, K. 2006. Lineage-specific hematopoietic growth factors. *N Engl J Med* 354 (19):2034-2045.

Kaushansky, K., S. Lok, R. D. Holly, V. C. Broudy, N. Lin, M. C. Bailey, J. W. Forstrom, M. M. Buddle, P. J. Oort, F. S. Hagen, and et al. 1994. Promotion of megakaryocyte progenitor expansion and differentiation by the c-Mpl ligand thrombopoietin. *Nature* 369 (6481):568-571.

Kawaki, H., S. Kubota, A. Suzuki, M. Suzuki, K. Kohsaka, K. Hoshi, T. Fujii, N. Lazar, T. Ohgawara, T. Maeda, B. Perbal, T. Takano-Yamamoto, and M. Takigawa. 2011. Differential roles of CCN family proteins during osteoblast differentiation: Involvement of Smad and MAPK signaling pathways. *Bone* 49 (5):975-989.

Kawamoto, H., T. Ikawa, K. Masuda, H. Wada, and Y. Katsura. 2010. A map for lineage restriction of progenitors during hematopoiesis: the essence of the myeloid-based model. *Immunol Rev* 238 (1):23-36.

Kawamoto, H., and Y. Katsura. 2009. A new paradigm for hematopoietic cell lineages: revision of the classical concept of the myeloid-lymphoid dichotomy. *Trends Immunol* 30 (5):193-200.

Kawamoto, H., K. Ohmura, N. Hattori, and Y. Katsura. 1997. Hemopoietic progenitors in the murine fetal liver capable of rapidly generating T cells. *J Immunol* 158 (7):3118-3124.

Kiel, M. J., and S. J. Morrison. 2006. Maintaining hematopoietic stem cells in the vascular niche. *Immunity* 25 (6):862-864.

Kiel, M. J., O. H. Yilmaz, T. Iwashita, O. H. Yilmaz, C. Terhorst, and S. J. Morrison. 2005. SLAM family receptors distinguish hematopoietic stem and progenitor cells and reveal endothelial niches for stem cells. *Cell* 121 (7):1109-1121.

Kim, I., S. He, O. H. Yilmaz, M. J. Kiel, and S. J. Morrison. 2006. Enhanced purification of fetal liver hematopoietic stem cells using SLAM family receptors. *Blood* 108 (2):737-744.

Kimura, A., C. Martin, G. W. Robinson, J. M. Simone, W. Chen, M. C. Wickre, J. J. O'Shea, and L. Hennighausen. 2010. The gene encoding the hematopoietic stem cell regulator CCN3/NOV is under direct cytokine control through the transcription factors STAT5A/B. *J Biol Chem* 285 (43):32704-32709.

Kimura, A., M. A. Rieger, J. M. Simone, W. Chen, M. C. Wickre, B. M. Zhu, P. S. Hoppe, J. J. O'Shea, T. Schroeder, and L. Hennighausen. 2009. The transcription factors STAT5A/B regulate GM-CSF-mediated granulopoiesis. *Blood* 114 (21):4721-4728.

Kobayashi, M., J. H. Laver, T. Kato, H. Miyazaki, and M. Ogawa. 1995. Recombinant human thrombopoietin (Mpl ligand) enhances proliferation of erythroid progenitors. *Blood* 86 (7):2494-2499.

Kollet, O., A. Dar, S. Shivtiel, A. Kalinkovich, K. Lapid, Y. Sztainberg, M. Tesio, R. M. Samstein, P. Goichberg, A. Spiegel, A. Elson, and T. Lapidot. 2006. Osteoclasts degrade endosteal components and promote mobilization of hematopoietic progenitor cells. *Nat Med* 12 (6):657-664.

Kondo, M., I. L. Weissman, and K. Akashi. 1997. Identification of clonogenic common lymphoid progenitors in mouse bone marrow. *Cell* 91 (5):661-672.

Kopp, H. G., S. T. Avecilla, A. T. Hooper, and S. Rafii. 2005. The bone marrow vascular niche: home of HSC differentiation and mobilization. *Physiology (Bethesda)* 20:349-356.

Koury, M. J., and M. C. Bondurant. 1990. Erythropoietin retards DNA breakdown and prevents programmed death in erythroid progenitor cells. *Science* 248 (4953):378-381.

Krause, D. S. 2002. Regulation of hematopoietic stem cell fate. *Oncogene* 21 (21):3262-3269.

Kular, L., Pakradouni, J., Kitabgi, P., Laurent, M., & Martinerie, C. (2011). The CCN family: a new class of inflammation modulators? Biochimie, 93(3), 377-388.

Kulessa, H., J. Frampton, and T. Graf. 1995. GATA-1 reprograms avian myelomonocytic cell lines into eosinophils, thromboblasts, and erythroblasts. *Genes Dev* 9 (10):1250-1262.

Kurth, I., K. Franke, T. Pompe, M. Bornhauser, and C. Werner. 2009. Hematopoietic stem and progenitor cells in adhesive microcavities. *Integr Biol (Camb)* 1 (5-6):427-434.

Lafont, J., H. Thibout, C. Dubois, M. Laurent, and C. Martinerie. 2005. NOV/CCN3 induces adhesion of muscle skeletal cells and cooperates with FGF2 and IGF-1 to promote proliferation and survival. *Cell Commun Adhes* 12 (1-2):41-57.

Lazar, N., C. Manara, S. Navarro, A. M. Bleau, A. Llombart-Bosch, K. Scotlandi, N. Planque, and B. Perbal. 2007. Domain-specific CCN3 antibodies as unique tools for structural and functional studies. *J Cell Commun Signal* 1 (2):91-102.

Letting, D. L., Y. Y. Chen, C. Rakowski, S. Reedy, and G. A. Blobel. 2004. Context-dependent regulation of GATA-1 by friend of GATA-1. *Proc Natl Acad Sci U S A* 101 (2):476-481.

Levesque, J. P. 2012. N(o)-cadherin role for HSCs. *Blood* 120 (2):237-238.

Li, C. L., V. Martinez, B. He, A. Lombet, and B. Perbal. 2002. A role for CCN3 (NOV) in calcium signalling. *Mol Pathol* 55 (4):250-261.

Li, J. 2011. Quiescence regulators for hematopoietic stem cell. *Exp Hematol* 39 (5):511-520.

Lin, C. G., S. J. Leu, N. Chen, C. M. Tebeau, S. X. Lin, C. Y. Yeung, and L. F. Lau. 2003. CCN3 (NOV) is a novel angiogenic regulator of the CCN protein family. *J Biol Chem* 278 (26):24200-24208.

Lind, E. F., S. E. Prockop, H. E. Porritt, and H. T. Petrie. 2001. Mapping precursor movement through the postnatal thymus reveals specific microenvironments supporting defined stages of early lymphoid development. *J Exp Med* 194 (2):127-134.

Liu, C., X. J. Liu, P. D. Crowe, G. S. Kelner, J. Fan, G. Barry, F. Manu, N. Ling, E. B. De Souza, and R. A. Maki. 1999. Nephroblastoma overexpressed gene (NOV) codes for a growth factor that induces protein tyrosine phosphorylation. *Gene* 238 (2):471-478.

Lu, M., H. Kawamoto, Y. Katsube, T. Ikawa, and Y. Katsura. 2002. The common myelolymphoid progenitor: a key intermediate stage in hemopoiesis generating T and B cells. *J Immunol* 169 (7):3519-3525.

Lu, M., R. Tayu, T. Ikawa, K. Masuda, I. Matsumoto, H. Mugishima, H. Kawamoto, and Y. Katsura. 2005. The earliest thymic progenitors in adults are restricted to T, NK, and dendritic cell lineage and have a potential to form more diverse TCRbeta chains than fetal progenitors. *J Immunol* 175 (9):5848-5856.

Lu, P., V. M. Weaver, and Z. Werb. 2012. The extracellular matrix: a dynamic niche in cancer progression. *J Cell Biol* 196 (4):395-406.

Lymperi, S., A. Ersek, F. Ferraro, F. Dazzi, and N. J. Horwood. 2010. Inhibition of osteoclast function reduces hematopoietic stem cell numbers in vivo. *Blood* 117 (5):1540-1549.

Lymperi, S., F. Ferraro, and D. T. Scadden. 2010. The HSC niche concept has turned 31. Has our knowledge matured? *Ann N Y Acad Sci* 1192:12-18.

Manara, M. C., B. Perbal, S. Benini, R. Strammiello, V. Cerisano, S. Perdichizzi, M. Serra, A. Astolfi, F. Bertoni, J. Alami, H. Yeger, P. Picci, and K. Scotlandi. 2002. The expression of ccn3(nov) gene in musculoskeletal tumors. *Am J Pathol* 160 (3):849-859.

Mansour, A., G. Abou-Ezzi, E. Sitnicka, S. E. Jacobsen, A. Wakkach, and C. Blin-Wakkach. 2012. Osteoclasts promote the formation of hematopoietic stem cell niches in the bone marrow. *J Exp Med* 209 (3):537-549.

Mansson, R., A. Hultquist, S. Luc, L. Yang, K. Anderson, S. Kharazi, S. Al-Hashmi, K. Liuba, L. Thoren, J. Adolfsson, N. Buza-Vidas, H. Qian, S. Soneji, T. Enver, M. Sigvardsson, and S. E. Jacobsen. 2007. Molecular evidence for hierarchical transcriptional lineage priming in fetal and adult stem cells and multipotent progenitors. *Immunity* 26 (4):407-419.

Manz, M. G., D. Traver, T. Miyamoto, I. L. Weissman, and K. Akashi. 2001. Dendritic cell potentials of early lymphoid and myeloid progenitors. *Blood* 97 (11):3333-3341.

Martin, P., G. M. del Hoyo, F. Anjuere, S. R. Ruiz, C. F. Arias, A. R. Marin, and C. Ardavin. 2000. Concept of lymphoid versus myeloid dendritic cell lineages revisited: both CD8alpha(-) and CD8alpha(+) dendritic cells are generated from CD4(low) lymphoid-committed precursors. *Blood* 96 (7):2511-2519.

Martinerie, C., C. Gicquel, A. Louvel, M. Laurent, P. N. Schofield, and Y. Le Bouc. 2001. Altered expression of novH is associated with human adrenocortical tumorigenesis. *J Clin Endocrinol Metab* 86 (8):3929-3940.

McCallum, L., and A. E. Irvine. 2009. CCN3--a key regulator of the hematopoietic compartment. *Blood Rev* 23 (2):79-85.

McCallum, L., W. Lu, S. Price, N. Lazar, B. Perbal, and A. E. Irvine. 2009. CCN3: a key growth regulator in Chronic Myeloid Leukaemia. *J Cell Commun Signal* 3 (2):115-124.

McCallum, L., 2012. CCN3 suppresses mitogenic signalling and reinstates growth control mechanisms in Chronic Myeloid Leukaemia. *J Cell Commun Signal* 6 (1):27-35.

McCallum, L., S. Price, N. Planque, B. Perbal, A. Pierce, A. D. Whetton, and A. E. Irvine. 2006. A novel mechanism for BCR-ABL action: stimulated secretion of CCN3 is involved in growth and differentiation regulation. *Blood* 108 (5):1716-1723.

Mendez-Ferrer, S., D. Lucas, M. Battista, and P. S. Frenette. 2008. Haematopoietic stem cell release is regulated by circadian oscillations. *Nature* 452 (7186):442-447.

Mendez-Ferrer, S., T. V. Michurina, F. Ferraro, A. R. Mazloom, B. D. Macarthur, S. A. Lira, D. T. Scadden, A. Ma'ayan, G. N. Enikolopov, and P. S. Frenette. 2010. Mesenchymal and haematopoietic stem cells form a unique bone marrow niche. *Nature* 466 (7308):829-834.

Mercier, F. E., C. Ragu, and D. T. Scadden. 2012. The bone marrow at the crossroads of blood and immunity. *Nat Rev Immunol* 12 (1):49-60.

Metcalf, D. 1986. The molecular biology and functions of the granulocyte-macrophage colony-stimulating factors. *Blood* 67 (2):257-267.

Metcalf, D. 2007. Concise review: hematopoietic stem cells and tissue stem cells: current concepts and unanswered questions. *Stem Cells* 25 (10):2390-2395.

Minamizato, T., K. Sakamoto, T. Liu, H. Kokubo, K. Katsube, B. Perbal, S. Nakamura, and A. Yamaguchi. 2007. CCN3/NOV inhibits BMP-2-induced osteoblast differentiation by interacting with BMP and Notch signaling pathways. *Biochem Biophys Res Commun* 354 (2):567-573.

Mohrin, M., E. Bourke, D. Alexander, M. R. Warr, K. Barry-Holson, M. M. Le Beau, C. G. Morrison, and E. Passegue. 2010. Hematopoietic stem cell quiescence promotes error-prone DNA repair and mutagenesis. *Cell Stem Cell* 7 (2):174-185.

Montecino-Rodriguez, E., and K. Dorshkind. 2001. Regulation of hematopoiesis by gap junction-mediated intercellular communication. *J Leukoc Biol* 70 (3):341-347.

Morrison, S. J., and I. L. Weissman. 1994. The long-term repopulating subset of hematopoietic stem cells is deterministic and isolatable by phenotype. *Immunity* 1 (8):661-673.

Nagasawa, T., Y. Omatsu, and T. Sugiyama. 2011. Control of hematopoietic stem cells by the bone marrow stromal niche: the role of reticular cells. *Trends Immunol* 32 (7):315-320.

Nakada, D., T. L. Saunders, and S. J. Morrison. 2010. Lkb1 regulates cell cycle and energy metabolism in haematopoietic stem cells. *Nature* 468 (7324):653-658.

Nakamura, Y., F. Arai, H. Iwasaki, K. Hosokawa, I. Kobayashi, Y. Gomei, Y. Matsumoto, H. Yoshihara, and T. Suda. 2010. Isolation and characterization of endosteal niche cell populations that regulate hematopoietic stem cells. *Blood* 116 (9):1422-1432.

Naveiras, O., V. Nardi, P. L. Wenzel, P. V. Hauschka, F. Fahey, and G. Q. Daley. 2009. Bone-marrow adipocytes as negative regulators of the haematopoietic microenvironment. *Nature* 460 (7252):259-263.

Nemeth, M. J., and D. M. Bodine. 2007. Regulation of hematopoiesis and the hematopoietic stem cell niche by Wnt signaling pathways. *Cell Res* 17 (9):746-758.

Netelenbos, T., J. van den Born, F. L. Kessler, S. Zweegman, P. A. Merle, J. W. van Oostveen, J. J. Zwaginga, P. C. Huijgens, and A. M. Drager. 2003. Proteoglycans on bone marrow endothelial cells bind and present SDF-1 towards hematopoietic progenitor cells. *Leukemia* 17 (1):175-184.

Novershtern, N., A. Subramanian, L. N. Lawton, R. H. Mak, W. N. Haining, M. E. McConkey, N. Habib, N. Yosef, C. Y. Chang, T. Shay, G. M. Frampton, A. C. Drake, I. Leskov, B. Nilsson, F. Preffer, D. Dombkowski, J. W. Evans, T. Liefeld, J. S. Smutko, J. Chen, N. Friedman, R. A. Young, T. R. Golub, A. Regev, and B. L. Ebert. 2011. Densely interconnected transcriptional circuits control cell states in human hematopoiesis. *Cell* 144 (2):296-309.

Olesen, G., H. Tonder, M. S. Holm, and P. Hokland. 2001. Long-term culture of hematopoietic stem cells - validating the stromal component of the CAFC assay. *Cytotherapy* 3 (2):107-116.

Orkin, S. H. 1995. Transcription factors and hematopoietic development. *J Biol Chem* 270 (10):4955-4958.

Orkin, S. H., and L. I. Zon. 2008. Hematopoiesis: an evolving paradigm for stem cell biology. *Cell* 132 (4):631-644.

Oshima, M., M. Endoh, T. A. Endo, T. Toyoda, Y. Nakajima-Takagi, F. Sugiyama, H. Koseki, M. Kyba, A. Iwama, and M. Osawa. 2011. Genome-wide analysis of target genes regulated by HoxB4 in hematopoietic stem and progenitor cells developing from embryonic stem cells. *Blood* 117 (15):e142-150.

Ouellet, V., and P. M. Siegel. 2012. CCN3 modulates bone turnover and is a novel regulator of skeletal metastasis. *J Cell Commun Signal* 6 (2):73-85.

Park, I. K., D. Qian, M. Kiel, M. W. Becker, M. Pihalja, I. L. Weissman, S. J. Morrison, and M. F. Clarke. 2003. Bmi-1 is required for maintenance of adult self-renewing haematopoietic stem cells. *Nature* 423 (6937):302-305.

Perbal, B. 2001. NOV (nephroblastoma overexpressed) and the CCN family of genes: structural and functional issues. *Mol Pathol* 54 (2):57-79.

Perbal, B. (2006). New insight into CCN3 interactions--nuclear CCN3 : fact or fantasy? *Cell Commun Signal, 4*, 6

Pietras, E. M., M. R. Warr, and E. Passegue. 2011. Cell cycle regulation in hematopoietic stem cells. *J Cell Biol* 195 (5):709-720.

Ploemacher, R. E., J. P. van der Sluijs, J. S. Voerman, and N. H. Brons. 1989. An in vitro limiting-dilution assay of long-term repopulating hematopoietic stem cells in the mouse. *Blood* 74 (8):2755-2763.

Porritt, H. E., K. Gordon, and H. T. Petrie. 2003. Kinetics of steady-state differentiation and mapping of intrathymic-signaling environments by stem cell transplantation in nonirradiated mice. *J Exp Med* 198 (6):957-962.

Pronk, C. J., D. J. Rossi, R. Mansson, J. L. Attema, G. L. Norddahl, C. K. Chan, M. Sigvardsson, I. L. Weissman, and D. Bryder. 2007. Elucidation of the phenotypic, functional, and molecular topography of a myeloerythroid progenitor cell hierarchy. *Cell Stem Cell* 1 (4):428-442.

Rafii, S., F. Shapiro, R. Pettengell, B. Ferris, R. L. Nachman, M. A. Moore, and A. S. Asch. 1995. Human bone marrow microvascular endothelial cells support long-term proliferation and differentiation of myeloid and megakaryocytic progenitors. *Blood* 86 (9):3353-3363.

Rafii, S., F. Shapiro, J. Rimarachin, R. L. Nachman, B. Ferris, B. Weksler, M. A. Moore, and A. S. Asch. 1994. Isolation and characterization of human bone marrow microvascular endothelial cells: hematopoietic progenitor cell adhesion. *Blood* 84 (1):10-19.

Ramsfjell, V., D. Bryder, H. Bjorgvinsdottir, S. Kornfalt, L. Nilsson, O. J. Borge, and S. E. Jacobsen. 1999. Distinct requirements for optimal growth and In vitro expansion of human CD34(+)CD38(-) bone marrow long-term culture-initiating cells (LTC-IC), extended LTC-IC, and murine in vivo long-term reconstituting stem cells. *Blood* 94 (12):4093-4102.

Ratajczak, M. Z., C. Kim, A. Janowska-Wieczorek, and J. Ratajczak. 2012. The expanding family of bone marrow homing factors for hematopoietic stem cells: stromal derived factor 1 is not the only player in the game. *ScientificWorldJournal* 2012:758512.

Reilly, G. C., and A. J. Engler. 2010. Intrinsic extracellular matrix properties regulate stem cell differentiation. *J Biomech* 43 (1):55-62.

Reya, T., A. W. Duncan, L. Ailles, J. Domen, D. C. Scherer, K. Willert, L. Hintz, R. Nusse, and I. L. Weissman. 2003. A role for Wnt signalling in self-renewal of haematopoietic stem cells. *Nature* 423 (6938):409-414.

Robin, C., K. Ottersbach, J. C. Boisset, A. Oziemlak, and E. Dzierzak. 2011. CD41 is developmentally regulated and differentially expressed on mouse hematopoietic stem cells. Blood 117 (19):5088-509

Rosler, E. S., J. E. Brandt, J. Chute, and R. Hoffman. 2000. An in vivo competitive repopulation assay for various sources of human hematopoietic stem cells. *Blood* 96 (10):3414-3421.

Sakamoto, K., S. Yamaguchi, R. Ando, A. Miyawaki, Y. Kabasawa, M. Takagi, C. L. Li, B. Perbal, and K. Katsube. 2002. The nephroblastoma overexpressed gene (NOV/ccn3) protein associates with Notch1 extracellular domain and inhibits myoblast differentiation via Notch signaling pathway. *J Biol Chem* 277 (33):29399-29405.

Schajnovitz, A., T. Itkin, G. D'Uva, A. Kalinkovich, K. Golan, A. Ludin, D. Cohen, Z. Shulman, A. Avigdor, A. Nagler, O. Kollet, R. Seger, and T. Lapidot. 2011. CXCL12 secretion by bone marrow stromal cells is dependent on cell contact and mediated by connexin-43 and connexin-45 gap junctions. *Nat Immunol* 12 (5):391-398.

Sharma, M. B., L. S. Limaye, and V. P. Kale. 2012. Mimicking the functional hematopoietic stem cell niche in vitro: recapitulation of marrow physiology by hydrogel-based three-dimensional cultures of mesenchymal stromal cells. *Haematologica* 97 (5):651-660.

Shen, Y., and S. K. Nilsson. 2012. Bone, microenvironment and hematopoiesis. *Curr Opin Hematol* 19 (4):250-255.

Shimoyama, T., S. Hiraoka, M. Takemoto, M. Koshizaka, H. Tokuyama, T. Tokuyama, A. Watanabe, M. Fujimoto, H. Kawamura, S. Sato, Y. Tsurutani, Y. Saito, B. Perbal, H. Koseki, and K. Yokote. 2010. CCN3 inhibits neointimal hyperplasia through modulation of smooth muscle cell growth and migration. *Arterioscler Thromb Vasc Biol* 30 (4):675-682.

Sin, W. C., J. F. Bechberger, W. J. Rushlow, and C. C. Naus. 2008. Dose-dependent differential upregulation of CCN1/Cyr61 and CCN3/NOV by the gap junction protein Connexin43 in glioma cells. *J Cell Biochem* 103 (6):1772-1782.

Sin, W. C., M. Tse, N. Planque, B. Perbal, P. D. Lampe, and C. C. Naus. 2009. Matricellular protein CCN3 (NOV) regulates actin cytoskeleton reorganization. *J Biol Chem* 284 (43):29935-29944.

Sitnicka, E., D. Bryder, K. Theilgaard-Monch, N. Buza-Vidas, J. Adolfsson, and S. E. Jacobsen. 2002. Key role of flt3 ligand in regulation of the common lymphoid

progenitor but not in maintenance of the hematopoietic stem cell pool. *Immunity* 17 (4):463-472.

Sitnicka, E., N. Buza-Vidas, S. Larsson, J. M. Nygren, K. Liuba, and S. E. Jacobsen. 2003. Human CD34+ hematopoietic stem cells capable of multilineage engrafting NOD/SCID mice express flt3: distinct flt3 and c-kit expression and response patterns on mouse and candidate human hematopoietic stem cells. *Blood* 102 (3):881-886.

Sitnicka, E., N. Lin, G. V. Priestley, N. Fox, V. C. Broudy, N. S. Wolf, and K. Kaushansky. 1996. The effect of thrombopoietin on the proliferation and differentiation of murine hematopoietic stem cells. *Blood* 87 (12):4998-5005.

Soret, J., G. Dambrine, and B. Perbal. 1989. Induction of nephroblastoma by myeloblastosis-associated virus type 1: state of proviral DNAs in tumor cells. *J Virol* 63 (4):1803-1807.

Spangrude, G. J., S. Heimfeld, and I. L. Weissman. 1988. Purification and characterization of mouse hematopoietic stem cells. *Science* 241 (4861):58-62.

Strobel, E. S., D. Mobest, S. von Kleist, M. Dangel, S. Ries, R. Mertelsmann, and R. Henschler. 1997. Adhesion and migration are differentially regulated in hematopoietic progenitor cells by cytokines and extracellular matrix. *Blood* 90 (9):3524-3532.

Su, B. Y., W. Q. Cai, C. G. Zhang, V. Martinez, A. Lombet, and B. Perbal. 2001. The expression of ccn3 (nov) RNA and protein in the rat central nervous system is developmentally regulated. *Mol Pathol* 54 (3):184-191.

Suarez-Alvarez, B., A. Lopez-Vazquez, and C. Lopez-Larrea. 2012. Mobilization and homing of hematopoietic stem cells. *Adv Exp Med Biol* 741:152-170.

Suda, T., K. Takubo, and G. L. Semenza. 2010. Metabolic regulation of hematopoietic stem cells in the hypoxic niche. *Cell Stem Cell* 9 (4):298-310.

Sugimura, R., X. C. He, A. Venkatraman, F. Arai, A. Box, C. Semerad, J. S. Haug, L. Peng, X. B. Zhong, T. Suda, and L. Li. 2012. Noncanonical Wnt signaling maintains hematopoietic stem cells in the niche. *Cell* 150 (2):351-365.

Sugiyama, T., H. Kohara, M. Noda, and T. Nagasawa. 2006. Maintenance of the hematopoietic stem cell pool by CXCL12-CXCR4 chemokine signaling in bone marrow stromal cell niches. *Immunity* 25 (6):977-988.

Suresh, S., L. McCallum, W. Lu, N. Lazar, B. Perbal, and A. E. Irvine. 2011. MicroRNAs 130a/b are regulated by BCR-ABL and downregulate expression of CCN3 in CML. *J Cell Commun Signal*.

Tan, T. W., Y. L. Huang, J. T. Chang, J. J. Lin, Y. C. Fong, C. C. Kuo, C. H. Tsai, Y. J. Chen, H. C. Hsu, D. Y. Cho, Y. H. Chen, and C. H. Tang. 2012. CCN3 increases BMP-4 expression and bone mineralization in osteoblasts. *J Cell Physiol* 227 (6):2531-2541.

Taniguchi Ishikawa, E., D. Gonzalez-Nieto, G. Ghiaur, S. K. Dunn, A. M. Ficker, B. Murali, M. Madhu, D. E. Gutstein, G. I. Fishman, L. C. Barrio, and J. A. Cancelas. 2012. Connexin-43 prevents hematopoietic stem cell senescence through transfer of

reactive oxygen species to bone marrow stromal cells. *Proc Natl Acad Sci U S A* 109 (23):9071-9076.

Thibout, H., C. Martinerie, C. Creminon, F. Godeau, P. Boudou, Y. Le Bouc, and M. Laurent. 2003. Characterization of human NOV in biological fluids: an enzyme immunoassay for the quantification of human NOV in sera from patients with diseases of the adrenal gland and of the nervous system. *J Clin Endocrinol Metab* 88 (1):327-336.

Thorsteinsdottir, U., G. Sauvageau, and R. K. Humphries. 1999. Enhanced in vivo regenerative potential of HOXB4-transduced hematopoietic stem cells with regulation of their pool size. *Blood* 94 (8):2605-2612.

Toksoz, D., K. M. Zsebo, K. A. Smith, S. Hu, D. Brankow, S. V. Suggs, F. H. Martin, and D. A. Williams. 1992. Support of human hematopoiesis in long-term bone marrow cultures by murine stromal cells selectively expressing the membrane-bound and secreted forms of the human homolog of the steel gene product, stem cell factor. *Proc Natl Acad Sci U S A* 89 (16):7350-7354.

Trowbridge, J. J., R. T. Moon, and M. Bhatia. 2006. Hematopoietic stem cell biology: too much of a Wnt thing. *Nat Immunol* 7 (10):1021-1023.

Tzeng, H. E., J. C. Chen, C. H. Tsai, C. C. Kuo, H. C. Hsu, W. L. Hwang, Y. C. Fong, and C. H. Tang. 2011. CCN3 increases cell motility and MMP-13 expression in human chondrosarcoma through integrin dependent pathway. *J Cell Physiol*.

Ulyanova, T., G. V. Priestley, B. Nakamoto, Y. Jiang, and T. Papayannopoulou. 2007. VCAM-1 ablation in nonhematopoietic cells in MxCre+ VCAM-1f/f mice is variable and dictates their phenotype. *Exp Hematol* 35 (4):565-571.

Vallacchi, V., M. Daniotti, F. Ratti, D. Di Stasi, P. Deho, A. De Filippo, G. Tragni, A. Balsari, A. Carbone, L. Rivoltini, G. Parmiani, N. Lazar, B. Perbal, and M. Rodolfo. 2008. CCN3/nephroblastoma overexpressed matricellular protein regulates integrin expression, adhesion, and dissemination in melanoma. *Cancer Res* 68 (3):715-723.

Vallacchi, V., and M. Rodolfo. 2009. Regulatory role of CCN3 in melanoma cell interaction with the extracellular matrix. *Cell Adh Migr* 3 (1):7-10.

Visnjic, D., Z. Kalajzic, D. W. Rowe, V. Katavic, J. Lorenzo, and H. L. Aguila. 2004. Hematopoiesis is severely altered in mice with an induced osteoblast deficiency. *Blood* 103 (9):3258-3264.

Wada, H., K. Masuda, R. Satoh, K. Kakugawa, T. Ikawa, Y. Katsura, and H. Kawamoto. 2008. Adult T-cell progenitors retain myeloid potential. *Nature* 452 (7188):768-772.

Wang, L. D., and A. J. Wagers. 2011. Dynamic niches in the origination and differentiation of haematopoietic stem cells. *Nat Rev Mol Cell Biol* 12 (10):643-655.

Weaver, A., D. Ryder, D. Crowther, T. M. Dexter, and N. G. Testa. 1996. Increased numbers of long-term culture-initiating cells in the apheresis product of patients randomized to receive increasing doses of stem cell factor administered in combination with chemotherapy and a standard dose of granulocyte colony-stimulating factor. *Blood* 88 (9):3323-3328.

Welch, J. J., J. A. Watts, C. R. Vakoc, Y. Yao, H. Wang, R. C. Hardison, G. A. Blobel, L. A. Chodosh, and M. J. Weiss. 2004. Global regulation of erythroid gene expression by transcription factor GATA-1. *Blood* 104 (10):3136-3147.

Wilson, A., M. J. Murphy, T. Oskarsson, K. Kaloulis, M. D. Bettess, G. M. Oser, A. C. Pasche, C. Knabenhans, H. R. Macdonald, and A. Trumpp. 2004. c-Myc controls the balance between hematopoietic stem cell self-renewal and differentiation. *Genes Dev* 18 (22):2747-2763.

Wilson, A., and A. Trumpp. 2006. Bone-marrow haematopoietic-stem-cell niches. *Nat Rev Immunol* 6 (2):93-106.

Winkler, I. G., N. A. Sims, A. R. Pettit, V. Barbier, B. Nowlan, F. Helwani, I. J. Poulton, N. van Rooijen, K. A. Alexander, L. J. Raggatt, and J. P. Levesque. 2010. Bone marrow macrophages maintain hematopoietic stem cell (HSC) niches and their depletion mobilizes HSCs. *Blood* 116 (23):4815-4828.

Wontakal, S. N., X. Guo, C. Smith, T. MacCarthy, E. H. Bresnick, A. Bergman, M. P. Snyder, S. M. Weissman, D. Zheng, and A. I. Skoultchi. 2012. A core erythroid transcriptional network is repressed by a master regulator of myelo-lymphoid differentiation. *Proc Natl Acad Sci U S A* 109 (10):3832-3837.

Wright, D. E., E. P. Bowman, A. J. Wagers, E. C. Butcher, and I. L. Weissman. 2002. Hematopoietic stem cells are uniquely selective in their migratory response to chemokines. *J Exp Med* 195 (9):1145-1154.

Wright, D. E., A. J. Wagers, A. P. Gulati, F. L. Johnson, and I. L. Weissman. 2001. Physiological migration of hematopoietic stem and progenitor cells. *Science* 294 (5548):1933-1936.

Wu, H., X. Liu, R. Jaenisch, and H. F. Lodish. 1995. Generation of committed erythroid BFU-E and CFU-E progenitors does not require erythropoietin or the erythropoietin receptor. *Cell* 83 (1):59-67.

Xie, Y., T. Yin, W. Wiegraebe, X. C. He, D. Miller, D. Stark, K. Perko, R. Alexander, J. Schwartz, J. C. Grindley, J. Park, J. S. Haug, J. P. Wunderlich, H. Li, S. Zhang, T. Johnson, R. A. Feldman, and L. Li. 2009. Detection of functional haematopoietic stem cell niche using real-time imaging. *Nature* 457 (7225):97-101.

Yamazaki, S., H. Ema, G. Karlsson, T. Yamaguchi, H. Miyoshi, S. Shioda, M. M. Taketo, S. Karlsson, A. Iwama, and H. Nakauchi. 2011. Nonmyelinating Schwann cells maintain hematopoietic stem cell hibernation in the bone marrow niche. *Cell* 147 (5):1146-1158.

Yamazaki, S., A. Iwama, S. Takayanagi, K. Eto, H. Ema, and H. Nakauchi. 2009. TGF-beta as a candidate bone marrow niche signal to induce hematopoietic stem cell hibernation. *Blood* 113 (6):1250-1256.

Yang, L., D. Bryder, J. Adolfsson, J. Nygren, R. Mansson, M. Sigvardsson, and S. E. Jacobsen. 2005. Identification of Lin(-)Sca1(+)kit(+)CD34(+)Flt3- short-term hematopoietic stem cells capable of rapidly reconstituting and rescuing myeloablated transplant recipients. *Blood* 105 (7):2717-2723.

Yang, L., L. Wang, H. Geiger, J. A. Cancelas, J. Mo, and Y. Zheng. 2007. Rho GTPase Cdc42 coordinates hematopoietic stem cell quiescence and niche interaction in the bone marrow. *Proc Natl Acad Sci U S A* 104 (12):5091-5096.

Yilmaz, O. H., M. J. Kiel, and S. J. Morrison. 2006. SLAM family markers are conserved among hematopoietic stem cells from old and reconstituted mice and markedly increase their purity. *Blood* 107 (3):924-930.

Yoshihara, H., F. Arai, K. Hosokawa, T. Hagiwara, K. Takubo, Y. Nakamura, Y. Gomei, H. Iwasaki, S. Matsuoka, K. Miyamoto, H. Miyazaki, T. Takahashi, and T. Suda. 2007. Thrombopoietin/MPL signaling regulates hematopoietic stem cell quiescence and interaction with the osteoblastic niche. *Cell Stem Cell* 1 (6):685-697.

Zandstra, P. W., E. Conneally, A. L. Petzer, J. M. Piret, and C. J. Eaves. 1997. Cytokine manipulation of primitive human hematopoietic cell self-renewal. *Proc Natl Acad Sci U S A* 94 (9):4698-4703.

Zandstra, P. W., E. Conneally, J. M. Piret, and C. J. Eaves. 1998. Ontogeny-associated changes in the cytokine responses of primitive human haemopoietic cells. *Br J Haematol* 101 (4):770-778.

Zeng, H., R. Yucel, C. Kosan, L. Klein-Hitpass, and T. Moroy. 2004. Transcription factor Gfi1 regulates self-renewal and engraftment of hematopoietic stem cells. *Embo J* 23 (20):4116-4125.

Zetterblad, J., H. Qian, S. Zandi, R. Mansson, A. Lagergren, F. Hansson, D. Bryder, N. Paulsson, and M. Sigvardsson. 2010. Genomics based analysis of interactions between developing B-lymphocytes and stromal cells reveal complex interactions and two-way communication. *BMC Genomics* 11:108.

Zhang, C. C., and H. F. Lodish. 2008. Cytokines regulating hematopoietic stem cell function. *Curr Opin Hematol* 15 (4):307-311.

Zhang, J., C. Niu, L. Ye, H. Huang, X. He, W. G. Tong, J. Ross, J. Haug, T. Johnson, J. Q. Feng, S. Harris, L. M. Wiedemann, Y. Mishina, and L. Li. 2003. Identification of the haematopoietic stem cell niche and control of the niche size. *Nature* 425 (6960):836-841.

Zhang, Y., and C. Wang. 2011. Nephroblastoma overexpressed (NOV/CCN3) gene: a paired-domain-specific PAX3-FKHR transcription target that promotes survival and motility in alveolar rhabdomyosarcoma cells. *Oncogene*.

Zhu, J., and S. G. Emerson. 2002. Hematopoietic cytokines, transcription factors and lineage commitment. *Oncogene* 21 (21):3295-3313.

Zon, L. I. 2008. Intrinsic and extrinsic control of haematopoietic stem-cell self-renewal. *Nature* 453 (7193):306-313.

Appendix: publications

1. Genetic variegation of clonal architecture and propagating cells in leukemia.

   Anderson K, Lutz C, van Delft FW, Bateman CM, **Guo Y**, Colman SM, Kempski H, Moorman AV, Titley I, Swansbury J, Kearney L, **Enver T**, Greaves M.
   Nature. 2011 Jan 20; 469(7330):356-61. doi: 10.1038/nature09650.

2. Dynamic analysis of gene expression and genome wide transcription factor binding during lineage-specification of multipotent progenitors.

   Gillian May, Shamit Soneji, Alex J. Tipping, Jose Teles, Simon J. McGowan, Mengchu Wu, **Yanping Guo,** Cristina Fugazza, John Brown, Cristina Pina, Victor Olariu, Stephen Taylor, Daniel G. Tenen, Carsten Peterson, **Tariq Enver**
   Cell Stem Cell, manuscripts under revision